AD-A179 776 EFFECTS OF CCN-FCN (CLOUD CONDENSATION NUCLEI-FOG CONDENSATION NUCLEI) SP..(U) NEVADA UNIV RENO DESERT RESEARCH INST J G HUDSON 05 MAR 87 ARO-22342.1-GS 1/3

UNCLASSIFIED DAAG29-85-K-0037 F/G 4/1 NL

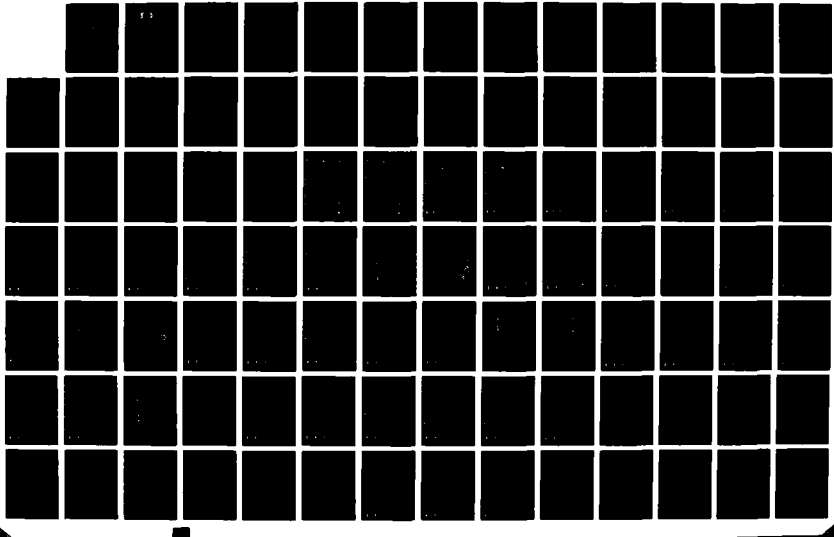

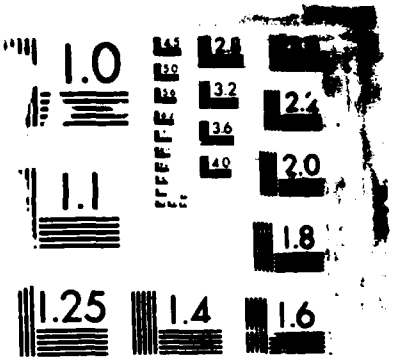
1.0
1.1
1.25
1.4
1.6
2.0
1.8

DTIC

AD-A179 776

REPORT DOCUMENTATION PAGE

DTIC ELECTE MAY 0 1 1987 S D

1b RESTRICTIVE MARKINGS

Unclassified

2a SECURITY CLASSIFICATION AUTHORITY

3 DISTRIBUTION/AVAILABILITY OF REPORT

Approved for public release; distribution unlimited.

2b DECLASSIFICATION/DOWNGRADING SCHEDULE

4 PERFORMING ORGANIZATION REPORT NUMBER(S)

5. MONITORING ORGANIZATION REPORT NUMBER(S)

ARO 22342.1-GS

6a NAME OF PERFORMING ORGANIZATION	6b OFFICE SYMBOL (If applicable)	7a. NAME OF MONITORING ORGANIZATION
Desert Research Institute University of Nevada System		U. S. Army Research Office
6c ADDRESS (City, State, and ZIP Code) P. O. Box 60220, Reno, Nevada 89506		7b. ADDRESS (City, State, and ZIP Code) P. O. Box 12211 Research Triangle Park, NC 27709-2211
8a NAME OF FUNDING/SPONSORING ORGANIZATION U. S. Army Research Office	8b. OFFICE SYMBOL (If applicable)	9. PROCUREMENT INSTRUMENT IDENTIFICATION NUMBER DAAG29-85-K-0037
8c ADDRESS (City, State, and ZIP Code) P. O. Box 12211 Research Triangle Park, NC 27709-2211		10 SOURCE OF FUNDING NUMBERS

PROGRAM ELEMENT NO	PROJECT NO.	TASK NO.	WORK UNIT ACCESSION NO

11 TITLE (Include Security Classification)
Effects of CCN-FCN Spectra on Droplet Spectra in the Albany Fog Project

12 PERSONAL AUTHOR(S) James G. Hudson

13a TYPE OF REPORT	13b. TIME COVERED	14. DATE OF REPORT (Year, Month, Day)	15. PAGE COUNT
Final	FROM 1, 85 TO 10, 86	87, 3, 5	202

16 SUPPLEMENTARY NOTATION The view, opinions and/or findings contained in this report are those of the author(s) and should not be construed as an official Department of the Army position, policy or decision, unless so designated by other documentation.

17 COSATI CODES		
FIELD	GROUP	SUB-GROUP

18. SUBJECT TERMS (Continue on reverse if necessary and identify by block number)
Fog, haze, supersaturation, visibility, electromagnetic propagation, aerosol, optics

19 ABSTRACT (Continue on reverse if necessary and identify by block number)

Analysis of aerosol and fog droplet data has shown that fogs are composed of zones with various supersaturations and subsaturations. A technique to quantify the subsaturations as well as the supersaturations has been developed. This has enabled calculations to be made of droplet growth and evaporation of the droplet spectra. These preliminary approximations are consistent with the measured time evolution of the fog. The largest nuclei (lowest critical supersaturation) FCN were definitely found to be the only ones upon which fog droplets condense. Droplet concentrations and visibility in subsaturated conditions especially were found to be determined by the preexisting nuclei. Droplet concentrations and visibility in supersaturated conditions were found to be related to the preexisting nuclei.

(Keywords)

20 DISTRIBUTION/AVAILABILITY OF ABSTRACT	21 ABSTRACT SECURITY CLASSIFICATION
☐ UNCLASSIFIED/UNLIMITED ☐ SAME AS RPT ☐ DTIC USERS	Unclassified

22a NAME OF RESPONSIBLE INDIVIDUAL	22b TELEPHONE (Include Area Code)	22c. OFFICE SYMBOL

DD FORM 1473, 84 MAR 83 APR edition may be used until exhausted. All other editions are obsolete.

SECURITY CLASSIFICATION OF THIS PAGE
UNCLASSIFIED

TABLE OF CONTENTS

Final Report of Effects of CCN-FCN Spectra on Droplet Spectra in the Albany Fog Project

by James G. Hudson

1. Introduction

Fog condensation nuclei (FCN) spectra and cloud condensation nuclei (CCN) concentrations were collected continuously from Sept. 24 to Nov. 9, 1982 at Albany, New York during a fog field project organized by the University of New York. The CCN were measured with a DRI continuous flow thermal diffusion chamber (Hudson and Squires, 1976) which was operated at 0.4% supersaturation. The FCN were measured with the DRI isothermal haze chamber (IHC) (Hudson, 1980) which obtained five supersaturations simultaneously (0.12%, 0.08%, 0.04%, 0.03%, and 0.02%). Most of the data was recorded on cassette tape every two minutes. Much of the effort with this project involved the processing of this data. For convenience the data was stored on 3.5 inch floppy disks which could be used with the PI's personal computer for analysis. Some of the gaps in the data had to be filled by manually reading data from paper tapes. These nuclei data were then compared with droplet spectra provided by the University of New York. The droplet spectra was also loaded onto the 3.5 inch floppy disks so that they could be directly compared electronically and simultaneous droplet and nuclei data could be plotted from both data sets. Comparisons were also made with the humidity and visibility which was provided in graphical form by U. of N.Y. During the seven fog events when all data was available time plots were made identical so that they could be overlayed for convenient comparisons. Two major new findings have come from the analysis. Other evidence to confirm and delineate past work was also obtained. Moreover it is apparent that further analysis of this data would yield significant results. Furthermore, techniques have been developed which would be valuable in future field efforts.

One of the two significant new findings clears up the mystery of the apparent disappearance of the submicron droplets upon cloud or fog formation. These observations were previously explained as a malfunction or artifact of the instruments. In the cases where CCN-FCN measurements were not available the observations were not necessarily anomalalous as it was always possible that a peculiar particle spectrum might produce such phenomena. It will be shown that after a careful analysis of the Albany data (many

comparisons of the simultaneous droplet and nuclei spectra) that the most likely explanation is that the small droplets do indeed evaporate under subsaturated conditions. However many of the observations which will be presented demonstrate no contradictions between the droplet and nuclei spectra. These observations are indicative of zones of supersaturation within the fog. Hence it appears that this technique (comparisons of droplet and nuclei spectra which will be described in detail later) can be used to actually measure the instantaneous super/subsaturation within the fog. Since this is a most useful piece of information and there is practically no other way to obtain a measurement of the relative humidity (R.H.) near saturation or any level of supersaturation this will be a valuable research tool.

The second important finding from this analysis is that the CCN-FCN spectrum can be used to predict the haze droplet spectrum before fog onset. Along with this is the fact that with low FCN concentrations, fog onset (R.H. > 100%) is much more sudden. A corolary to this is the fact that when the FCN concentrations are high the haze droplet concentrations before actual fog onset (100% R.H.) are quite similar to the total droplet concentrations in the fog.

The low supersaturations (<0.1%) previously measured in fogs have been thoroughly confirmed in this study. The supersaturations in Albany may be a little higher than in most of the previous measurement projects. A weak correlation was found between the FCN concentrations and the total droplet concentrations in the fogs. However the extent of variation was much less than at other locations (other field projects). Nevertheless since the correlation increased for the lowest supersaturations and was nonexistant for the higher Sc's this gave further confirmation to the fact that fog droplets condense only on the largest nuclei (the FCN). Therefore the term FCN has been upheld.

2. Level of Fog Supersaturation

Figure 1 displays the ambient droplet spectra and the simultaneous ambient CCN spectra. These CCN spectra are plotted as described by Hudson (1980) in order to compute the effective supersaturation, Seff, in the fog or cloud. The CCN spectra are plotted as two nearly parallel lines while the droplet spectra often intersects one or both of the CCN lines. The lefthand CCN spectrum is actually a direct plot of the cumulative data from the isothermal haze chamber (IHC). This instrument exposes the sample aerosol to 100% R.H. for enough time that the particles grow to their equilibrium sizes. This size d(0) is related to the critical

supersaturation, Sc, of the particles through the equation

$$d(0) = 8x10(-4)/Sc$$

Hence the x axis can be transcribed so that traditional CCN plot can be made (cumulative number vs. Sc). However since these are not very useful for the comparisons with droplet spectra they will not be presented here. The righthand CCN curve which is plotted in these figures is an artificial curve which is obtained by multiplying the sizes by 1.73 which is the ratio of the critical diameter, dc, of a nucleus to d(0) (the ratio is the square root of three). Whereas the lefthand nucleus distribution is possible in the ambient air when the ambient humidity is 100%; a droplet distribution which coincides with the nuclei critical diameter, dc, is not possible. This second CCN distribution is used only as a device to determine the Seff within the fog. The critical size represents the peak of the Kohler curve. The Kohler curve is the equilibrium humidity for a particle as a function of droplet size. Growth of droplets to supermicron sizes is only possible if the humidity has at one time exceeded the peak value which is the critical supersaturation, Sc, of the particle's Kohler curve and the particle (droplet) has thus exceeded its dc. Growth beyond the dc is not possible unless the Sc of the nucleus has been exceeded in the ambient air for a long enough period that the droplet has also been able to grow beyond dc.

Generally in a cloud a peak supersaturation is reached early in the life cycle and then declines. At that point the number of activated droplets is determined because all particles with Sc less than this supersaturation can exceed their critical sizes and grow without limit while those with Sc less then the peak supersaturation can not exceed their dc. These droplets will actually shrink as the humidity decreases while those which have exceeded their critical values can continue to grow even if the supersaturation decreases. Of course if the humidity goes below 100% all droplets will tend to evaporate. However the unactivated ones (which are of course smaller) will attain smaller sizes much more rapidly. This type of analysis assumes homogeneous unmixed cloud conditions. Therefore it assumes that larger droplets are always grown on larger nuclei. However Hudson (1984) and Hudson and Rogers (1986) seem to have confirmed this fact. If the cumulative ambient droplet curve intersects the critical CCN-FCN spectrum then an Seff is obtainable. In figure 1 the part of the droplet curve which is to the right of the intersection with the dc curve displays the droplets which have exceeded their critical sizes. The rest of the droplets the smaller ones are smaller than their critical sizes; these are the unactivated haze droplets.

The size corresponding to this intersection can be derived from each figure. The corresonding effective supersaturation, Seff, is then calculated from the above equation. Tables of Seff for the various fog events are shown later. Seff was generally in keeping with past measurements in various fogs (e.g. Hudson, 1980; Meyer et. al., 1980; Hudson and Rogers, 1986). This supersaturation was generally less than 0.1%. This is quite encouraging because much of the past data was obtained with a Royco optical particle counter instead of a PMS probe measuring the ambient droplets. It is also quite encouraging that the cumulative droplet curves usually have flat areas near the intersection with the dc lines. This is indicative of a size separation of the activated droplets from the unactivated droplets. A flat area in a cumulative distribution represents a size range over which there are no particles. This is predicted from the theory of cloud droplet growth because the activated droplets grow to larger sizes but the unactivated ones do not. This then leaves a gap in the size distribution. The excellent agreement of the droplet line with the d(0) line at the lower size range is also predicted from the theory of droplet growth as these smaller (higher Sc nuclei) should achieve a size only slightly more than d(0) but less than dc. The various agreements cited here indicate that there was very little disagreement in number concentration or size between the PMS probe used to count ambient droplets and the Royco used to count and size the CCN in the cloud chambers. Therefore the comparisons seem to be quite valid. Scores of simultaneous droplet and nuclei spectra are presented in the appendix.

3. The apparent disappearance of small droplets in fog

This matter concerns a mystery which has been standing for several years. This mystery which was described in the proposal concerns the apparent disappearance of the smallest haze droplets in cloud or fog. It has been observed by the PI and by various investigators (e.g. Noonkester, 1984) that as the supersaturation increases and large droplets are produced as some nuclei become activated, the concentration of small droplets actually appears to decrease. When this was observed by the PI in west coast fogs during the late 70's it was a mystery because measurements of the nuclei indicated that this should not be happening. The concentration of nuclei was such that at even 100% R.H. there should have been many more submicron sized droplets than were measured. At the same time there were higher concentrations of larger droplets than there were nuclei. The comparison of these two spectra in fact yielded the Seff in the fog (Hudson, 1980). Hence the large part of the droplet spectrum was indicating supersaturation but the small end of the droplet spectrum was indicating subsaturation.

Fig. 2 displays the same type of observation in the Albany project. Figure 1 however displays data from the Albany project which does not show any conflict between the two parts of the spectrum. Many figures like this one (see appendix) show that the concentration of haze droplets is exactly what would be predicted from the nuclei measurements. Hence the two extremes of the droplet spectrum are not in conflict as they appear in figure 2. One explanation for the observations like figure 2 had been that the droplet probe was missing the smallest droplets. However this conclusion is severely weakened by the abundance of observations such as figure 1 (see appendix). An artifact of the equipment should not come and go.

When the sizes of the small droplets are compared with the nucleus spectrum the effective humidity can be inferred. The d(0) lines on these figures are the actual particle spectra in the isothermal haze chamber. This should also be the equilibrium sizes of all of the particles when the humidity is 100%. The humidity vs. size relationships which were determined by Fitzgerald (1975) were applied to the data to show what the relative humidity of the ambient air must be. The concentration of particles and nuclei is assumed to be homogeneous. The number of particles at 100% R.H. (from the FCN measurements) is compared to the sizes with the same number concentration in the simultaneous droplet measurements. When these sizes are compared on the diagrams presented by Fitzgerald (1975) the relative humidity of the ambient air can be inferred. This does require some assumptions about the composition of the particles. However using the two extreme compositions presented in the article by Fitzgerald indicates little difference in the deduced R.H. In many of the figures like fig. 2 the subsaturation was determined to be about 1%. This means that the relative humidity would be 99%. The largest droplets could still survive such a humidity and apparently that is what is happening. The fog is apparently made of parcels with various humidity histories (above and below 100%). In those parcels which are above 100% droplets can grow whereas in the subsaturated parcels the droplets evaporate.

The sizes of the smallest droplets are much more susceptible to changes in R.H. and in fact are an excellent indicator of the instantaneous ambient humidity. A crude approximation of droplet growth is given as

$$d(r2)/dt = 10 (-8) S$$

where r is droplet radius in centimeters, t is time in seconds, and S is supersaturation is percent. Thus

$$r2 - r(0)2 = 10 (-8) St$$

and then a change in radius from 0.5 micrometers to 0.4 micrometers at a subsaturation of 0.1% would take place within a second. On the otherhand it would take a 5 micrometer droplet nearly 100 seconds to evaporate down to 4 micrometers at the same subsaturation. It would take even 10 seconds to change from 5 micrometers to 4.9 micrometers at this subsaturation. This analysis shows that the sizes of the small droplets respond to the ambient humidity quite readily. Therefore there is probably nothing wrong with measurements such as fig. 2. They are in fact excellent indicators of the subsaturated conditions within the fog. One percent subsaturation is not enough to evaporate the larger droplets. In fact the largest droplets which have the smallest surface to volume ratio remain the longest. For example a 10 micrometer droplet would require 19 seconds to change to a 9 micrometer droplet at 1% subsaturation and 75 seconds to evaporate to 5 micrometers radius. On the otherhand a 0.5 micrometer droplet evaporates to 0.3 micrometers in 0.16 seconds.

4. Climatology

The CCN and FCN climatology was determined by taking the average hourly values and plotting these over the several days of the project. Figures 3-6 show the data plotted over the time period between Sept. 22 and Oct. 18. Figure 3 presents the CCN concentration (0.4%) and the largest FCN (0.02%) concentration. Since these are all cumulative the concentrations at the higher critical supersaturatons, Sc, include all nuclei at the lower Sc'. This is done because the nuclei act cumulatively. When a certain ambient supersaturation is achieved all nuclei with Sc less than that value produce activated cloud droplets. Figures 4 and 5 display each of the three adjacent supersaturations out of the total of six supersaturations which were used. It is readily seen that the lower Sc nuclei display much more variability. For instance the 0.02% Sc particles vary over 3 orders of magnitude whereas the CCN (0.4%) generally vary over only 1 order of magnitude. Figure 6 displays the simultaneous CCN concentration at Whiteface Mountain which is about 150 miles to the north and at a much higher elevation (5000 ft.). This data which was obtained from another project shows much more variability than at Albany.

The most notable event of the period was the sharp decrease in nucleus concentrations on Oct. 2. Although this was measured at all supersaturations the decrease at the lovest supersaturations was the most significant. The return to higher values was much faster for the smaller particles.

It is also noteworthy that this same decrease was measured at Whiteface Mountain. This indicates that the change in the aerosol occurred over a wide area. It will be shown later that this produced profound changes in the fog. Figures 7 and 8 extend the climatology through the entire period.

5. Description of events.

A complete data set--droplet spectra, CCN-FCN spectra, relative humidity, and visibility--exists for only seven fog events. These events occurred on Sept. 30-Oct. 1, Oct. 2-3, Oct. 4-5, Oct. 10-11, Oct. 24-25, Oct. 26-27, and Oct. 27-28. Three other events are also discussed here although these lacked either humidity or visibility data.

Sept. 29-30. (Table 1)

This event contained only limited CCN-FCN data from 6:30 to 7:30. A consistent Seff of 0.03% was derived from comparisons of the droplet and nucleus spectra (table 1). The agreement between the two spectra at smaller sizes was quite good but since the droplet spectra was generally slightly to the left of the nucleus spectra (see appendix) a slight subsaturation was indicated for this event (see appendix). This would indicate that the fog at the time of the measurements may have been in an evaporating stage even though activated droplets were detected. The degree of subsaturation was less than 0.1%. This subsaturation is the same order of magnitude as the the Seff.

Sept. 30-Oct. 1 (Figs. 9-17) (Table 2)

This event had the highest FCN concentrations of the seven events with complete data (see table 11 and fig. 3). Like the previous event the Seff was consistently found to be 0.03% (table 2). The real supersaturated fog occurred between 3 and 10 A.M. when the relative humidity peaked at 100% (Fig. 16), the visibility went to "zero" (Fig. 17), and very large droplets were produced (fig. 14 and 15). Prior to this time the relative humidity gradually worked its way up toward saturation. The total droplet concentration (>0.5 micrometers) (fig. 11) also gradually increased as saturation was approached. The CCN-FCN concentrations were quite steady throughout the fog (fig. 9 and 10). There is some indication that the concentration of the largest nuclei decreased during the fog and then increased toward the end of the fog. This decrease could be due to droplet fallout during the peak of the fog when the largest droplets were produced. The later

decrease may be due to chemical conversion processes within the fog droplets which would increase the solution strength of the droplets and thus increase the size of the nuclei when these droplets evaporated. The total CCN concentration did not display such an increase (fig. 9). The total haze droplet concentration prior to the fog was very high because of the high FCN concentrations (fig. 11). The FCN measurements seemed to predict the haze droplet concentrations.

The agreement between the droplet and nucleus spectrum was often quite good (see appendix) indicating that the measured fog was supersaturated as the Seff would seem to indicate. However often in the small portion of the spectrum the droplet concentrations were lower than the nucleus concentrations indicating subsaturations (appendix). This was especially noticable toward the end of this fog event but it even began at about 6:20. It can be noted that the droplet sizes and concentration showed a gradual decrease after this time as the peak occurred between 5:30 and 6:30 when the concentration of 40 micrometer droplets peaked. According to the crude growth equation two hours would be required to grow 40 micrometer droplets from 25 micrometer droplets with a 0.03% supersaturation. This is consistent with figs. 14 and 15. Thus the apparent sub/supersaturation determined from the comparison of the nucleus and droplet spectra seems to be an indicator of the vigor of the fog. It shows a subsaturated fog after this time where droplets are evaporating. Therefore this tool predicted the fog dissipation.

Oct. 2-3 (Figs. 18-26) (table 3)

This event shows a considerable contrast with the last event mainly because the FCN concentration is so much lower (1/cm3 as opposed to 20/cm3 active at 0.02% in the previous event see fig. 3 and table 11) (figs. 18 and 19). This produces the much lower haze droplet (0.5 micrometer) concentrations prior to the fog (fig. 20) (1/cm3 compared to at least 20/cm3 in the previous event) (fig. 11). The relative humidity was about the same prior to fog in each case (figs. 25 and 16). One consequence of this is that the droplet concentration showed a very abrupt increase when saturation was reached at about 1:40 (fig. 20-22). The visibility prior to saturation was thus much higher for this event as compared to the previous one (fig. 26 and 17). The nuclei as measured by the isothermal haze chamber (FCN) are the controlling factor. It should be noted that there is very little contrast between the CCN concentrations at 0.4% and 0.12% with the previous event (figs. 18 and 9).

The Seff of this fog is considerably higher (up to 0.12%) than the previous two events (table 3). It is probable that the lack of nuclei at low supersaturations is the one factor which allowed the supersaturation to get so much higher. The total droplet concentration during the supersaturated fog was actually higher 300/cm3 than the previous fog (100-200/cm3) because of the higher supersaturations which were indeed measured in this fog (tables 3 and 2).

The nucleus-droplet comparisons reveal subsaturated conditions from fog onset at 1:40 until about 4:30 (appendix). Droplet sizes during this period are much smaller than those found later. Subsaturations of as much as 1% were measured during this period. It is apparent that this was not a vigorous fog and that droplets were being produced at another location (perhaps above) and advected to the site. Beginning at about 4:30 the nucleus and droplet spectra begin to match (appendix) at the small sizes indicating supersaturated conditions. Seff is also much larger after this period (up to 0.12%) and the droplet sizes show the largest values (figs. 23 and 24). This is evidently a period of supersaturation and droplet growth. An increase in droplet size from 10 micrometers diameter to 20 micrometers would be predicted to occur in about 12 minutes with a 0.1% supersaturation (according to the crude growth equation). These supersaturations predict the droplet growth which occurrs after this time and culminates in peak growth of the 30 to 35 micron droplets between 7:00 and 8:00. For instance the increase from 25 to 35 micrometers diameter which is measured here between about 6 and 7 A.M. would require about 35 minutes with a 0.07% supersaturation according to the crude growth equation. The supersaturatin during this period was fairly steady with a slight gradual decline from 0.1 to 0.06% so this is in keeping with the observed droplet spectrum. The supersaturation shows a decline beginning at 8:00 when the small droplet concentration moves to the left of the nucleus curve indicating subsaturation in spite of the persistence of activated droplets. These require several minutes to evaporate under the subsaturated conditions. In the next few minutes the subsaturation increases rapidly leading to a rapid decrease in droplets. At 8:20 a subsaturation of 10% is measured! At this humidity even a 40 micrometer diameter droplet would evaporate to 10 micrometers within 40 seconds. This of course leads to the rapid evaporation of droplets which is observed.

Oct. 4-5. (Figs. 27-33) (Table 4)

The relative humidity at the site never comes up to saturation during this event (fig. 32). However Seff's are

measured during this fog and these are substantial, averaging about 0.07% (table 4). The highest value is measured at the beginning 4:40-4:50 and there is an immediate decline to about 0.07% which remains until about 7:30. However the droplet distribution is rather peculiar in that it is very flat and decreases rapidly at the small sizes where it is consistently below the nucleus spectrum (appendix). This seems to indicate subsaturated conditions and advection of activated droplets to the site. Small droplets are not detected because of the subsaturated conditions. For instance a 1% subsaturation would reduce a 4 micrometer diameter droplet to less than 0.5 micrometers within 4 seconds. The largest droplets which were observed on this day, 15 micrometers diameter (fig. 30), would have evaporated from 15.5 micrometer droplets in 4 seconds at 1% subsaturation. This is then entirely in keeping with the observations and could be indicative of a fog aloft. Droplet fall speed is given by

$$v = 10^{(6)} r2$$

where r is in centimeters. Thus a 15 micrometer diameter droplet would fall at about 0.6 cm/sec and it would take one-half hour to fall 10 meters. If it started out as a 38 micrometer diameter droplet it would fall at about 3.6 cm/sec and would thus take only about 5 minutes to fall 10 meters. Such a droplet would be evaporated to about 18 micrometers diameter with a subsaturation of 1%. Without a more complete analysis this seems a plausable scenario. This subsaturation seems to prevent the observation of large droplets. This event also has a rather low FCN concentration which leads to the rather low haze droplet concentration prior to the fog. Higher FCN concentrations would probably have led to larger droplets before and during the fog.

Oct. 5-6. (Table 5)

This fog was somewhat similar to the last event except that the Seff was only about 0.02 to 0.03% (table 5). The small particle part of the spectrum showed that the ambient relative humidity was only about 90%. This was certainly the factor which limited the droplet size in this fog. These measurements were indicative of a fog or stratus cloud hanging just above the site as in the privious event. In fact fog aloft was reported for this event.

Oct. 10-11. (Figs. 34-41) (Table 6)

Supersaturated conditions occurred from 2 until 10 (fig. 40) when the droplet sizes were very large (fig. 37-39). The supersaturations during this fog were quite variable and were

often quite high (up to 0.13%, table 6). The supersaturated periods during this event directly coincided with periods when the droplet sizes and concentrations were highest. The agreement between the droplet and nuclei spectra was excellent during this event (appendix). Conditions appeared to be supersaturated most of the time; there was very little evidence of subsaturated conditions during this fog. Shorter time periods used during this event did not show any substantial differences in supersaturation (appendix).

Oct. 14. (Table 7)

Rather high supersaturations were found in this fog (table 7). Agreement between the two spectra was usually quite good indicating supersaturated conditions. However there were occasional subsaturated conditions.

Oct. 24-25. (Figs. 42-49) (Table 8)

These last three events are distinguished from the previous several events in that the FCN concentrations are considerably higher (figs. 42 and 43 and table 11). The FCN concentrations have now increased to the values found during the first two events in September (figs. 3-5 and 7). The relative humidity does not go to 100% during this event. However the comparison of droplet and nucleus spectra indicates that many of the droplets are activated (appendix). In fact the Seff was rather consistently 0.04% (table 8). Although the low end of the spectral comparisons usually indicated subsaturated conditions there are some occasions when the agreement between the spectra indicates supersaturation. The high FCN concentrations produce the high droplet concentrations in spite of the lack of humidity (fig. 48).

Oct. 26-27. (Fig. 50-57) (Table 9)

The humidity does appear to go to 100% between 8 and 9 o'clock (fig. 56) when the total droplet concentration reaches 600/cm3 (fig. 52). This high concentration (fig. 50 and 51) is apparently caused by the high nucleus concentration rather than a high supersaturation because the Seff at this time was about 0.04% (table 9). At that time no subsaturation was indicated (appendix) so the droplets were in a state of growth. Earlier some Seff's of about the same magnitude were measured however a subsaturation of 1% was indicated by the disagreement between the droplet and nucleus spectra (appendix). The haze droplet concentration (fig. 52) prior to the supersaturation was high because of the high FCN

concentrations.

Oct. 27-28. (Figs. 58-64) (Table 10)

The FCN concentrations were even higher for this event (figs. 58 and 59). The relative humidity did not reach 100% at all during this event (fig. 63). Seff were measured only very briefly during this event (0.03 to 0.04%) (table 10). However there were also no measurements of undersaturation as would be noted by the droplet spectra being to the left of the nucleus spectra (appendix). When an Seff was measured the droplets did not grow much beyond their critical sizes. This event of all events in this project was truely a haze. The droplets reached only their equilibrium sizes at 100% R.H., d(0). The visibility reached low values (5km) (fig. 64) only because of the high nucleus concentrations. The droplet concentrations (fig. 60) were so high only because of the high nucleus concentrations (figs. 58 and 59). The humidity was substantial (fig. 63).

6. Comparisons of fog events with complete data sets

Table 11 presents a syntheses of the data from the seven fog events which have all four types of data--droplets, CCN, R.H., and visibility. The considerable differences in the FCN concentrations are quite obvious (also see figs. 3-5 and 7). In order to intercompare the haze droplet concentrations for each date a period of similar relative humidities has been chosen from each event. Periods when the R.H. was 95% are compared (see figs. 16, 25, 32, 40, 48, 56, and 63). You can see that the estimate of 95% is very rough as the humidity varied considerably with height and time. Estimates of FCN concentrations were made using figures 9, 10, 18, 19, 27, 28, 34, 35, 42, 43, 50, 51, 58, and 59. Estimates of the total droplet concentrations were made from figures 11, 20, 29, 36, 44, 52, and 60. Linear correlations were then made between the FCN concentrations and the haze droplet concentrations at these humidities (table 12). The total droplet concentration, 0.5 micrometers, often showed considerable variability probably because the humidity was changing and because droplets were being advected into the measurement area (figs. 11, 20, 29, 36, 44, 52, and 60). The lower end of the droplet concentration range when R.H. was 95% was then chosen for comparisons because the higher concentrations were probably due to droplets which had been advected into the area and not a result of the humidity at the measuring site. The correlation between the FCN and the haze droplets is extremely high (table 12). The correlation with the visibility is not so high. However the visibility values taken here are quite variable and difficult to

interpret from the figures. Nevertheless there does appear to be a correlation. Since the visibility is actually a result of the entire droplet spectrum an integration over the entire spectrum would be necessary in order to produce a valid theoretical visibility. The results here show that the visibility at subsaturation is dependent on the haze droplet concentration and the FCN concentrations.

Correlations with droplet concentrations when the fog was supersaturated are not as good (table 13). However the range of variability is not nearly so great for these droplets or for the nuclei which are associated with them (higher Sc's). The lowest Sc FCN show the most variability (also see figs 3-5) and thus the droplet concentrations which depend on these nuclei (the haze droplet concentrations) display the most variability especially for conditions of less than 100% R.H. The concentrations of total droplets in the supersaturated fogs do not vary over as great a range. However they do vary over a greater range than the CCN concentrations (0.4%) which do not correlate with any droplet concentrations. The concentrations of larger droplets within the fogs depends on a variety of factors including the nuclei. Other factors of importance are the magnitude of the supersaturation and the duration of the supersaturation. However even these factors to some extent depend on the nuclei as has been demonstrated.

7. Summary and Conclusions

Much of the work of this contract was expended in compiling the data; therefore the analysis was somewhat limited. The results presented here although extensive and comprehensive are by no means complete. The development of a technique to determine the level of supersaturation and subsaturation within a fog is quite important for further analysis of this project and for future investigations. The discovery of zones of substantial subsaturation within the fog is quite important for fog physics and for visibility considerations. This means that when subsaturated the haze droplets play a less significant role in electromagnetic propagation. However in supersaturated conditions these small droplets must be considered in visibility reduction.

The second major finding from this effort concerns the conditions at the onset of the fog. The contrast between the fog of Oct. 2-3 and the others is quite apparent in the concentration of the smallest droplets. In all of the other fog events the concentration of all droplets (>0.5 micrometers) shows a gradual increase as the relative humidity increased toward 100%. However this one event is

characterized by the most sudden increase in the concentration of droplets of all sizes including the smallest droplets. This was apparently because of the lack of fog condensation nuclei. FCN concentrations were the lowest for this event. There was no contrast in the relative humidity between this event and others hence the contrast between the droplet distributions is exclusively due to the aerosol. This shows that the aerosol as measured by the CCN-FCN counters can be used to predict the droplet distributions in subsaturated conditions. Thus the CCN-FCN spectra can be used to predict the visibility in subsaturated conditions. It is noticably higher in the conditions where the CCN-FCN concentrations are lower. Otherwise there was not too much contrast in the concentration of FCN between fog events. Therefore Albany did not appear to be the best location to observe microphysical contrasts. Nevertheless the one event of Oct. 2-3 displayed such a contrast with the other fogs that the data is quite worthwhile from this point of view. It is also interesting that since the contrast in CCN concentrations was not great for even this event the results confirm that FCN and not CCN exert exclusive influence on fog and haze droplet concentrations.

The crude estimates of droplet growth were quite good. These should now be expanded upon by using more exact equations which among other factors include the effect of the nuclei on droplet growth. These efforts should be combined with the meteorological data--temperature and wind so that growth for specific parcels of air can be realistically calculated and compared with the droplet measurements. The fact that super/subsaturation levels can be measured allows this to be done for a large number of cases in a variety of conditions of super and subsaturation. This will yield a much greater understanding of fog physics and how the supersaturations and subsaturations are generated. An important observation which needs further analysis which has not yet been possible is the bimodal droplet distribution (two modes beyond dc) which was often observed (see appendix). Most of the time there was another supersaturation (below Seff) which seems to be related to the larger droplets (see appendix). This needs further exploration because it may be more important than the Seff which has been measured. The relationship with humidity and visibility needs to be done in more detail. This report has suggested that important relationships exist. A complete calculation of visibility needs to be made from the droplet distributions. The potential visibility based upon the nuclei distributions should also be calculated. This would allow many valid comparisons between predicted visibility and actual measured visibility. The predictions should also be extended to earlier times with respect to the fog events.

Quite often the nuclei spectrum did not extend to low

enough supersaturations to intersect with the droplet distributions. This is especially true for the bimodal distributions described above. This limitation has made it impossible to determine the level of supersaturation when it was very low (< 0.02%). This was quite often the case as can be seen from the appendix. In such cases it is impossible to even tell whether the fog was supersaturated at all. Hence it would be desirable to extend the nuclei distributions to lower Sc's (larger sizes).

Since the technique to determine subsaturation concerns the small end of the droplet spectrum it is apparent that an extension of these measurements to lower sizes would be valuable. This would allow more accuracy and an extension of the range of measurements. It would be good to be able to measure such small droplets and nuclei that the indicated subsaturation would be identical over a range of sizes. This should be possible if the nuclei and droplet spectra were extended to smaller sizes. This would allow a much higher level of certainty in estimating the subsaturation. Fortunately instruments are now available to make such measurements. A more detailed CCN-FCN spectrum would be desirable. A faster time response would be valuable to determine if the aerosol is as homogeneously distributed as it appears from these measurements. Interstitial measurements (Hudson and Rogers, 1986) over short time intervals would be valuable in making direct associations between nuclei and droplet spectra.

Further analysis is needed to determine if the nuclei concentration indeed has an effect on the fog supersaturation as is indicated in this preliminary analysis. Further work is needed to produce a model of the potential visibility impact of the measured FCN spectra under supersaturated conditions.

References

Fitzgerald, James W., 1975: Approximation formulas for the equilibrum size of an aerosol particle as a function of its dry size and composition and the ambient relative humidity. J. Appl. Meteor., 14, 1044-1049.

Hudson, James G. and P. Squires, 1976: An improved continuous flow diffusion cloud chamber. J. Appl. Meteorl., 15, 776-782.

Hudson, James G., 1980: Relationship between fog condensation nuclei and fog microstructure. J. Atmos. Sci., 37, 1854-1867.

Hudson, James G., 1984: CCN measurements within clouds. J. Climat. Appl. Meteor., 23, 42-51.

Hudson, James G. and C.F. Rogers, 1986: Relationship between critical supersaturation and cloud droplet size: Implications for cloud mixing processes. J. Atmos. Sci., 43, 2341-2359.

Meyer, M. B., J.E. Jiusto and G.G. Lala, 1980: Measurements of visual range and radiation-fog (haze) microphysics. J. Atmos. Sci., 37, 622-629.

Noonkester, R.V., 1984: Droplet spectra observed in marine stratus cloud layers. J. Atmos. Sci., 41, 829-845.

Sept. 30, 1982

start Time	N/cm3	Seff
06:30	14	0.028
06:40	26	0.035
07:10	20	0.031
07:20	20	0.028

Table 1

Oct. 1, 1982

start Time	N/cm3	Sc(%)
01:20	60	0.029
02:10	70	0.037
02:50	80	0.039
03:00	70	0.035
04:20	40	0.031
04:30	45	0.037
05:10	95	0.037
05:20	50	0.028
05:50	100	0.037
06:00	45	0.028
06:10	80	0.037
06:40	20	0.024
07:00	15	0.020
07:10	13	0.023
07:30	25	0.028
07:50	45	0.035
08:00	20	0.028
08:10	15	0.028
08:20	18	0.028

Table 2

Oct. 3. 1982

start Time	N/cm3	Sc(%)
01:30	22	0.037
01:40	82	0.067
01:50	51	0.054
02:00	71	0.061
02:10	70	0.056
02:20	60	0.047
02:30	50	0.040
02:40	50	0.047
02:50	80	0.052
03:00	50	0.044
03:10		
03:20	60	0.056
04:30	180	0.110
05:00	60	0.064
05:10	210	0.120
05:20	72	0.067
05:30	120	0.093
05:40	130	0.083
05:50	140	0.083
06:00	120	0.078
06:10	90	0.067
06:20	68	0.064
06:30	76	0.067
06:40	90	0.070
06:50	100	0.064
07:00	70	0.056
07:10	100	0.067
07:20	110	0.070
07:30	90	0.070
07:40	80	0.070
07:50	70	0.070
08:00	50	0.044
08:10	50	0.035

Table 3

Oct. 5, 1982

start Time	N/cm3	Sc(%)
02:20	18	0.038
02:30	6	0.033
03:20	4	0.033
04:30	17	0.038
04:40	125	0.100
04:50	85	0.093
05:00	55	0.070
05:10	52	0.067
05:20	52	0.067
05:30	110	0.093
05:40	52	0.070
05:50	52	0.070
06:00	70	0.078
06:10	54	0.064
06:20	59	0.074
06:30	110	0.087
06:40	51	0.078
06:50	57	0.078
07:00	70	0.078
07:10	55	0.070
07:20	40	0.056
07:30	7	0.035

Table 4

Oct. 5-6, 1982

start Time	N/cm3	Sc(%)
21:00	130	0.038
21:10	45	0.033
21:20	20	0.026
21:30	20	0.028
21:40	20	0.025
21:50	20	0.023
22:00	20	0.021
22:10	20	0.023
22:20	20	0.019
22:30	19	0.020
22:40	19	0.019
22:50	19	0.018
23:00	20	0.020
23:10	40	0.029
23:20	45	0.034
23:30	20	0.020
23:40	27	0.030
23:50	15	0.027
01:20	38	0.035
01:30	40	0.035
03:40	22	0.020

Table 5

Oct. 11, 1982

start Time	N(cm/3)	Sc(%)
01:10	37	0.042
01:20		
01:30		
01:40		
01:50	48	0.041
02:00	15	0.028
02:10	125	0.078
02:20	52	0.044
02:30	34	0.038
02:40	80	0.064
02:50	65	0.064
03:00	12	0.033
03:10	90	0.093
03:20	190	0.130
03:30	160	0.120
03:40	215	0.130
03:50	38	0.047
04:00	70	0.070
04:10	27	0.038
04:20	4	0.023
04:30	25	0.040
04:40	53	0.056
04:50	11	0.035
05:00		
05:10		
05:20	70	
05:30	28	0.040
05:40	52	0.047
05:50	22	0.037
06:00	37	0.037

Table 6

Oct. 14, 1982

start Time	N/cm3	Sc(%)
01:40	350	0.160
01:50	200	0.082
02:10	42	0.035
02:40	62	0.035
02:50	130	0.056
03:00	215	0.130
03:10	85	0.061
03:20	71	0.037
03:30	170	0.074
03:40	95	0.064
03:50	180	0.078
04:00	180	0.082
04:10	55	0.064
04:20	125	0.082
04:30	140	0.120
04:40	115	0.082
04:50		
05:00	170	0.120
05:10	160	0.082
05:20	190	0.130
05:30	150	0.110
05:40	90	0.078
05:50	78	0.064
06:00	140	0.080
06:10	160	0.110
06:20	43	0.050
06:30	75	0.061
06:40	27	0.040

Table 7

Oct. 25, 1982

start Time	N/cm3	Sc(%)
01:10	16	0.035
05:00	50	0.038
05:10	90	0.047
06:20	11	0.031
06:30	30	0.035
06:40	45	0.036
06:50	125	0.044
07:00	130	0.044
07:10	54	0.037
07:20	80	0.038
07:30	70	0.035

Table 8

Oct. 27, 1982

start Time	N/cm3	Sc(%)
06:40	140	0.047
06:50	60	0.036
07:10	11	0.033
07:30	39	0.035
07:50	60	0.036
08:00	140	0.047
08:10	85	0.038
08:20	35	0.035
08:30	7	0.020

Table 9

Oct. 28, 1982

start Time	N/cm3	Sc(%)
01:10	2	0.038
02:00	0.1	0.034
03:00	3	0.044

Table 10

Comparison of those fog events with complete data

Only for times when the R.H. was 95%

Date	Time	concentrations for Sc's in % .02	.03	.04	.12	.40	drop(>0.5mm)	Vis(km)	(1/V)1/2
Sept. 30	20-23	20	35	80	100	900	20-100	5-15	0.32
Oct. 2	22-01	1	3	20	110	800	1+	35-55	0.15
Oct. 4	01-03	2	4	35	150	900	2-100	5-30	0.24
Oct. 10	21-23	3	5	40	160	-	3-100	5-50	0.19
Oct. 24	04-08	3	8	80	400	-	10-500	0-10	0.45
Oct. 26	02-05	8	12	100	500	-	10- 40	5-25	0.26
Oct. 27	21-08	11	30	110	600	-	20-200	3-10	0.39

Table 11

Correlations between FCN and haze droplets/Visibility

95% R.H. from table 11

FCN(y) Sc	other(x)	No. cases	y intercept	slope	cor. coef.	conf. level
0.02%	drop(>0.5)	7	2.2	1.0	0.88	2%
0.03%	drop(>0.5)	7	1.2	0.58	0.95	0.5%
0.02%	(1/V)1/2	7	24	0.57	0.36	26%
0.03%	(1/V)1/2	7	22	0.41	0.50	20%

Table 12

Correlations between CCN-FCN concentrations and droplets during supersaturated conditions

CCN -FCN Sc	Drops min size	No. cases	y intercept	slope	cor.coef.	conf. level
0.4	0.5	11	251	5.1	0.59	4%
0.12	0.5	11	223	0.30	0.75	1%
0.4	2.0	11	217	-2.9	-0.46	
0.12	2.0	11	204	-0.1	-0.34	

Table 13

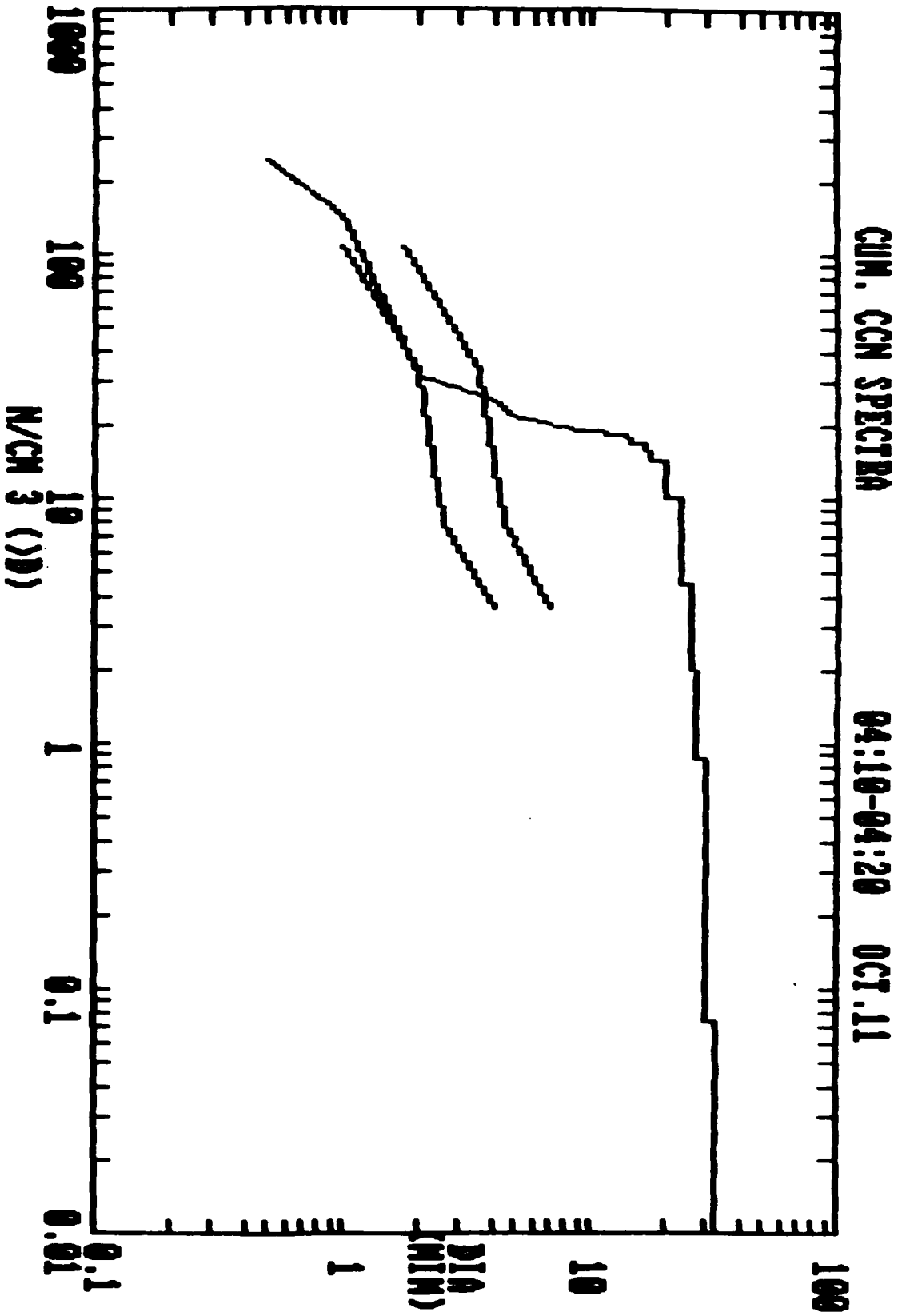

Fig. 1. An example of a CCN-FCN spectrum and a simultaneous droplet spectrum. The nucleus spectrum is displayed as two parallel lines. The line to the left is the d(0) line which is the concentration as a function of the equilibrium size at 100% R.H. The other nucleus line to the right is just a change of the sizes of the first line by multiplying by the square root of 3. These are the critical sizes of the nuclei. All of these lines are cumulative distributions--that is they represent concentrations greater than the designated sizes. The intersection of the critical line with the droplet spectrum determines Seff. This example shows a well explained droplet spectrum where the small haze droplets are the proper size for a supersaturated condition.

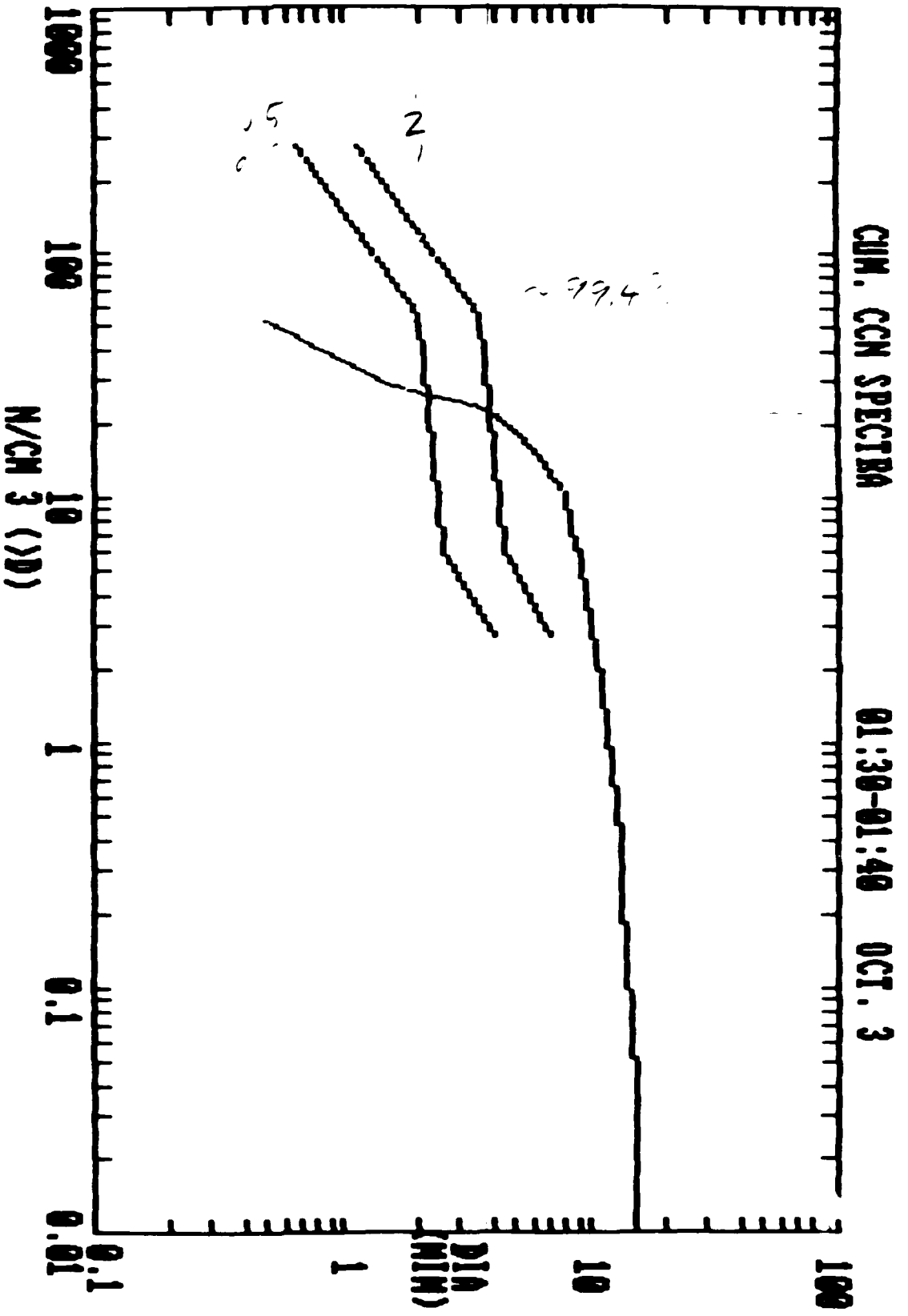

Fig. 2. Like figure 1 but the small droplets appear to be missing because the droplet line is to the left of the d(0) line at the small sizes. Therefore there appears to be an inconsistency between the small and large end of the spectrum.

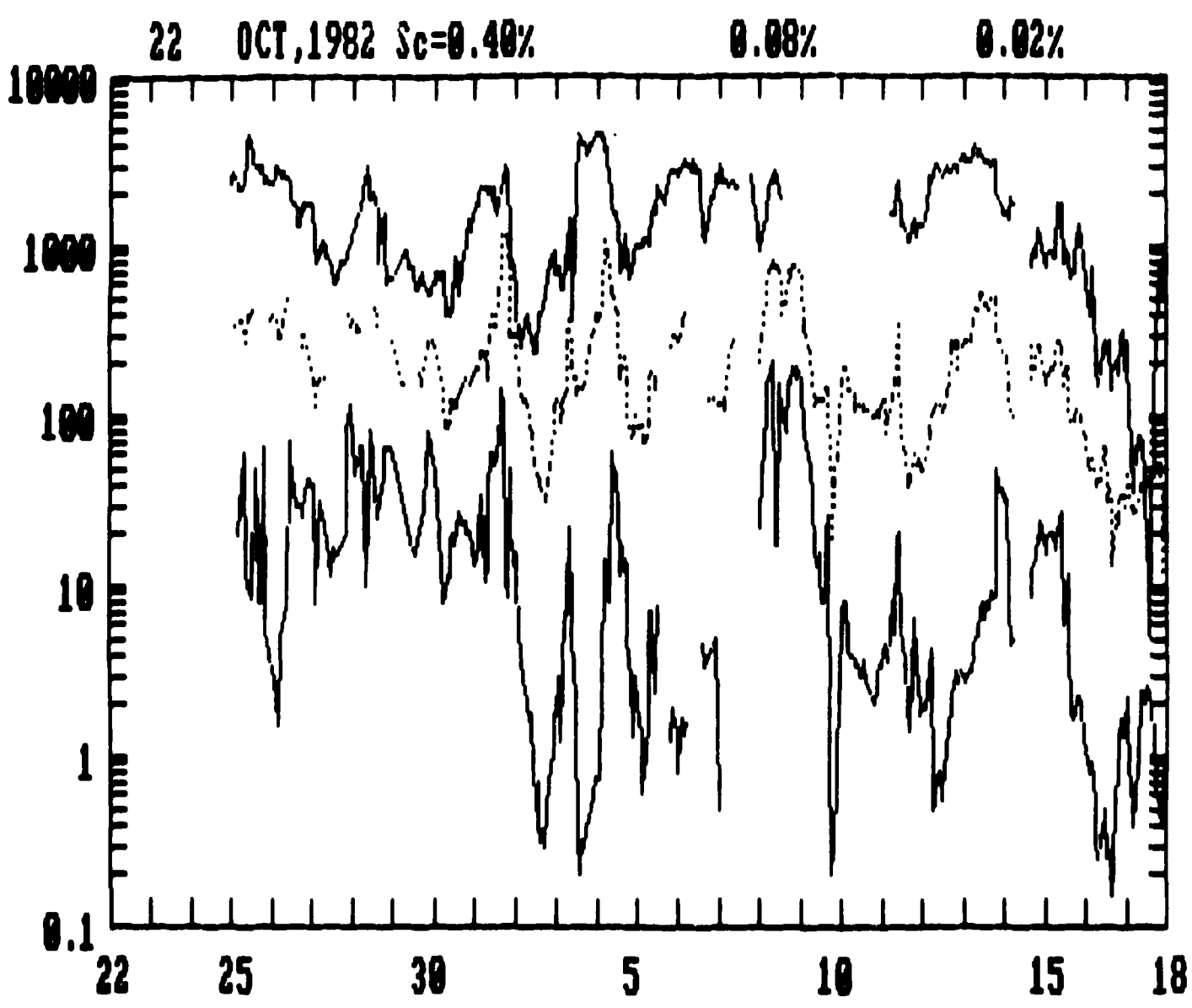

Fig. 3. CCN and FCN concentrations as a function of time from Sept. 22 to Oct. 18, 1982 at Albany.

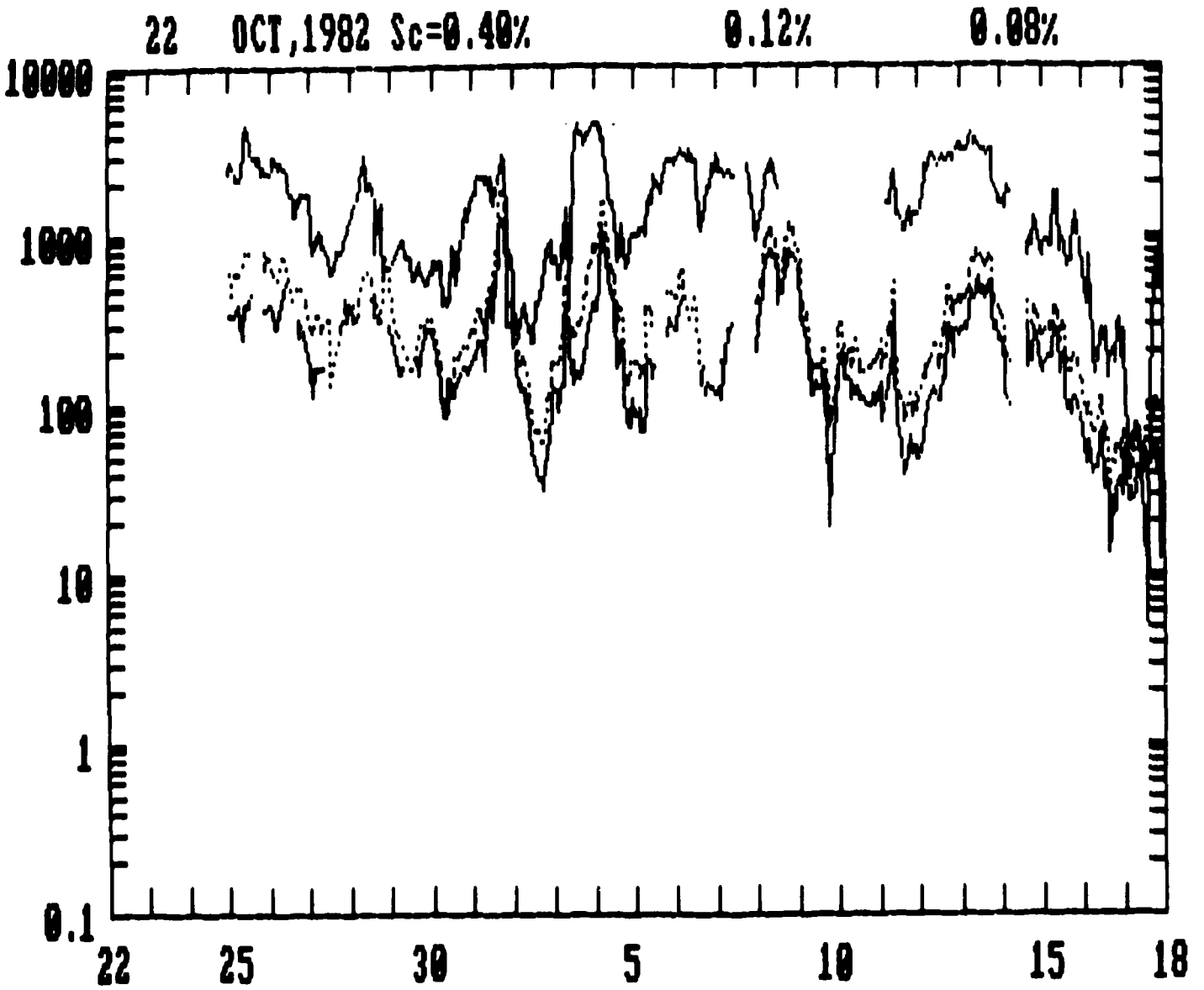

Fig. 4. Like fig. 2.

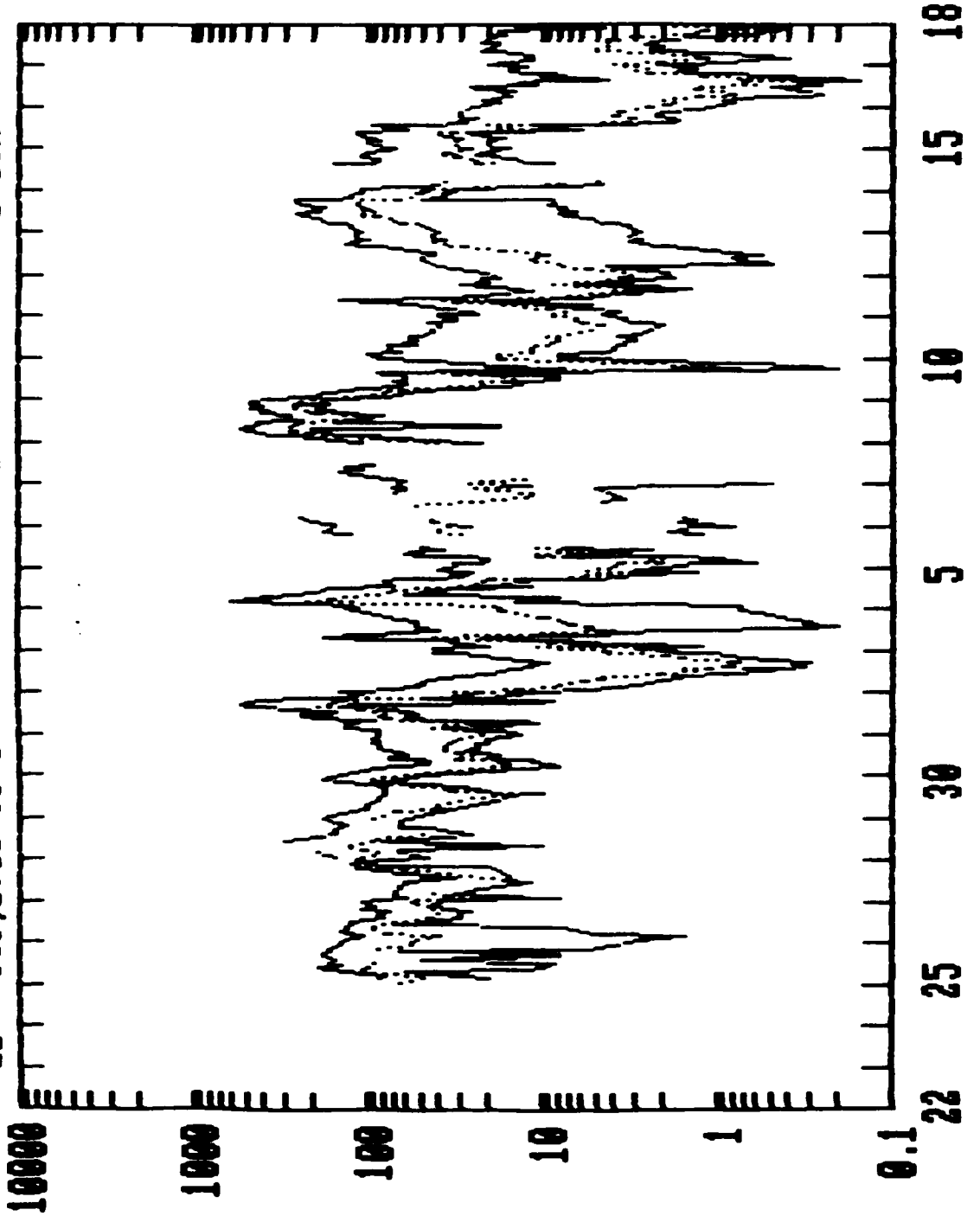

Fig. 5. Like fig. 2.

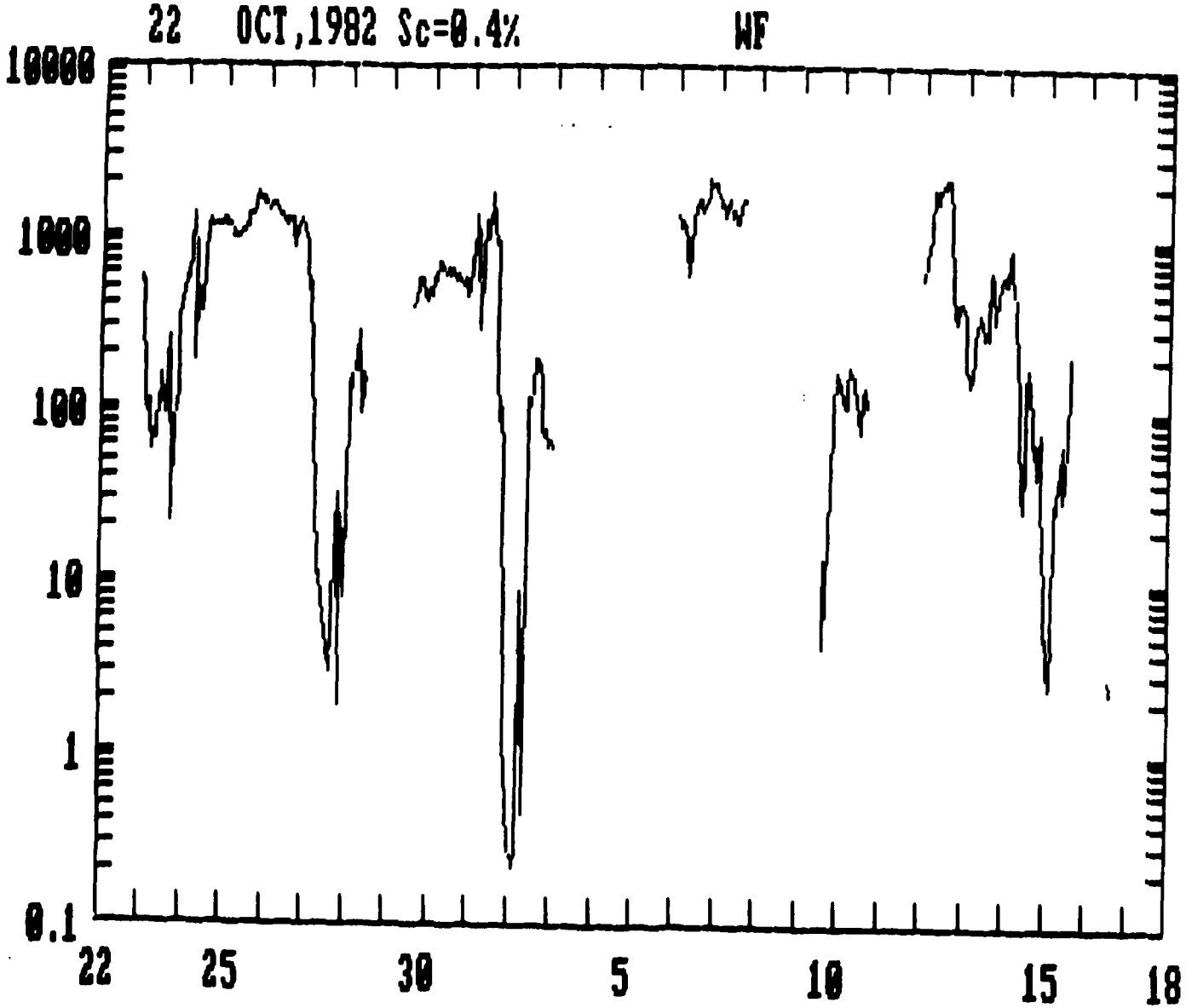

Fig. 6. Like fig. 2 except that the site of the measurements is Whiteface Mountain, N. Y.

B)

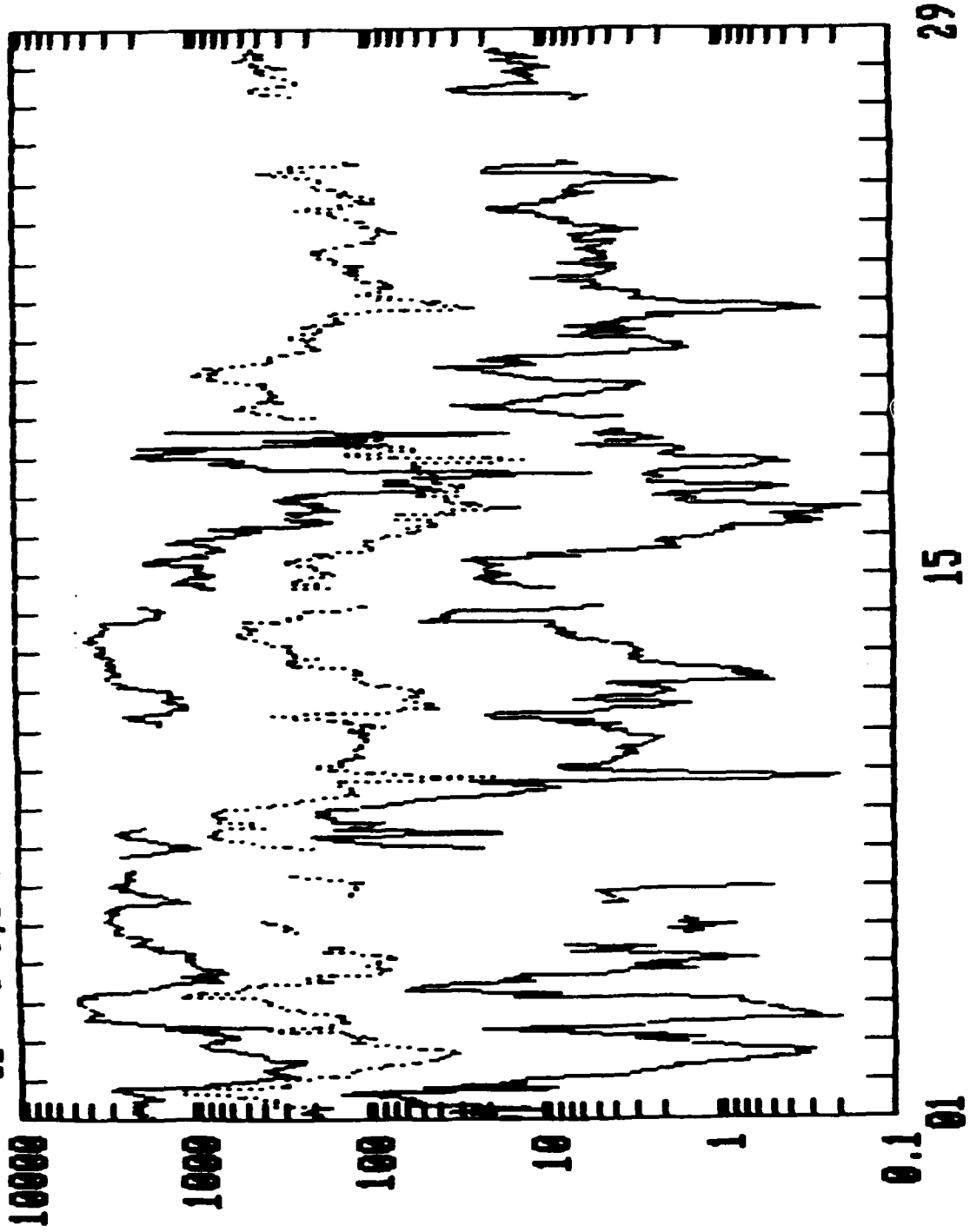

Fig. 7. Further CCN-FCN climatology at Albany.

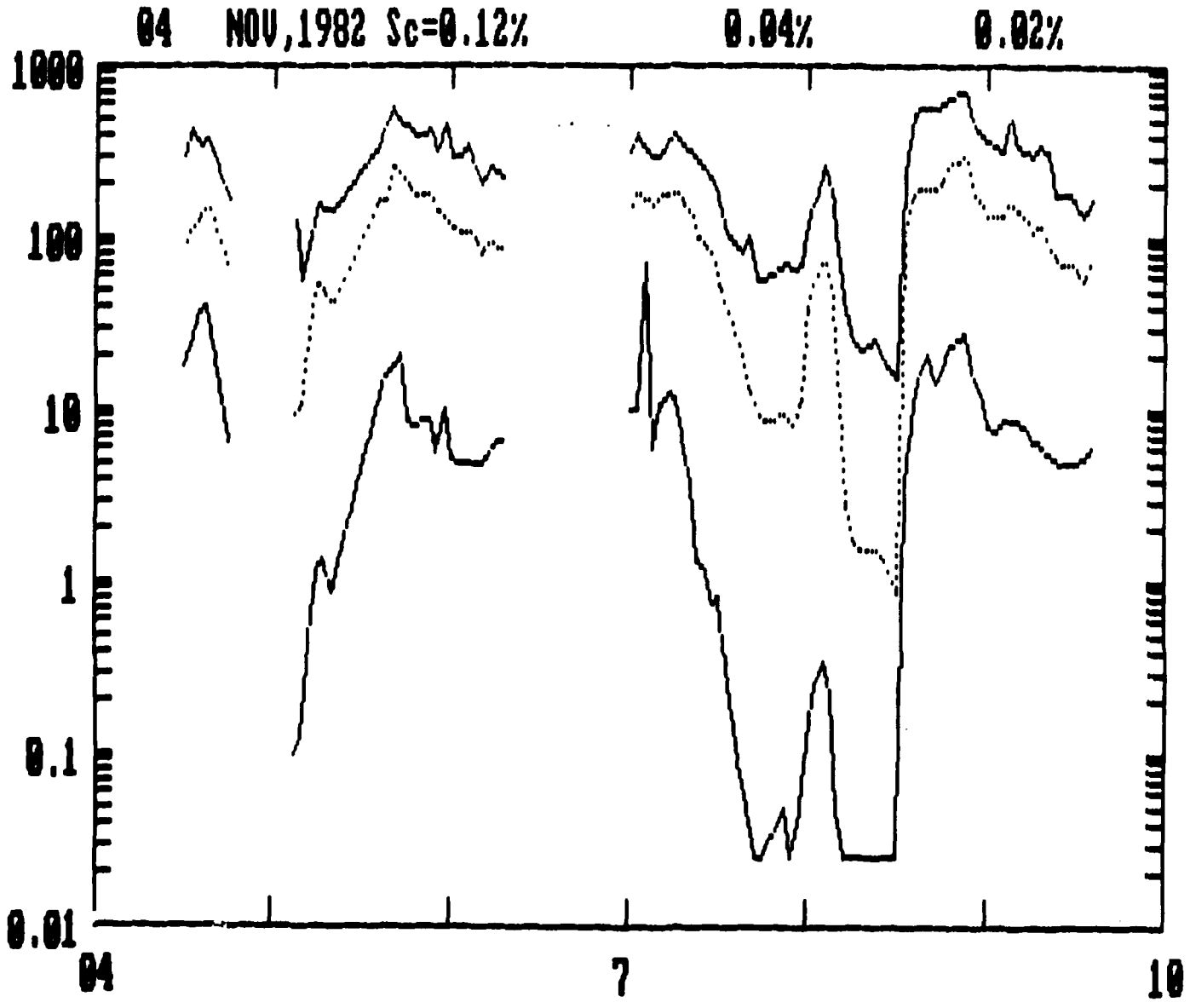

Fig. 8. Further CCN-FCN climatology at Albany.

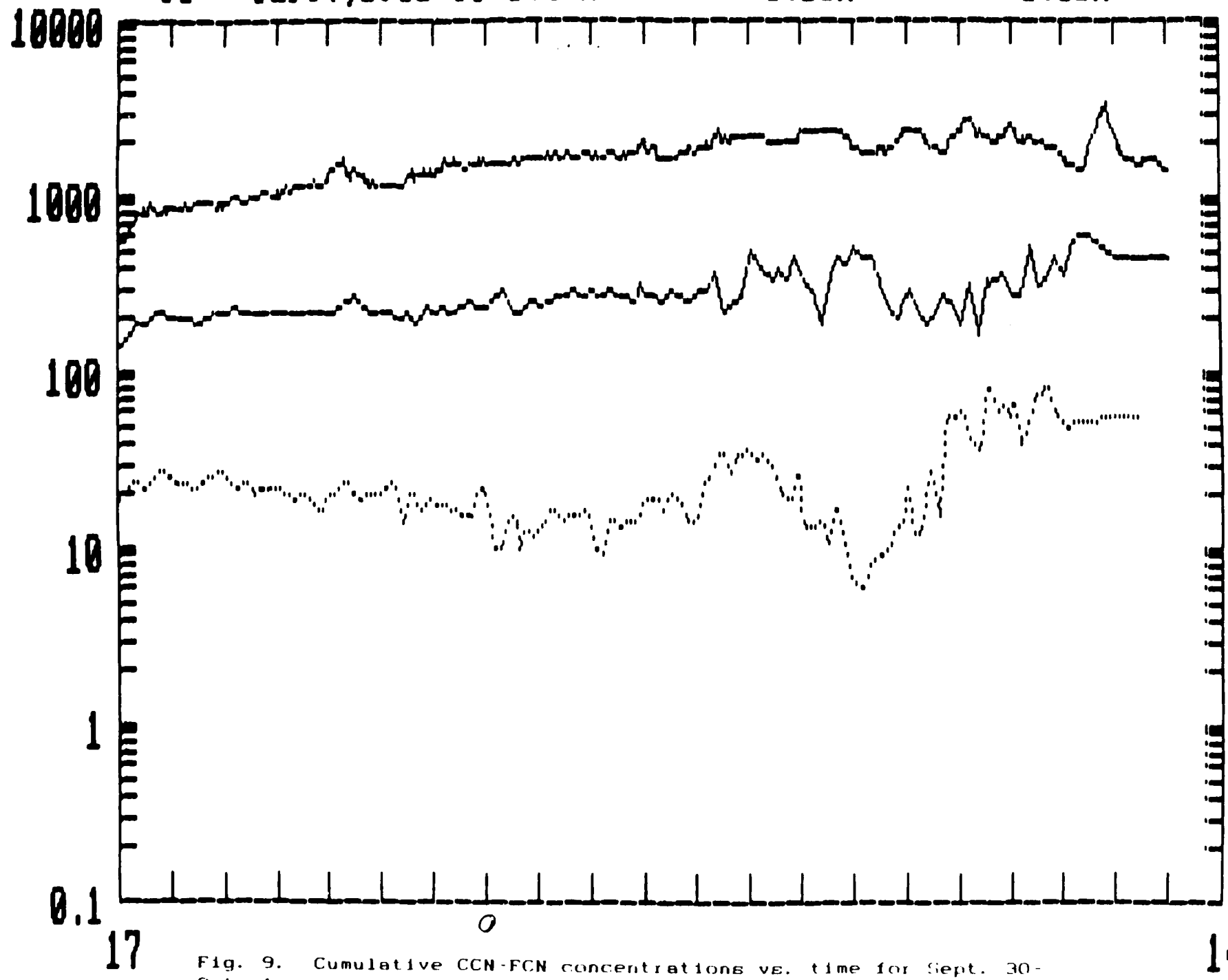

Fig. 9. Cumulative CCN-FCN concentrations vs. time for Sept. 30-Oct. 1.

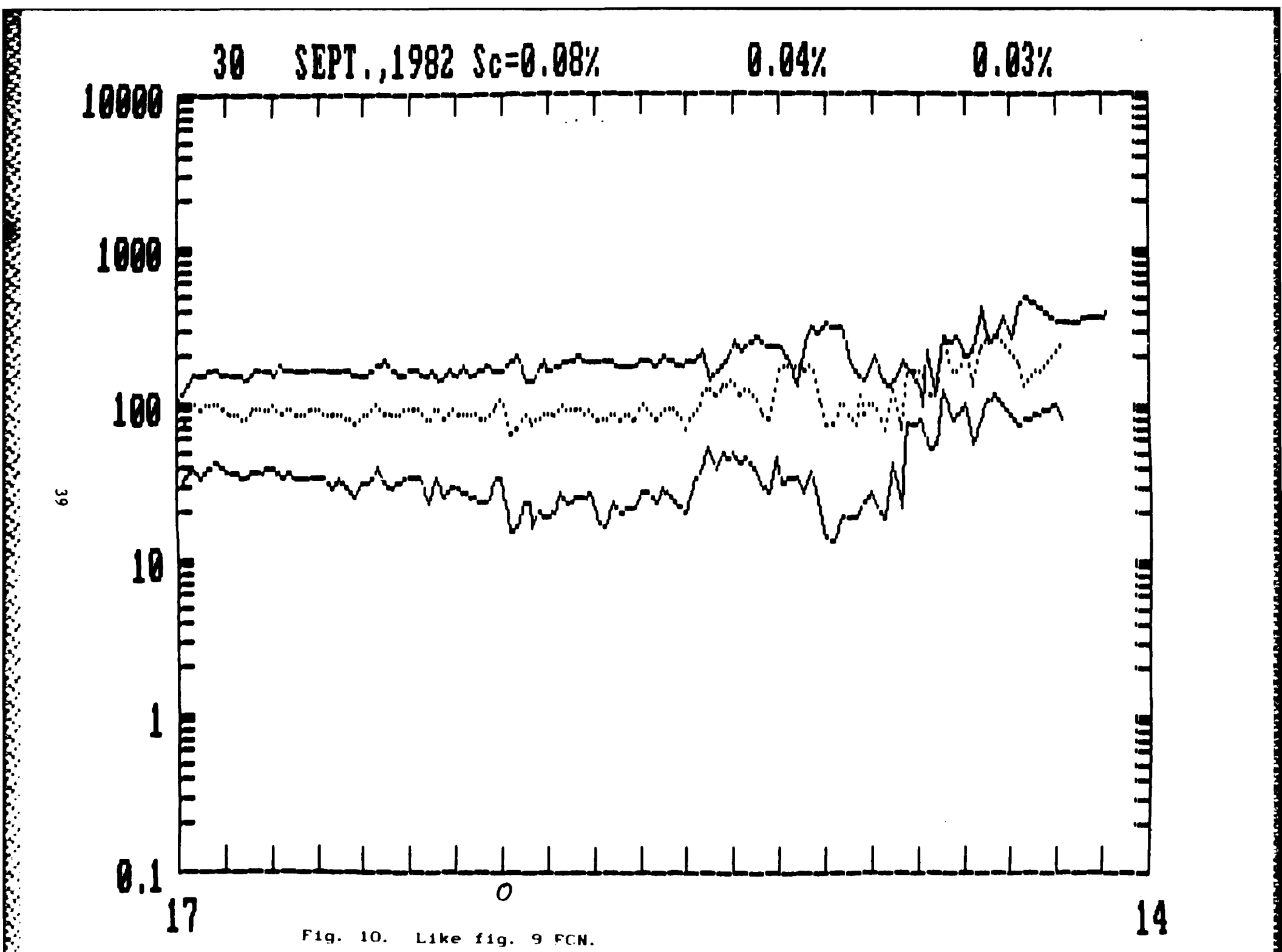

Fig. 10. Like fig. 9 FCN.

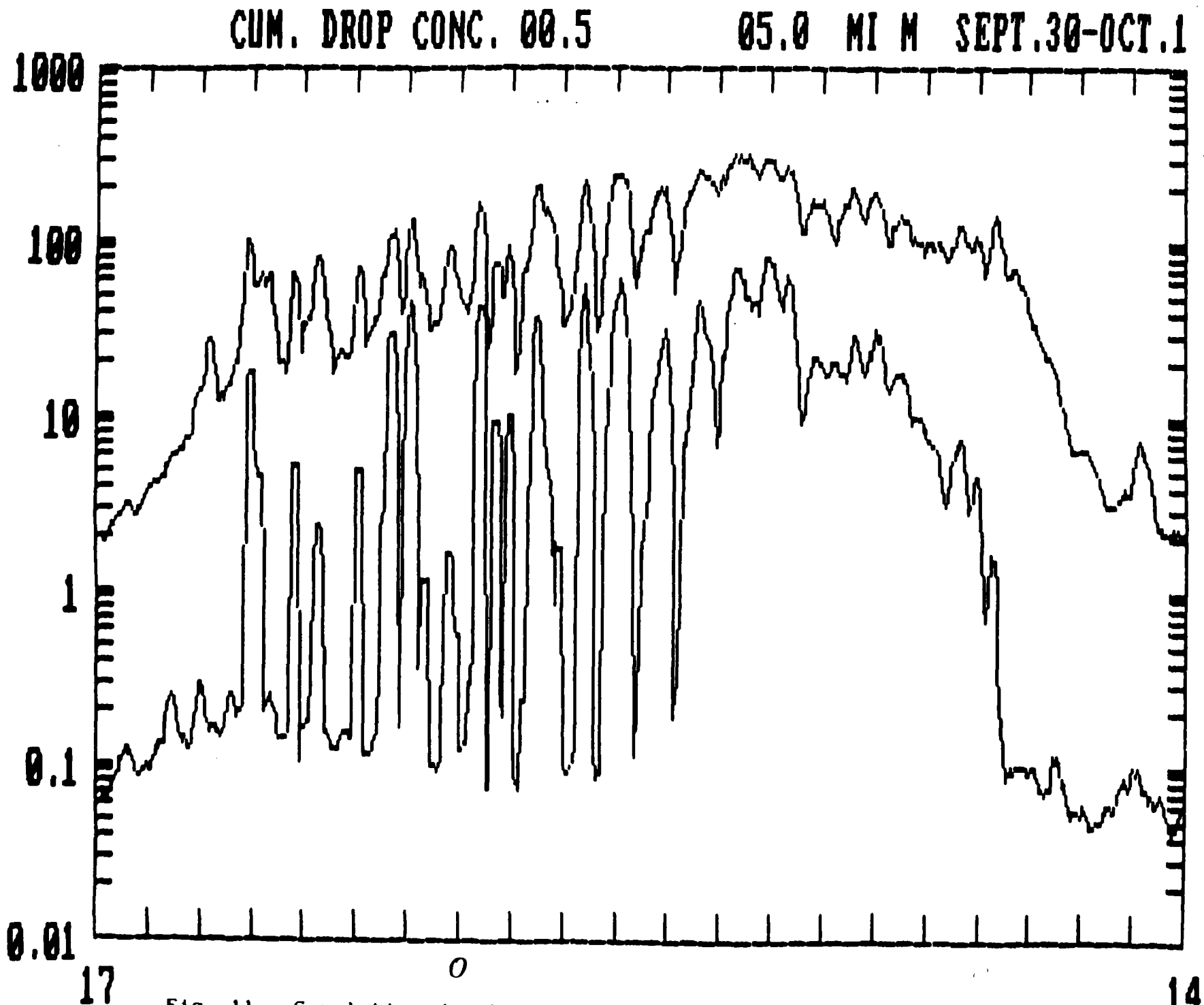

Fig. 11. Cumulative droplet concentrations vs. time for Sept. 30-Oct. 1.

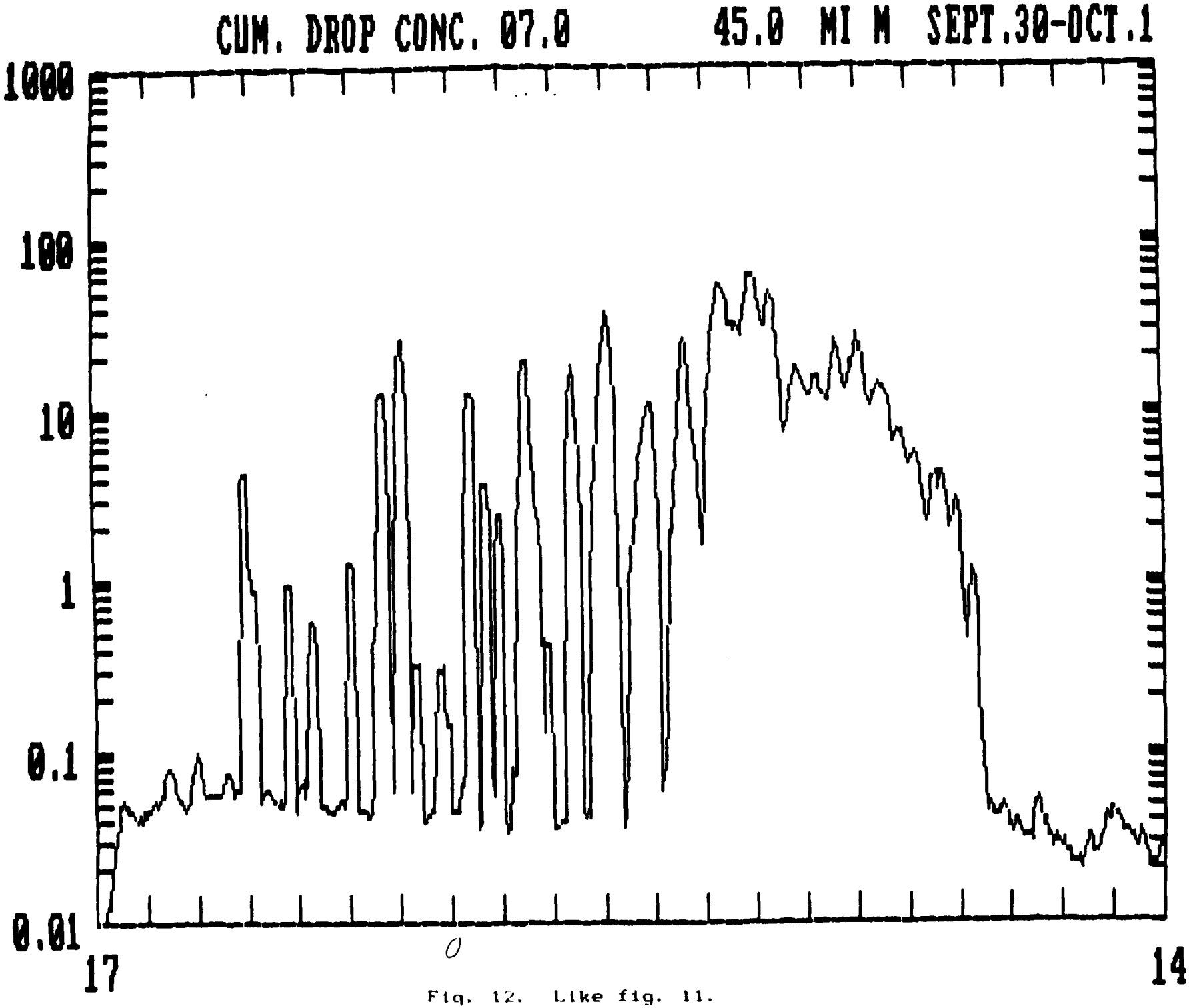

Fig. 12. Like fig. 11.

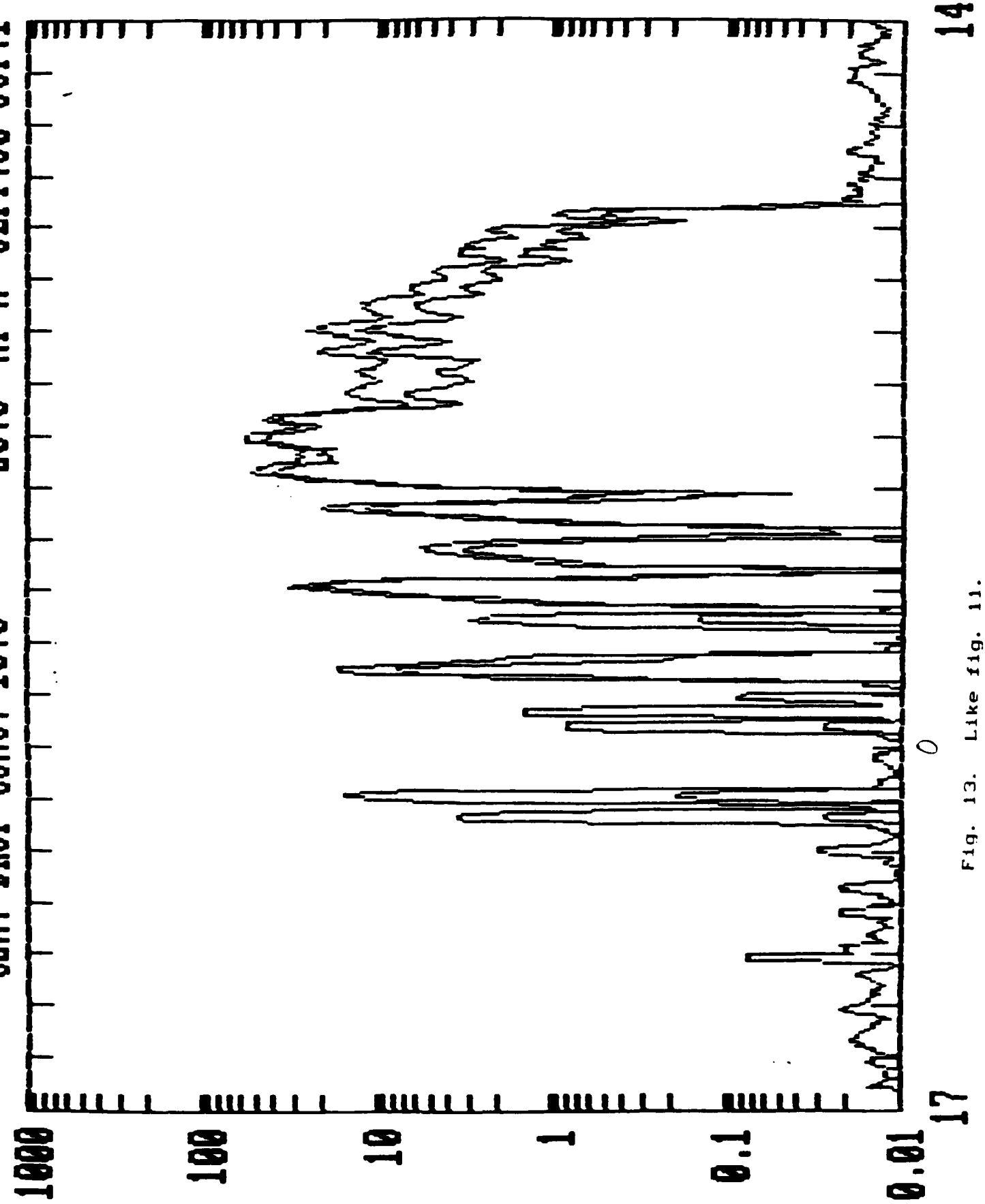

Fig. 13. Like fig. 11.

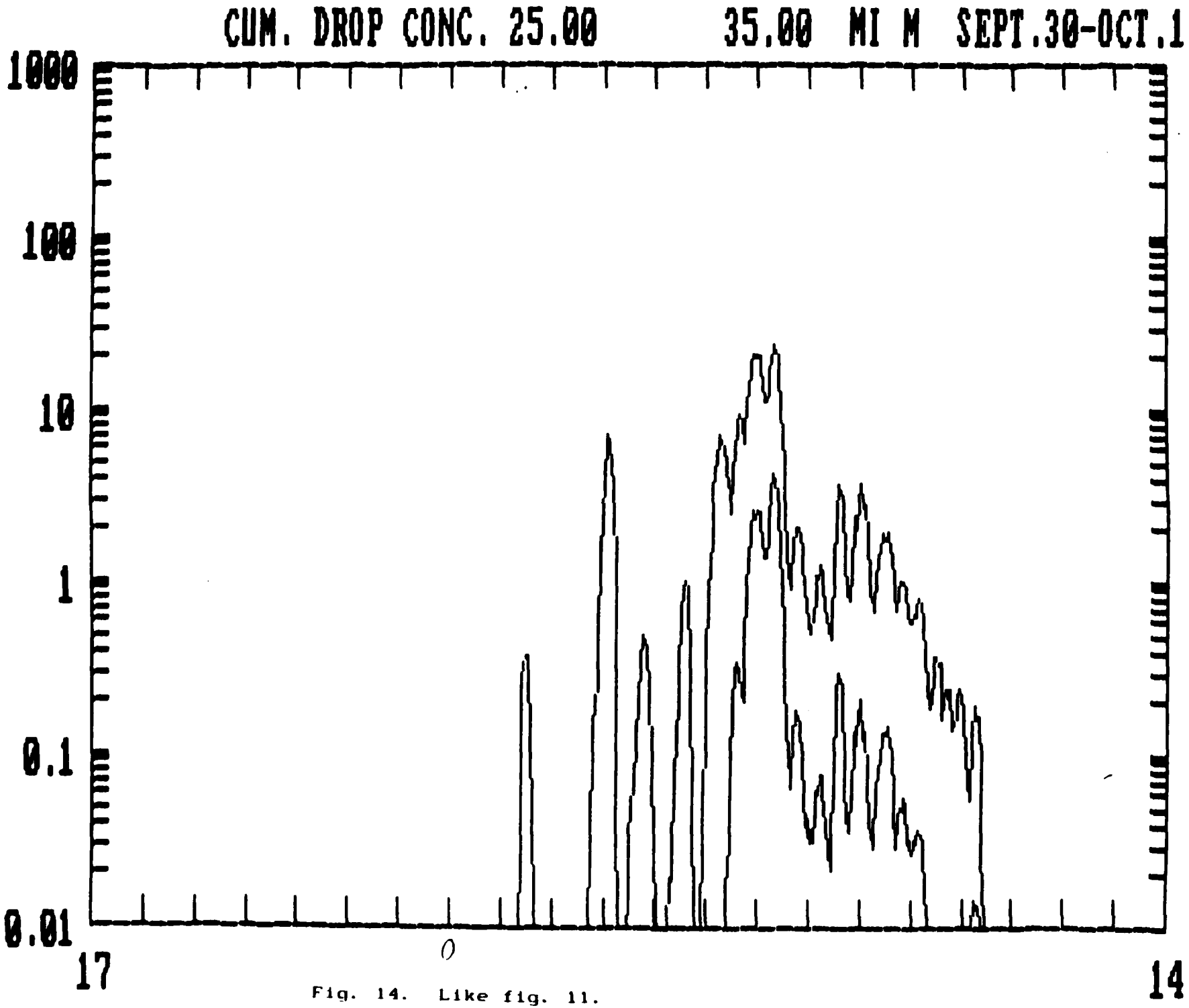

Fig. 14. Like fig. 11.

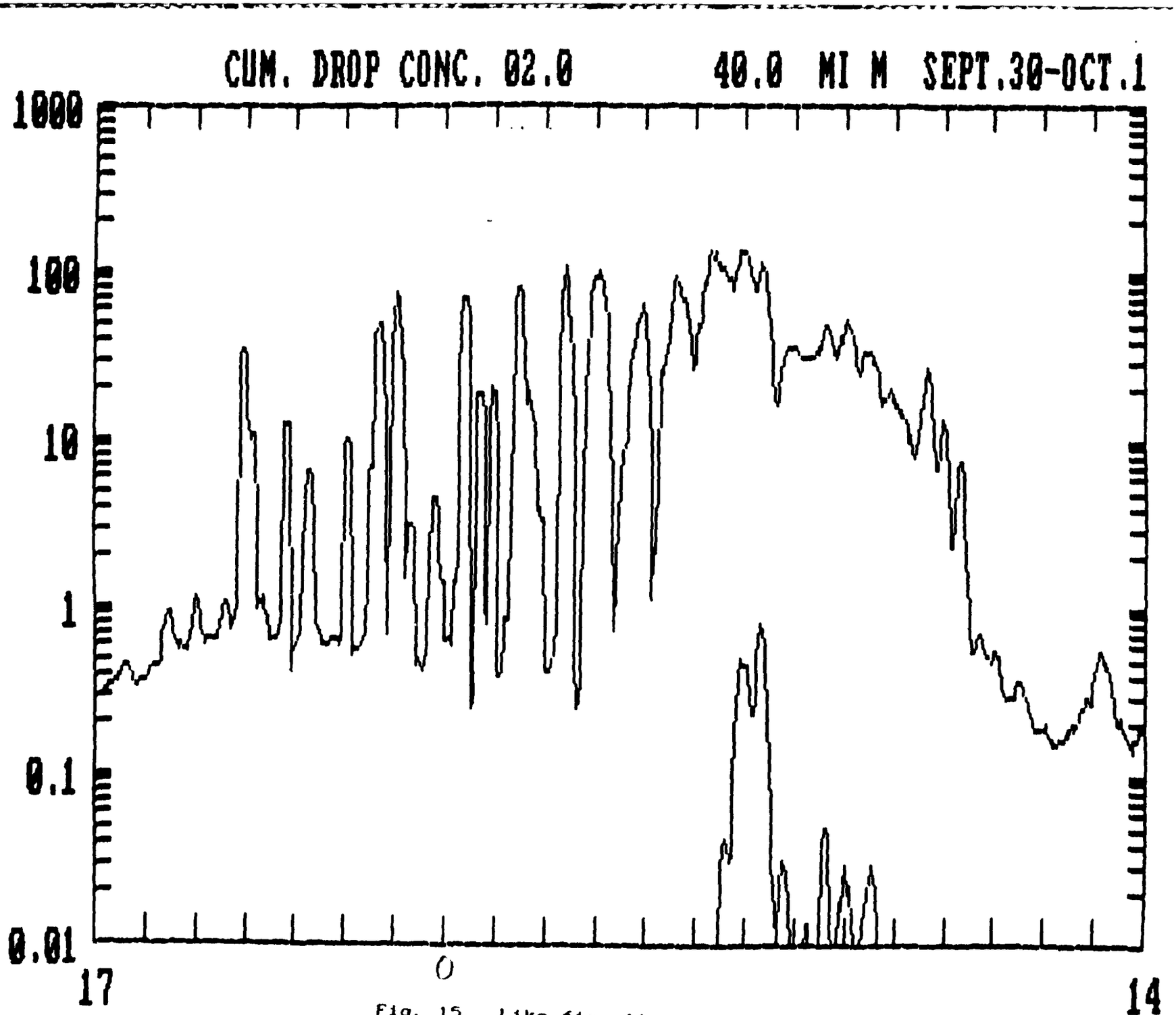

Fig. 15. Like fig. 11.

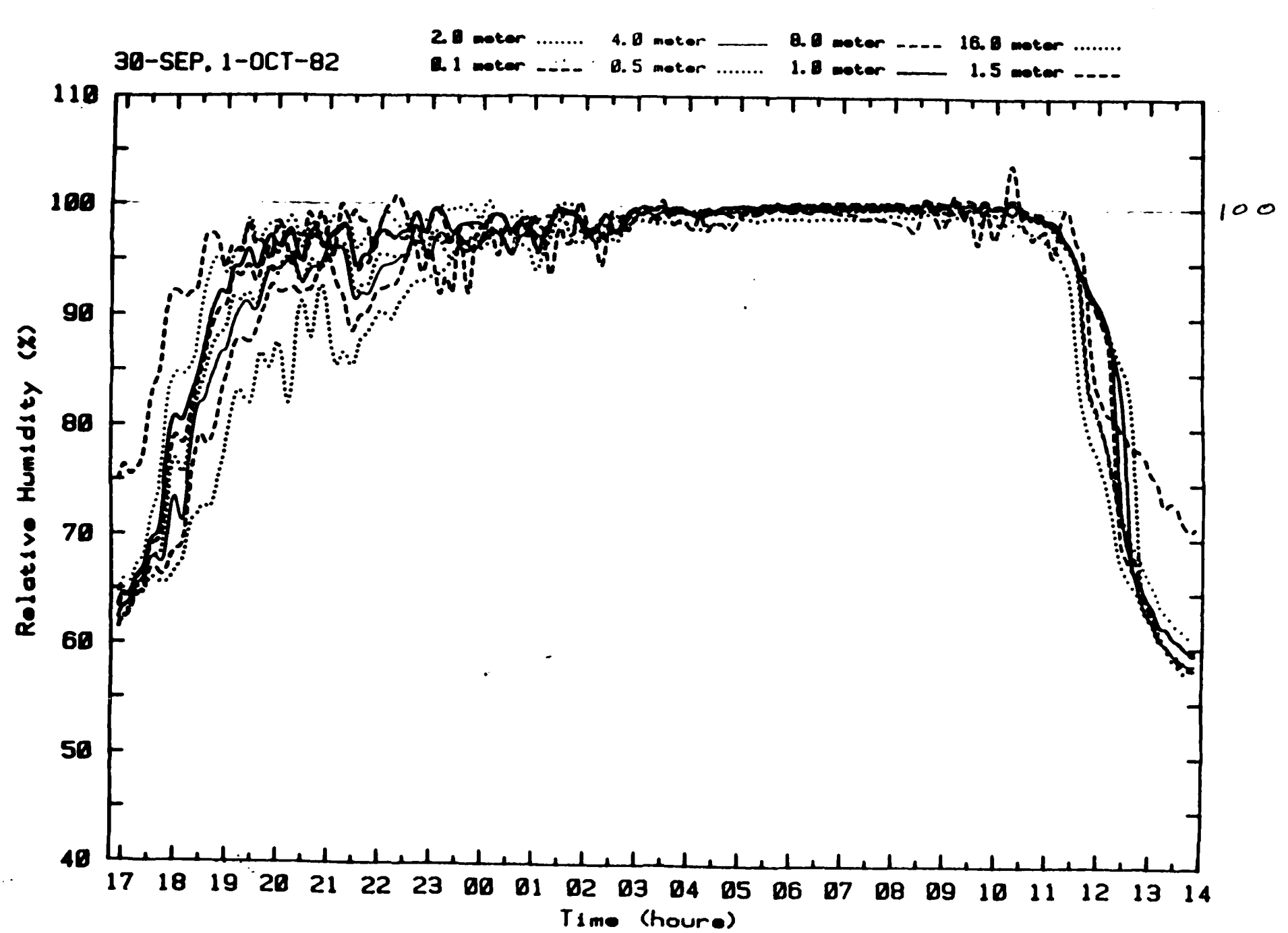

Fig. 16. Relative humidity vs. time for Sept. 30-Oct. 1.

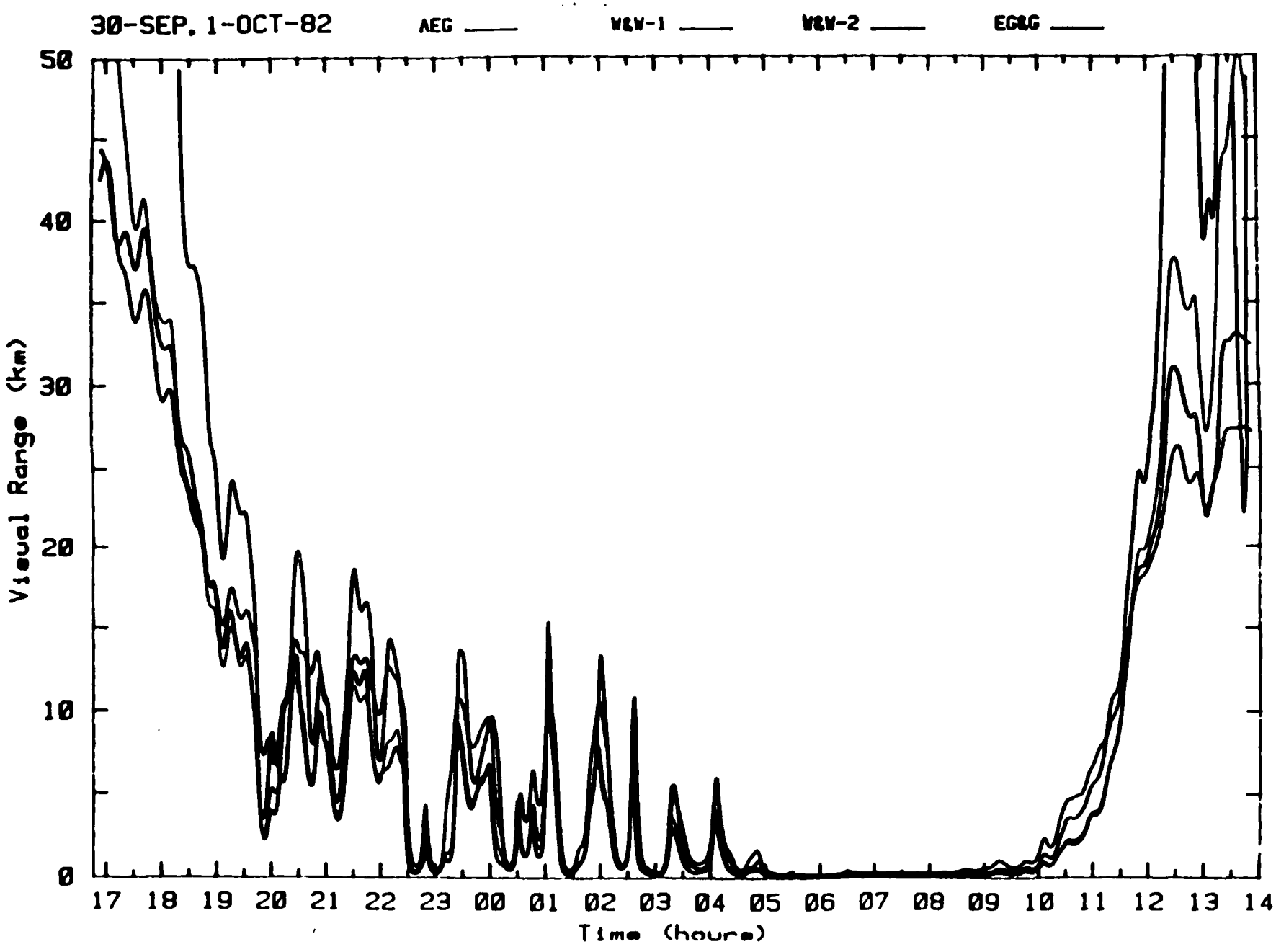

Fig. 17. Visibility vs. time for Sept. 30-Oct. 1.

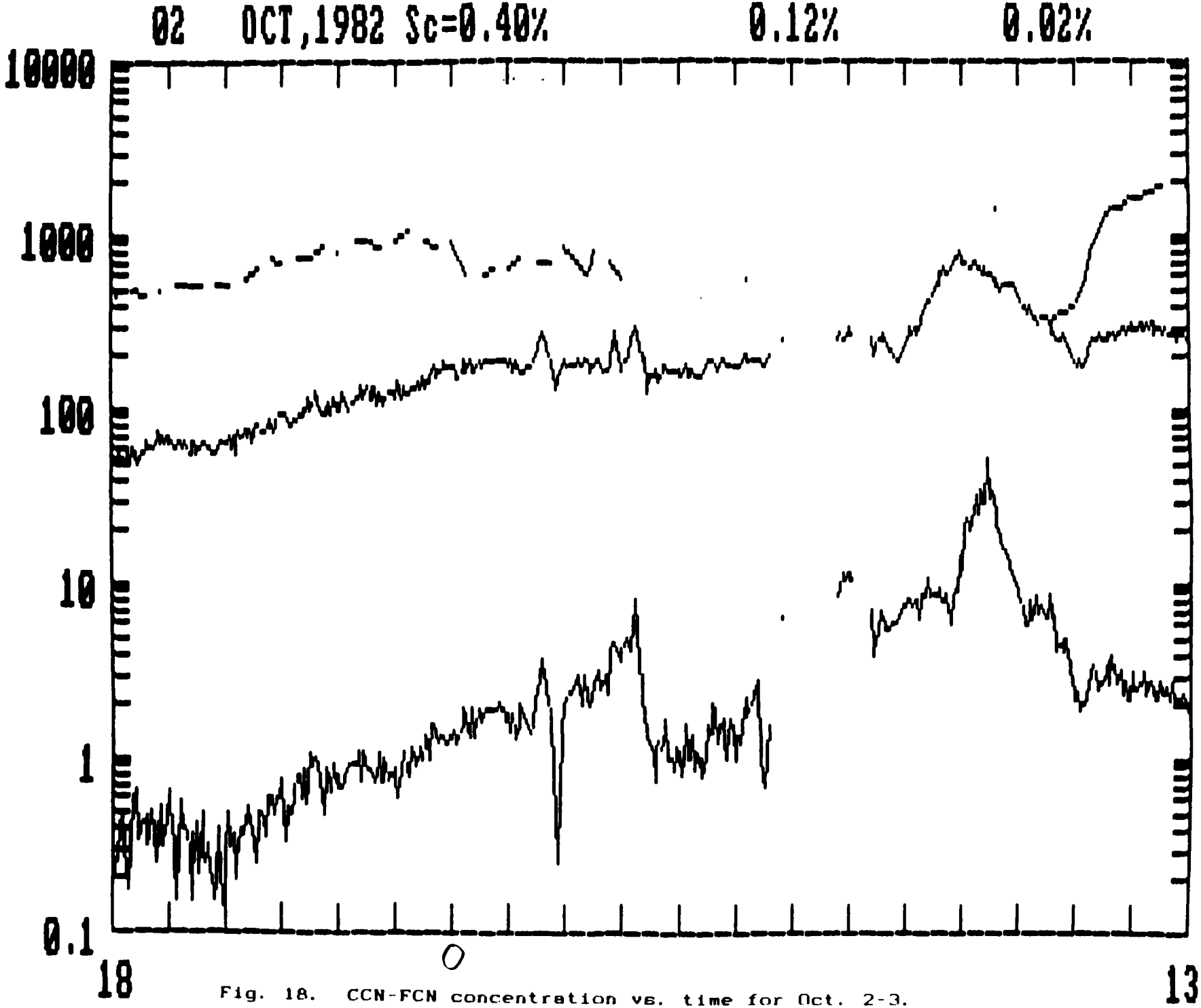

Fig. 18. CCN-FCN concentration vs. time for Oct. 2-3.

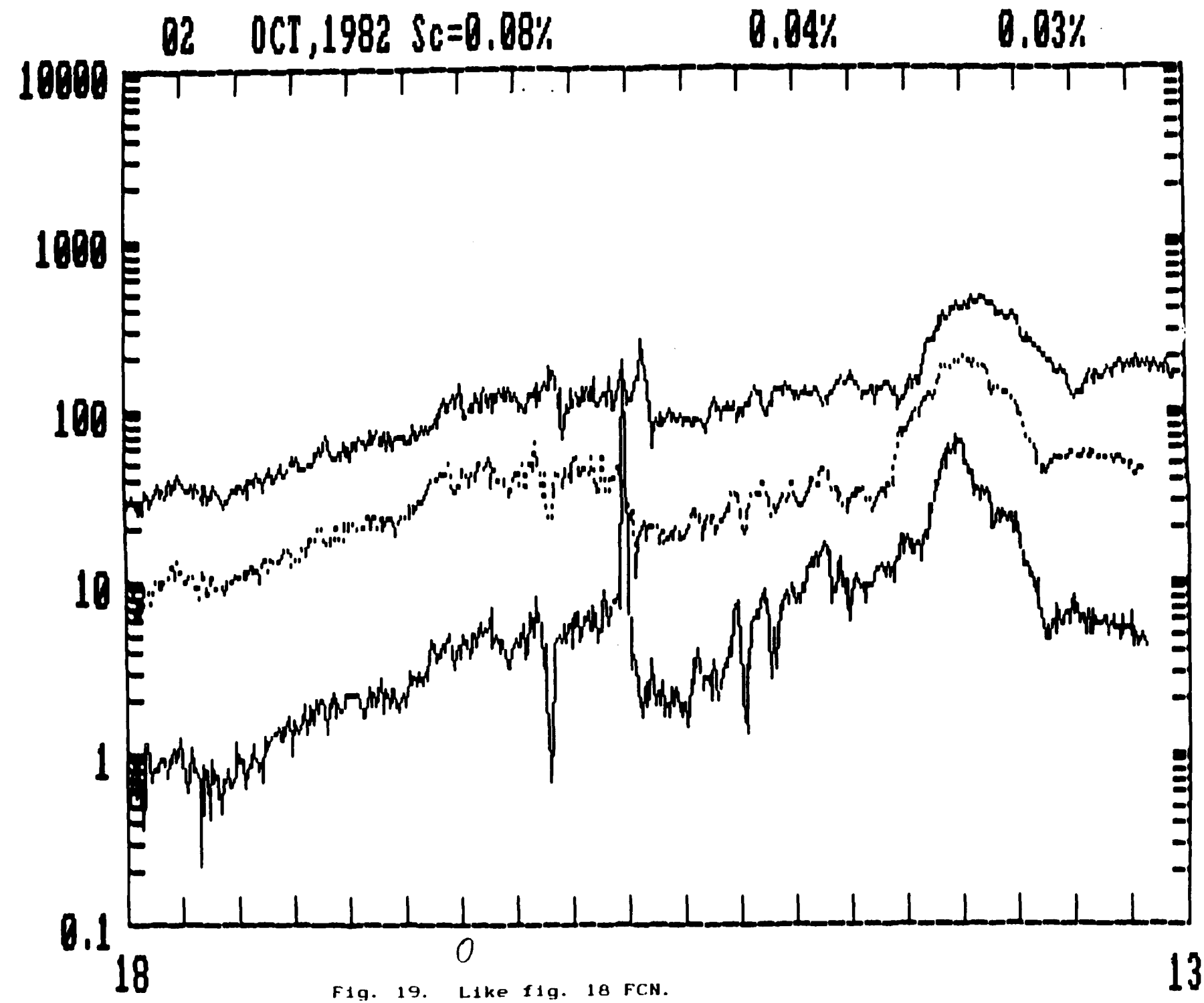

Fig. 19. Like fig. 18 FCN.

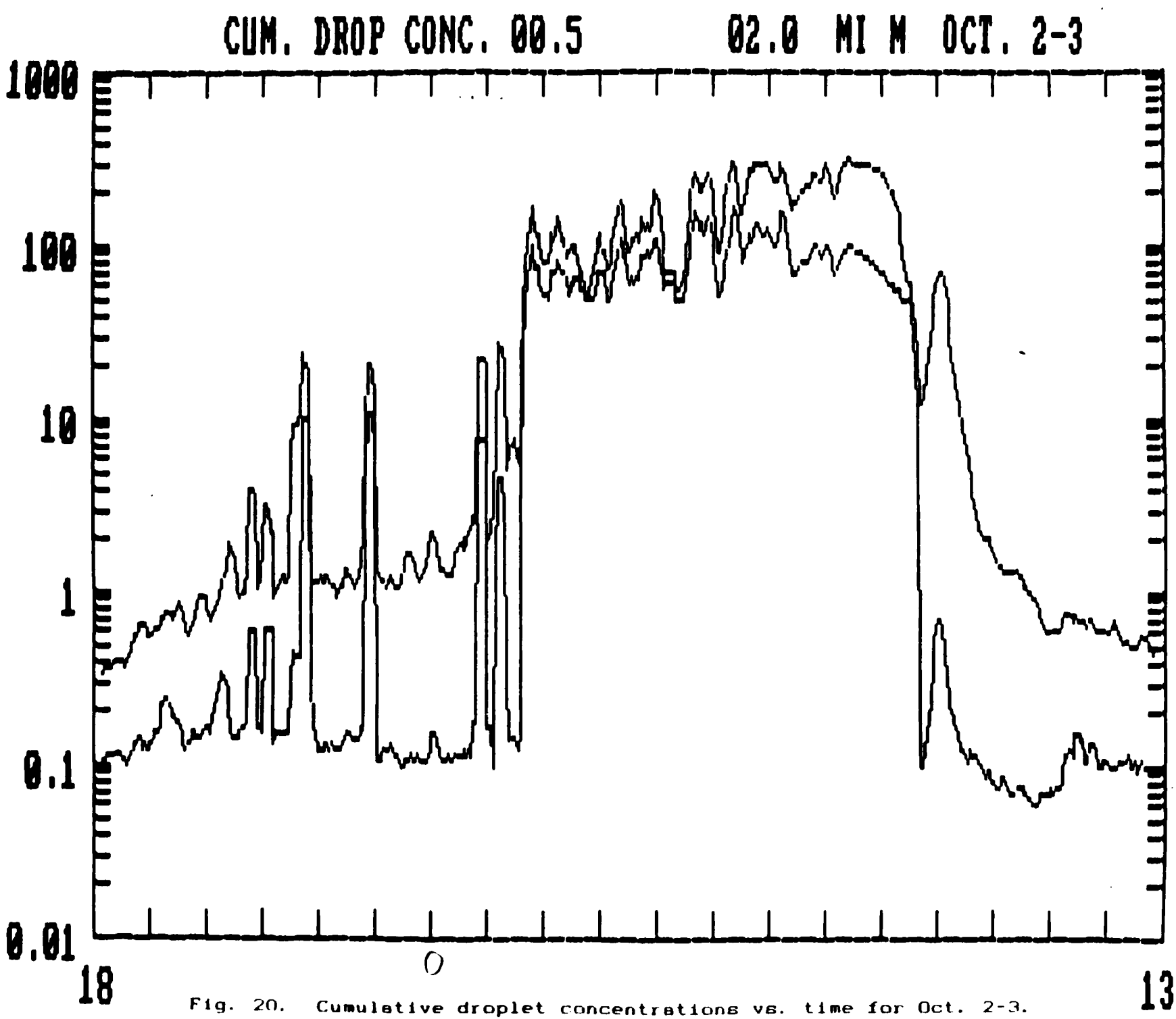

Fig. 20. Cumulative droplet concentrations vs. time for Oct. 2-3.

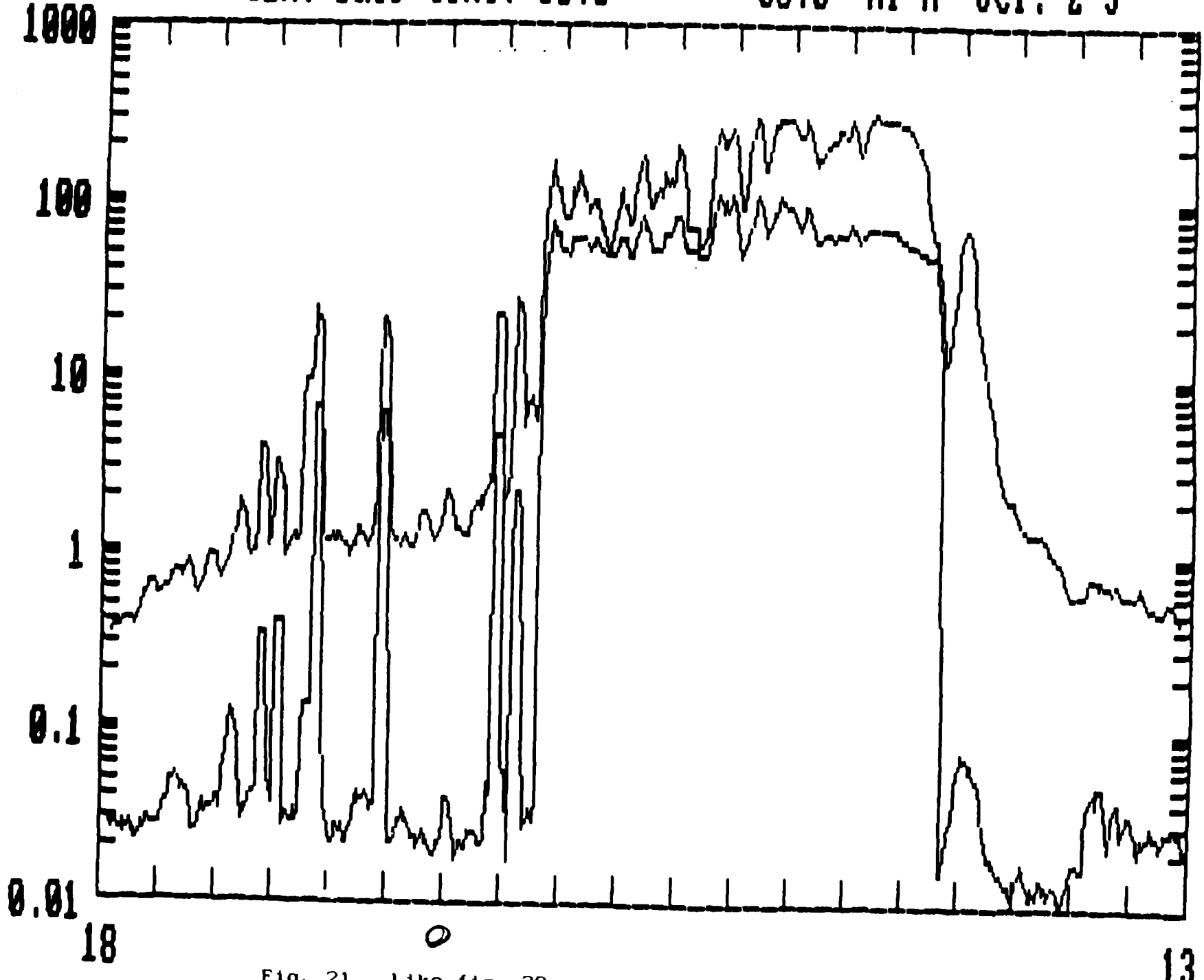

Fig. 21. Like fig. 20.

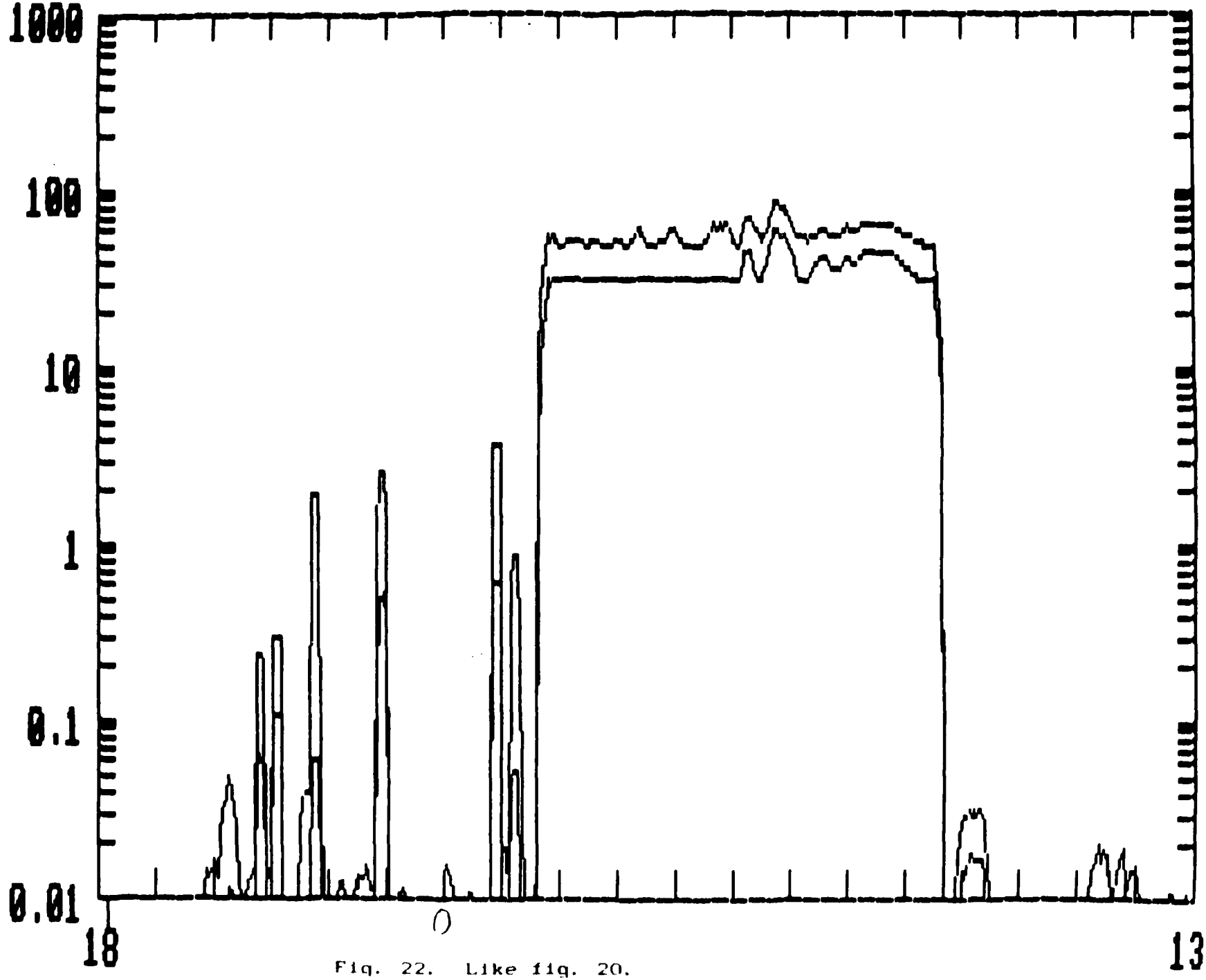

Fig. 22. Like fig. 20.

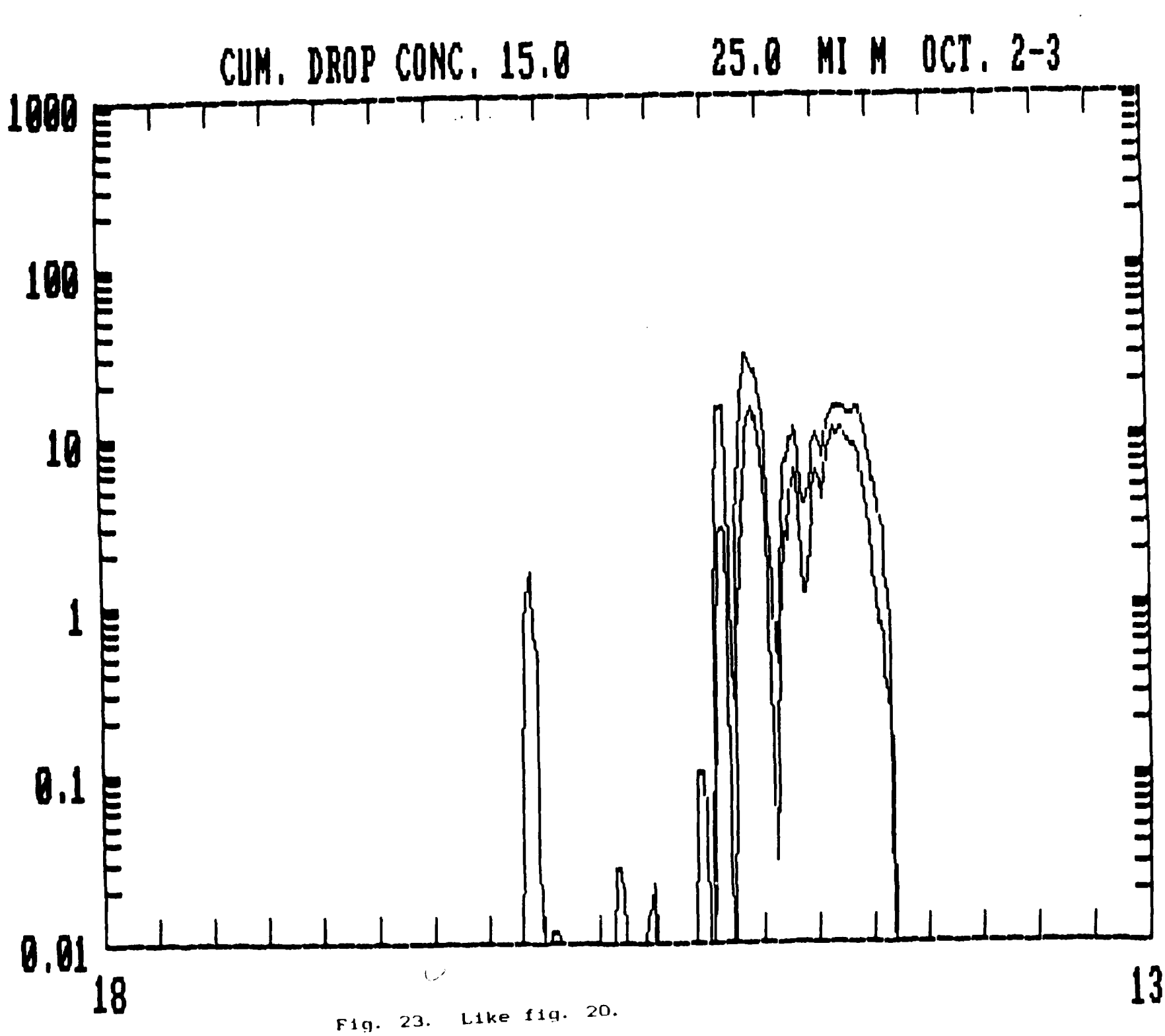

Fig. 23. Like fig. 20.

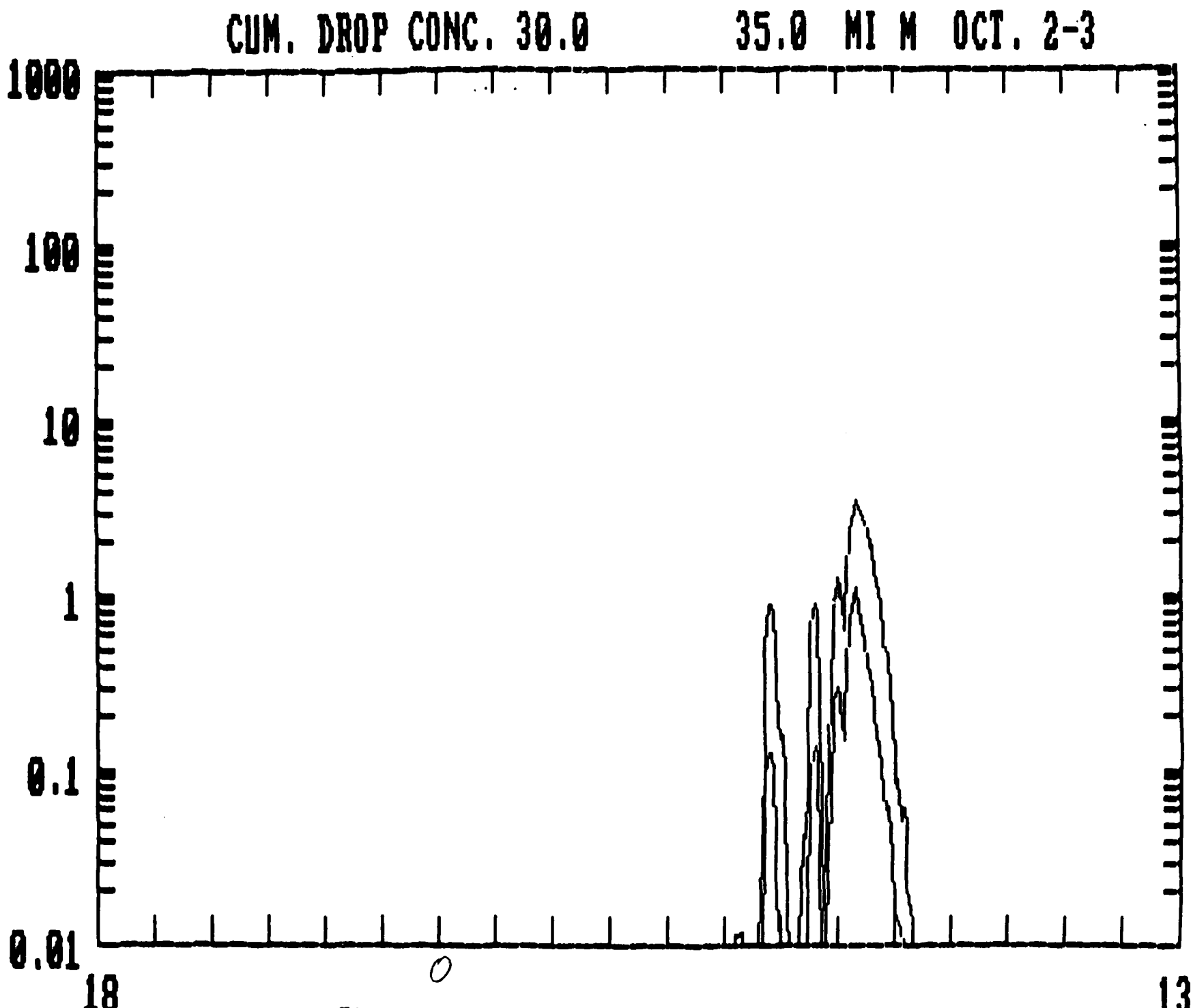

Fig. 24. Like fig. 20.

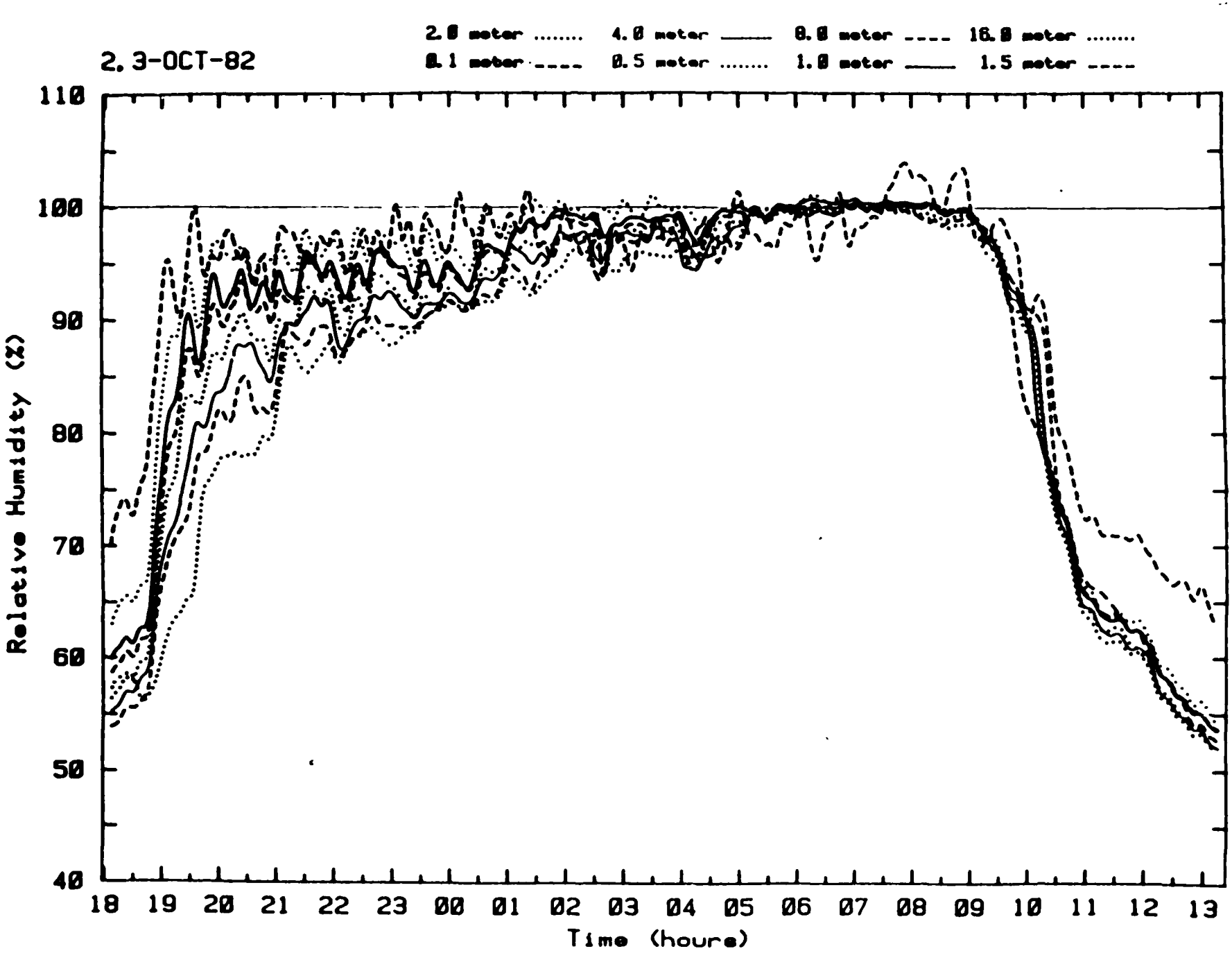

Fig. 25. Relative humidity vs. time for Oct. 2-3.

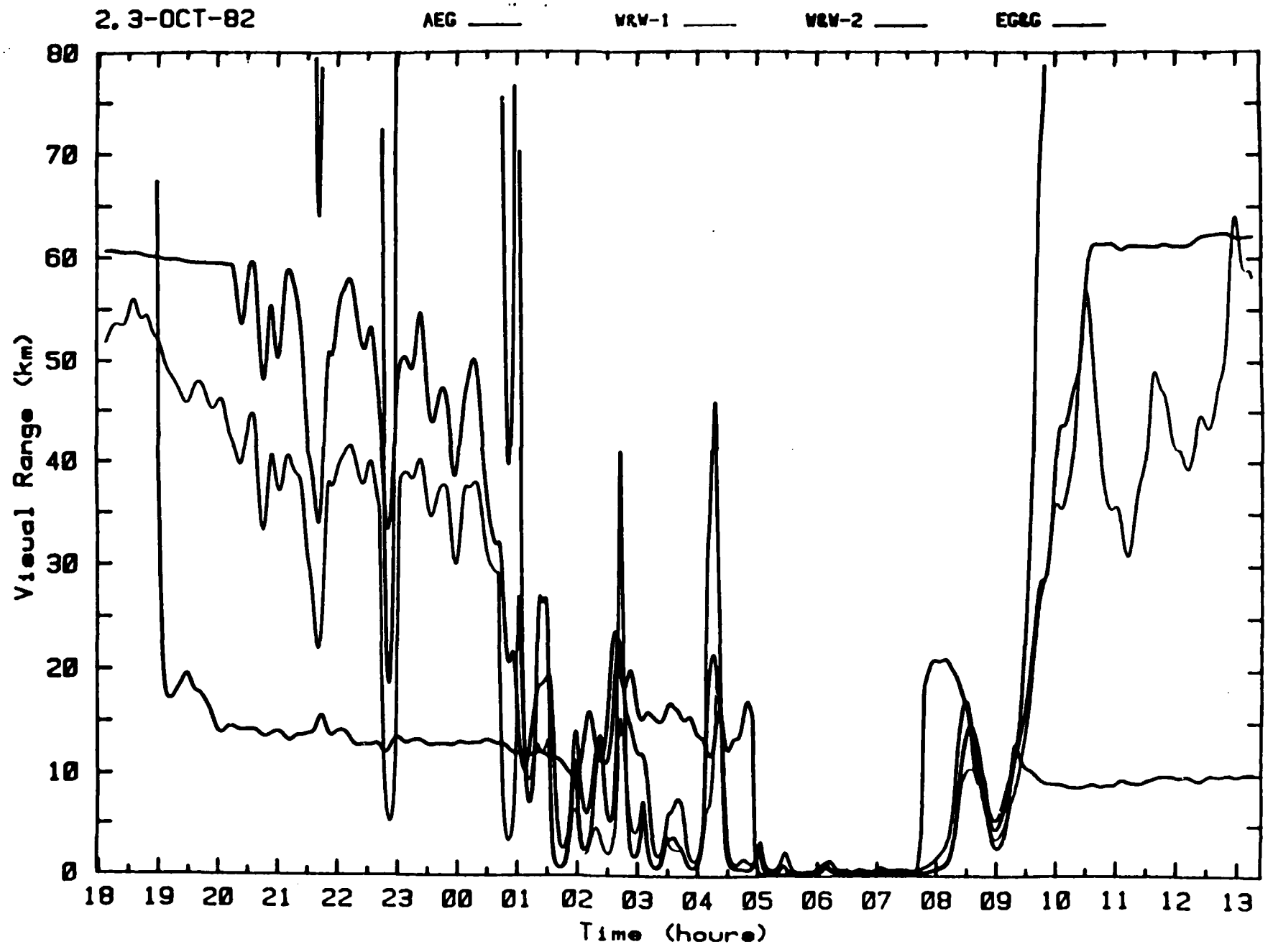

Fig. 26. Visibility vs. time for Oct. 2-3.

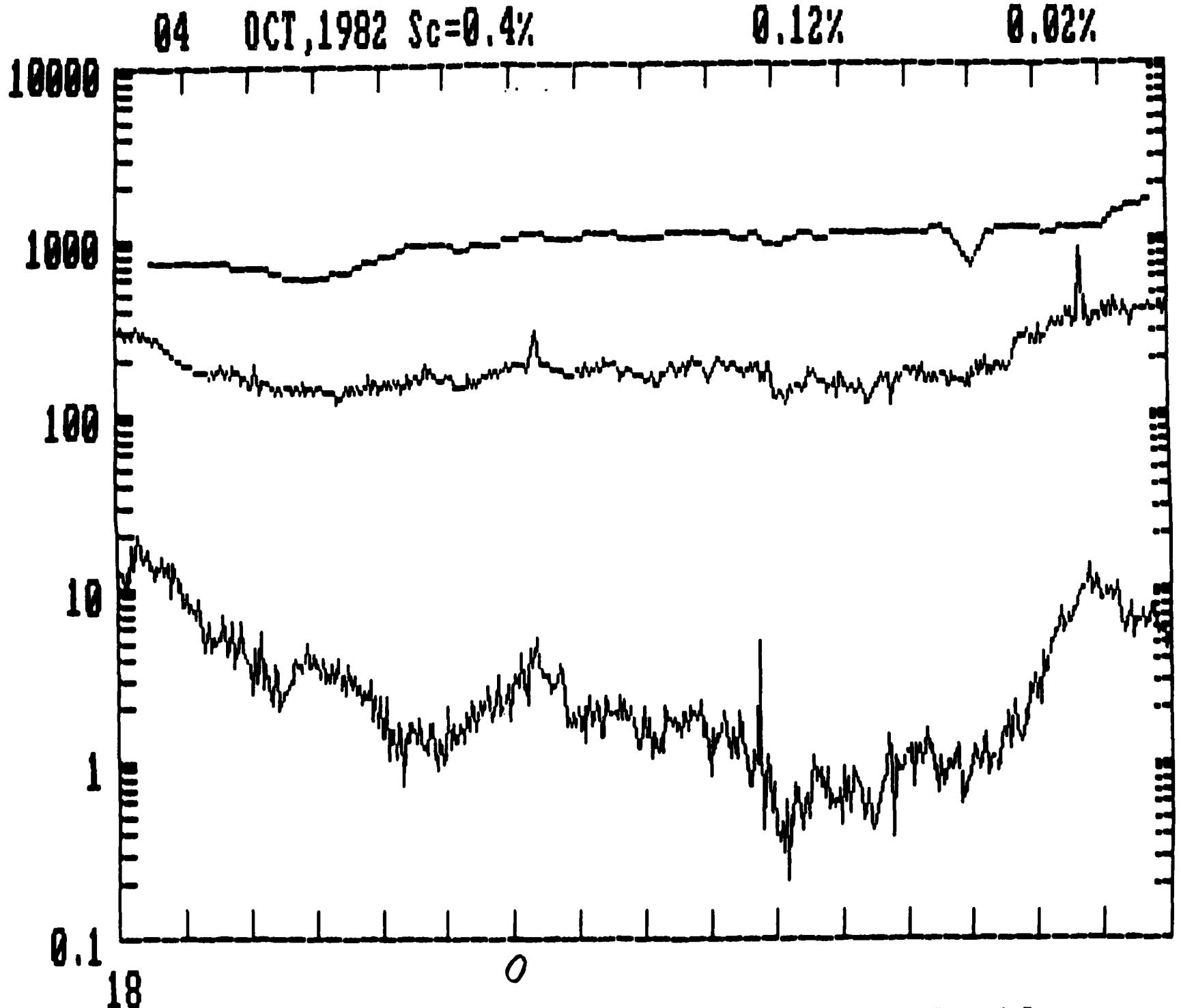

Fig. 27. Cumulative CCN-FCN concentrations vs. time for Oct. 4-5.

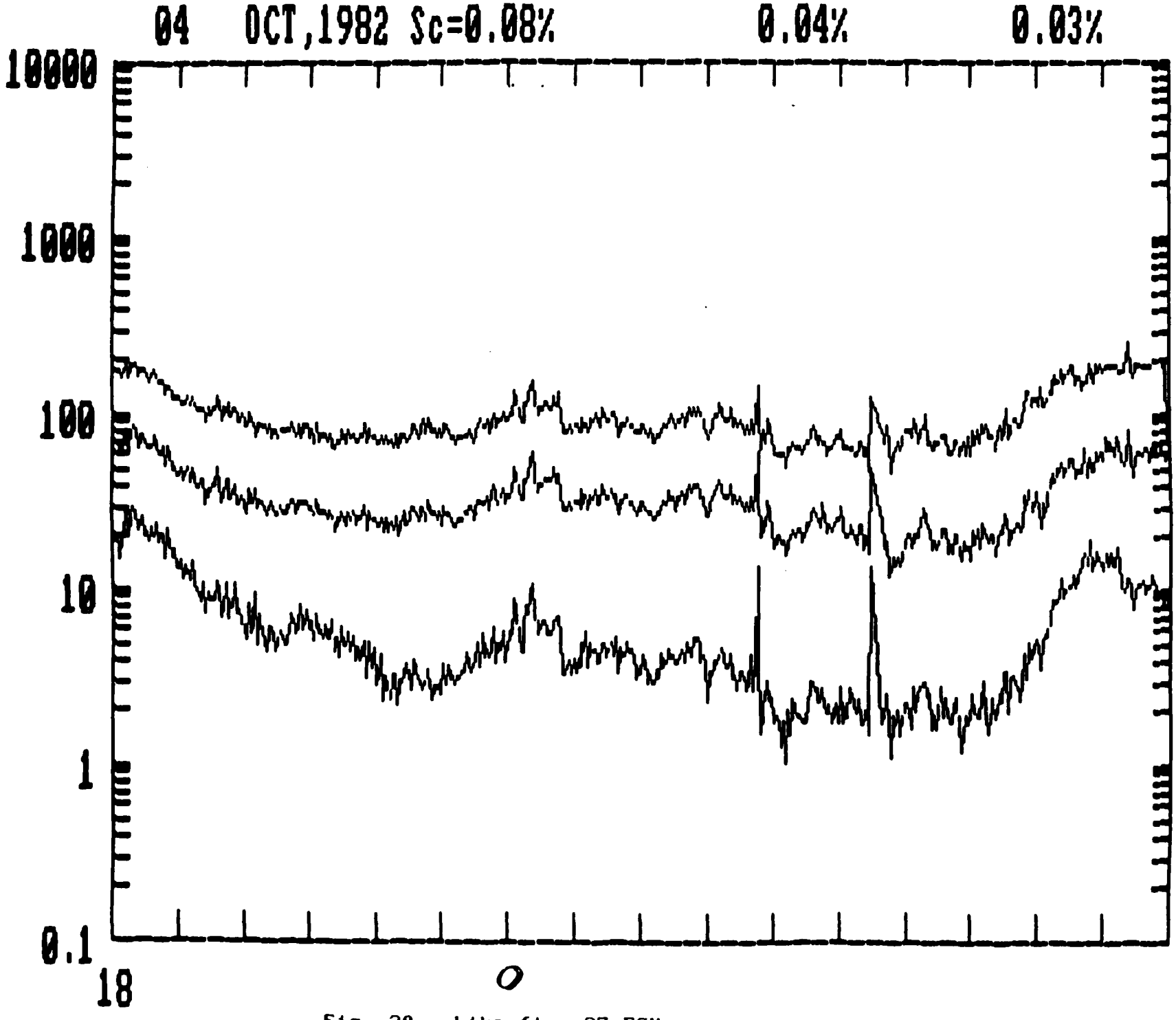

Fig. 28. Like fig. 27 FCN.

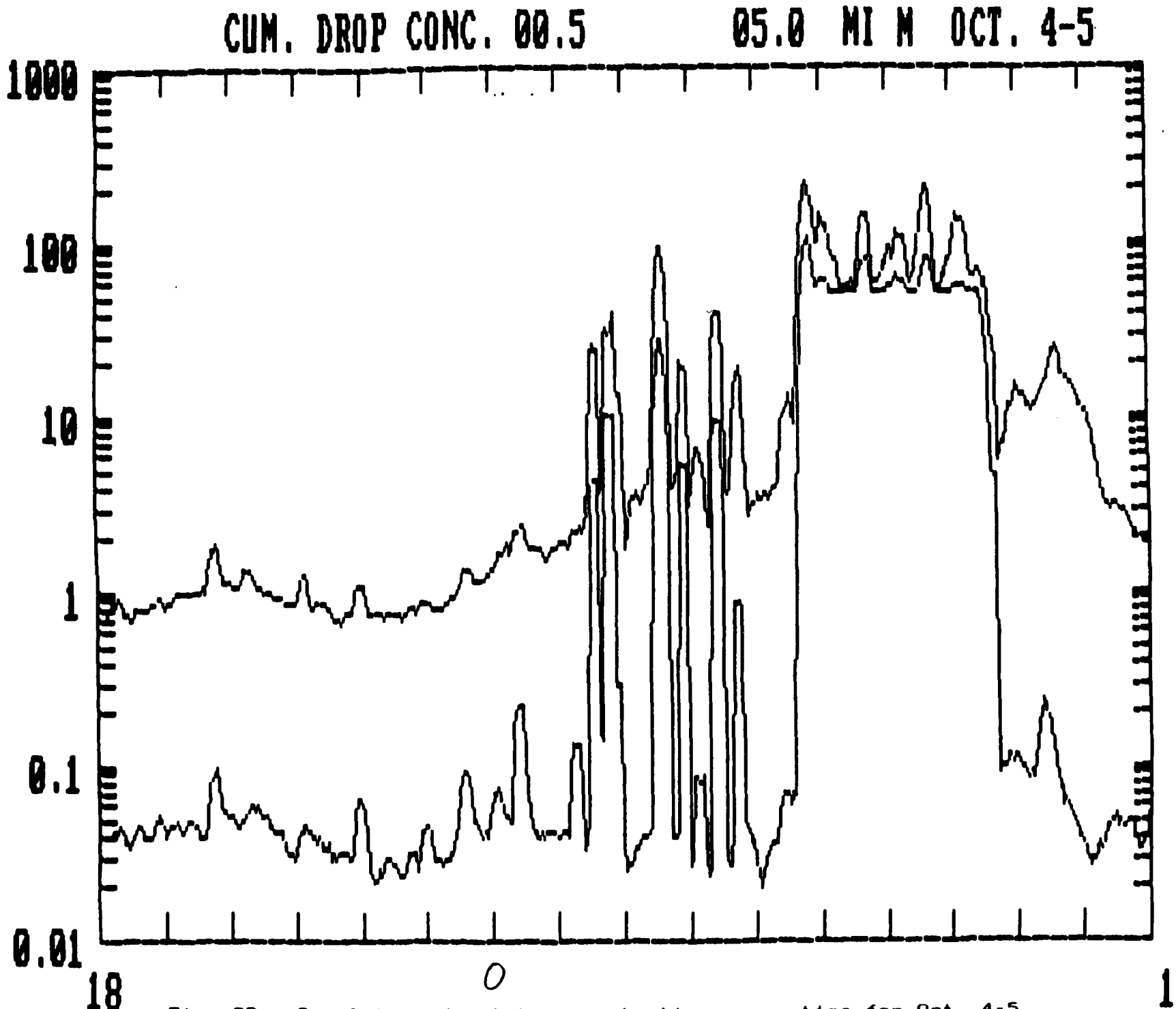

Fig. 29. Cumulative droplet concentrations. vs. time for Oct. 4-5.

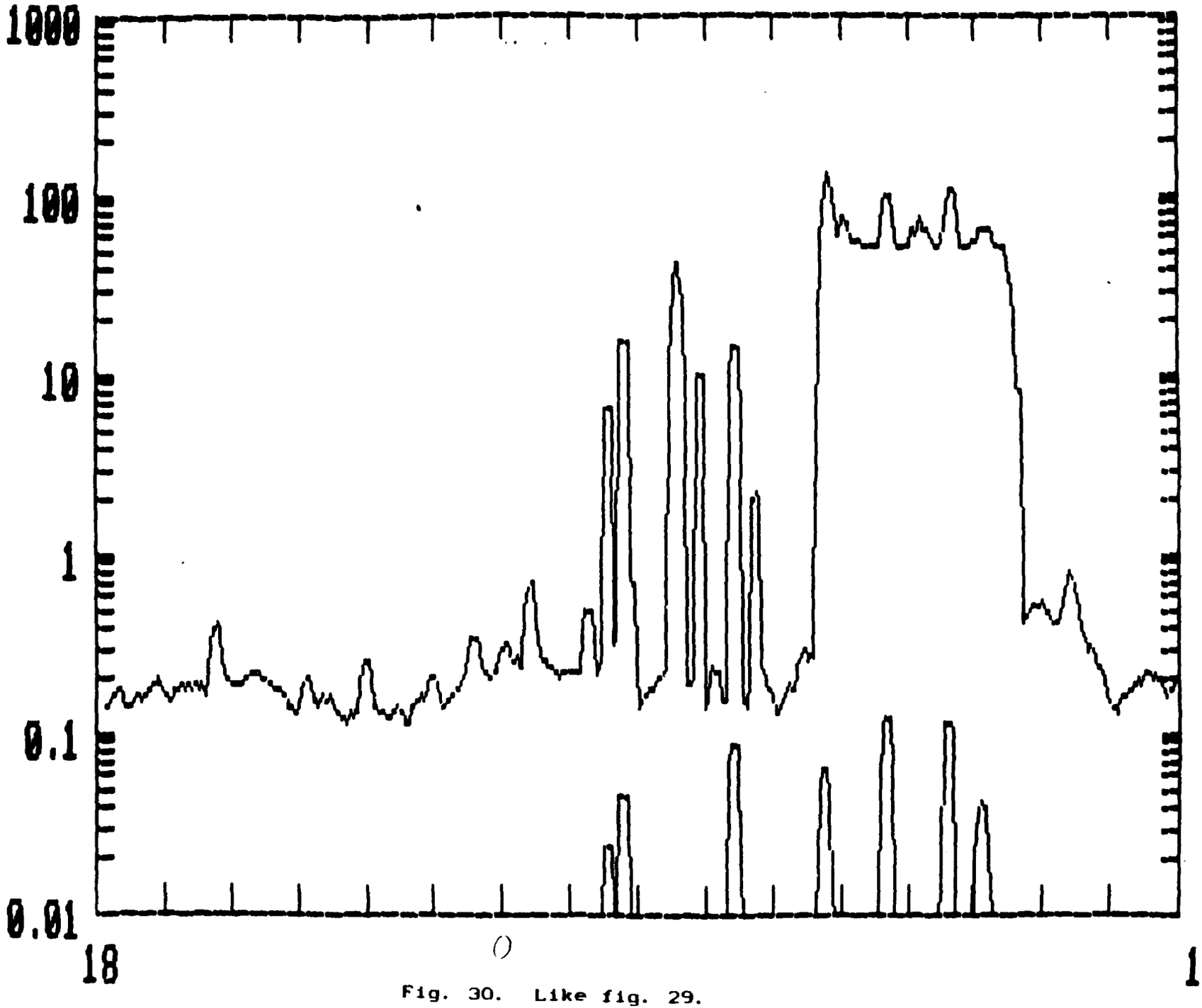

Fig. 30. Like fig. 29.

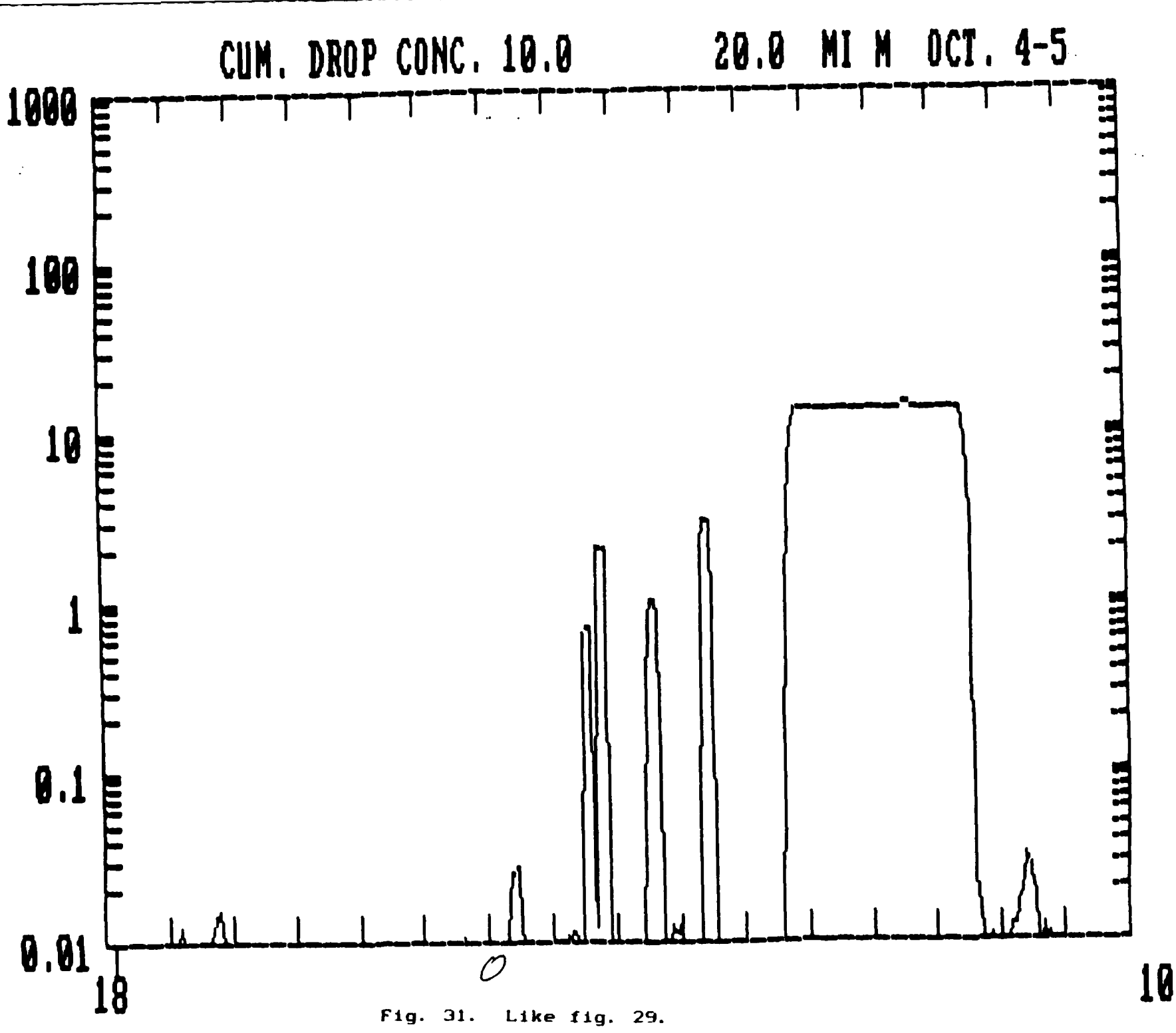

Fig. 31. Like fig. 29.

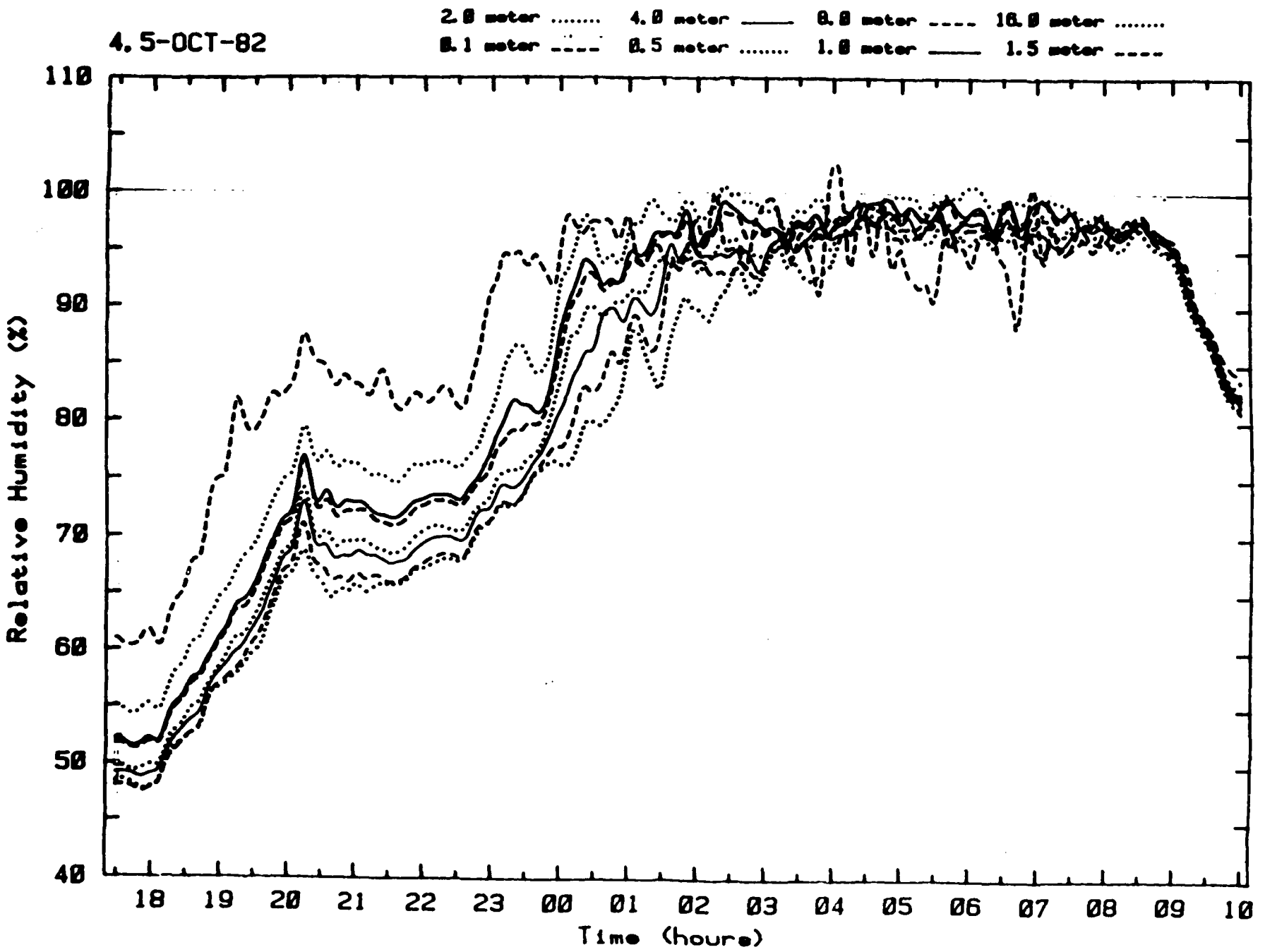

Fig. 32. Relative humidity vs. time for Oct. 4-5.

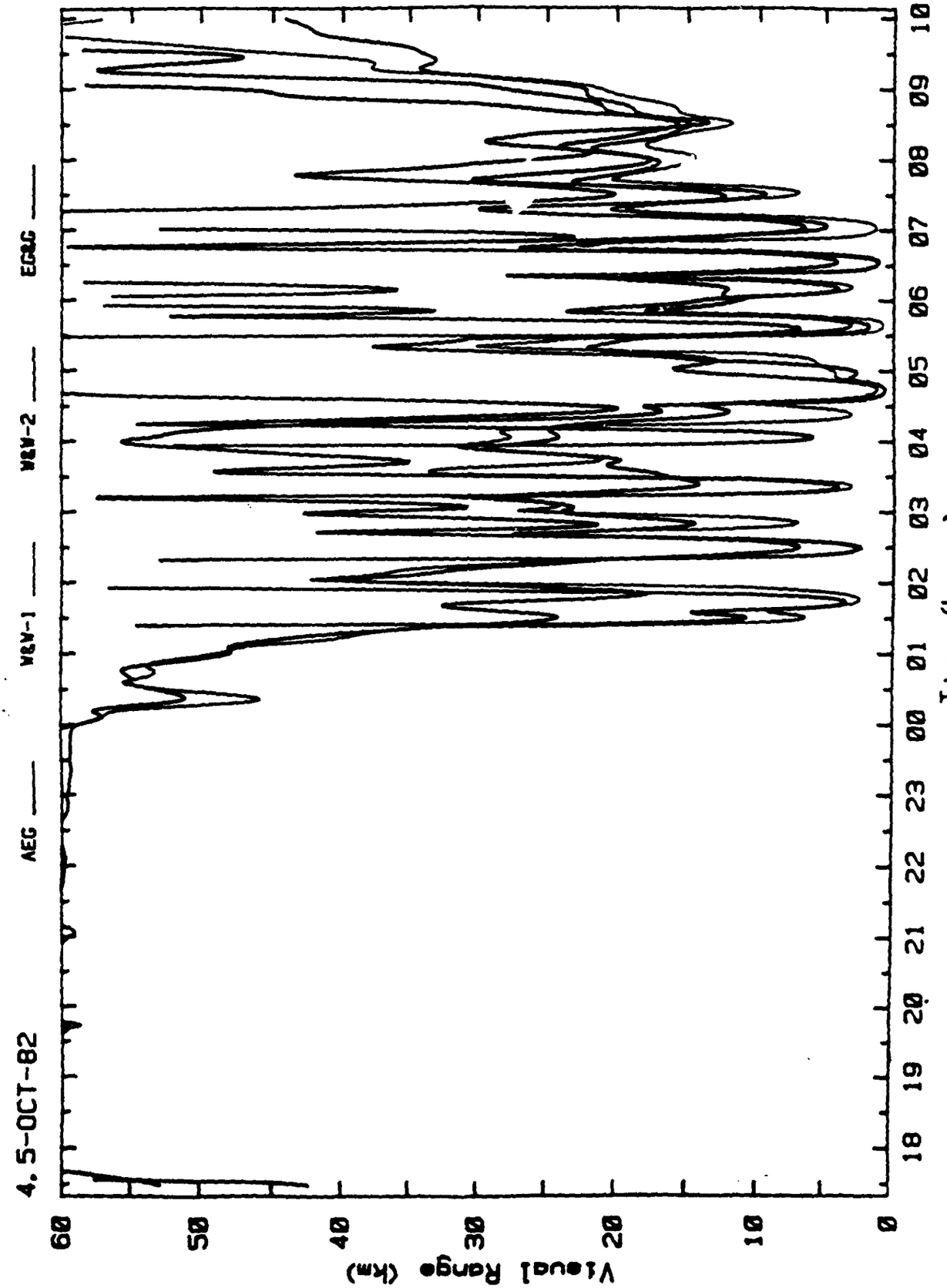

Fig. 33. Viability vs. time for Oct. 4-5.

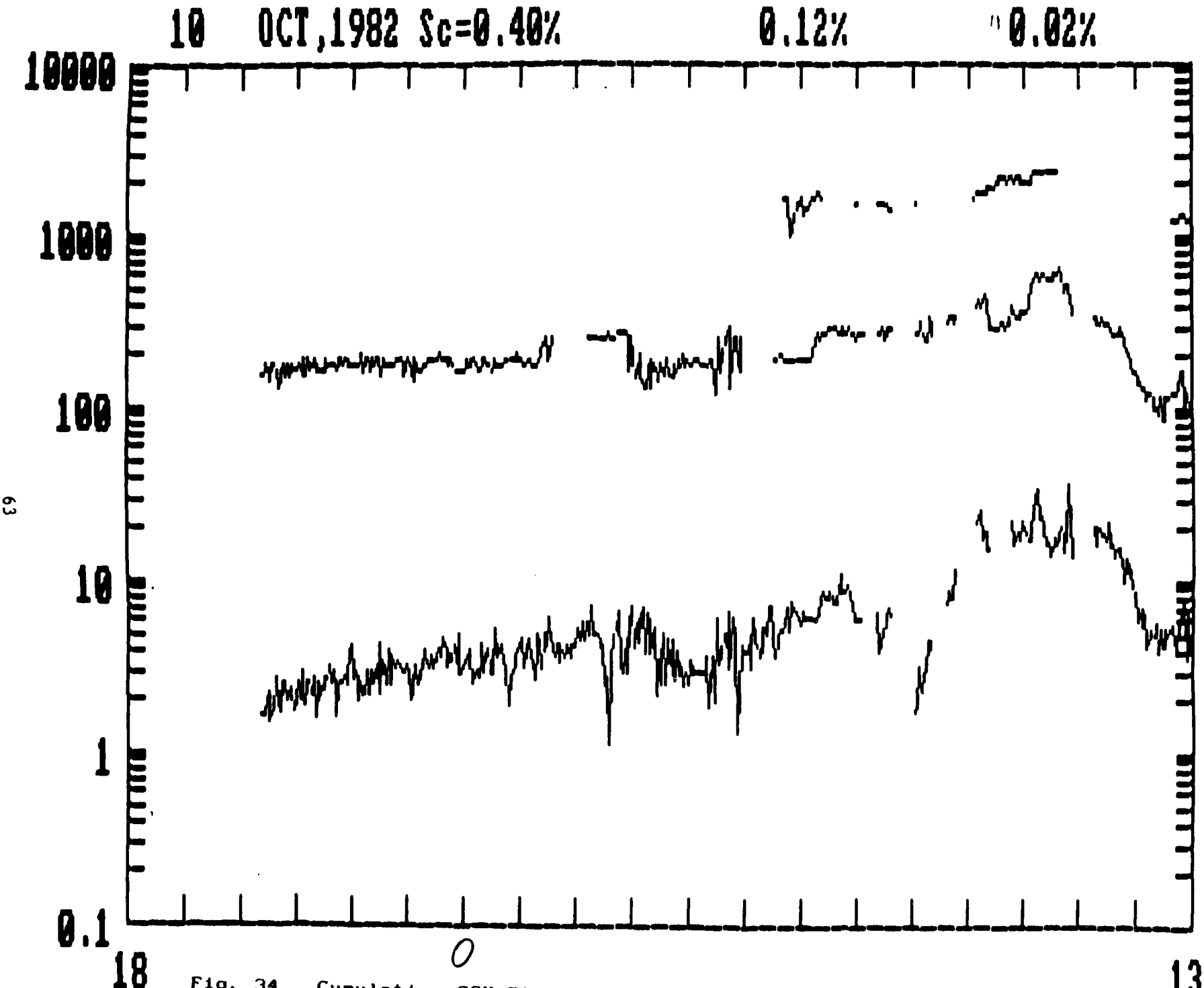

Fig. 34. Cumulative CCN-FCN concentrations vs. time for Oct. 10-11.

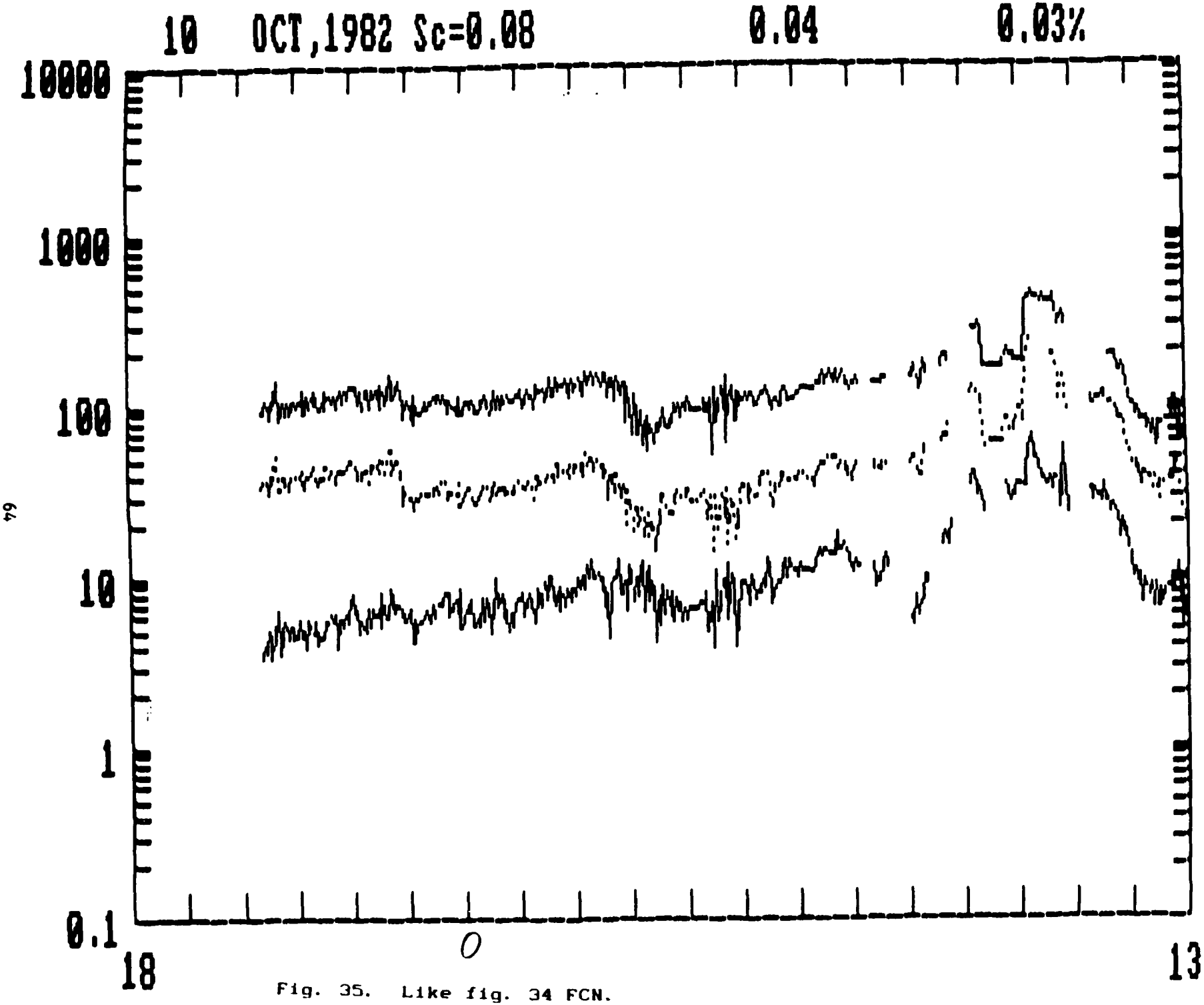

Fig. 35. Like fig. 34 FCN.

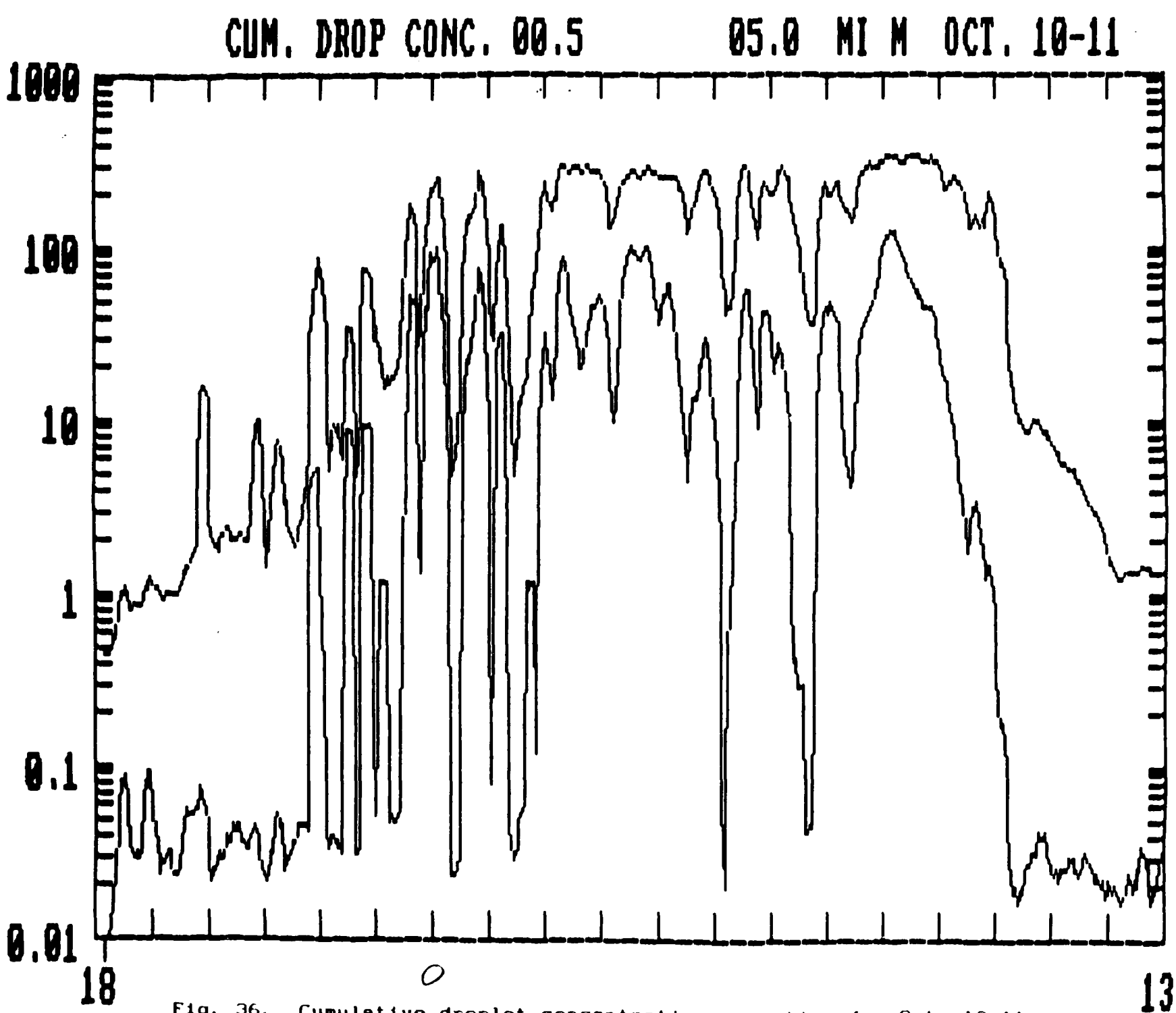

Fig. 36. Cumulative droplet concentrations vs. time for Oct. 10 11.

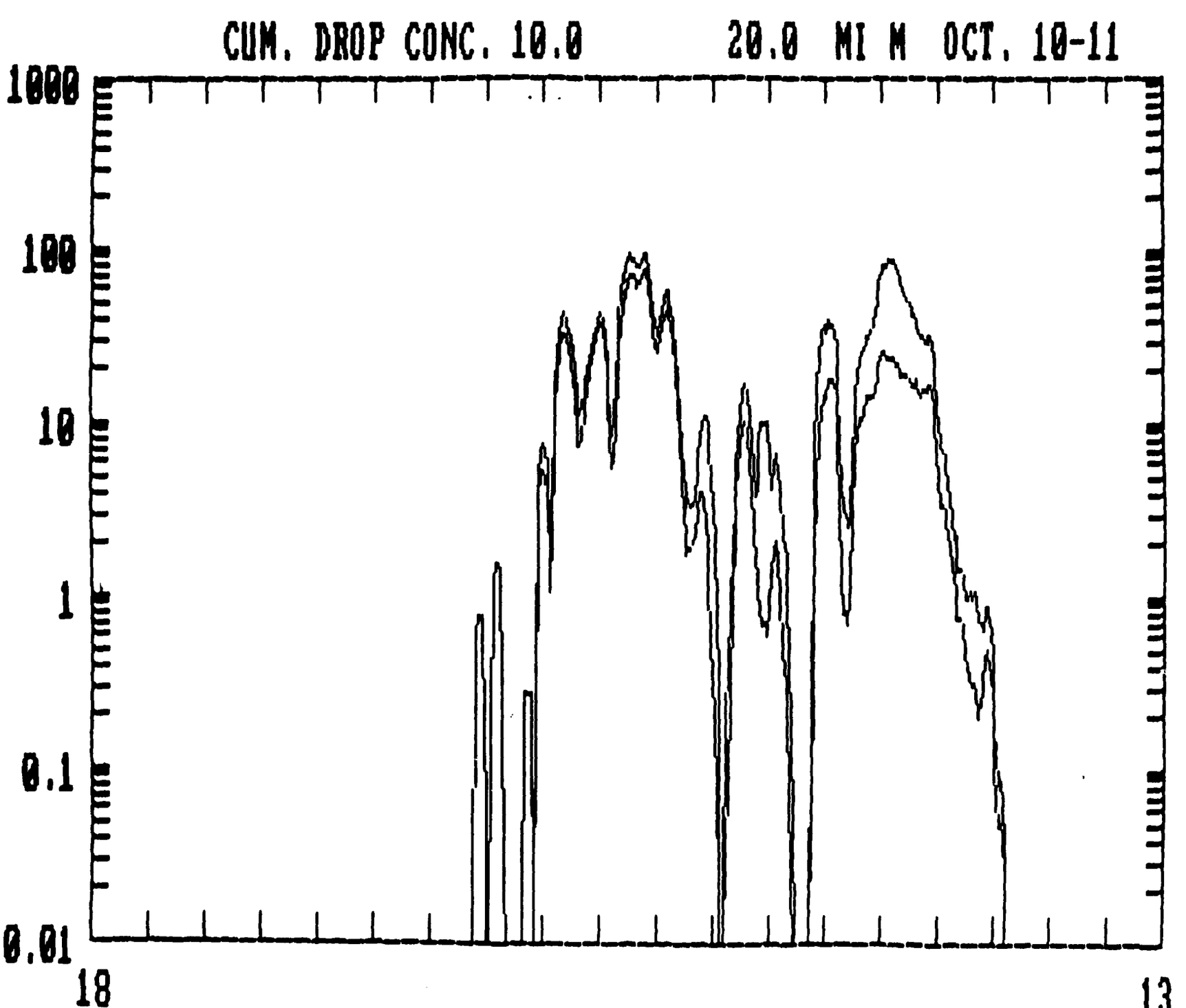

Fig. 37. Like fig. 36.

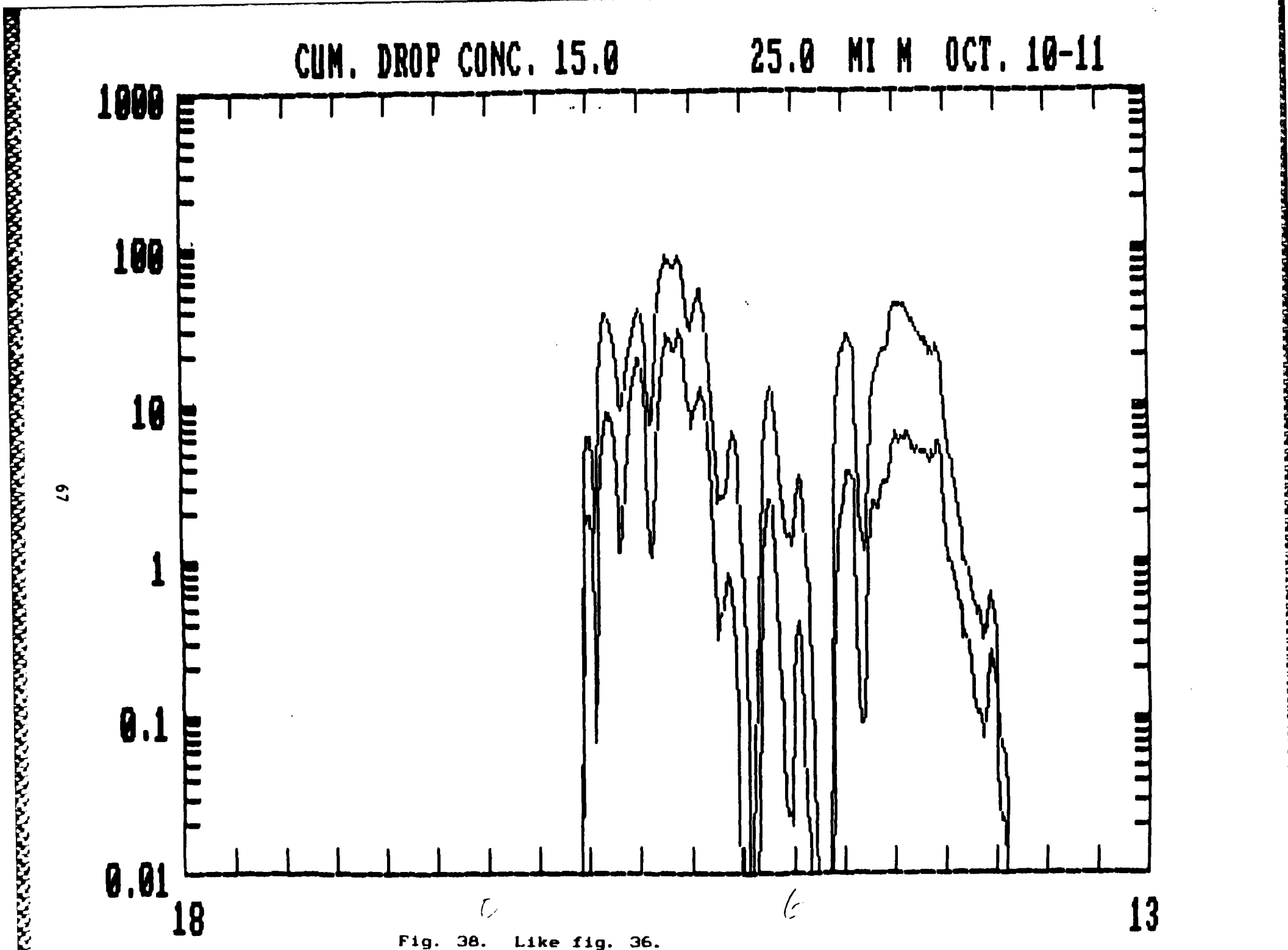

Fig. 38. Like fig. 36.

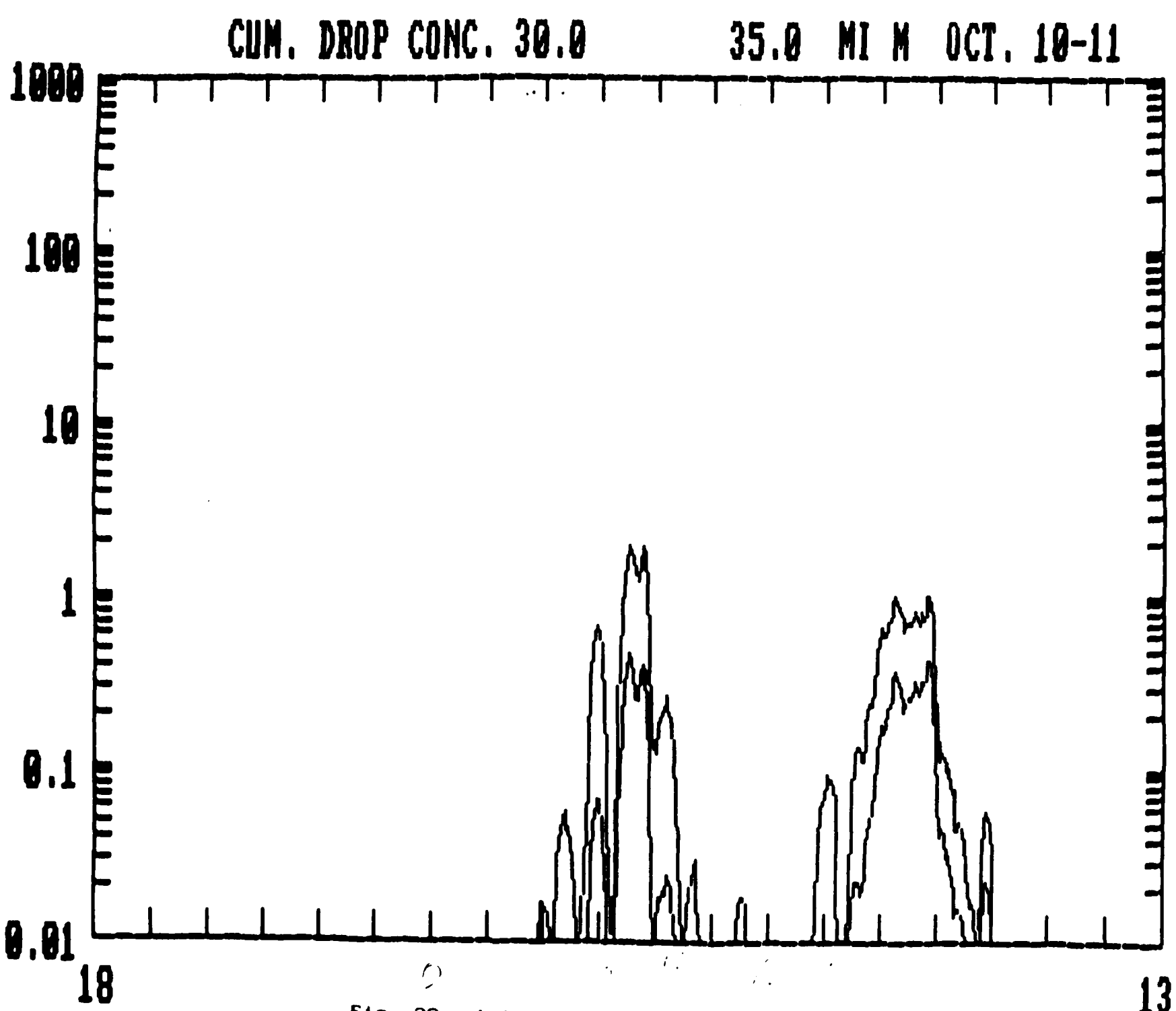

Fig. 39. Like fig. 36.

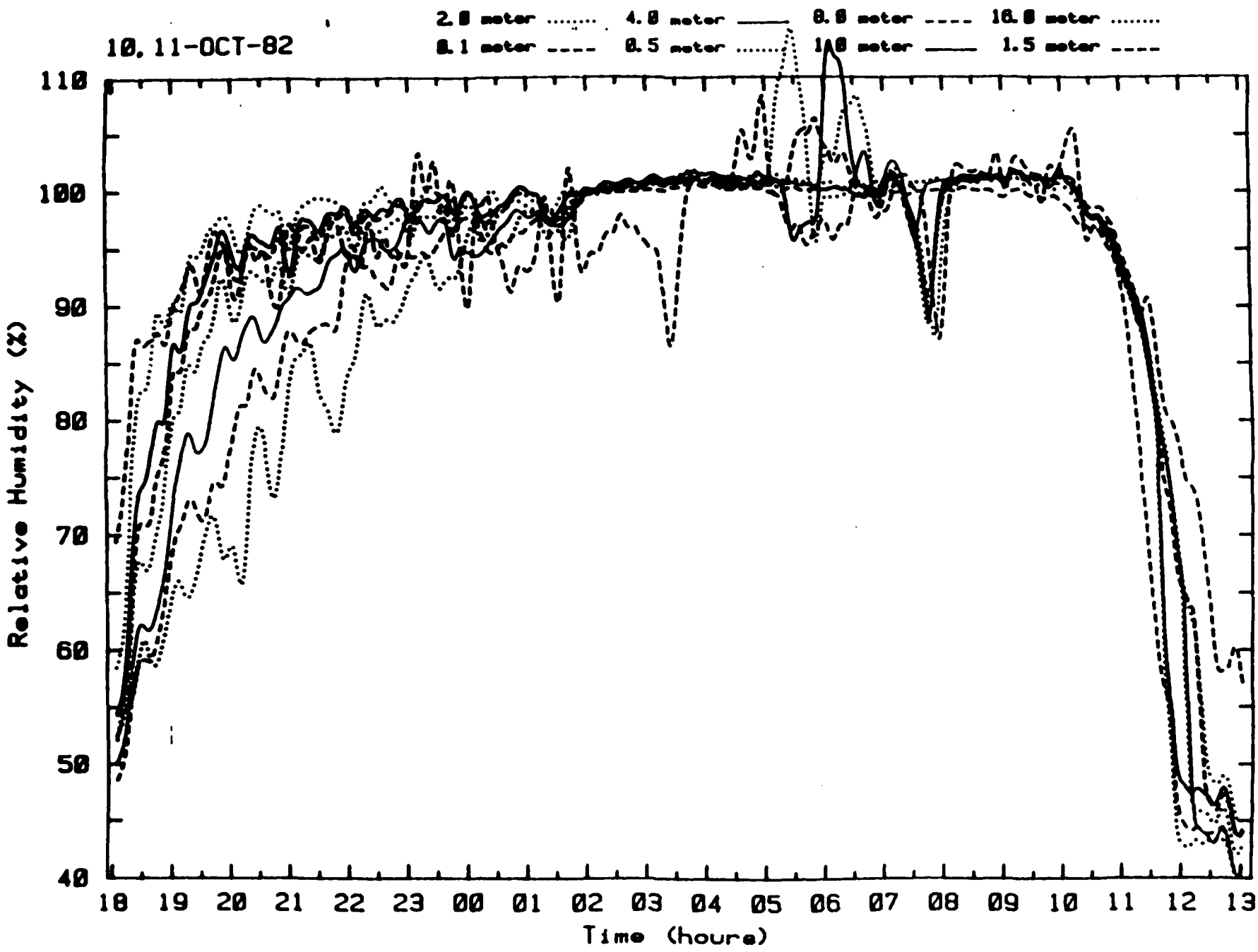

Fig. 40. Relative humidity vs. time for Oct. 10-11.

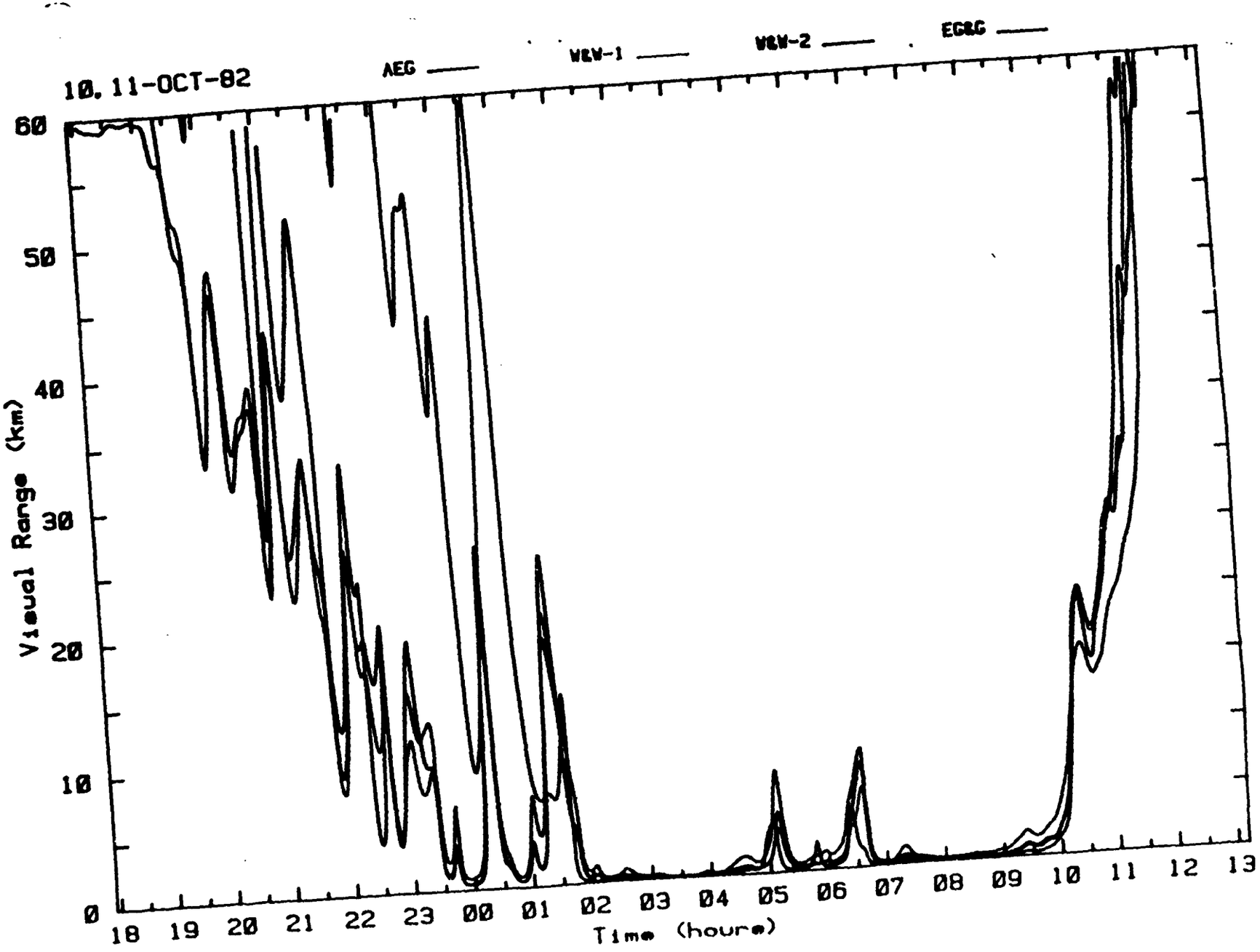

Fig. 41. Visibility vs. time for Oct. 10-11.

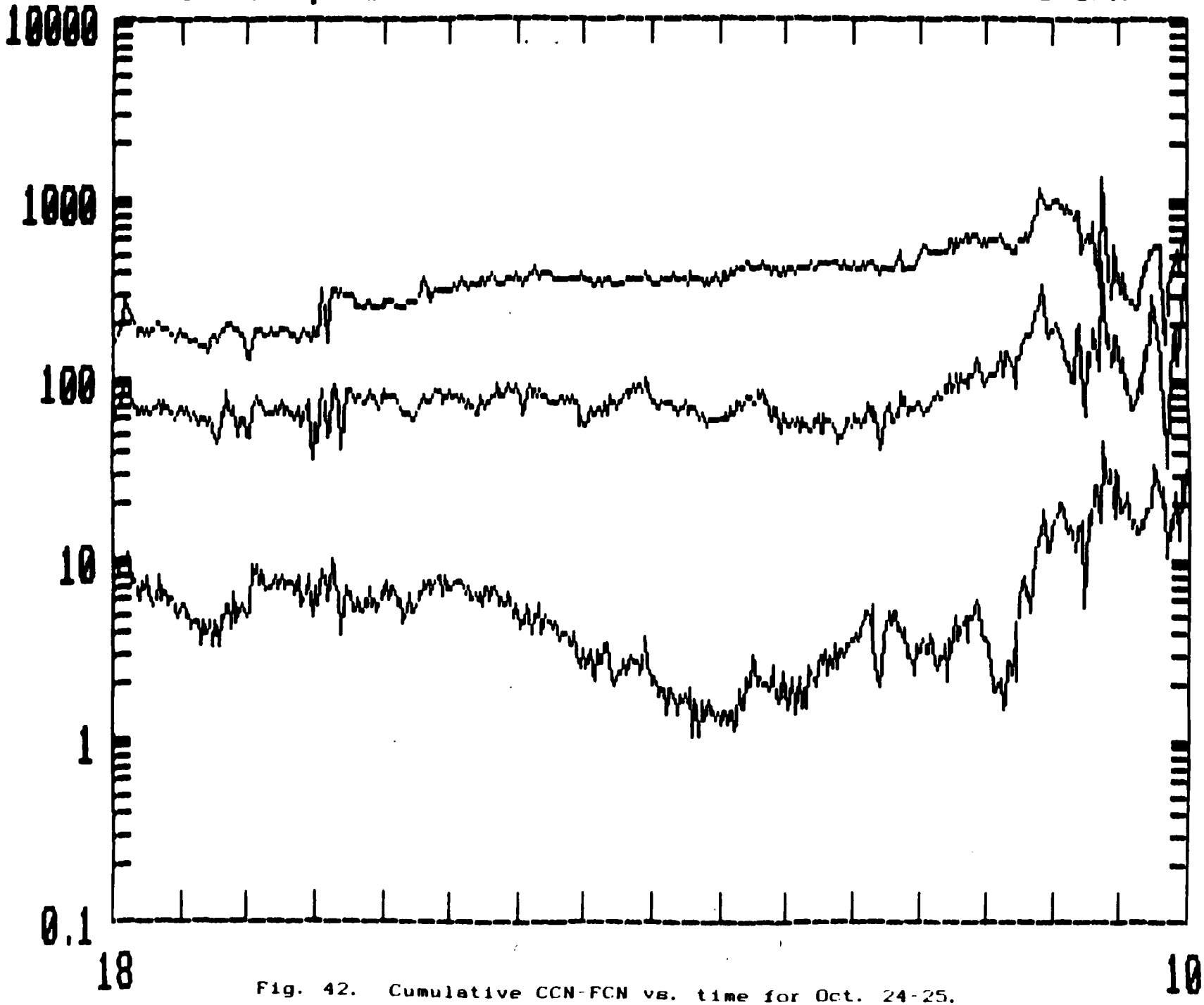

Fig. 42. Cumulative CCN-FCN vs. time for Oct. 24-25.

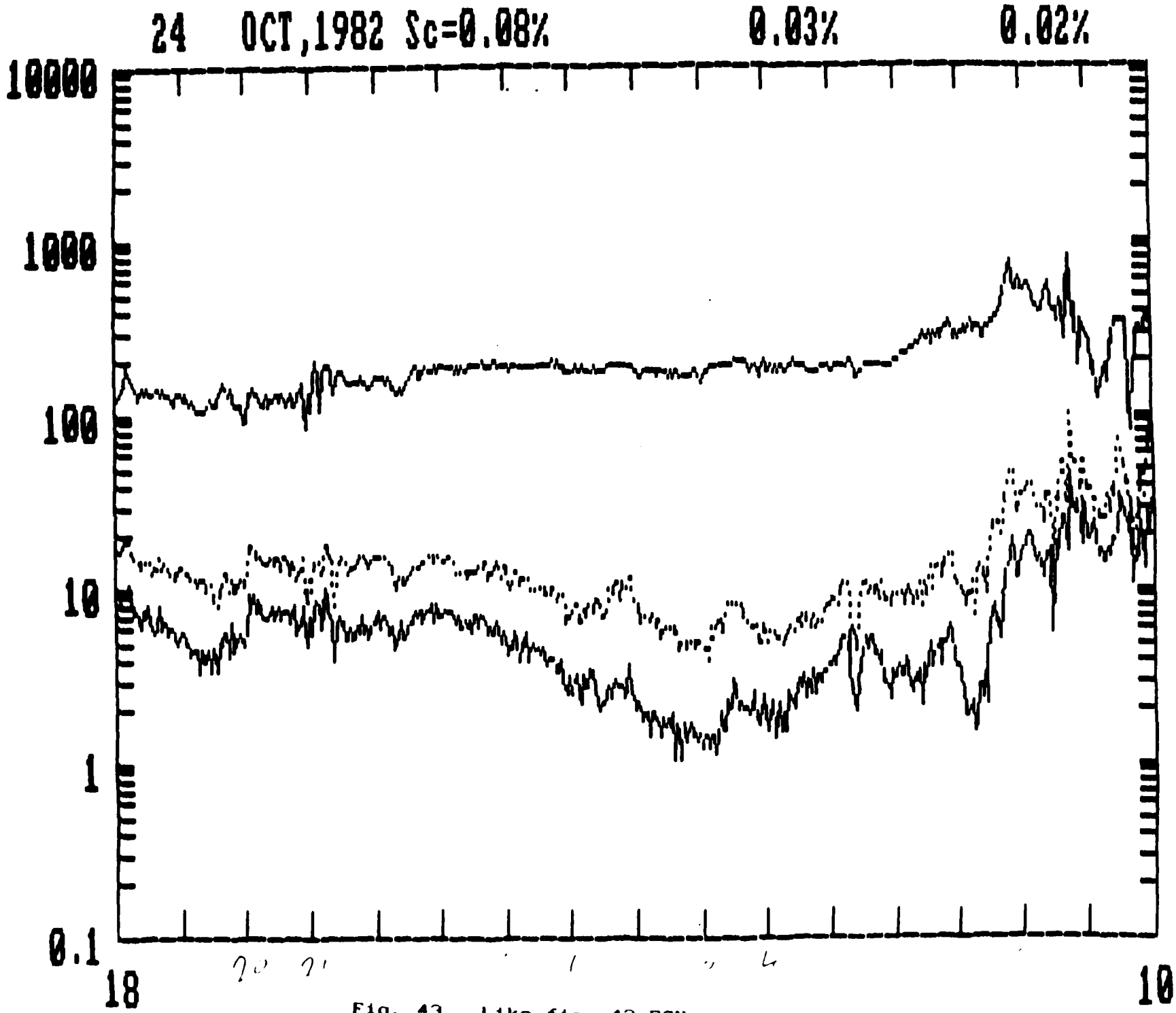

Fig. 43. Like fig. 42 FCN.

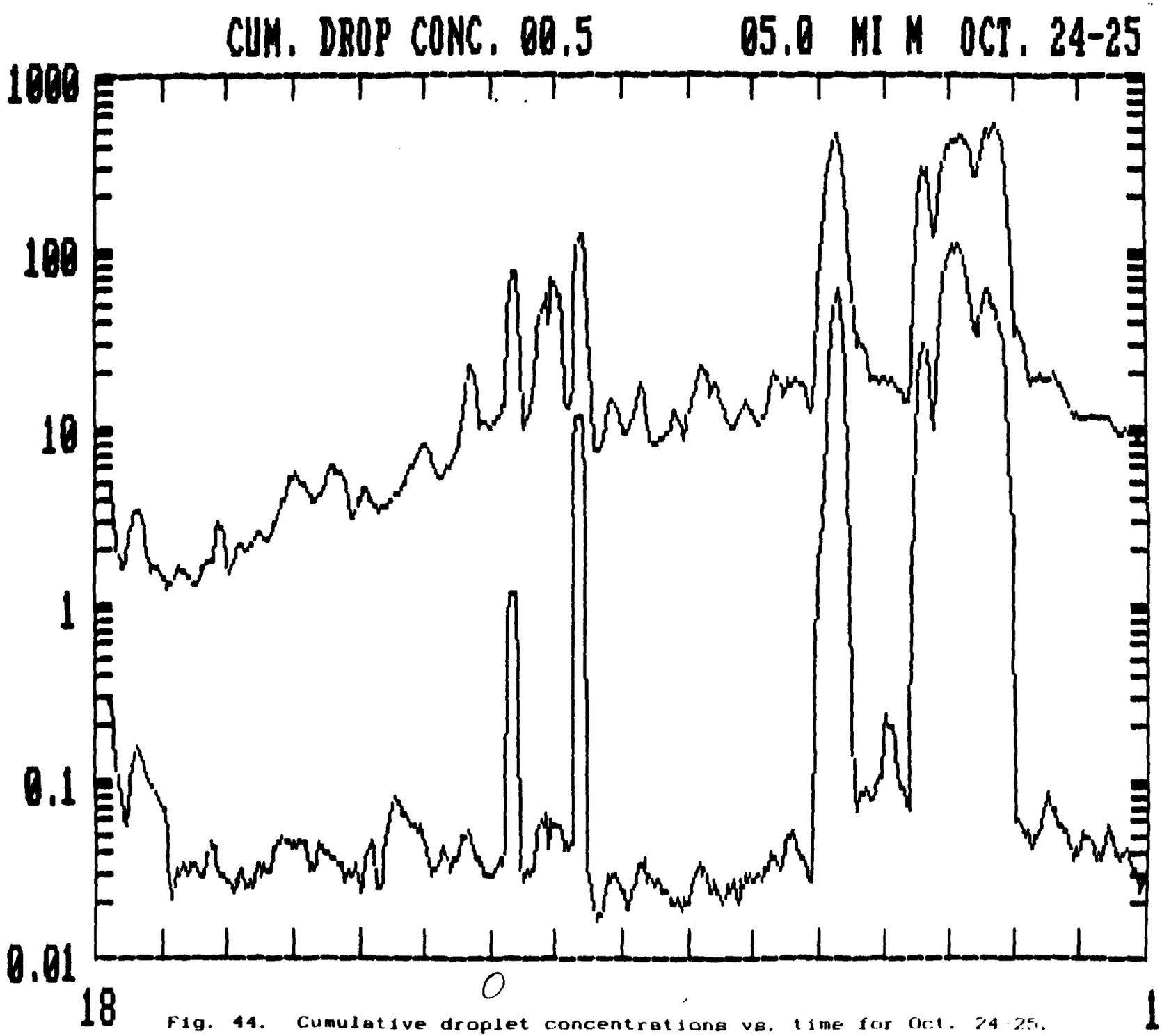

Fig. 44. Cumulative droplet concentrations vs. time for Oct. 24-25.

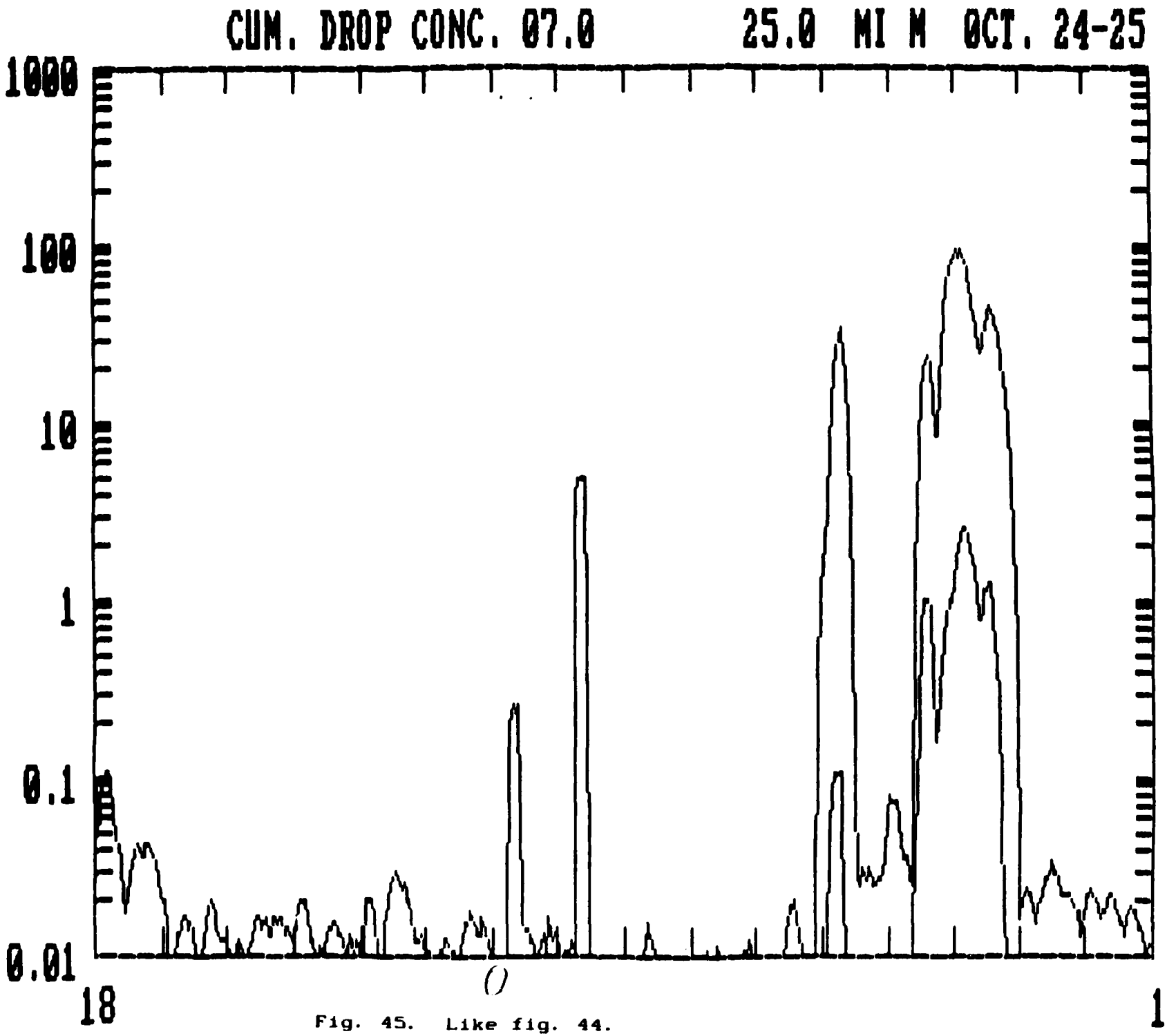

Fig. 45. Like fig. 44.

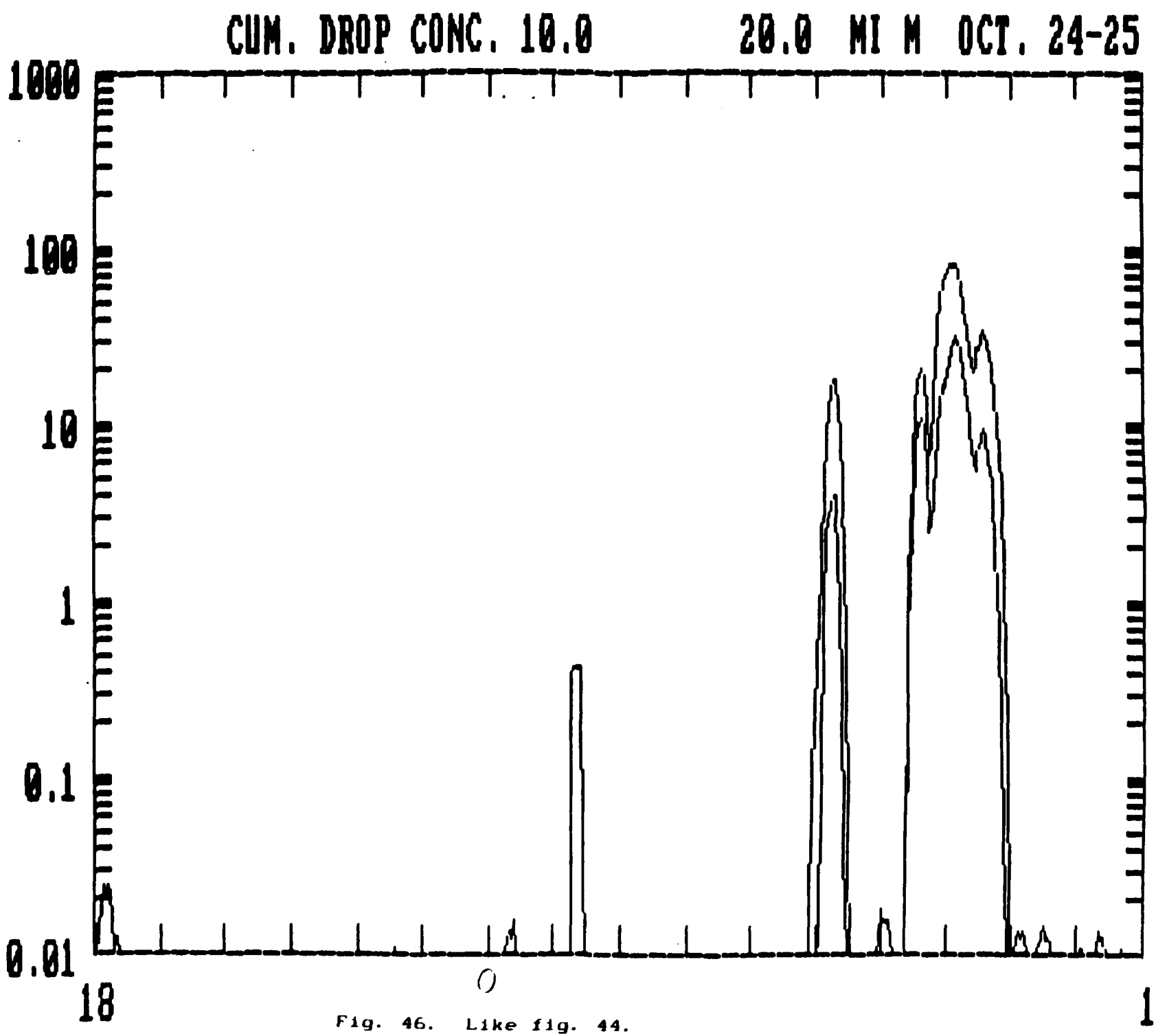

Fig. 46. Like fig. 44.

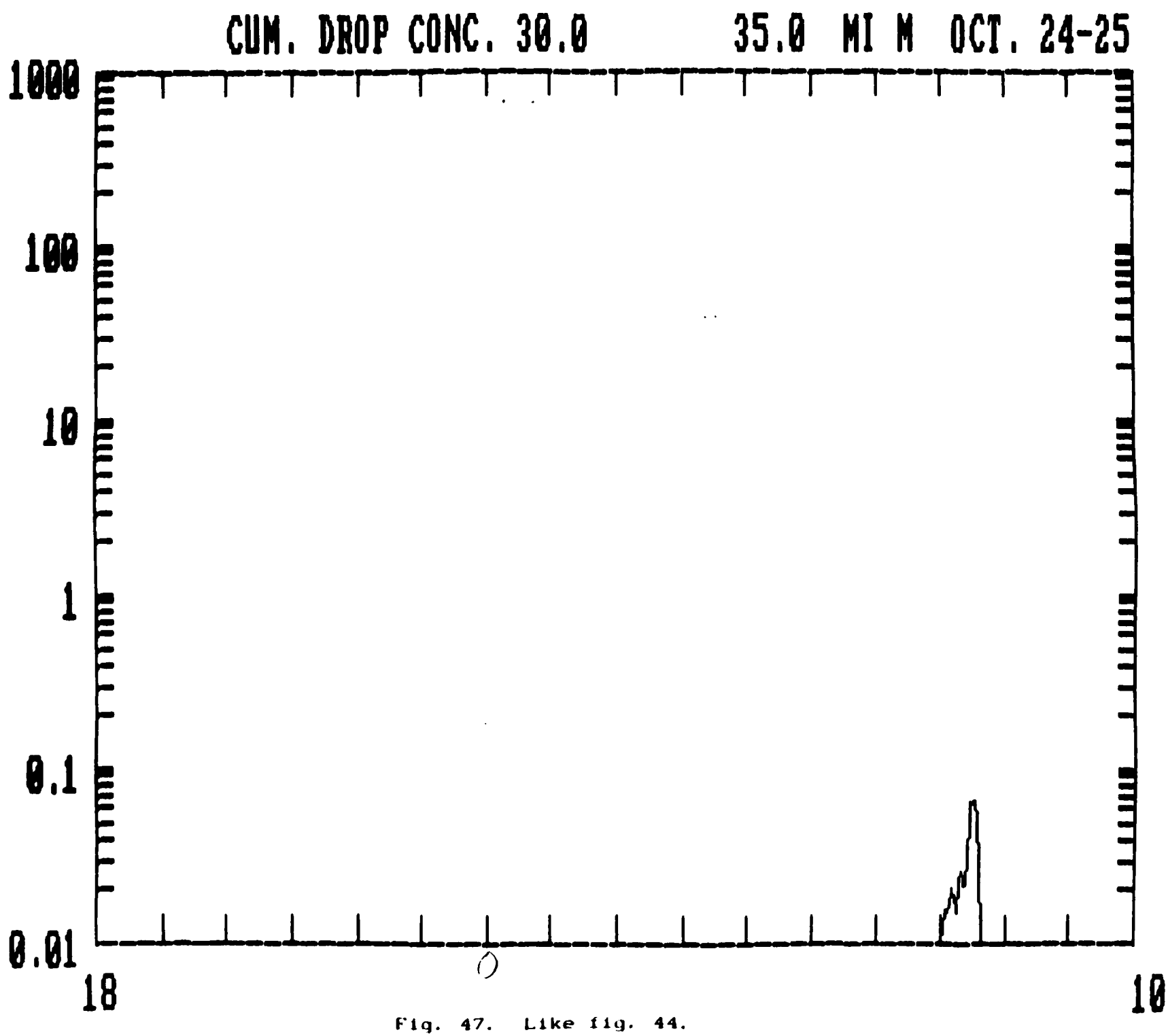

Fig. 47. Like fig. 44.

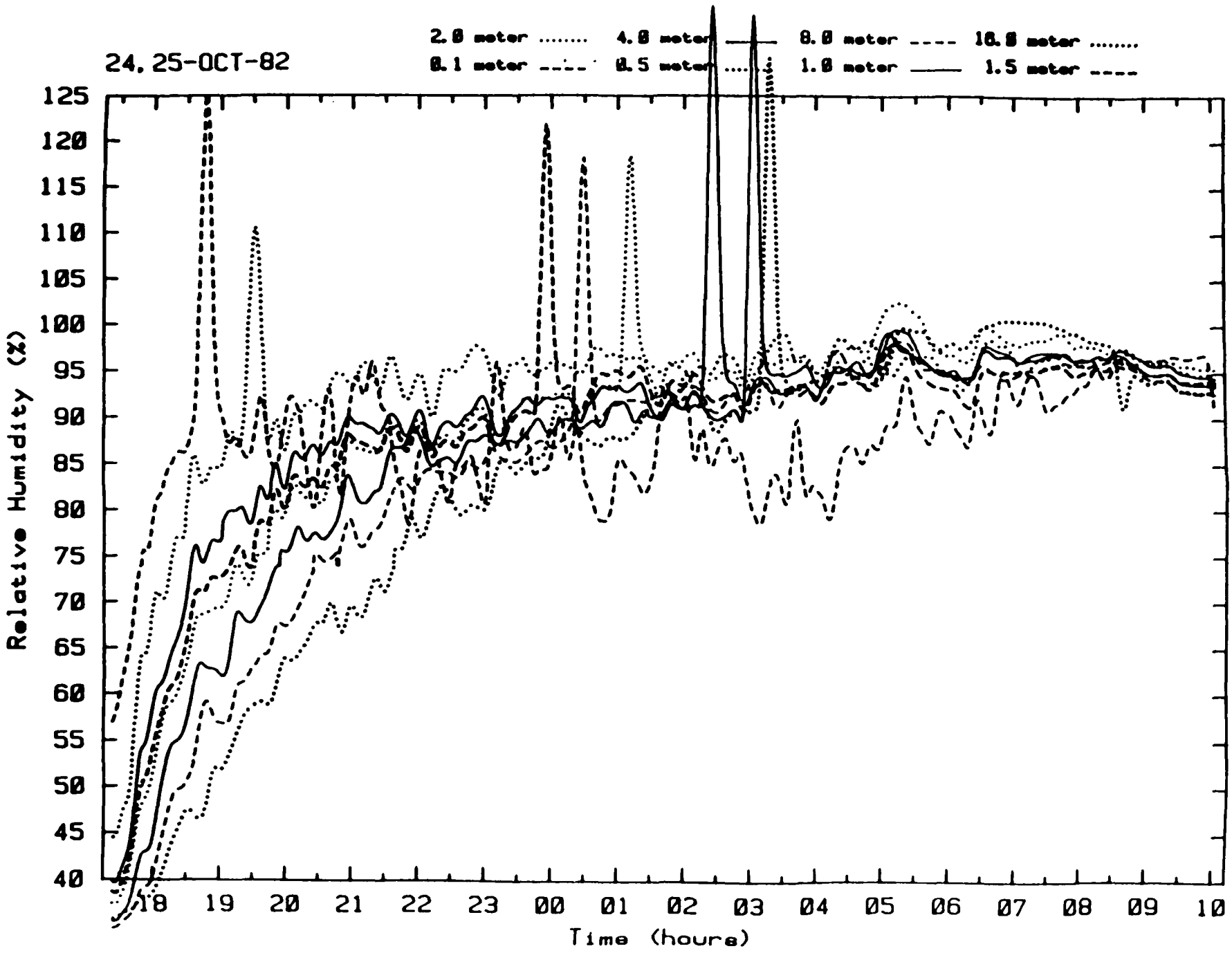

Fig. 48. Relative humidity vs. time for Oct. 24-25.

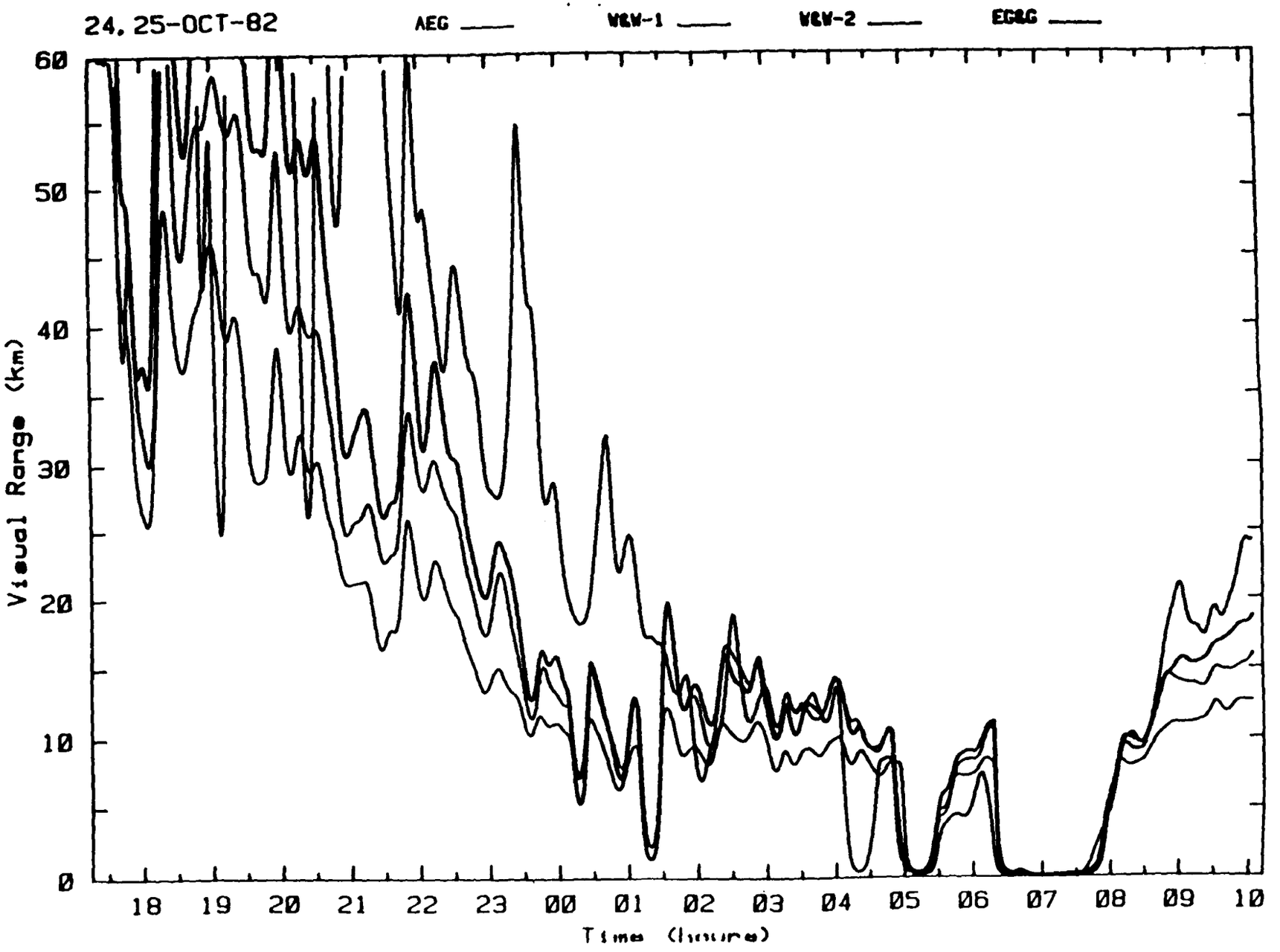

Fig. 49. Visibility vs. time for Oct. 24-25.

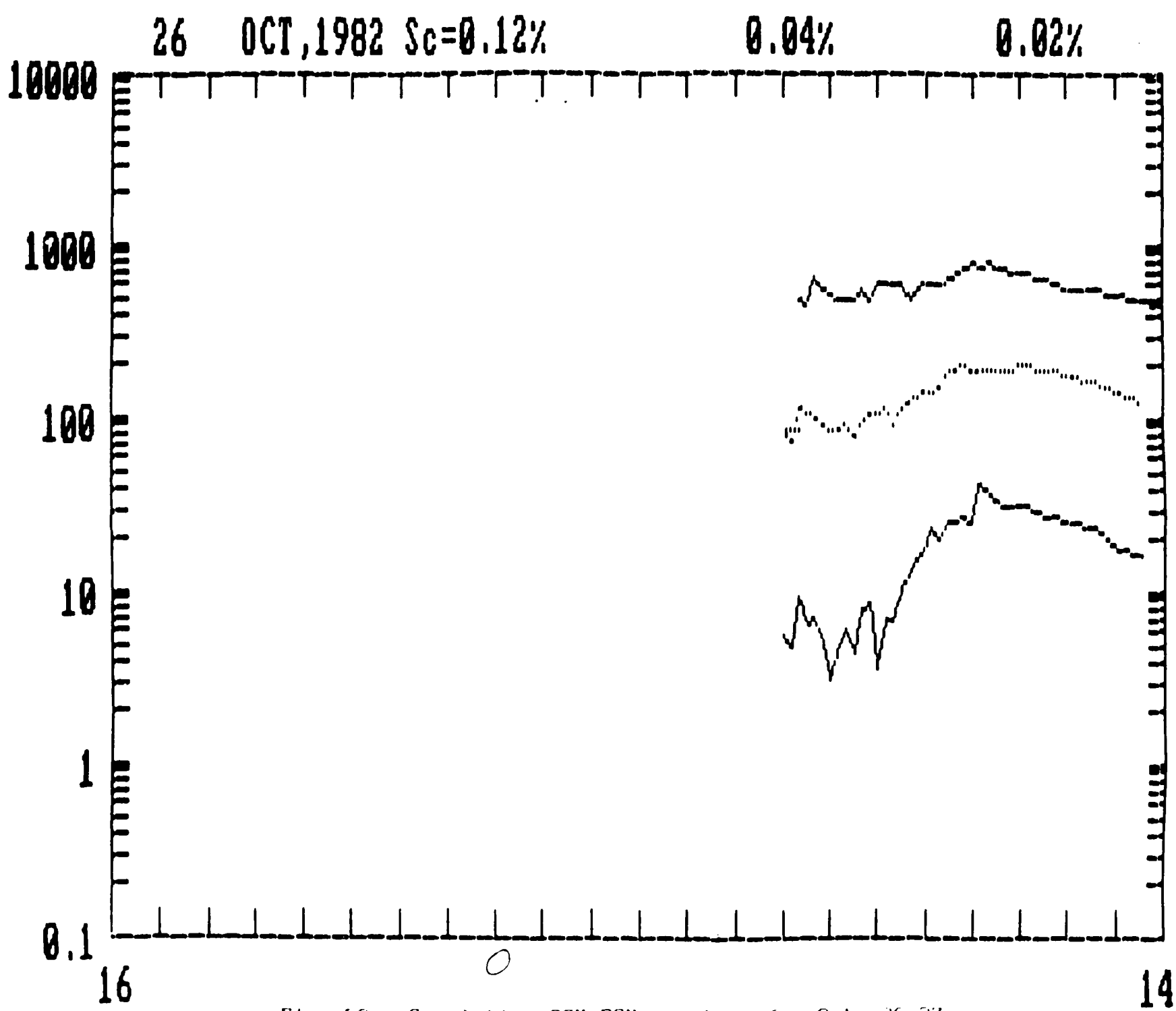

Fig. 50. Cumulative CCN-FCN vs. time for Oct. 26-27

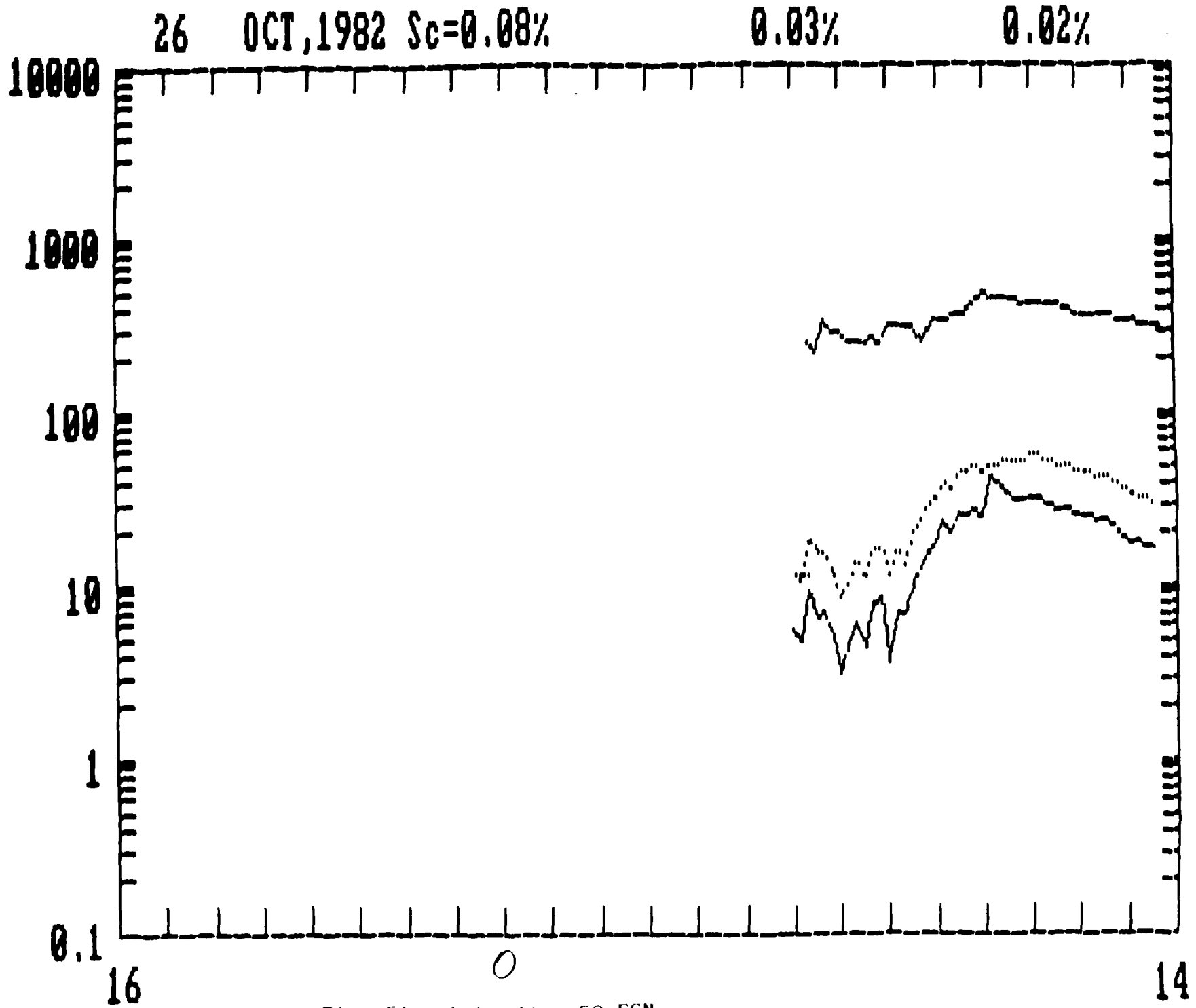

Fig. 51. Like fig. 50 FCN.

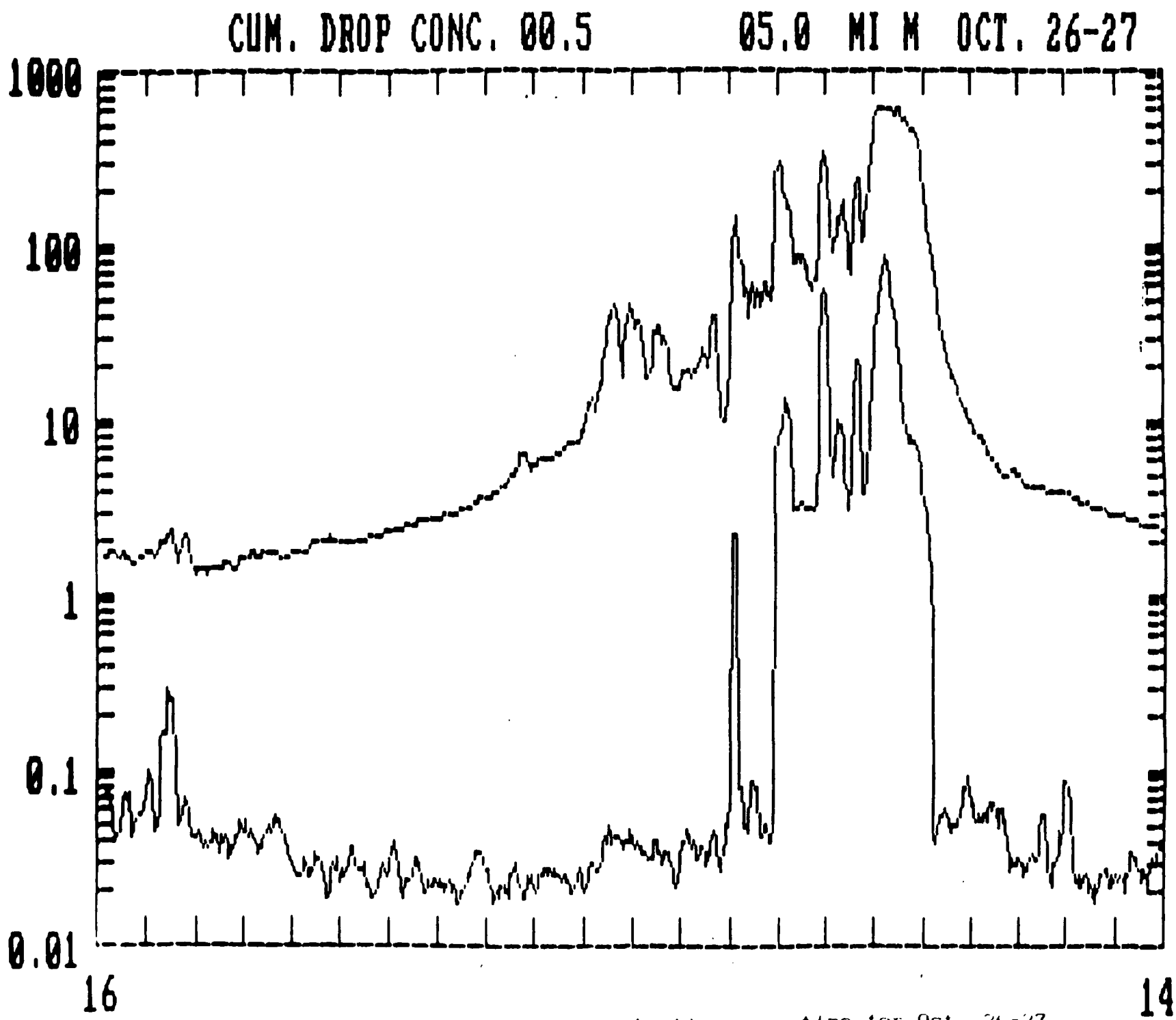

Fig. 52. Cumulative droplet concentrations vs. time for Oct. 26-27.

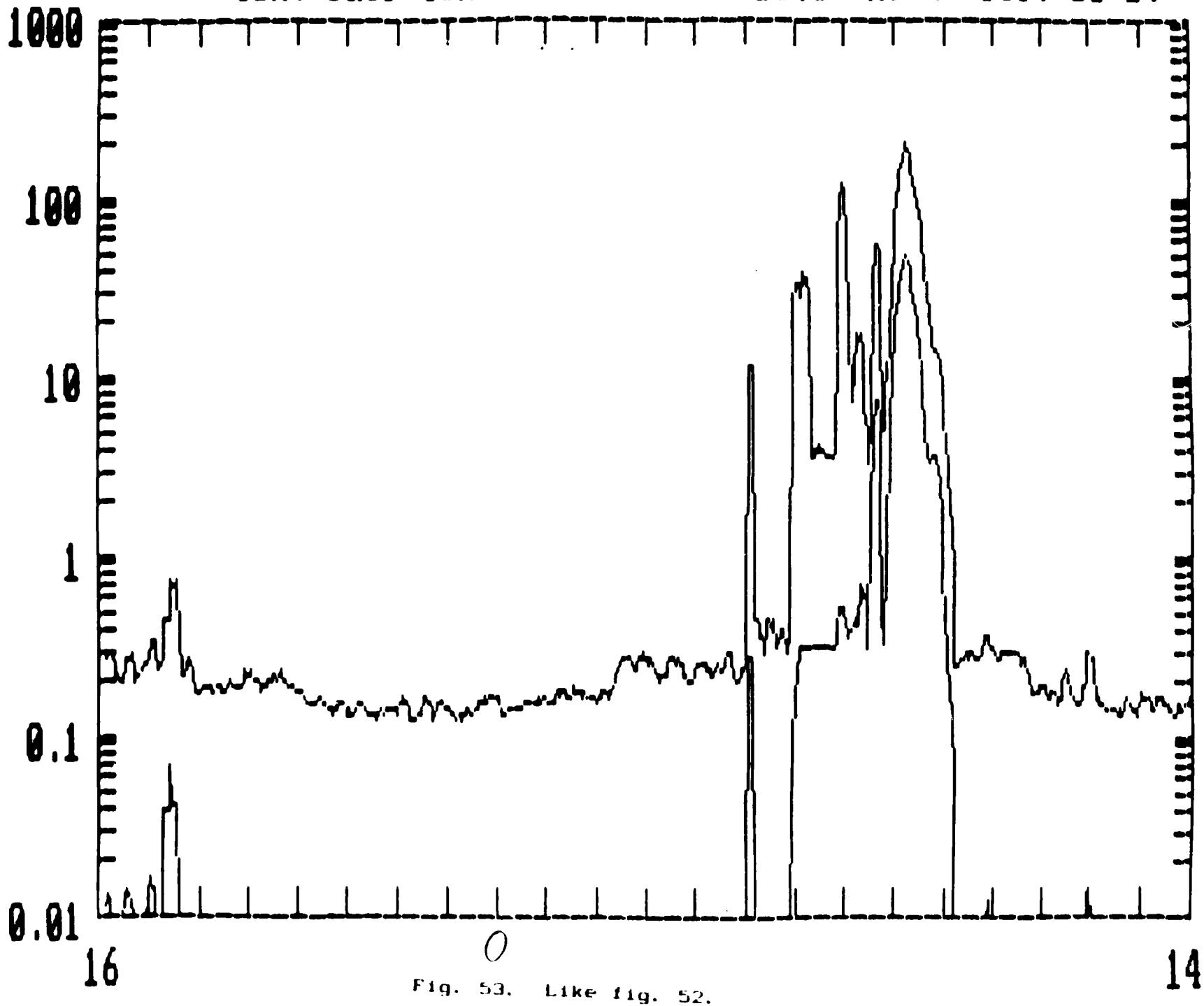

Fig. 53. Like fig. 52.

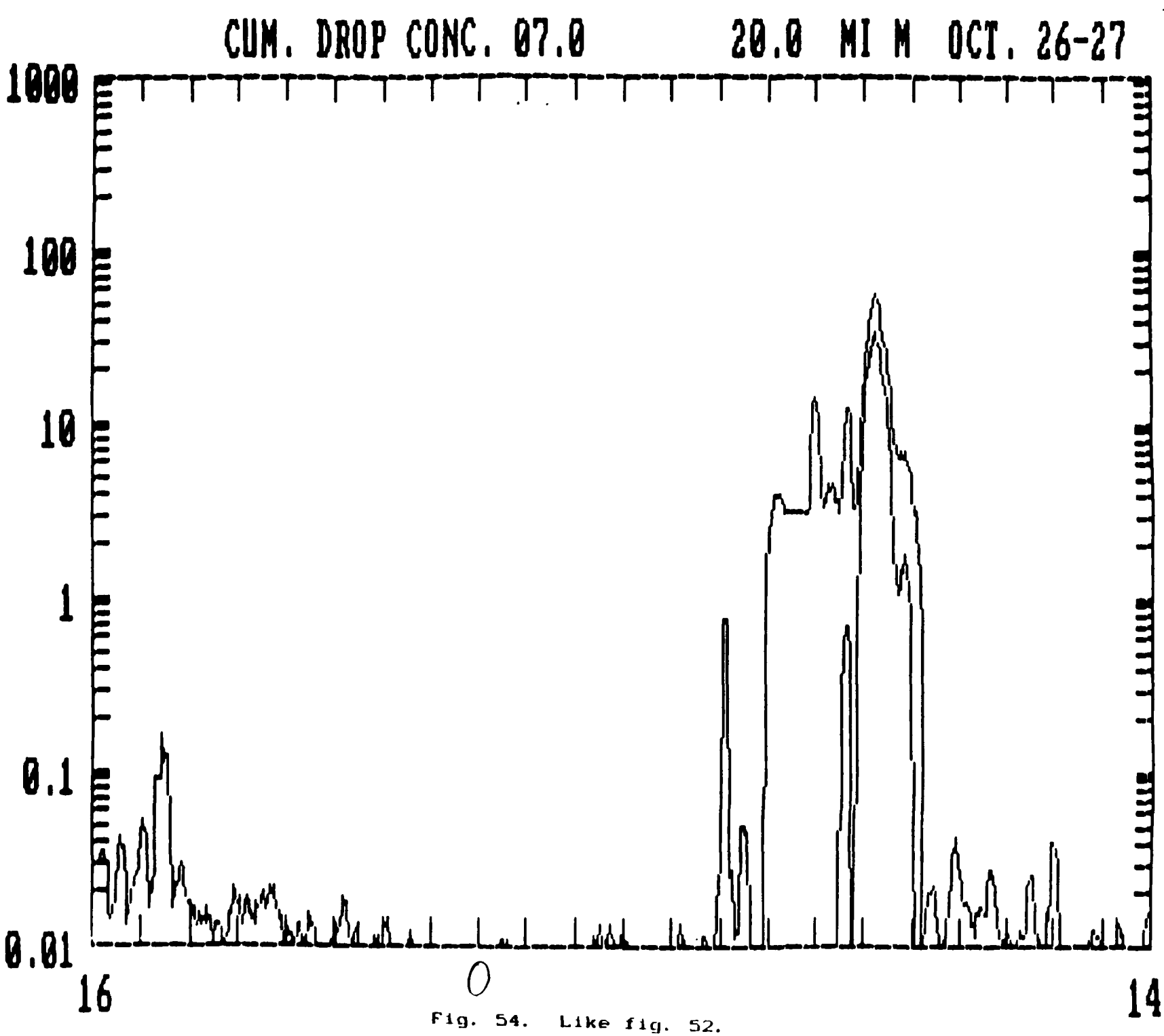

Fig. 54. Like fig. 52.

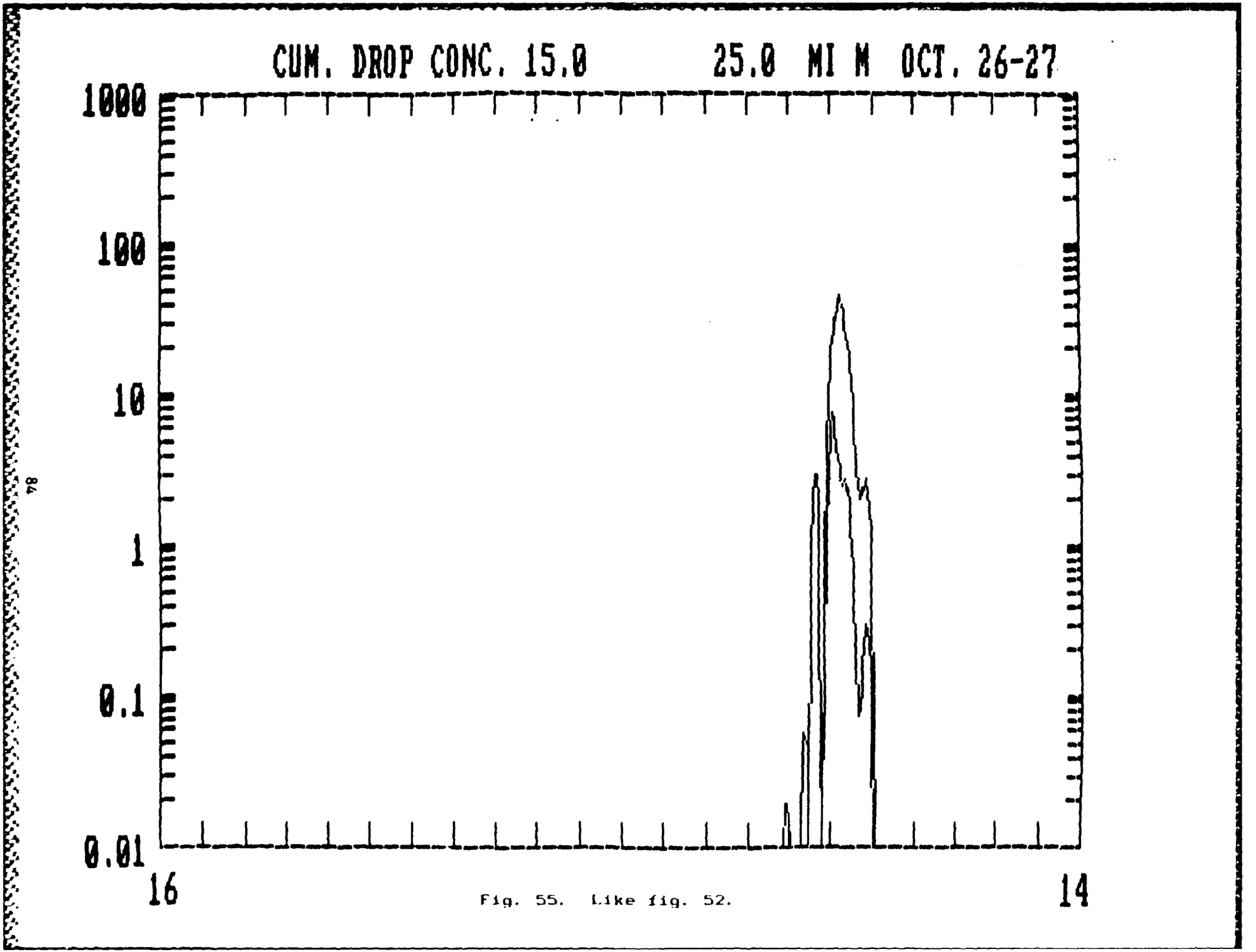

Fig. 55. Like fig. 52.

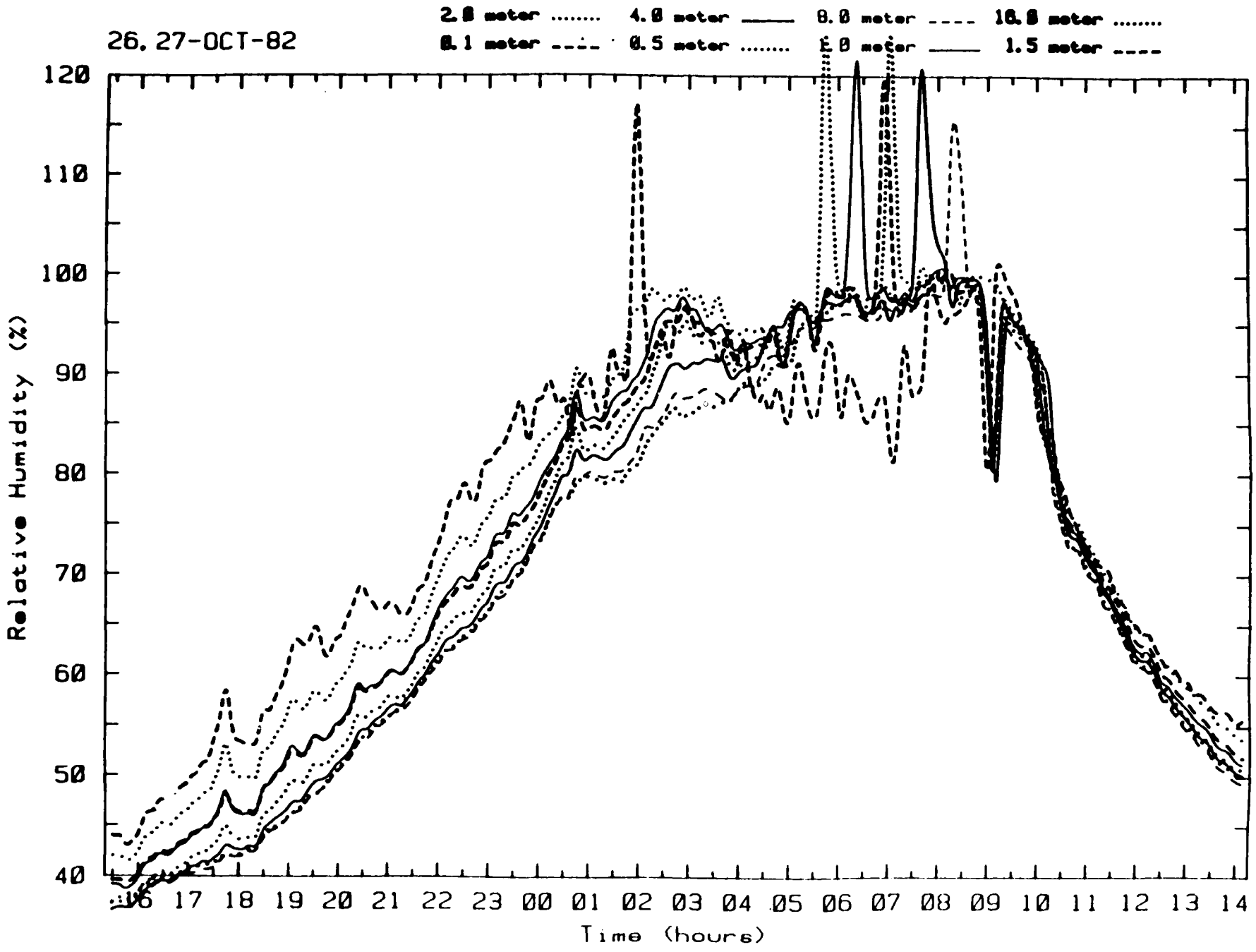

Fig. 56. Relative humidity vs. time for Oct. 26-27.

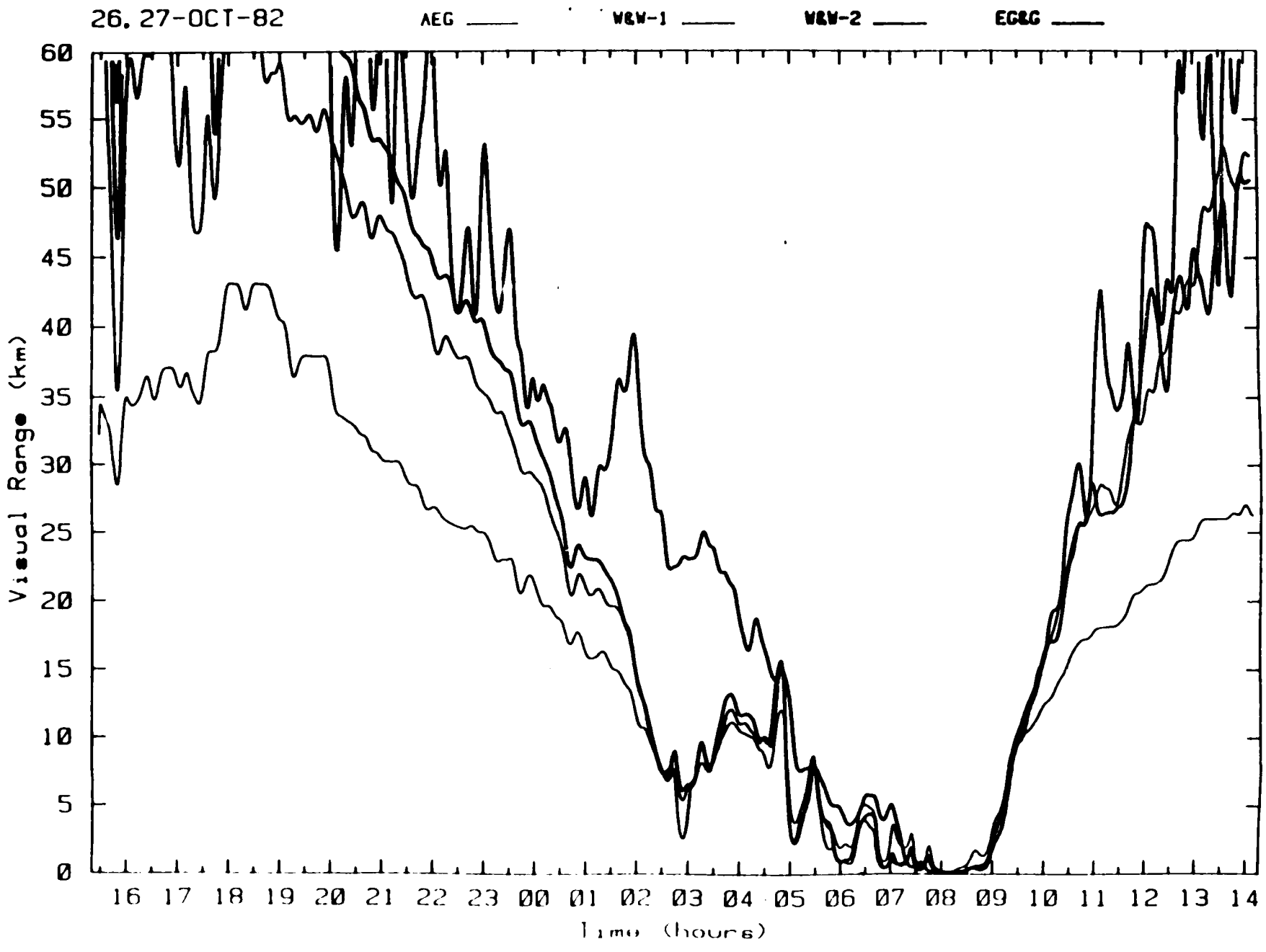

Fig. 57. Visibility vs. time for Oct. 26-27.

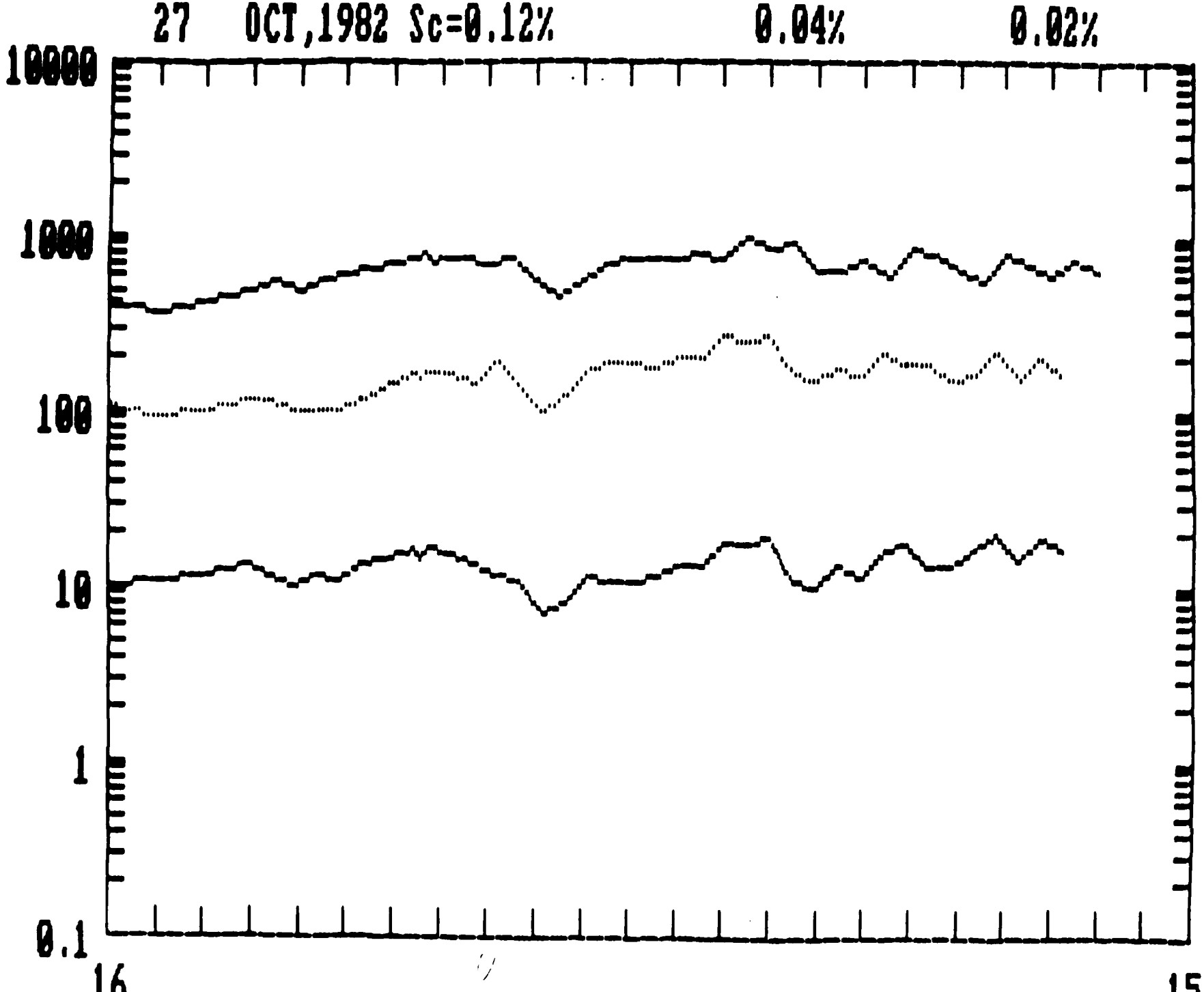

Fig. 58. Cumulative CCN-FCN concentrations vs. time for Oct. 27-28.

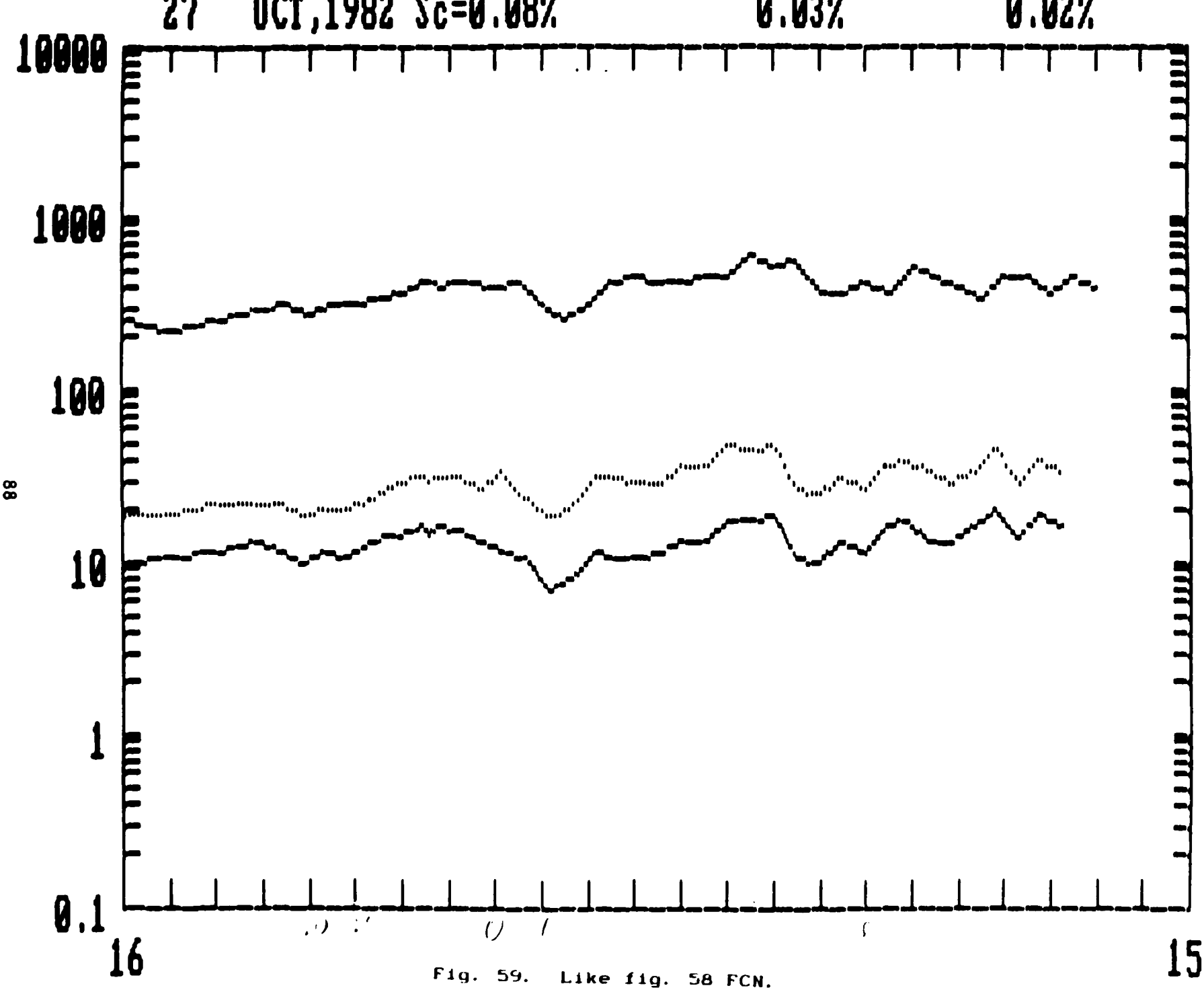

Fig. 59. Like fig. 58 FCN.

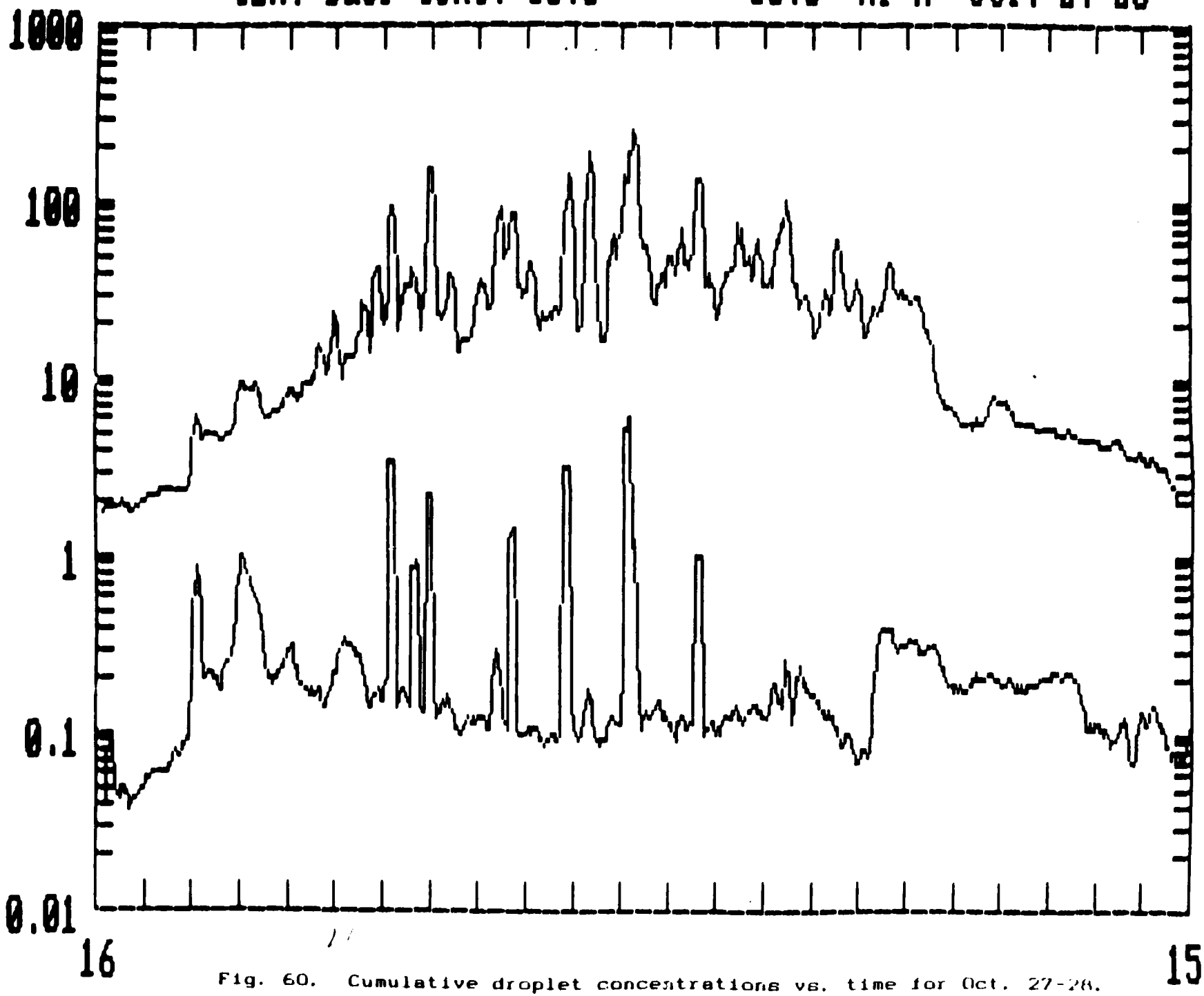

Fig. 60. Cumulative droplet concentrations vs. time for Oct. 27-28.

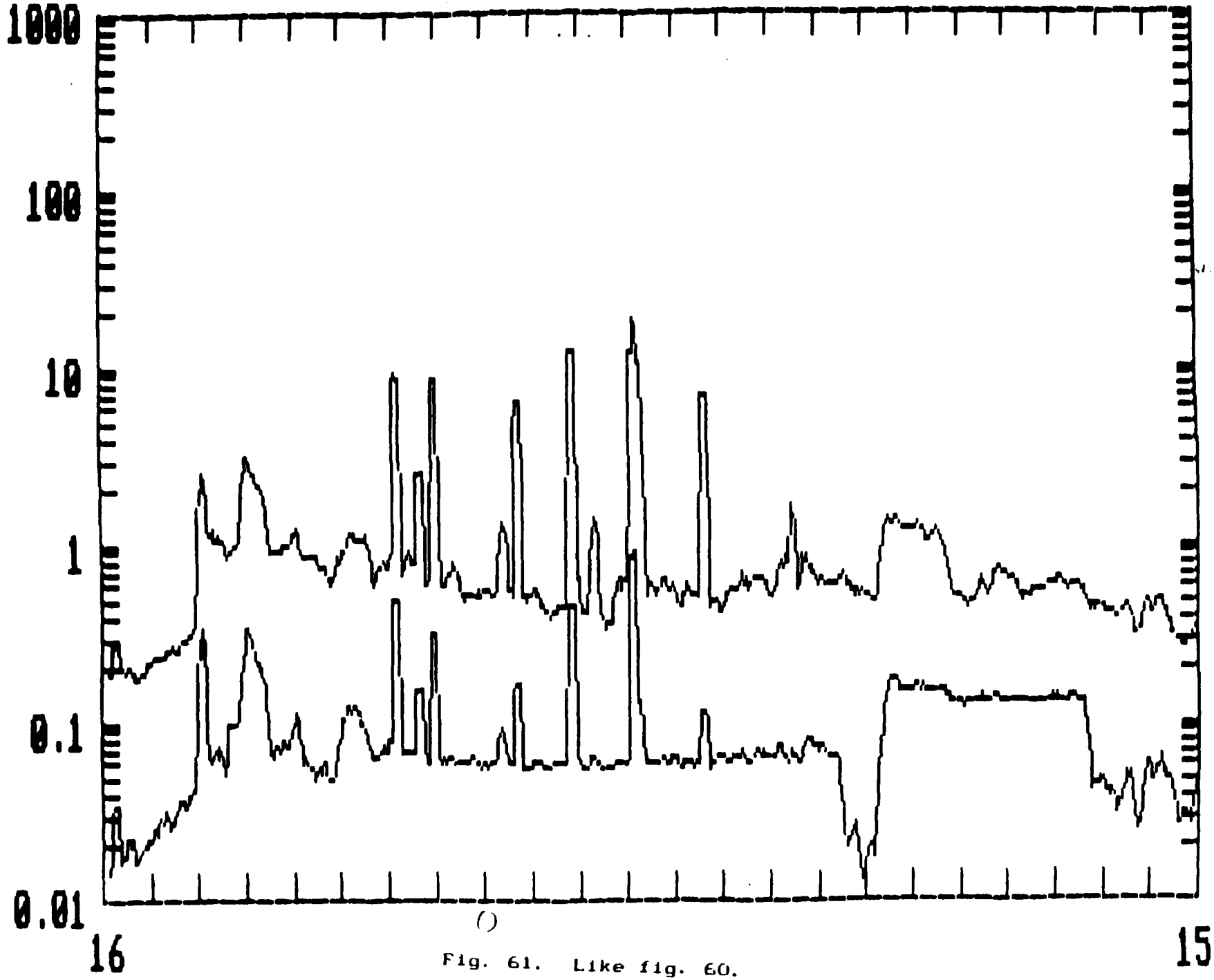

Fig. 61. Like fig. 60.

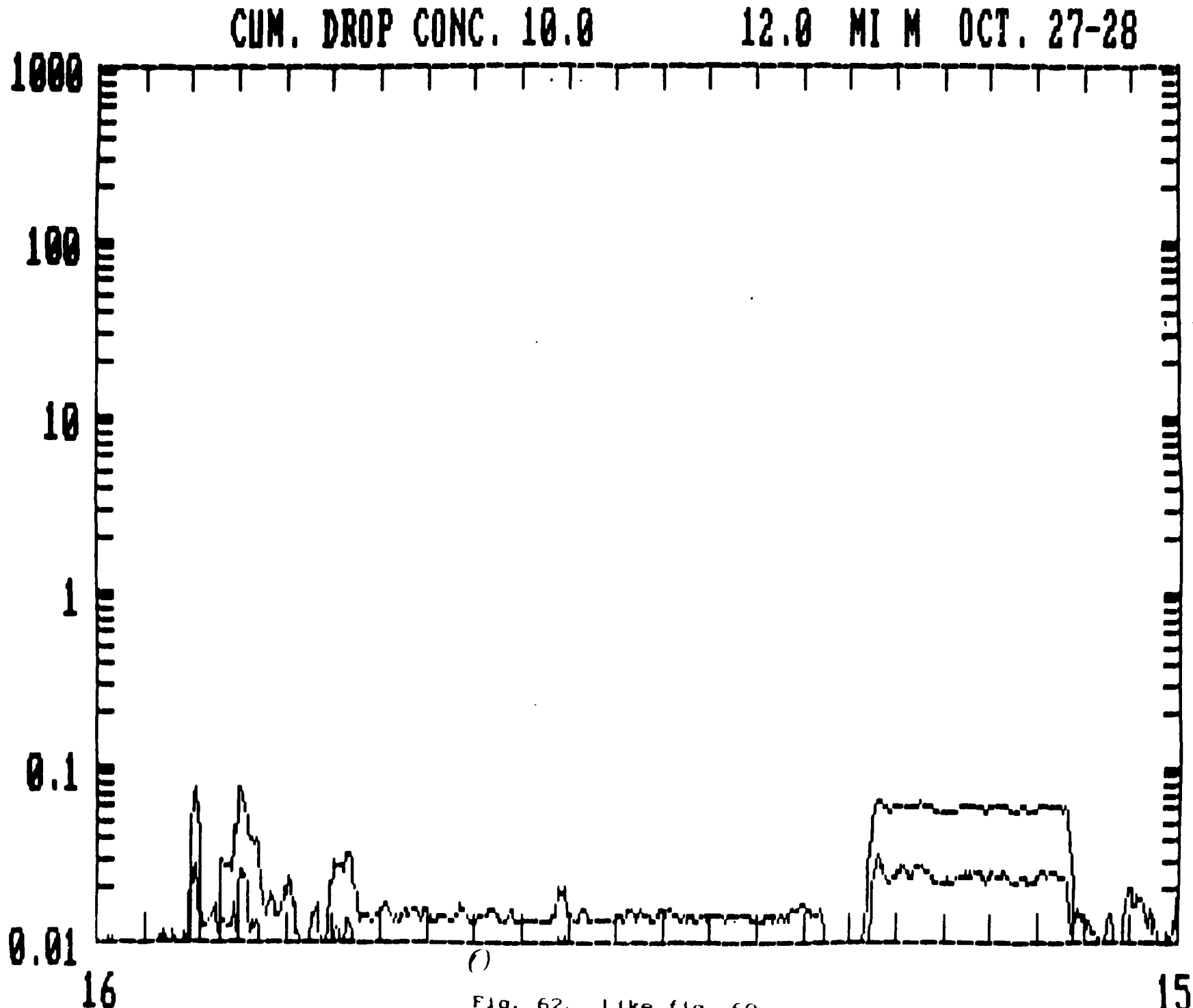

Fig. 62. Like fig. 60.

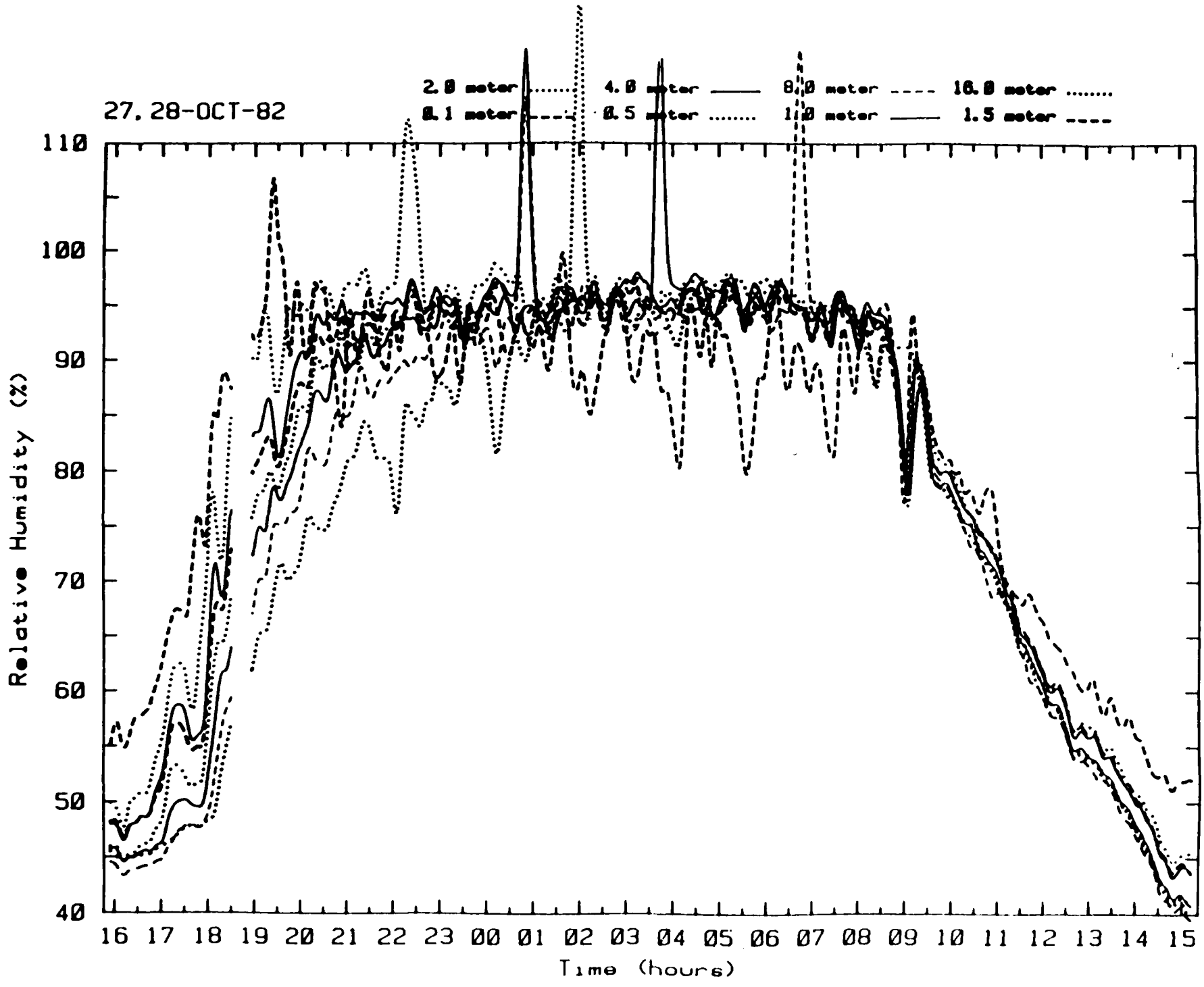

Fig. 64. Relative humidity vs. time for Oct. 27 28.

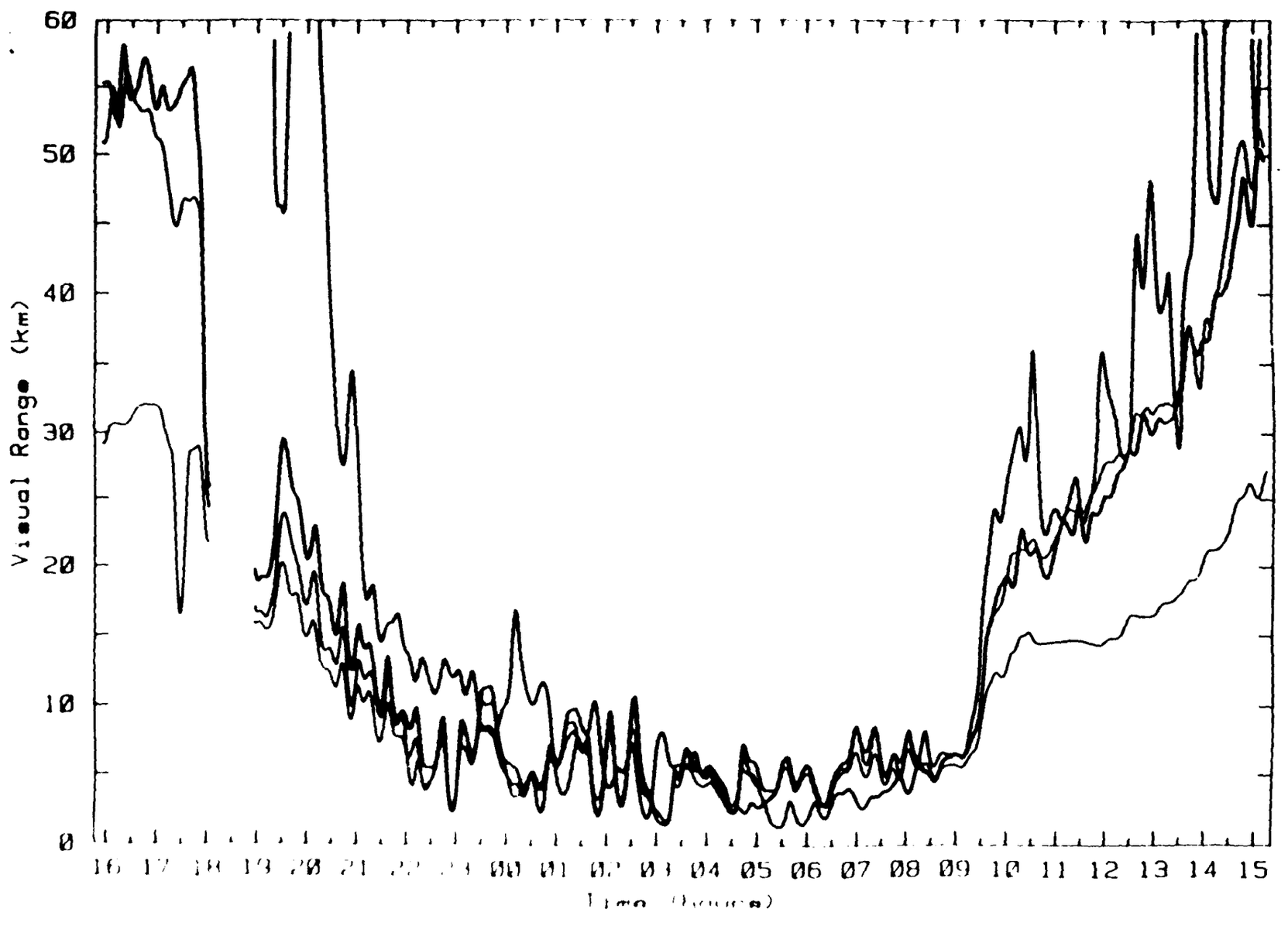

Fig. 64 Visibility vs. time for Oct. 27-28.

Appendix

to report Effects of CCN-FCN Spectra on Droplet Spectra in the Albany Fog Project

by James G. Hudson

The following figures are similar to figures 1 and 2 of the text. They display simultaneous droplet and nuclei spectra. The two nuclei spectra represent the equilibrum diameter of the droplets at 100% R.H. (left curve) and the critical diameter of the nuclei. These two curves are parallel and differ from each other in size by the factor 1.73. The other curve is the cumulative droplet spectra measured by a PMS probe. When the droplet curve intersects the critical diameter curve an effective supersaturation can be calculated. When the droplet curve is to the left of the critical curve the fog is probably not supersaturated. When the droplet curve is to the left of both nuclei curves the fog is subsaturated. When the small size portion of the droplet curve is to the left of both nuclei curves an instantaneous subsaturation is indicated. This can also be calculated (see text). Many more such curves were produced from the data but these are representative ones from the ten fog events. They display all of the possibilities in terms of humidity levels.

AD-A179 776 EFFECTS OF CCN-FCN (CLOUD CONDENSATION NUCLEI-FOG CONDENSATION NUCLEI) SP..(U) NEVADA UNIV RENO DESERT RESEARCH INST J G HUDSON 05 MAR 87 ARO-22342.1-GS 2/3

UNCLASSIFIED DAAG29-85-K-0037 F/G 4/1 NL

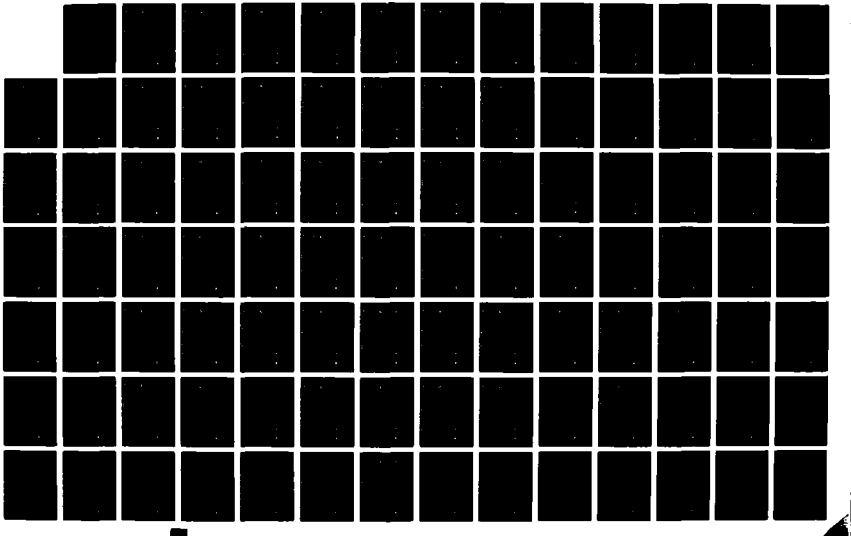


1.0
1.1
1.25
1.4
1.6
2.8
3.2
3.6
4.0
2.4
2.0
1.8

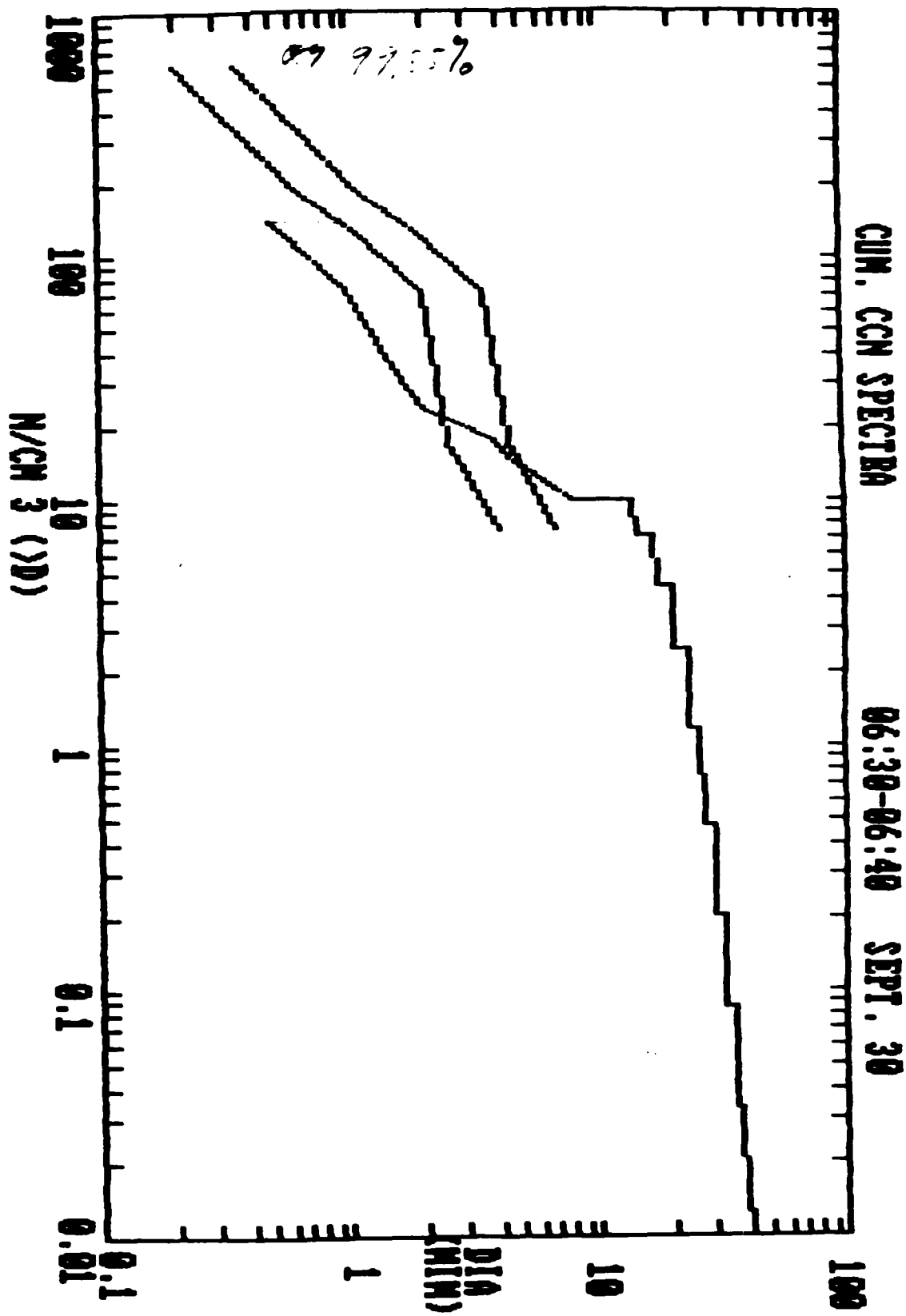
CUM. CCN SPECTRA
06:30-06:40 SEPT. 30
N/CM 3 (STP)
1000
100
10
1
0.1
0.01
0.1
1
10
100
DIA (MICRONS)

CUM. CCN SPECTRA
06:40-06:50 SEPT. 30
100
10
DIA (MIN)
1
0.1
0.01
0.1
1
10
100
1000
N/CM 3 (>D)

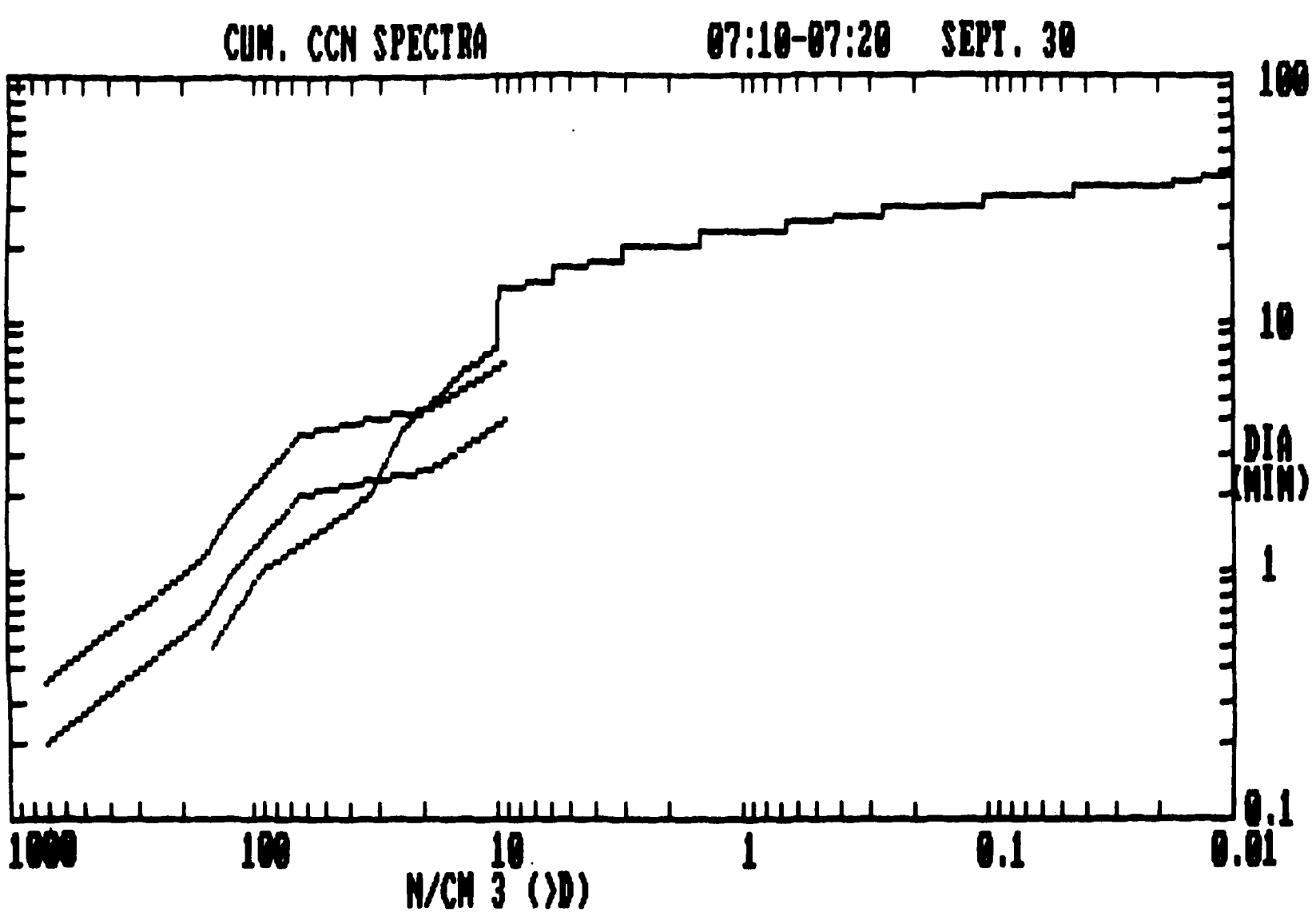
CUM. CCN SPECTRA
07:10-07:20 SEPT. 30
100
10
DIA
(MIM)
1
0.1
1000
100
10
1
0.1
0.01
N/CM 3 (>D)

CUM. CCN SPECTRA
07:20-07:30 SEPT. 30
100
10
DIA (MIN)
1
0.1
0.01
0.1
1
10
100
1000
N/CM 3 (>D)

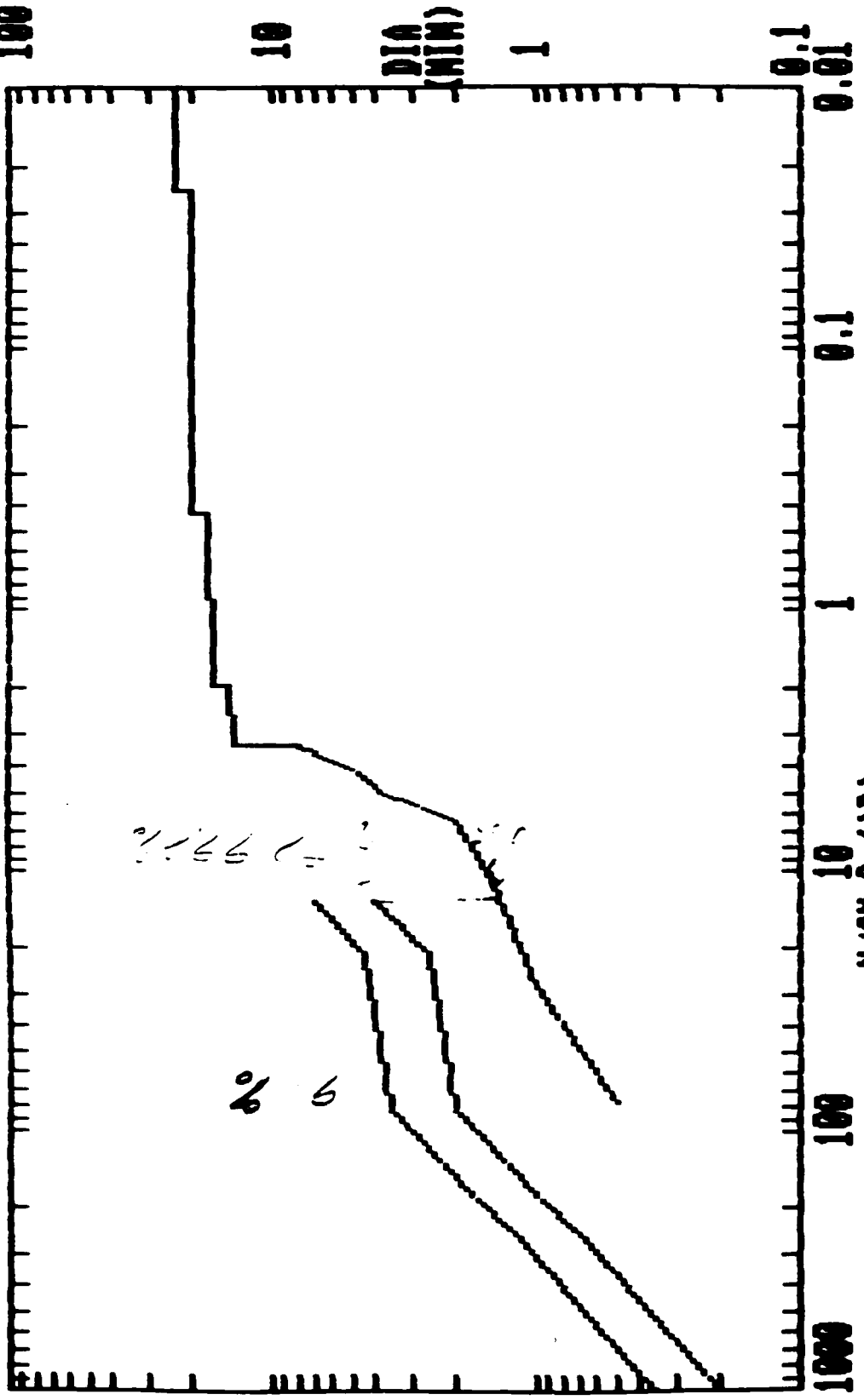
CUM. CCN SPECTRA
01:10-01:20 OCT.1
100
10
DIA (MIN)
1
0.1
0.01
0.1
1
10
100
1000
N/CM 3 (>D)

CUM. CCN SPECTRA
01:20-01:30 OCT. 1
100
10
DIA (MIN)
1
0.1
0.01
0.1
1
10
100
1000
N/CM 3 (>D)

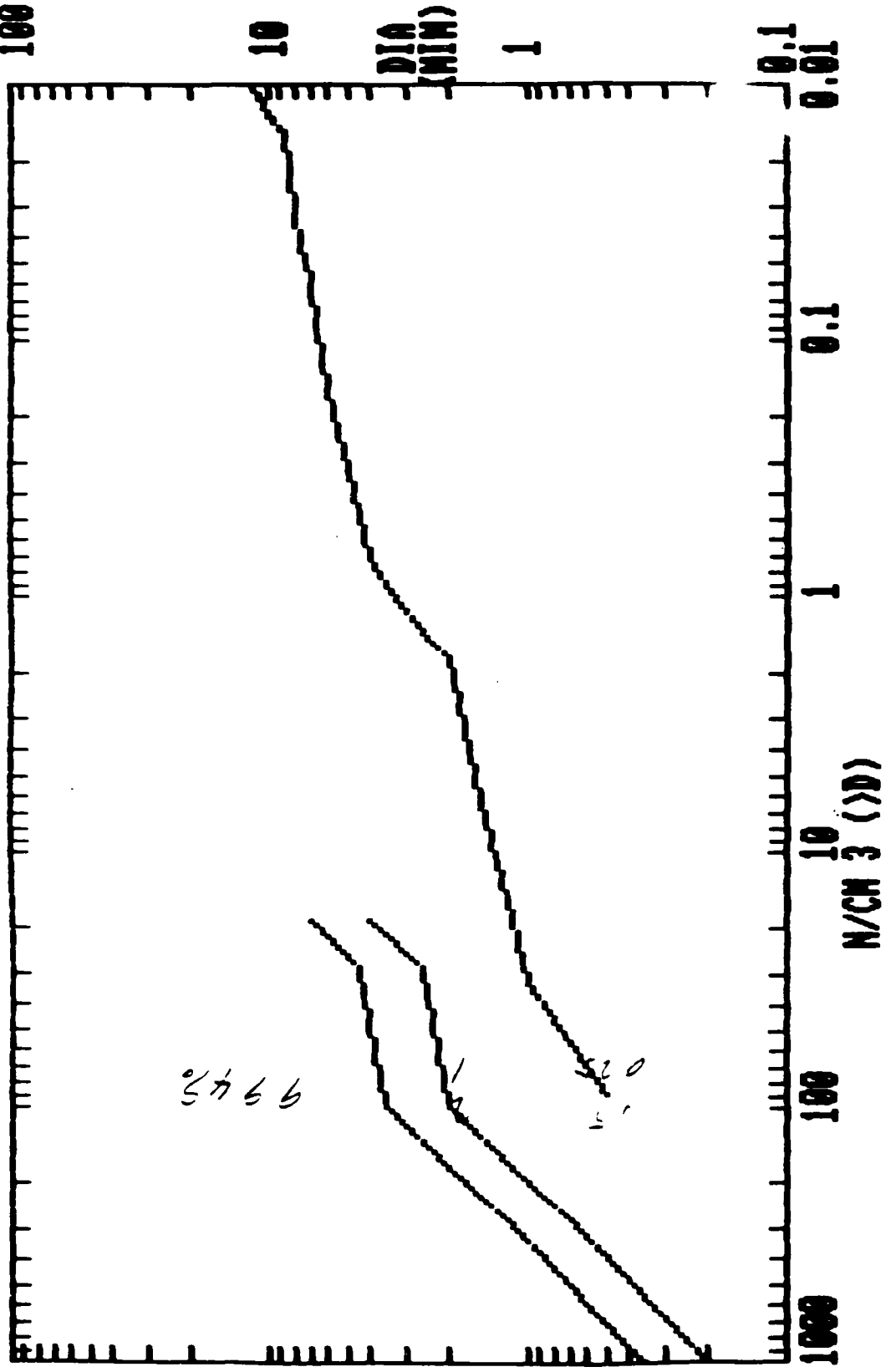
CUM. CCN SPECTRA
01:40-01:50 OCT. 1
DIA (MIN)
100
10
1
0.1
0.01
0.1
1
10
100
1000
N/CM 3 (>D)

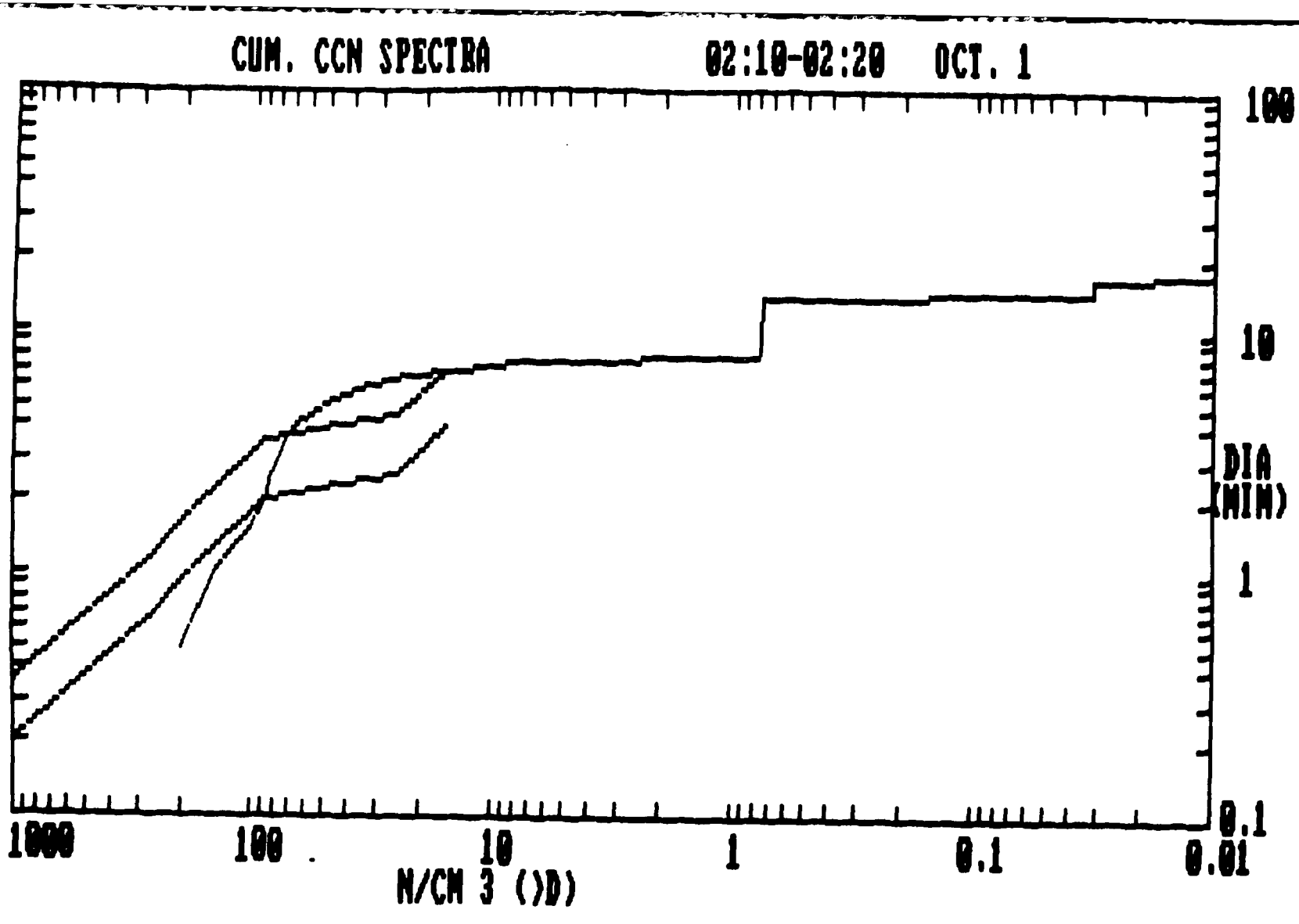
CUM. CCN SPECTRA
02:10-02:20 OCT. 1
100
10
DIA
(MIN)
1
0.1
1000
100
10
1
0.1
0.01
N/CM 3 ()D)

CUM. CCN SPECTRA
02:40-02:50 OCT. 1
100
10
DIA (MIM)
1
0.1
0.01
0.1
1
10
100
1000
N/CM 3 (>D)

CUM. CCN SPECTRA
02:50-03:00 OCT. 1
100
10
DIA (MICM)
1
0.1
0.01
0.1
1
10
100
1000
N/CM 3 (>D)

CUM. CCN SPECTRA
04:30-04:40 OCT. 1
100
10
DIA (MIN)
1
0.1
0.01
0.1
1
10
100
1000
N/CM 3 (>D)

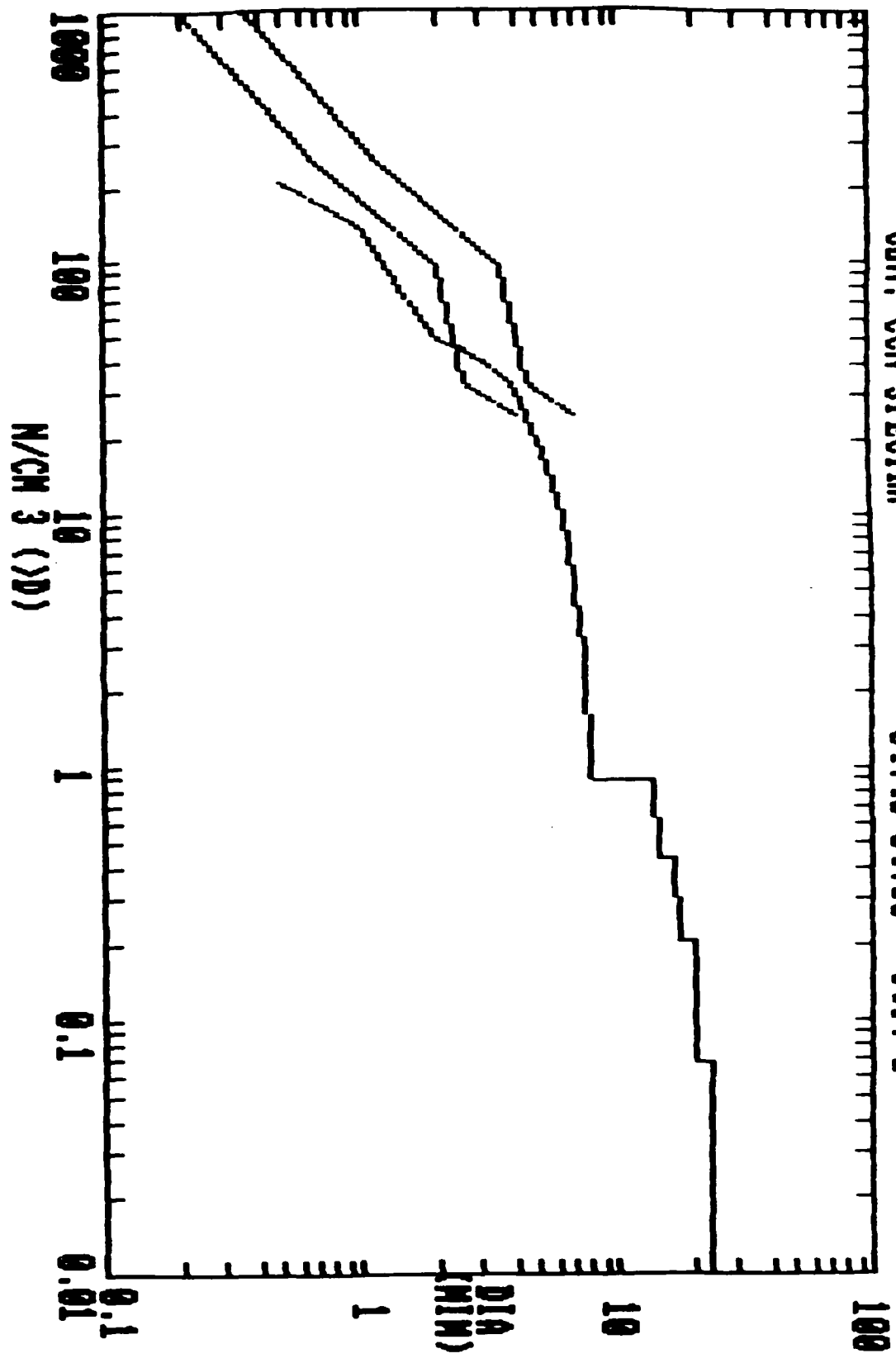
CUM. CCN SPECTRA
04:40-04:50 OCT. 1
N/CM 3 (>D)
1000
100
10
1
0.1
0.0
0.01
0.1
1
10
100
DIA (MICRON)

CUM. CCN SPECTRA
06:10-06:20 OCT. 1
100
10
DIA (MICRON)
1
0.1
0.01
0.1
1
10
100
1000
N/CM 3 (>D)

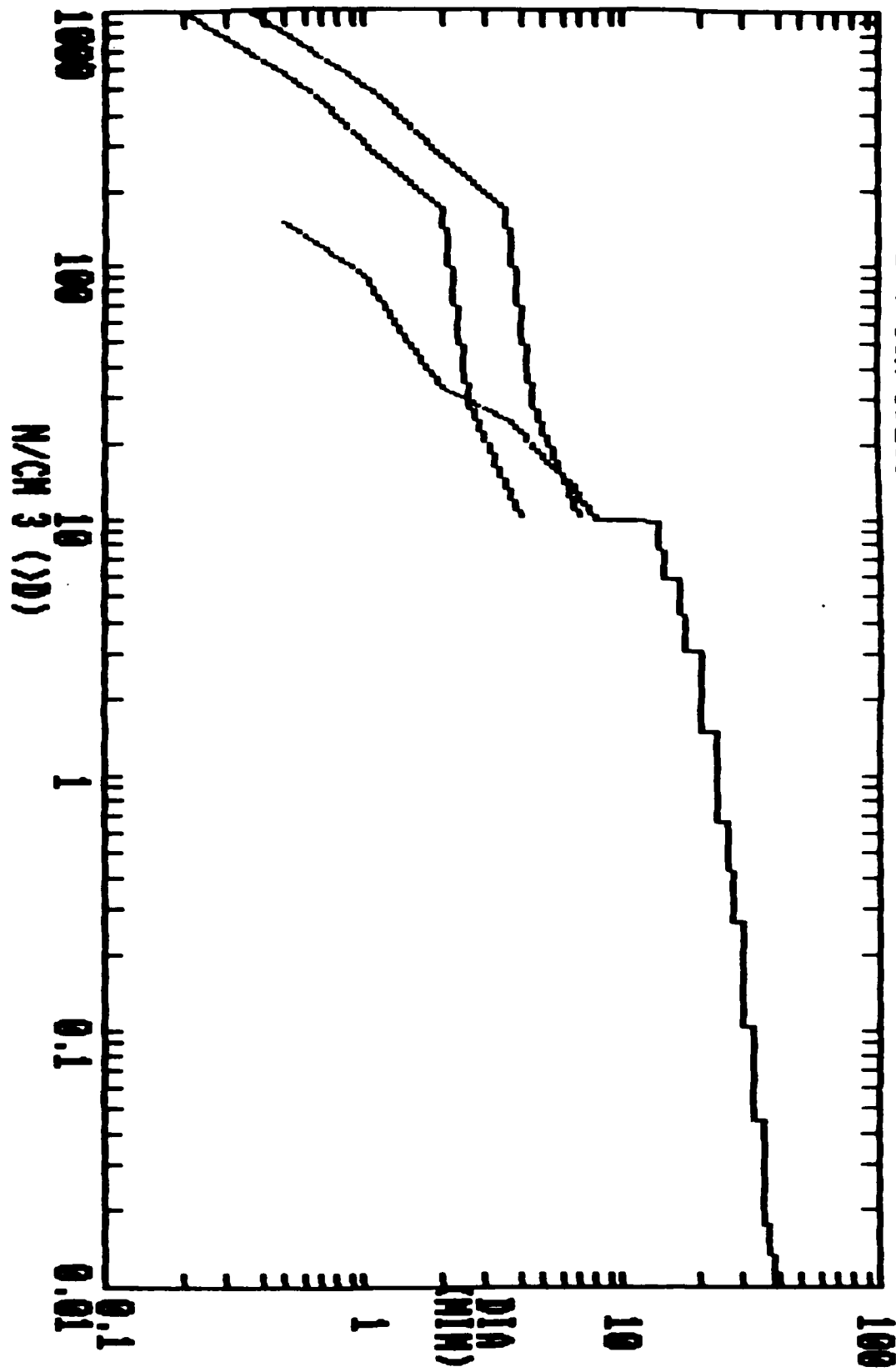
CUM. CCN SPECTRA
07:10-07:20 OCT. 1
N/CM 3 (STP)
1000
100
10
1
0.1
0.01
1.0
1
10
100
D(MIN) MICRONS

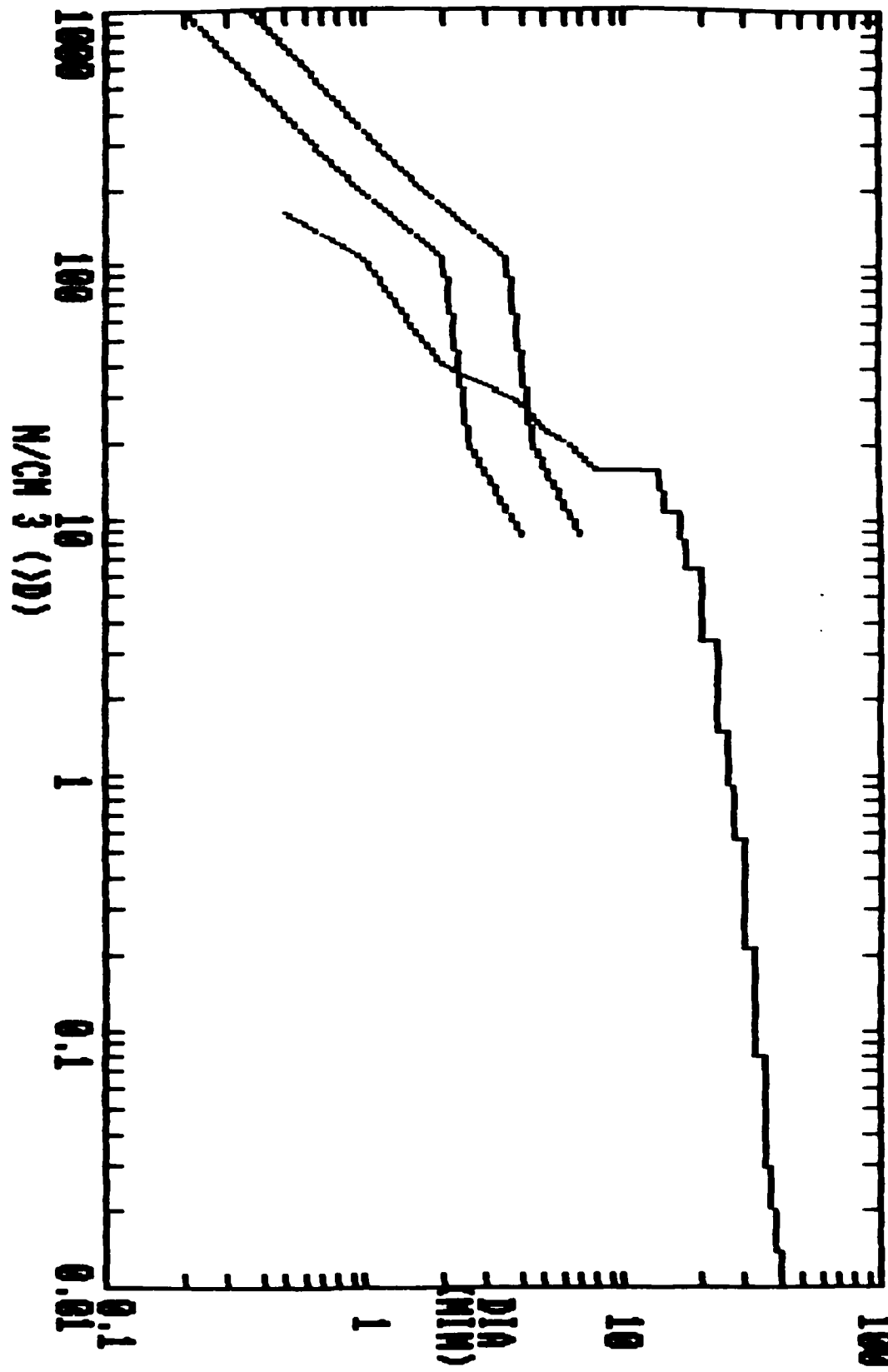
CUM. CCN SPECTRA
07:30-07:40 OCT. 1
N/CM 3 (D)
DIA (MICRON)
0.01
0.1
1
10
100
1000

CUM. CCN SPECTRA
07:40-07:50 OCT. 1
100
10
DIA (MIN)
1
0.1
0.01
0.1
1
10
100
1000
N/CM 3 (>D)

CUM. CCN SPECTRA
07:50-08:00 OCT. 1
100
10
DIA (MIN)
1
0.1
0.01
0.1
1
10
100
1000
N/CM 3 (>D)

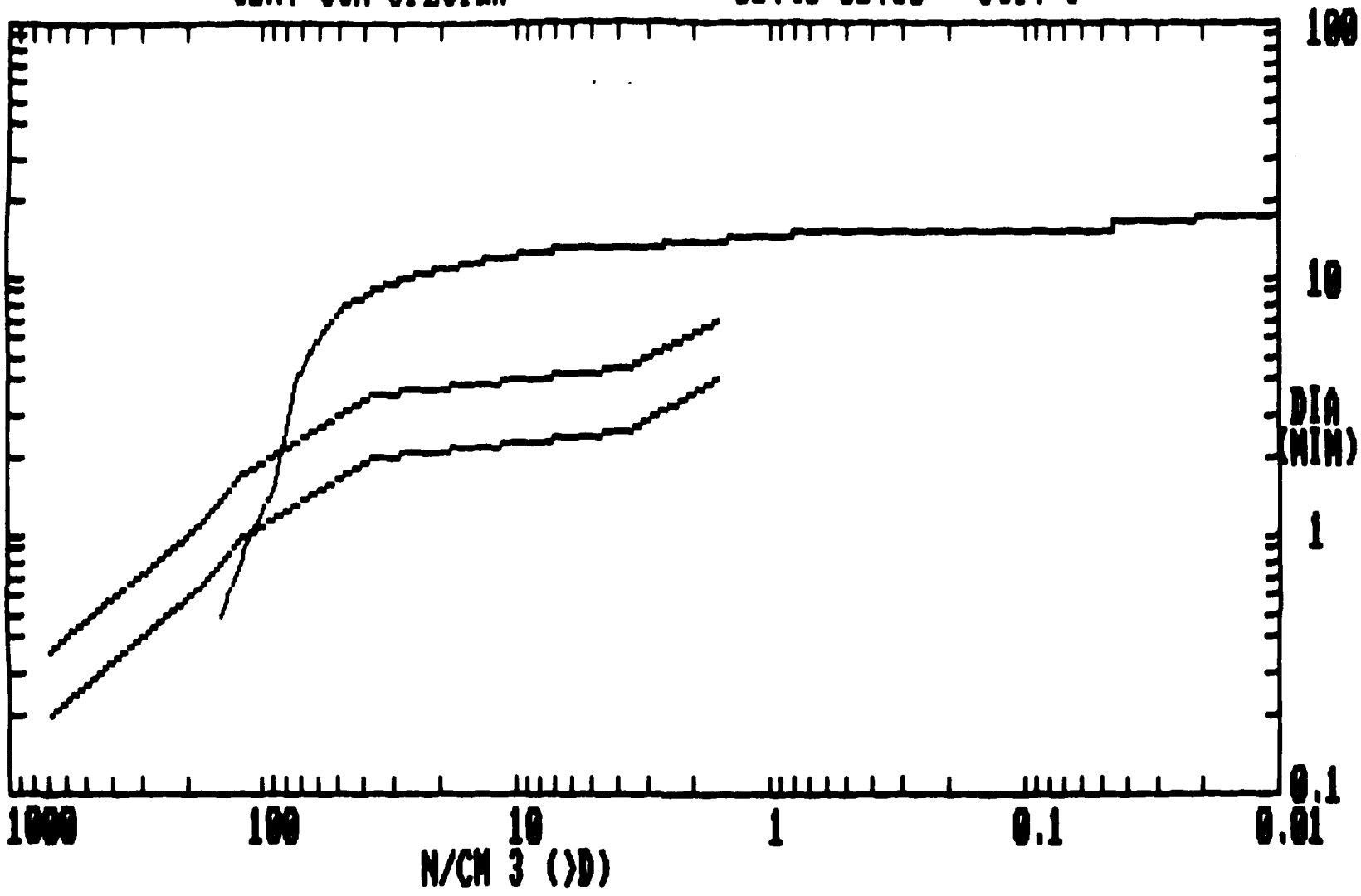
CUM. CCN SPECTRA
01:40-01:50 OCT. 3
100
10
DIA (MIN)
1
0.1
1000
100
10
1
0.1
0.01
N/CM 3 (>D)

CUM. CCN SPECTRA
01:50-02:00 OCT. 3
100
10
DIA (MIN)
1
0.1
0.01
0.1
1
10
100
1000
N/CM 3 (>D)

CUM. CCN SPECTRA
02:40-02:50 OCT. 3
DIA (MIN)
100
10
1
0.1
0.01
0.1
1
10
100
1000
N/CM 3 (>D)

CUM. CCN SPECTRA
02:50-03:00 OCT. 3
DIA (MIN)
100
10
1
0.1
0.01
0.1
1
10
100
1000
N/CM 3 (>D)

CUM. CCN SPECTRA
04:00-04:10 OCT. 3
DIA (MIN)
100
10
1
0.1
0.01
0.1
1
10
100
1000
N/CM 3 (>D)

CUM. CCN SPECTRA
04:10-04:20 OCT. 3
100
10
DIA (MICRON)
1
0.1
0.01
0.1
1
10
100
1000
N/CM 3 (>D)

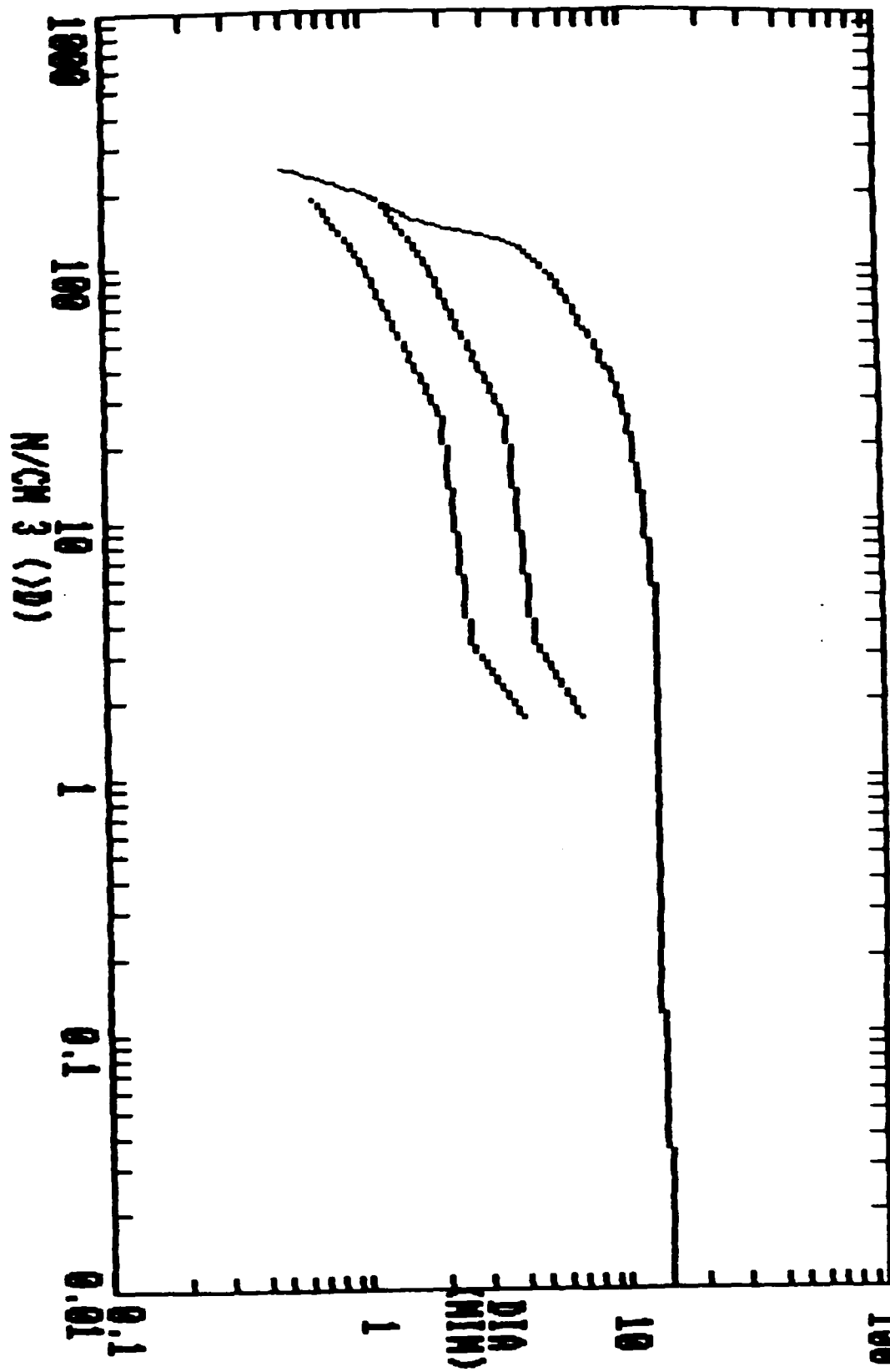
CUM. CCN SPECTRA
04:30-04:40 OCT. 3
N/CM 3 (>D)
1000
100
10
1
0.1
0.01
0.1
1
10
100
D1D (MICRON)

CUM. CCN SPECTRA
05:00-05:10 OCT. 3
DIA (MIN)
100
10
1
0.1
0.01
0.1
1
10
100
1000
N/CM 3 (>D)

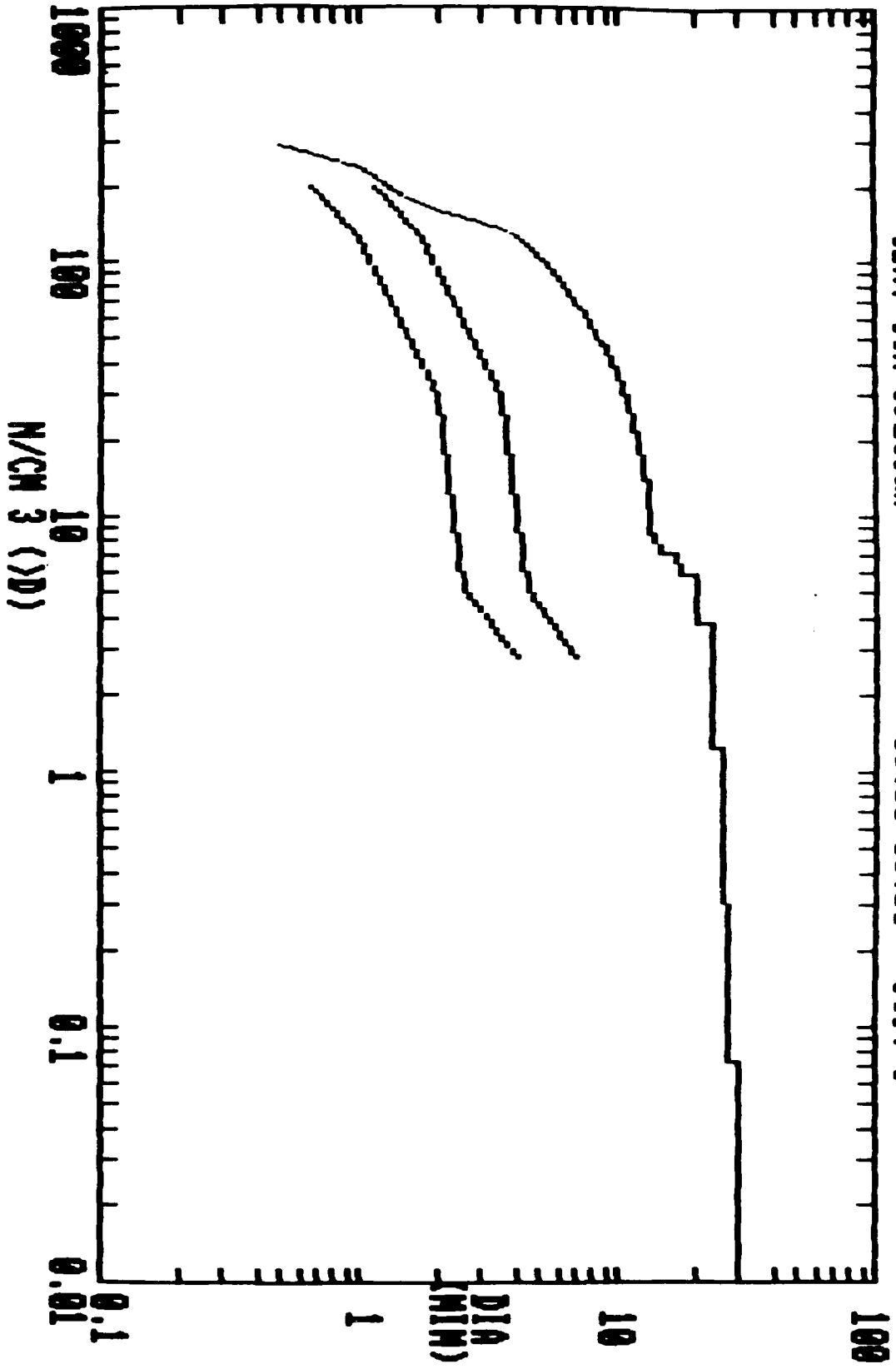
CUM. CCN SPECTRA
05:10-05:20 OCT. 3
N/CM 3 (>D)
DIA (MIN)
0.01
0.1
1
10
100
1000

CUM. CCN SPECTRA
06:00-06:10 OCT. 3
100
10
1
0.1
DIA (MIN)
0.01
1000
100
10
1
0.1
N/CM 3 (>D)

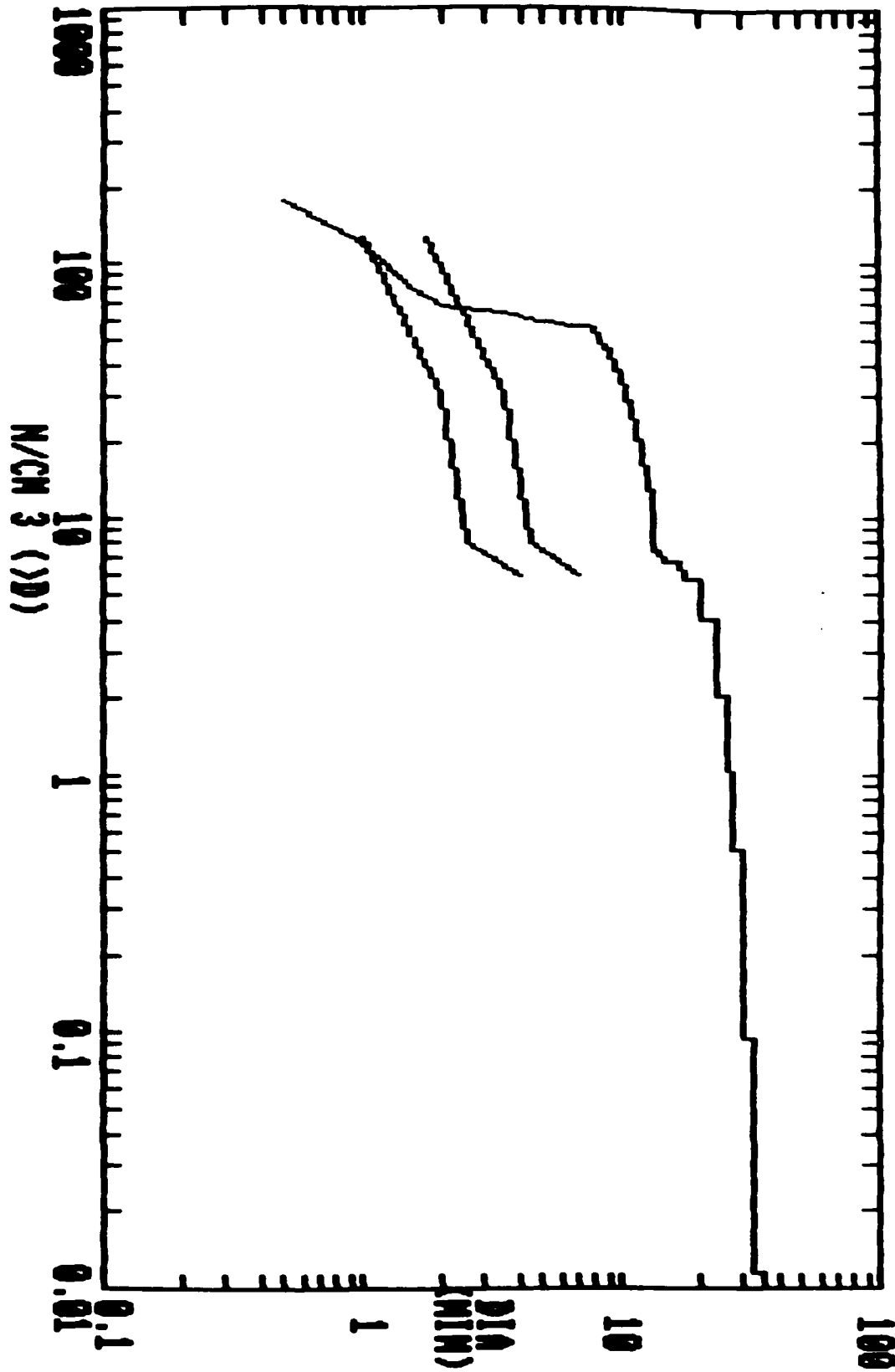
CUM. CCN SPECTRA
06:20-06:30 OCT. 3
N/CM 3 (K)
1000
100
10
1
0.1
0.01
0.1
1
10
100
(MICRON)

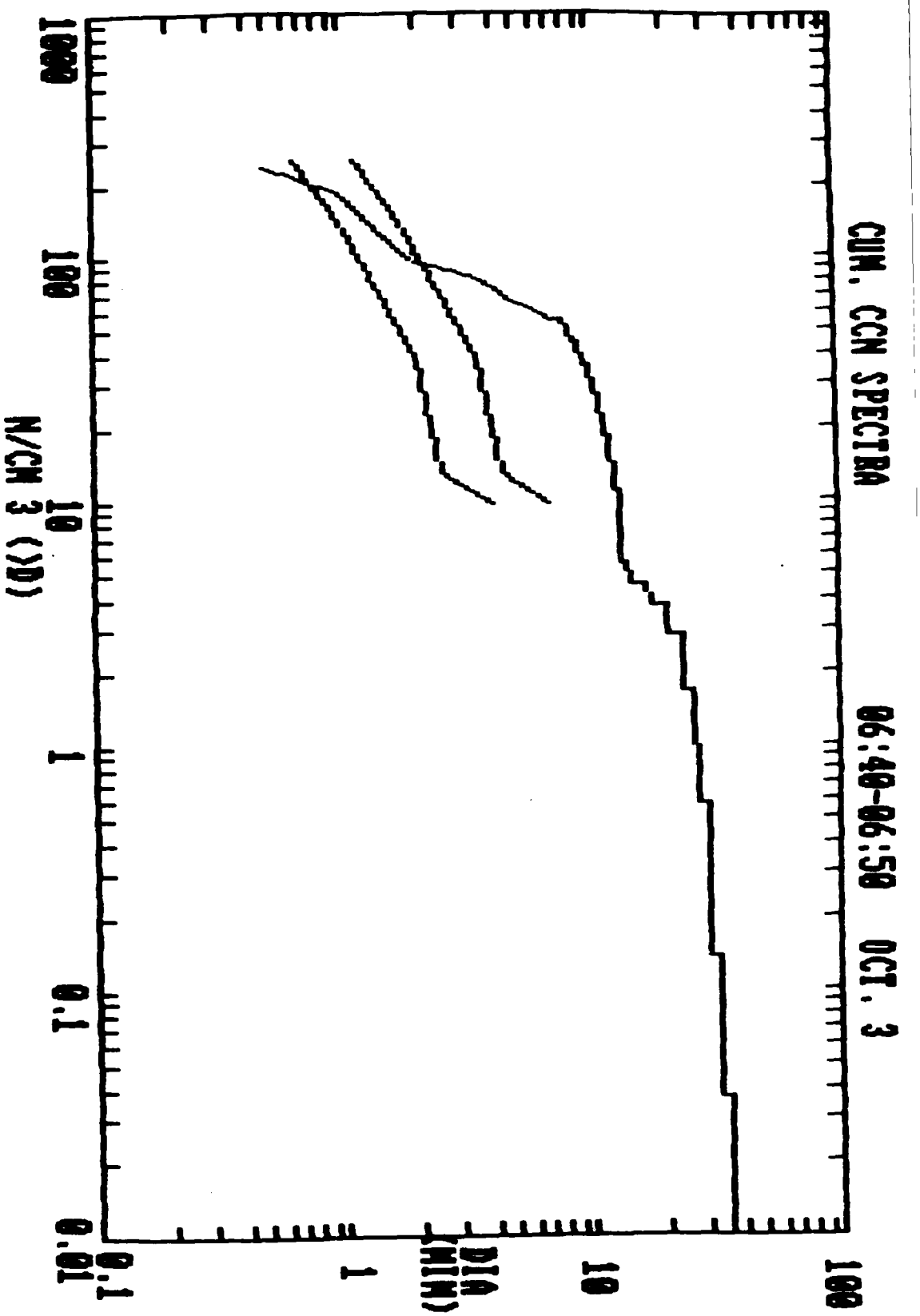
CUM. CCN SPECTRA
06:40-06:50 OCT. 3
N/CM 3 (>D)
DIA (MICRON)
0.01
0.1
1
10
100
1000

CUM. CCN SPECTRA
06:50-07:00 OCT. 3
100
10
DIA (MIN)
1
0.1
0.01
0.1
1
10
100
1000
N/CM 3 (>D)

CUM. CCN SPECTRA
07:00-07:10 OCT. 3
100
10
DIA (MIN)
1
0.1
0.01
0.1
1
10
100
1000
N/CM 3 (>D)

CUM. CCN SPECTRA
07:20-07:30 OCT. 3
100
10
DIA (MIN)
1
0.1
0.01
0.1
1
10
100
1000
N/CM 3 (>D)

CUM. CCN SPECTRA
07:40-07:50 OCT. 3
DIA (MIN)
100
10
1
0.1
0.01
1000
100
10
1
0.1
N/CM 3 (>D)

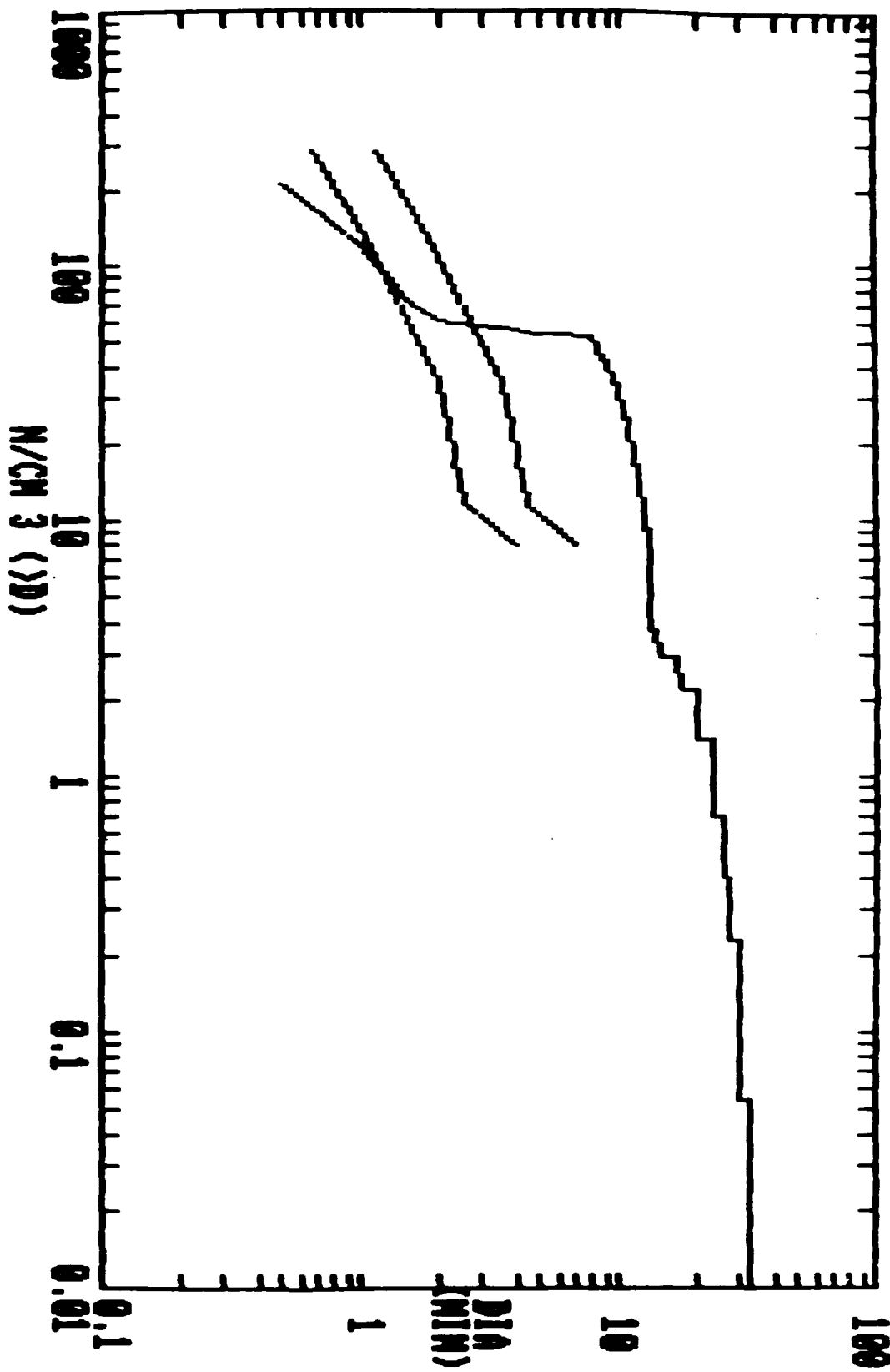
CUM. CCN SPECTRA
08:00-08:10 OCT. 3
N/CM 3 ()()
1000
100
10
1
0.1
0.01
0.1
1
10
100
DIA (MICRONS)

CUM. CCN SPECTRA
08:10-08:20 OCT. 3
100
10
DIA (MIN)
1
0.1
0.01
0.1
1
10
100
1000
N/CM 3 (>D)

CUM. CCN SPECTRA
08:20-08:30 OCT. 3
DIA (MIN)
100
10
1
0.1
0.01
0.1
1
10
100
1000
N/CM 3 (>D)

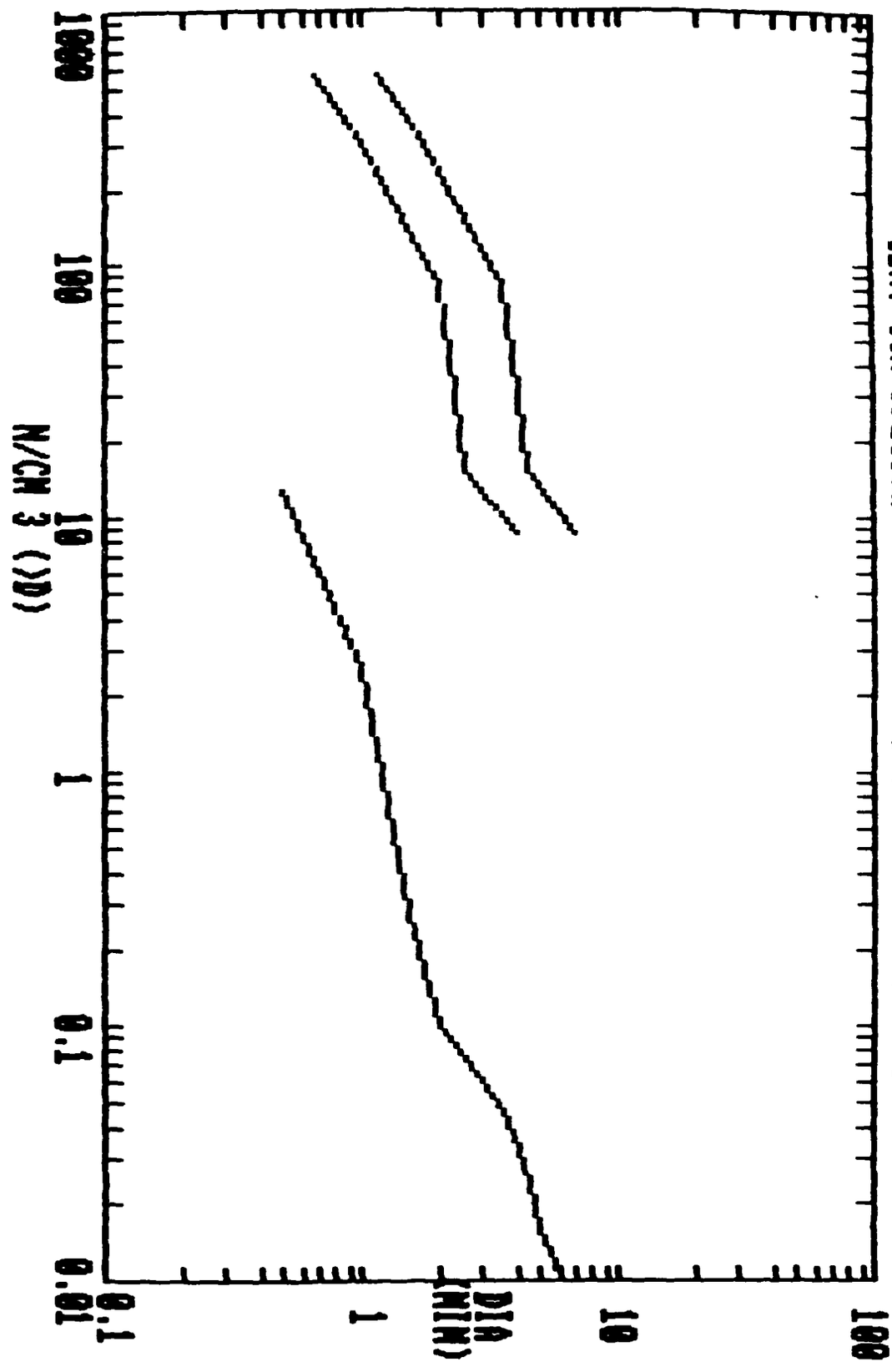
CUM. CCN SPECTRA
08:30-08:40 OCT. 3
N/CM 3 ()()
1000
100
10
1
0.1
0.0
0.01
0.1
1
10
100
DIA (MICRONS)

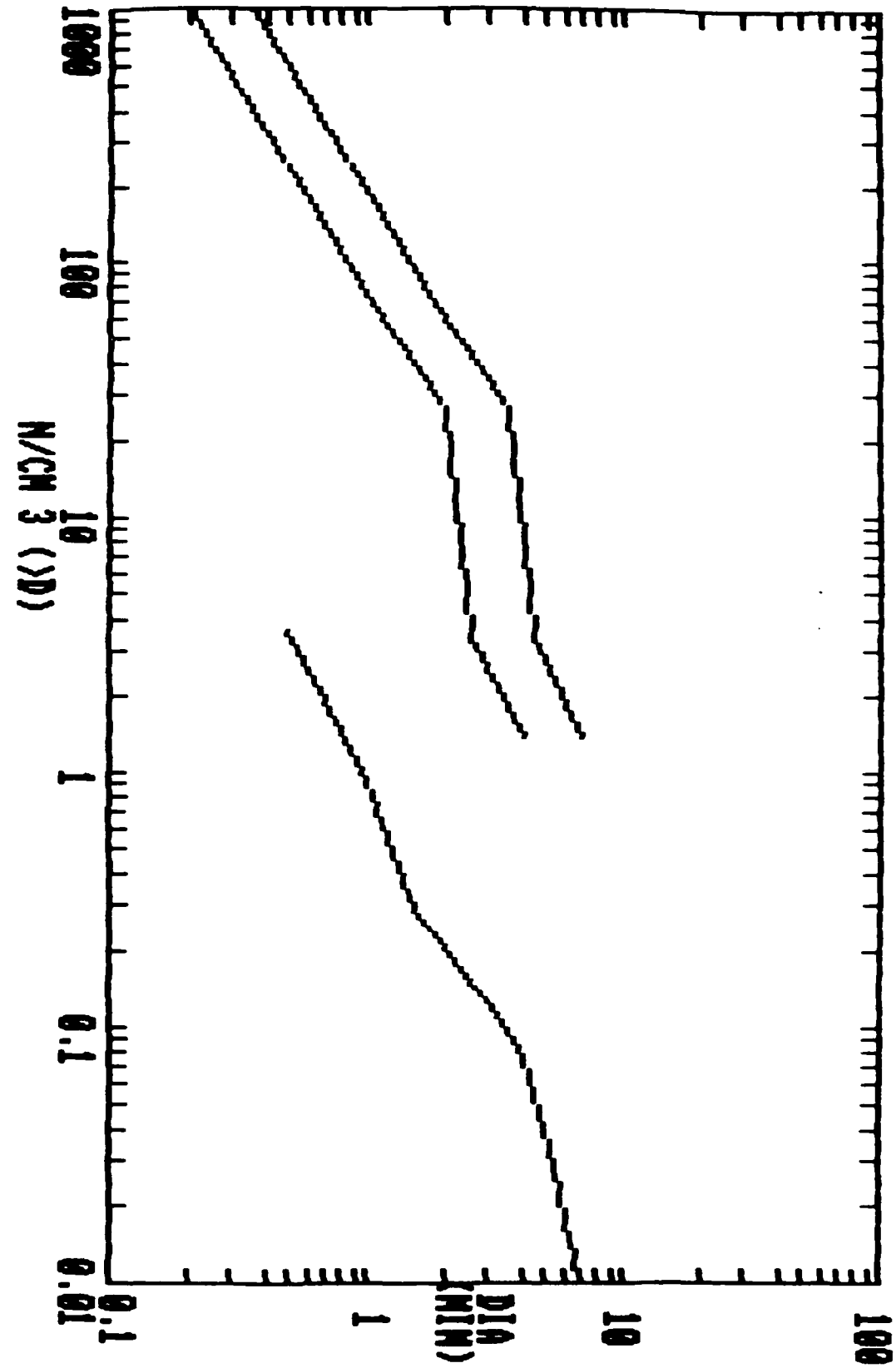
CUM. CCN SPECTRA
02:10-02:20 OCT. 5
N/CM 3 (D)
0.01
0.1
1
10
100
1000
0.01
0.1
1
10
100
DIA (MIN)

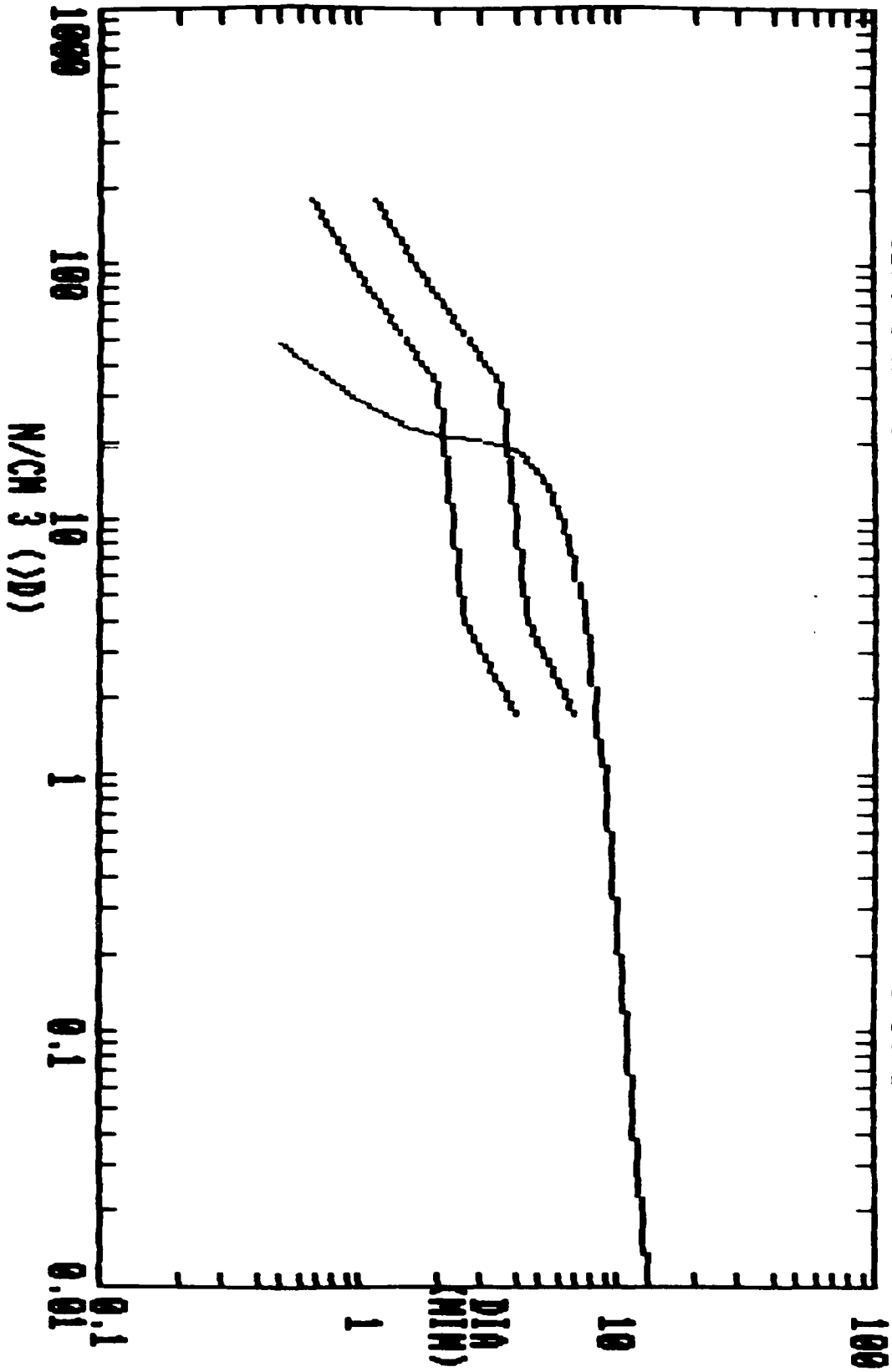
CUM. CCN SPECTRA
02:20-02:30 OCT. 5
N/CM 3 (>D)
DIA (MIN)
0.01
0.1
1
10
100
1000

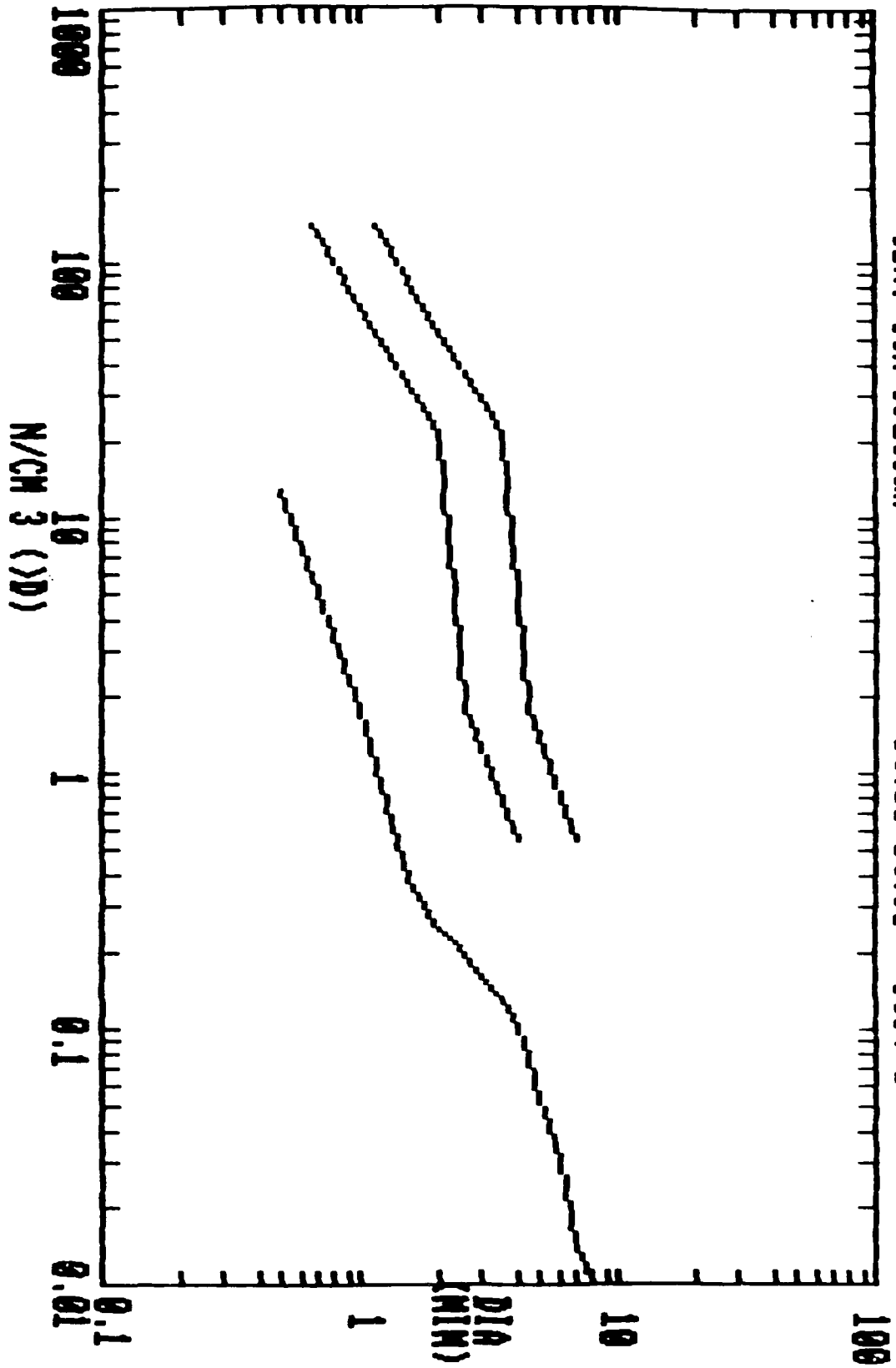
CUM. CCN SPECTRA
04:20-04:30 OCT. 5
N/CM 3 (D)
1000
100
10
1
0.1
0.01
0.1
1
10
100
DIA (MIN)

CUM. CCN SPECTRA
04:30-04:40 OCT. 5
100
10
DIA (MIN)
1
0.1
0.01
0.1
1
10
100
1000
N/CM 3 (>D)

CUM. CCN SPECTRA
04:40-04:50 OCT. 5
DIA (MIN)
100
10
1
0.1
0.01
0.1
1
10
100
1000
N/CM 3 (>D)

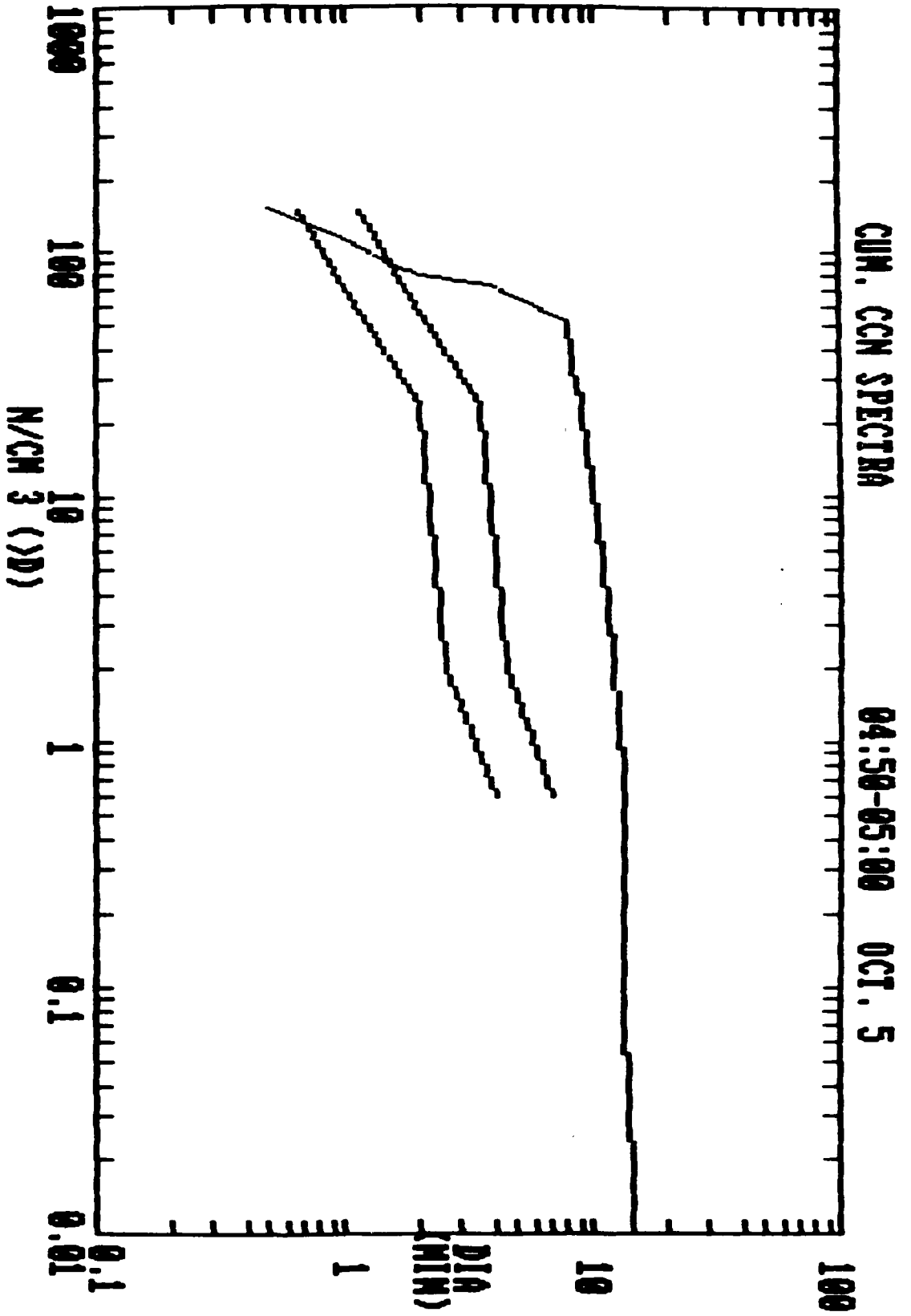
CUM. CCN SPECTRA
04:50-05:00 OCT. 5
N/CM 3 (>D)
DIA (MIN)
0.01
0.1
1
10
100
1000

CUM. CCN SPECTRA
05:00-05:10 OCT. 5
100
10
DIA (MIN)
1
0.1
0.01
0.1
1
10
100
1000
N/CM 3 (>D)

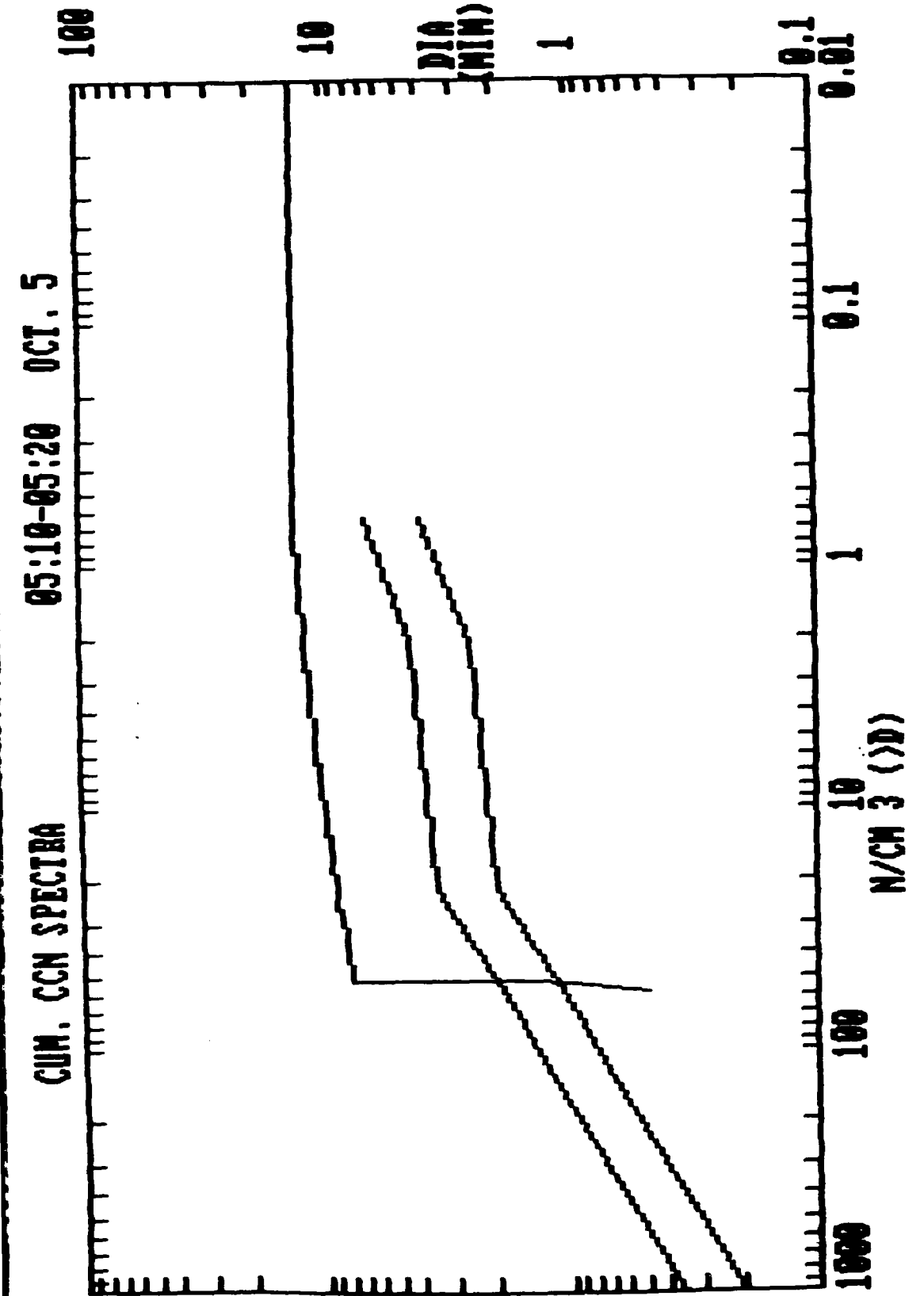
CUM. CCN SPECTRA
05:10-05:20 OCT. 5
DIA (MIM)
100
10
1
0.1
0.01
0.1
1
10
100
1000
N/CM 3 (>D)

CUM. CCN SPECTRA
06:40-06:50 OCT. 5
100
10
DIA (MIN)
1
0.1
0.01
0.1
1
10
100
1000
N/CM 3 (>D)

CUM. CCN SPECTRA
07:00-07:10 OCT. 5
100
10
DIA (MICR)
1
0.1
0.01
0.1
1
10
100
1000
N/CM 3 (>D)

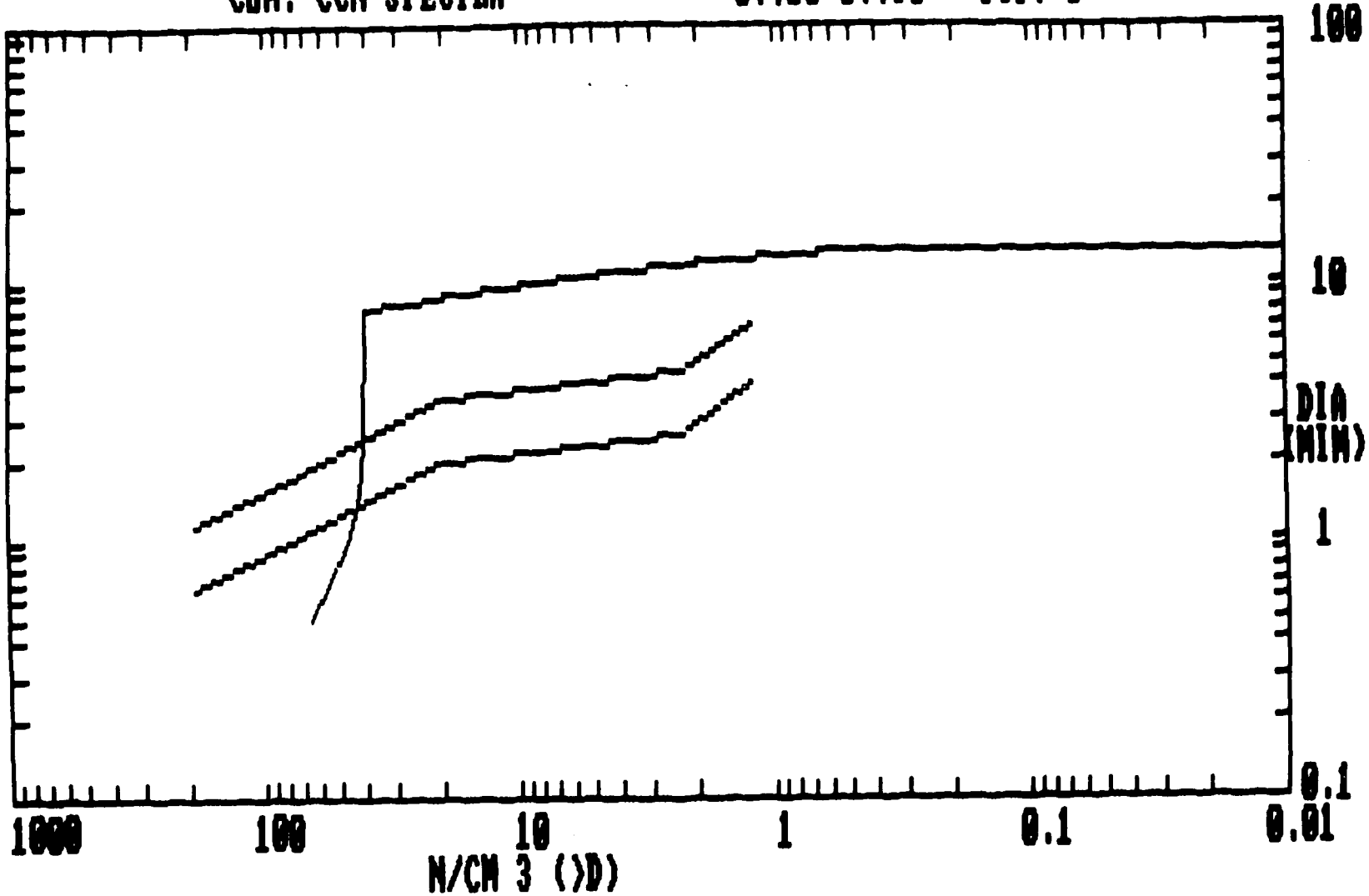
CUM. CCN SPECTRA
07:20-07:30 OCT. 5
100
10
DIA
(MIN)
1
0.1
1000
100
10
1
0.1
0.01
N/CM 3 (>D)

CUM. CCN SPECTRA
07:30-07:40 OCT. 5
100
10
DIA (MIN)
1
0.1
0.01
0.1
1
10
100
1000
N/CM 3 (>D)

CUM. CCN SPECTRA
07:40-07:50 OCT. 5
DIA (MICRON)
100
10
1
0.1
0.01
0.1
1
10
100
1000
N/CM 3 (>D)

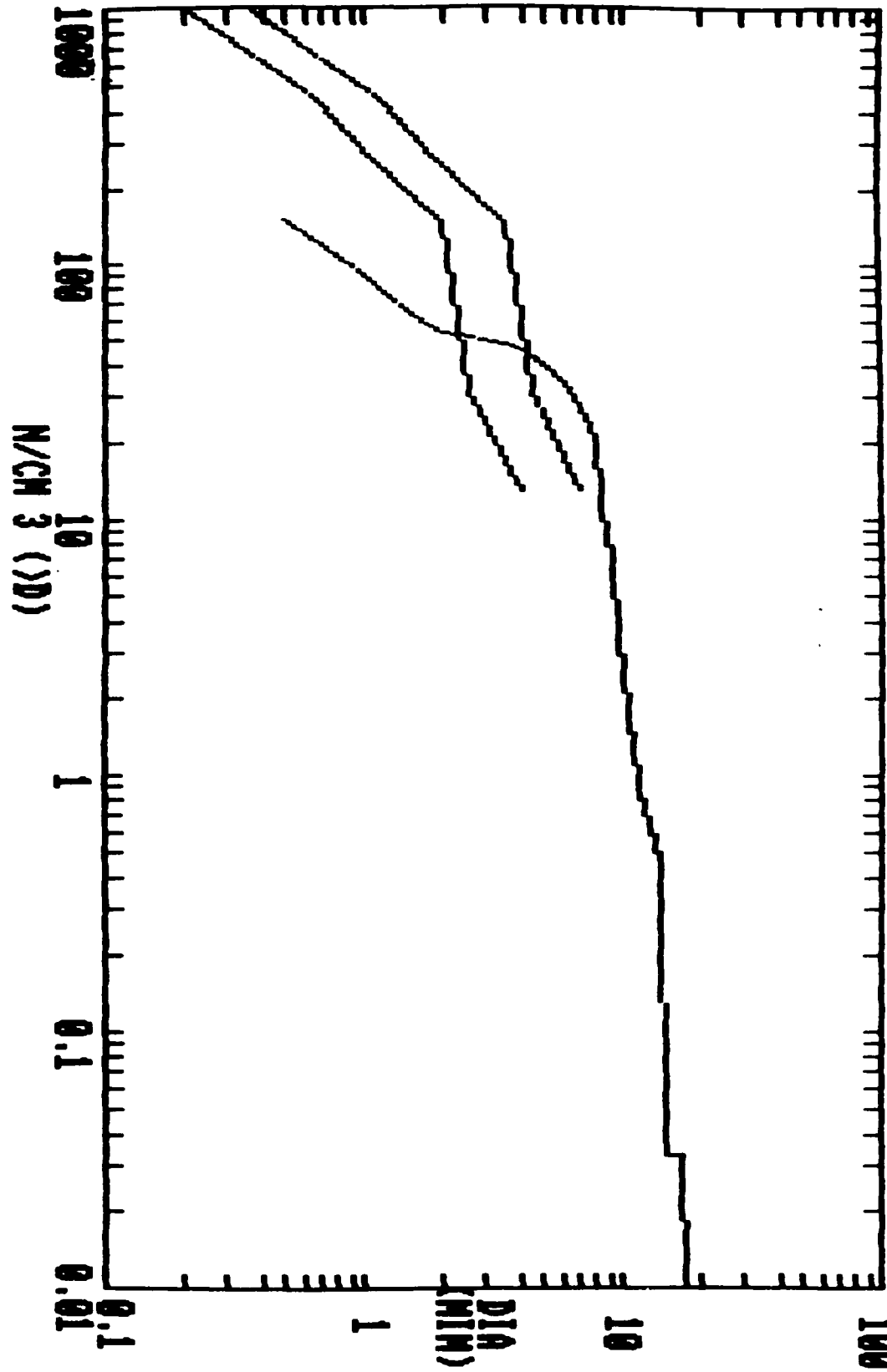
CUM. CCN SPECTRA
21:10-21:20 OCT. 5
N/CM 3 (D)
1000
100
10
1
0.1
0.01
0.1
1
10
100
DIA (MIN)

CUM. CCN SPECTRA
21:20-21:30 OCT. 5
100
10
DIA (MIN)
1
0.1
0.01
0.1
1
10
100
1000
N/CM 3 (>D)

CUM. CCN SPECTRA
21:30-21:40 OCT. 5
DIA (MIN)
100
10
1
0.1
0.01
0.1
1
10
100
1000
N/CM 3 (>D)

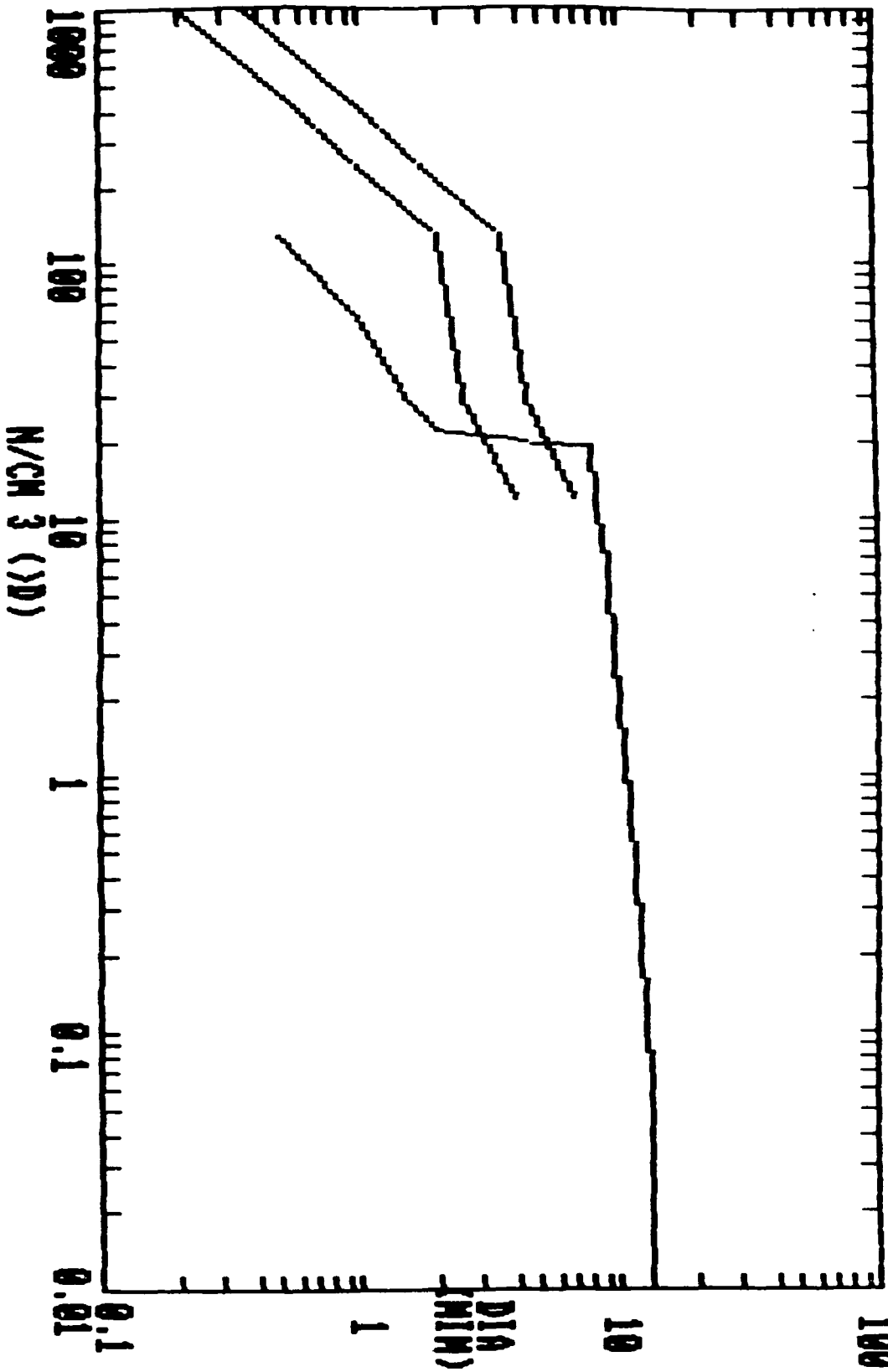
CUM. CCN SPECTRA
21:40-21:50 OCT. 5
N/CM 3 (>D)
DIA (MICRON)
0.01
0.1
1
10
100
1000

CUM. CCN SPECTRA
22:00-22:10 OCT. 5
100
10
DIA (MIN)
1
0.1
0.01
0.1
1
10
100
1000
N/CM 3 (>D)

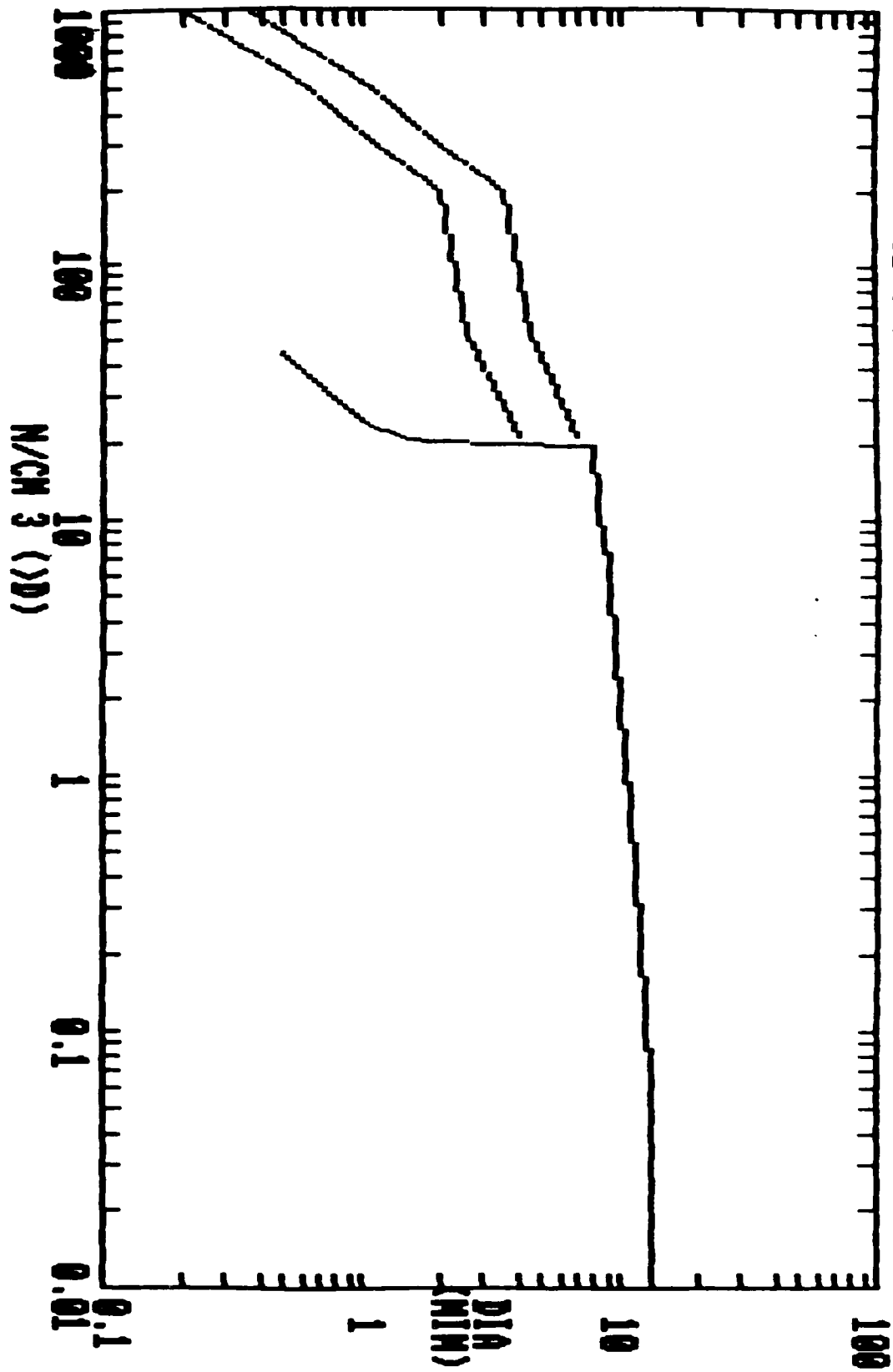
CUM. CCN SPECTRA
22:20-22:30 OCT. 5
N/CM 3 ((D))
1000
100
10
1
0.1
0.0
0.01
0.1
1
10
100
DIA (MIN)

CUM. CCN SPECTRA
23:50-24:00 OCT. 5
100
10
DIA (MIN)
1
0.1
0.01
0.1
1
10
100
1000
N/CM 3 ( )D)

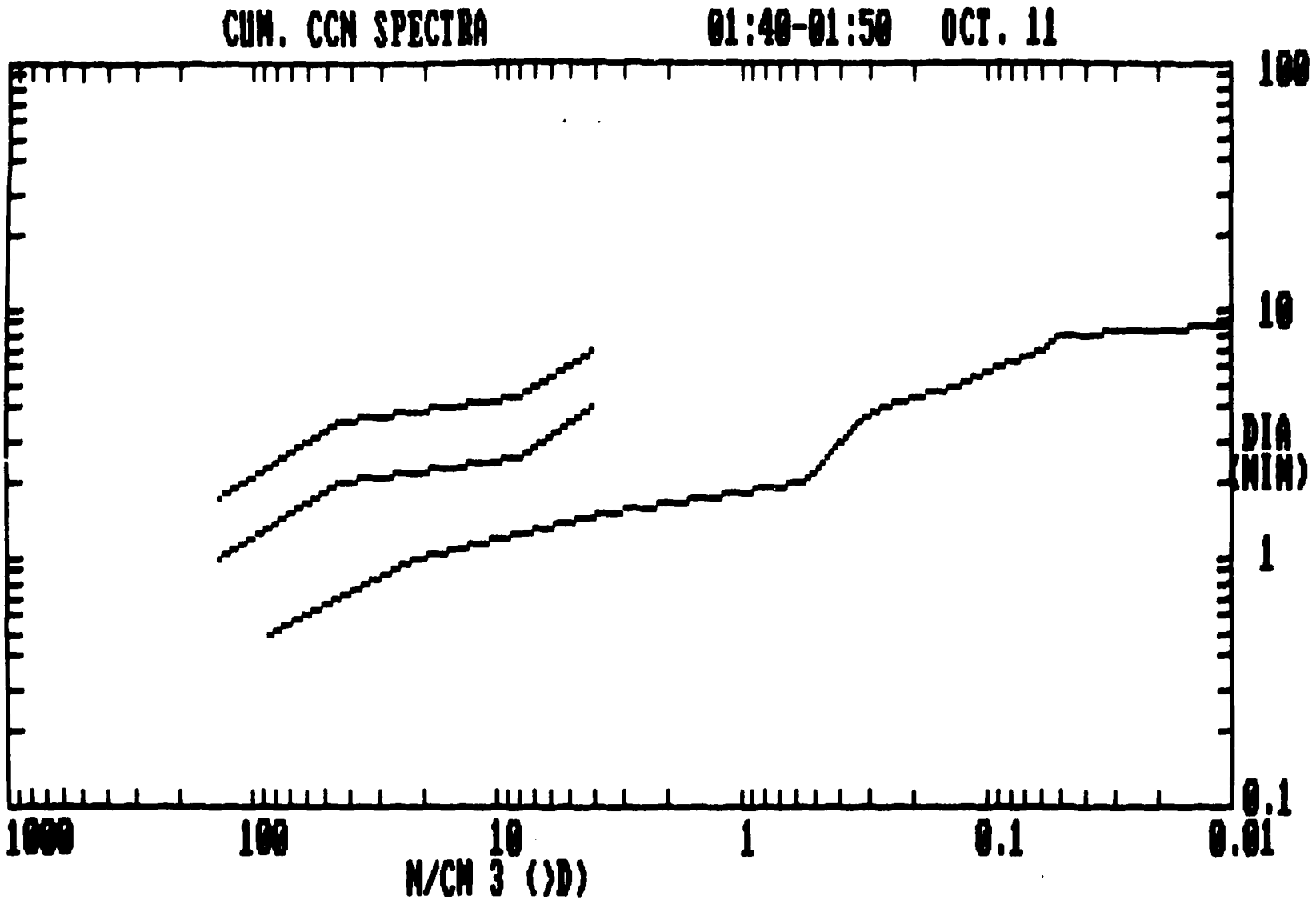
CUM. CCN SPECTRA
01:40-01:50 OCT. 11
100
10
DIA (MIN)
1
0.1
1000
100
10
1
0.1
0.01
N/CM 3 (>D)

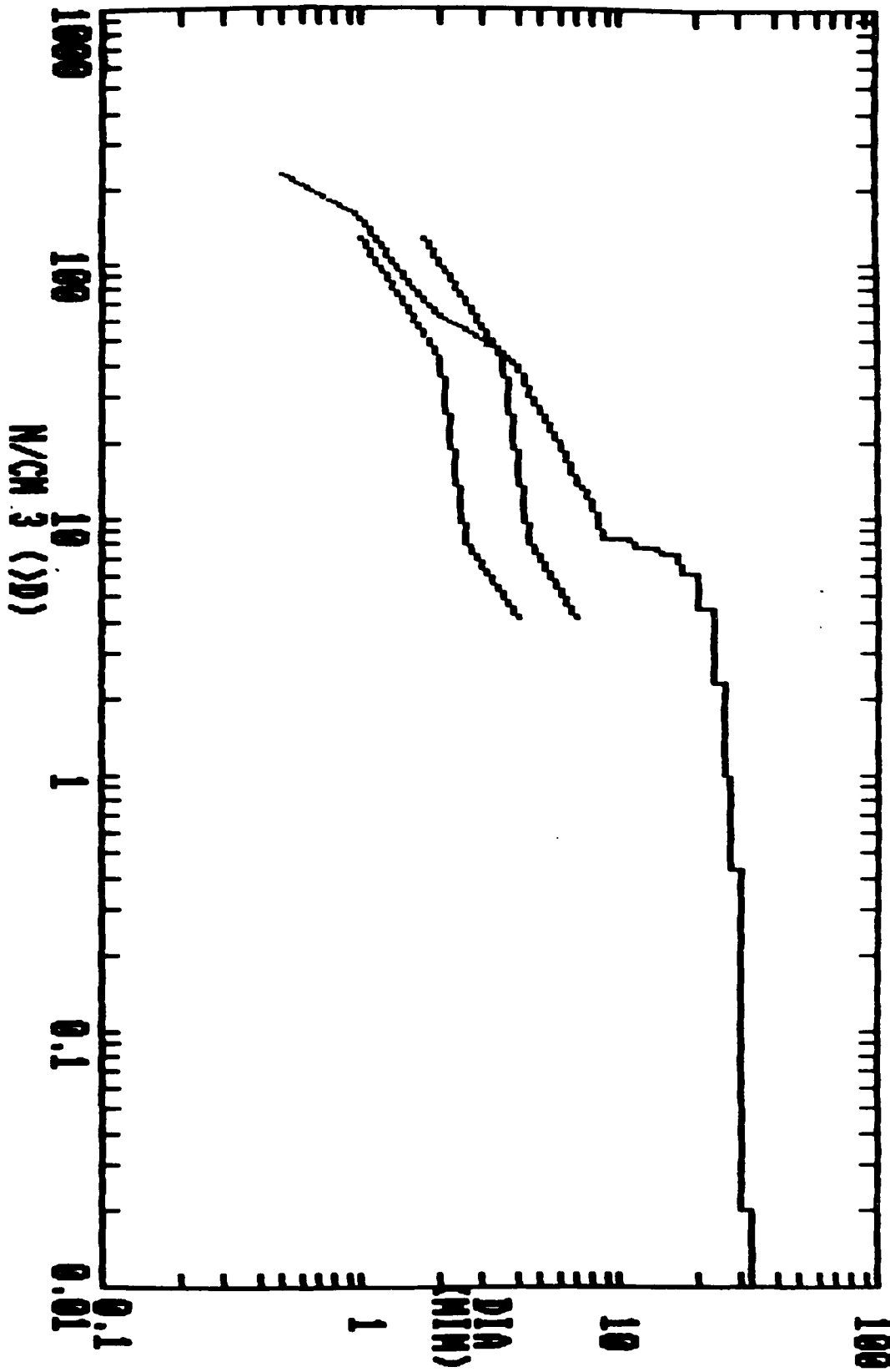
CUM. CCN SPECTRA
01:50-02:00 OCT. 11
N/CM 3 (D)
0.01
0.1
1
10
100
1000
0.01
0.1
1
10
100
D10 (MIN)

CUM. CCN SPECTRA
02:00-02:10 OCT. 11
100
10
DIA (MIN)
1
0.1
0.01
0.1
1
10
100
1000
N/CM 3 (>D)

CUM. CCN SPECTRA
02:10-02:20 OCT. 11
100
10
DIA (MIN)
1
0.1
0.01
0.1
1
10
100
1000
N/CM 3 (>D)

CUM. CCN SPECTRA
02:20-02:30 OCT. 11
100
10
DIA (MIN)
1
0.1
0.01
0.1
1
10
100
1000
N/CM 3 (>D)

CUM. CCN SPECTRA
03:00-03:10 OCT. 11
100
10
DIA (MIN)
1
0.1
0.01
0.1
1
10
100
1000
N/CM 3 (>D)

CUM. CCN SPECTRA
03:20-03:30 OCT. 11
100
10
DIA (MIN)
1
0.1
0.01
0.1
1
10
100
1000
N/CM 3 (>D)

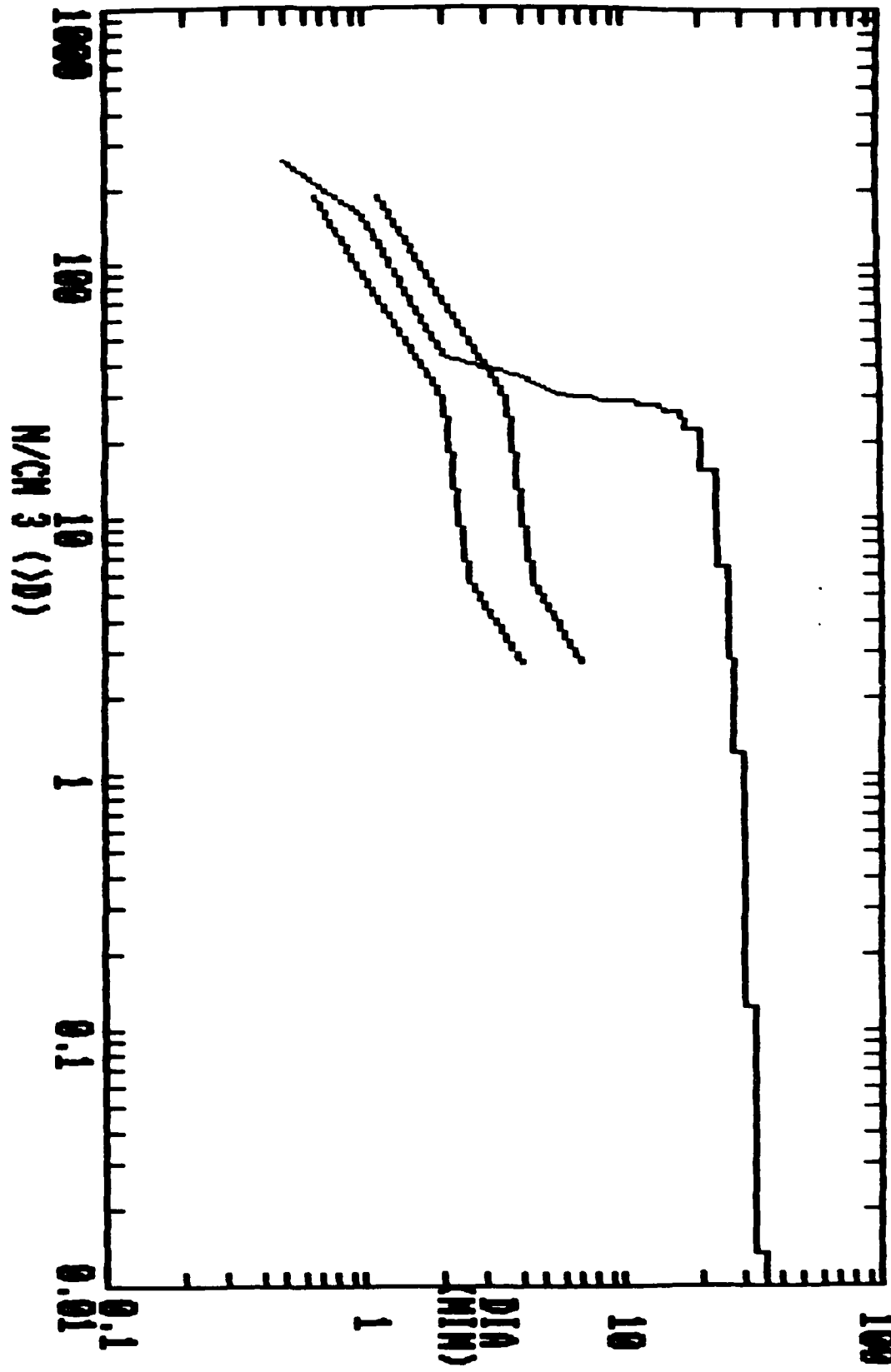
CUM. CCN SPECTRA
03:50-04:00 OCT. 11
N/CM 3 (STP)
1000
100
10
1
0.1
0.01
0.1
1
10
100
DIA (MICRONS)

CUM. CCN SPECTRA
04:30-04:40 OCT. 11
DIA (MIN)
100
10
1
0.1
0.01
0.1
1
10
100
1000
N/CM 3 (>D)

CUM. CCN SPECTRA
04:50-05:00 OCT. 11
100
10
DIA (MICR)
1
0.1
0.01
0.1
1
10
100
1000
N/CM 3 (>D)

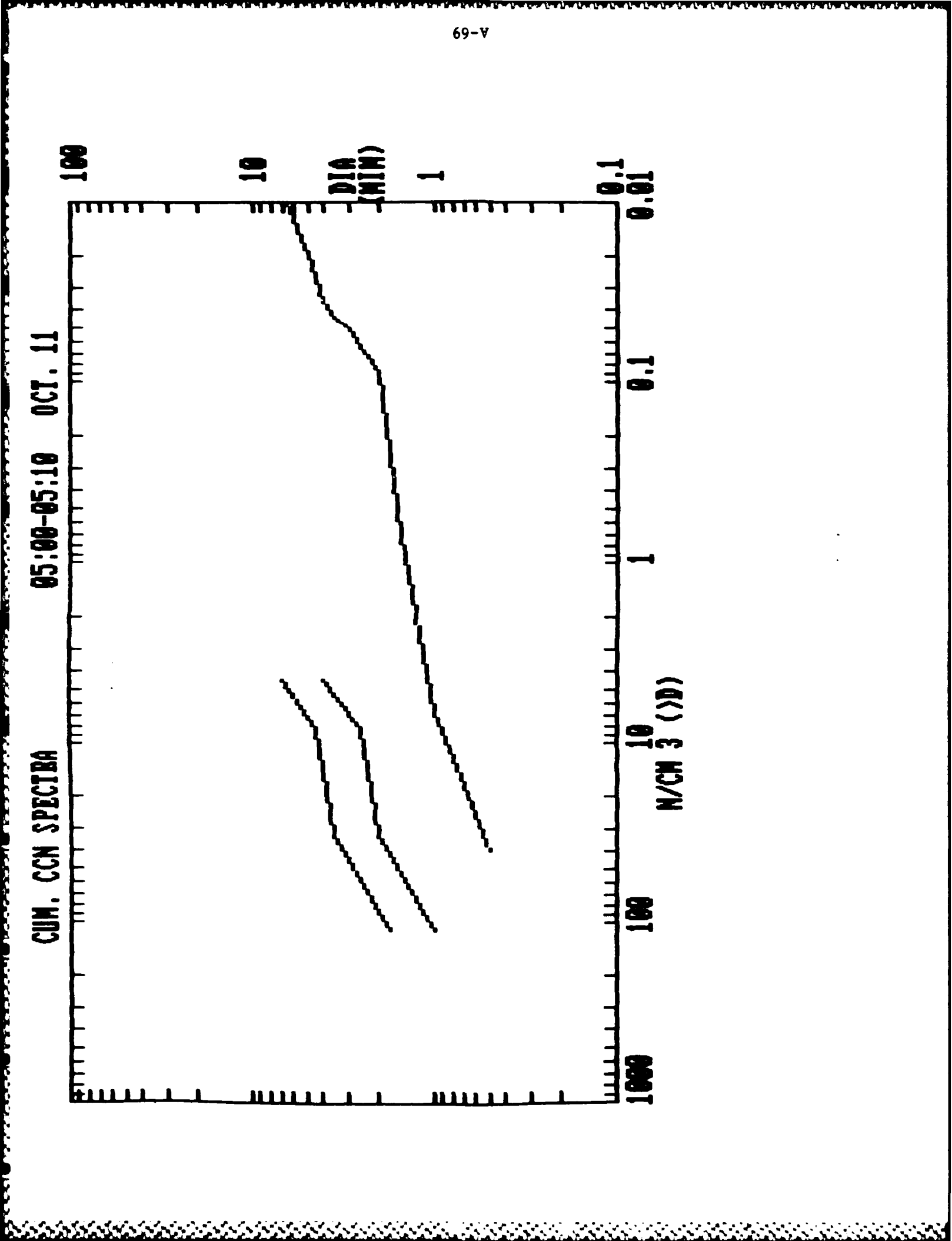
CUM. CCN SPECTRA
05:00-05:10 OCT. 11
DIA (MIN)
1000
10
1
0.1
0.01
0.1
1
10
100
1000
N/CM 3 (>D)

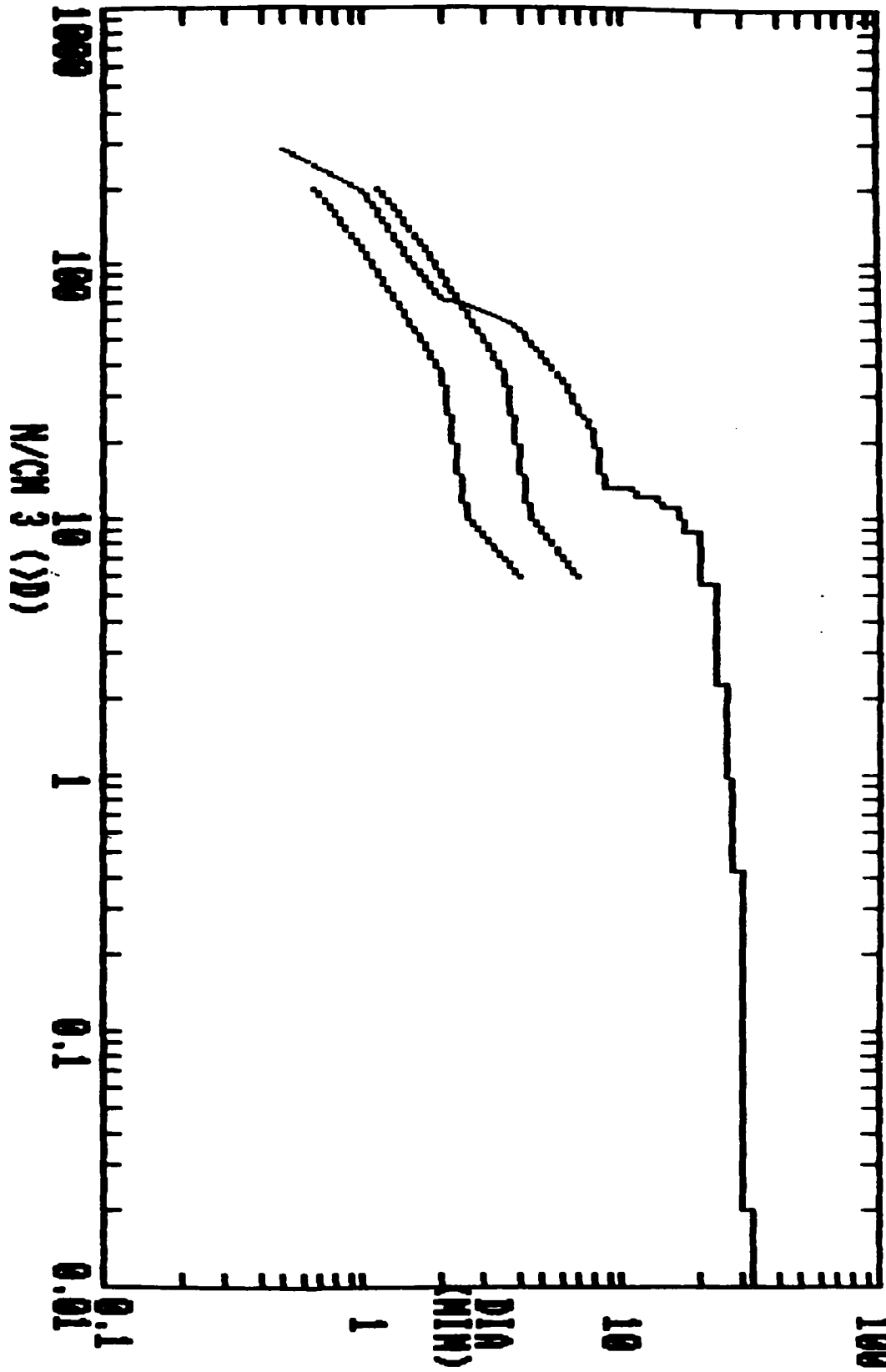
CUM. CCN SPECTRA
05:20-05:30 OCT. 11
N/CM 3 (STP)
1000
100
10
1
0.1
0.01
0.1
1
10
100
DIA (MICRONS)

CUM. CCN SPECTRA
05:40-05:50 OCT. 11
100
10
DIA (MIN)
1
0.1
0.01
1000
100
10
1
0.1
N/CM 3 (>D)

CUM. CCN SPECTRA
06:00-06:10 OCT. 11
DIA (MIN)
1000
10
1
0.1
0.01
0.1
1
10
100
1000
N/CM 3 (>D)

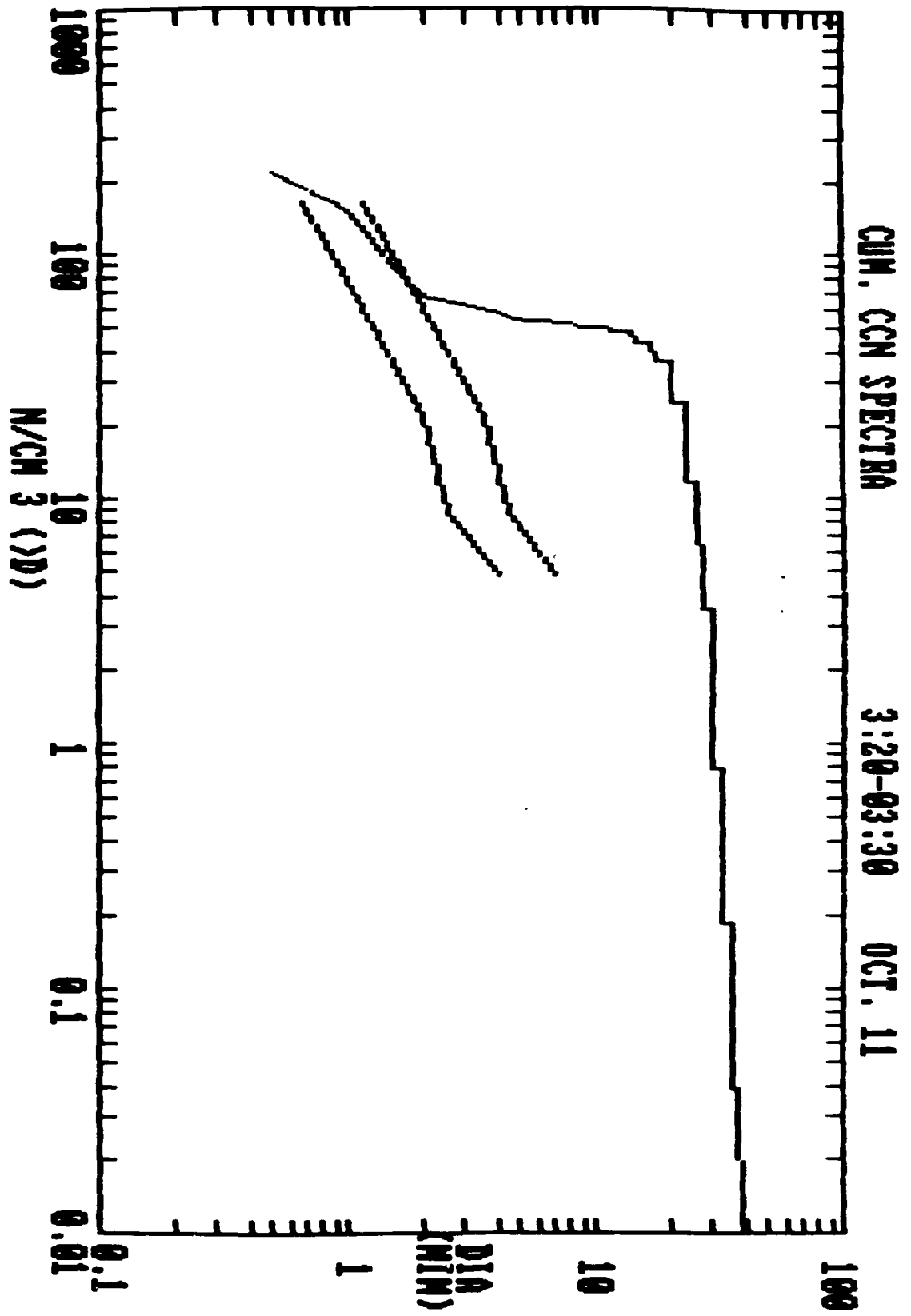
CUM. CCN SPECTRA
3:20-03:30 OCT. 11
N/CM 3 (>D)
D(MIN) (UM)
1000
100
10
1
0.1
0.01

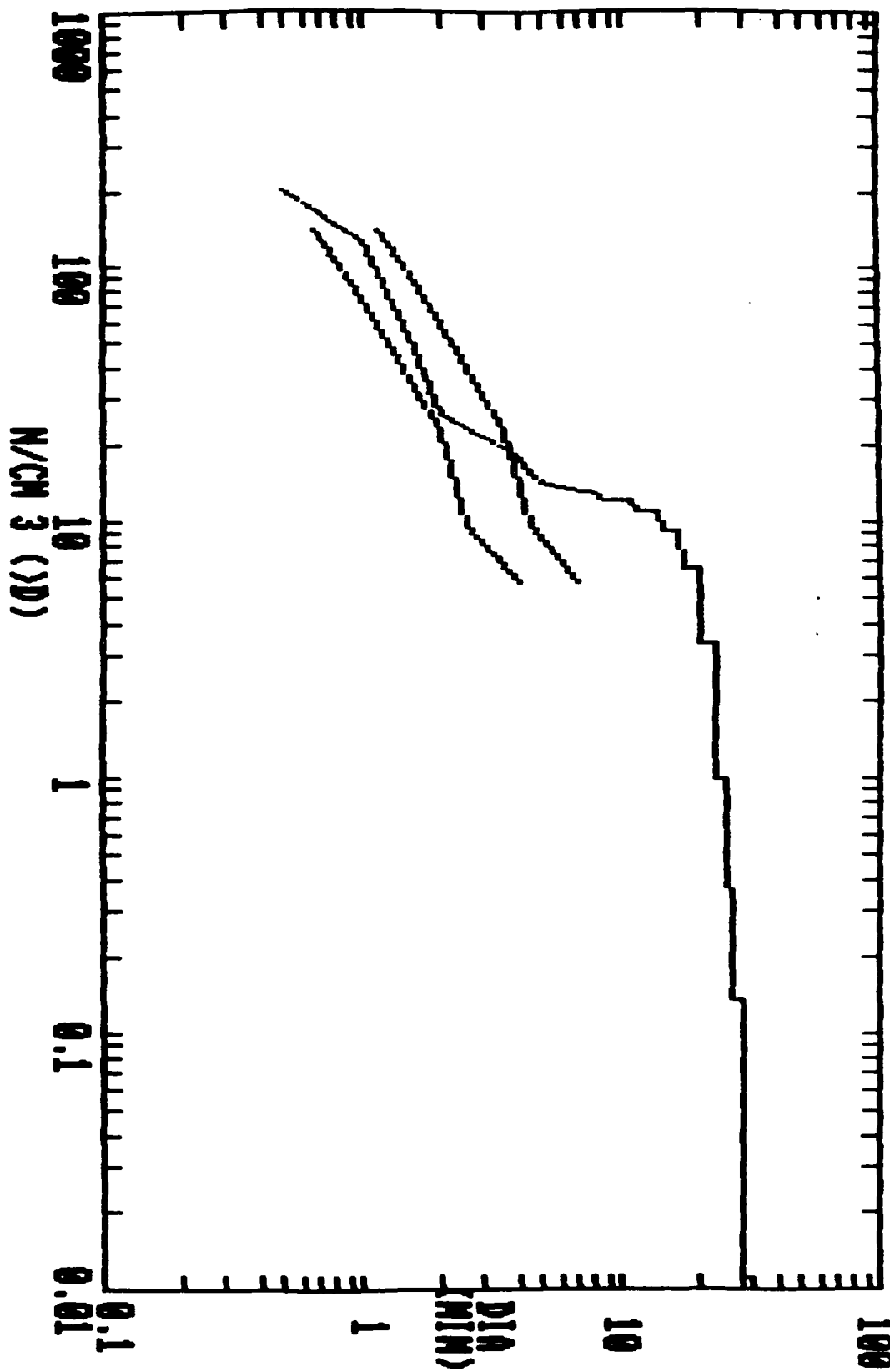
CUM. CCN SPECTRA
03:10-03:15 OCT. 11
N/CM 3 (STD)
1000
100
10
1
0.1
0.01
0.1
1
10
100
DIA (MIN)

CUM. CCN SPECTRA
03:15-03:20 OCT. 11
100
10
DIA (MIN)
1
0.1
0.01
0.1
1
10
100
1000
N/CM 3 (>D)

CUM. CCN SPECTRA
03:25-03:30 OCT. 11
100
10
DIA (MICRON)
1
0.1
0.01
0.1
1
10
100
1000
N/CM 3 (>D)

CUM. CCN SPECTRA
03:30-03:35 OCT. 11
DIA (MIN)
100
10
1
0.1
0.01
0.1
1
10
100
1000
N/CM 3 (>D)

CUM. CCN SPECTRA
03:40-03:50 OCT. 11
DIA (MIN)
100
10
1
0.1
0.01
0.1
1
10
100
1000
N/CM 3 (>D)

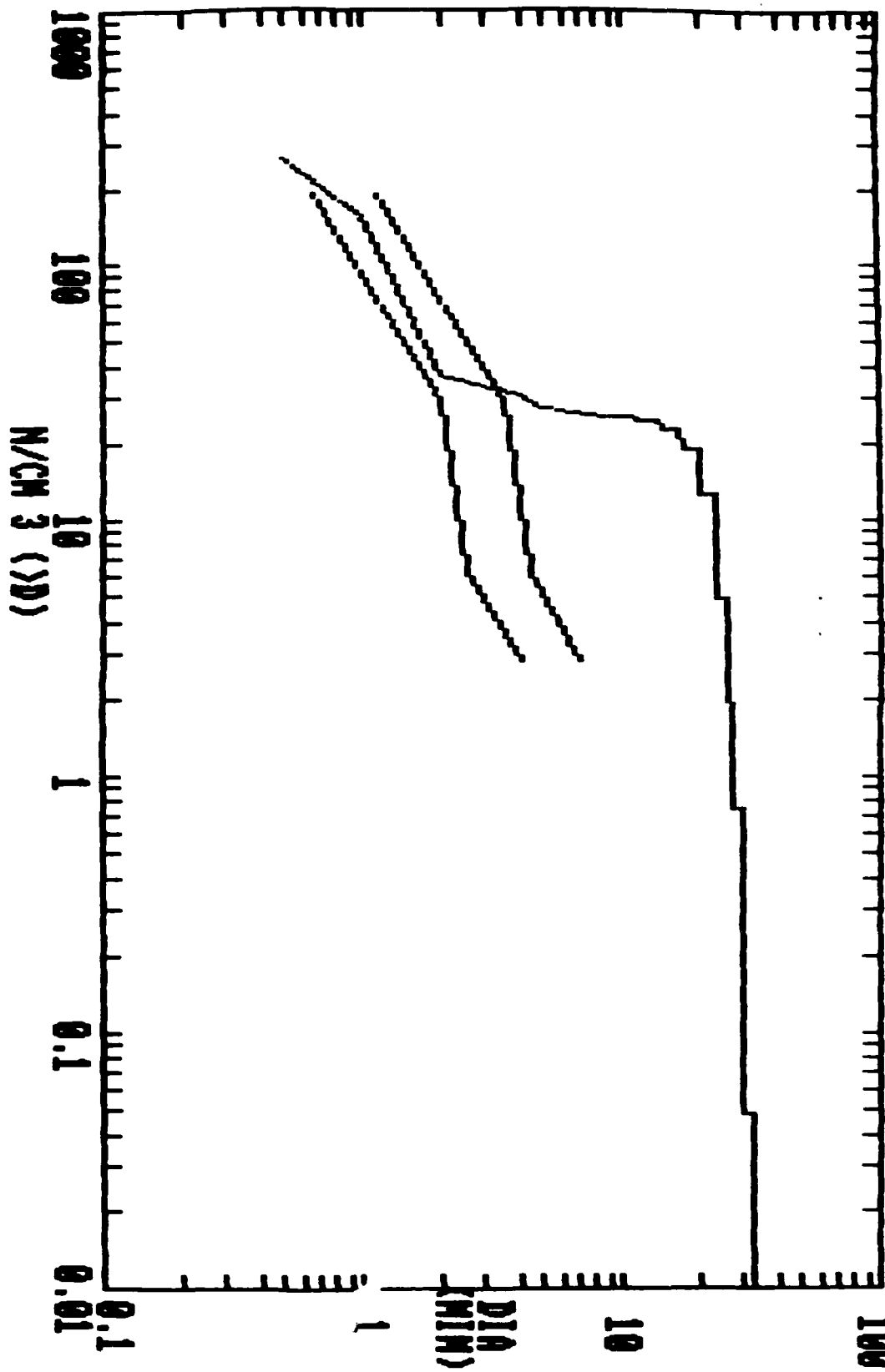
CUM. CCN SPECTRA
03:50-03:55 OCT. 11
N/CM 3 (>D)
1000
100
10
1
0.1
0.01
0.1
1
10
100
DIA (MICRONS)

CUM. CCN SPECTRA
03:55-04:00 OCT. 11
100
10
DIA (MIN)
1
0.1
0.01
0.1
1
10
100
1000
N/CM 3 (SD)

CUM. CCN SPECTRA
03:40-03:45 OCT. 11
100
10
DIA (MIN)
1
0.1
0.01
0.1
1
10
100
1000
N/CM 3 ()D)

CUM. CCN SPECTRA
03:45-03:50 OCT. 11
100
10
DIA (MIN)
1
0.1
0.01
0.1
1
10
100
1000
N/CM 3 (>D)

CUM. CCN SPECTRA
01:40-01:50 OCT. 14
100
10
1
0.1
DIA (MIM)
0.1
0.01
1000
100
10
1
N/CM 3 (>D)

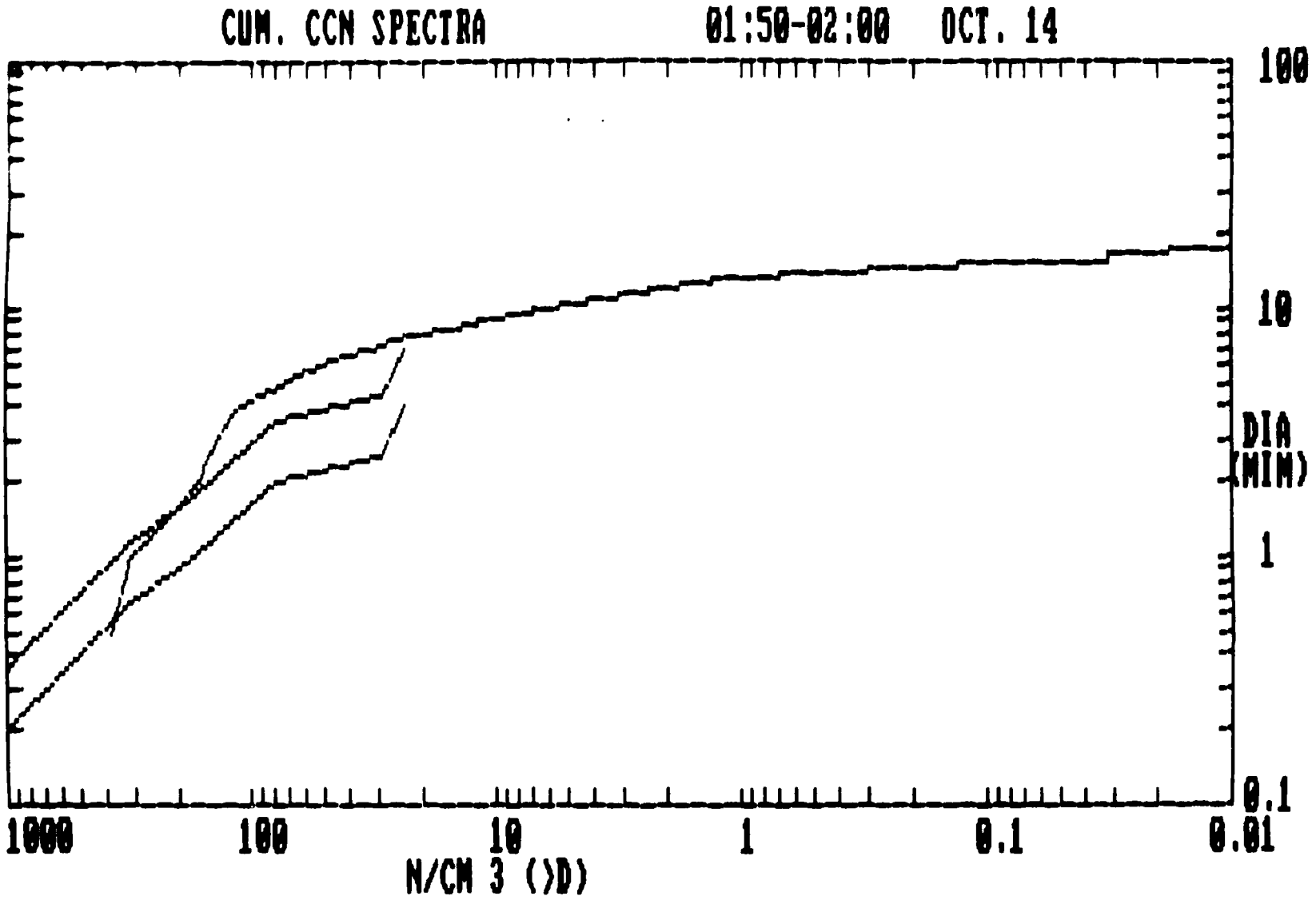
CUM. CCN SPECTRA
01:50-02:00 OCT. 14
100
10
DIA
(MIM)
1
0.1
1000
100
10
1
0.1
0.01
N/CM 3 ()D)

CUM. CCN SPECTRA
02:10-02:20 OCT. 14
100
10
DIA (MIN)
1
0.1
0.01
0.1
1
10
100
1000
N/CM 3 (>D)

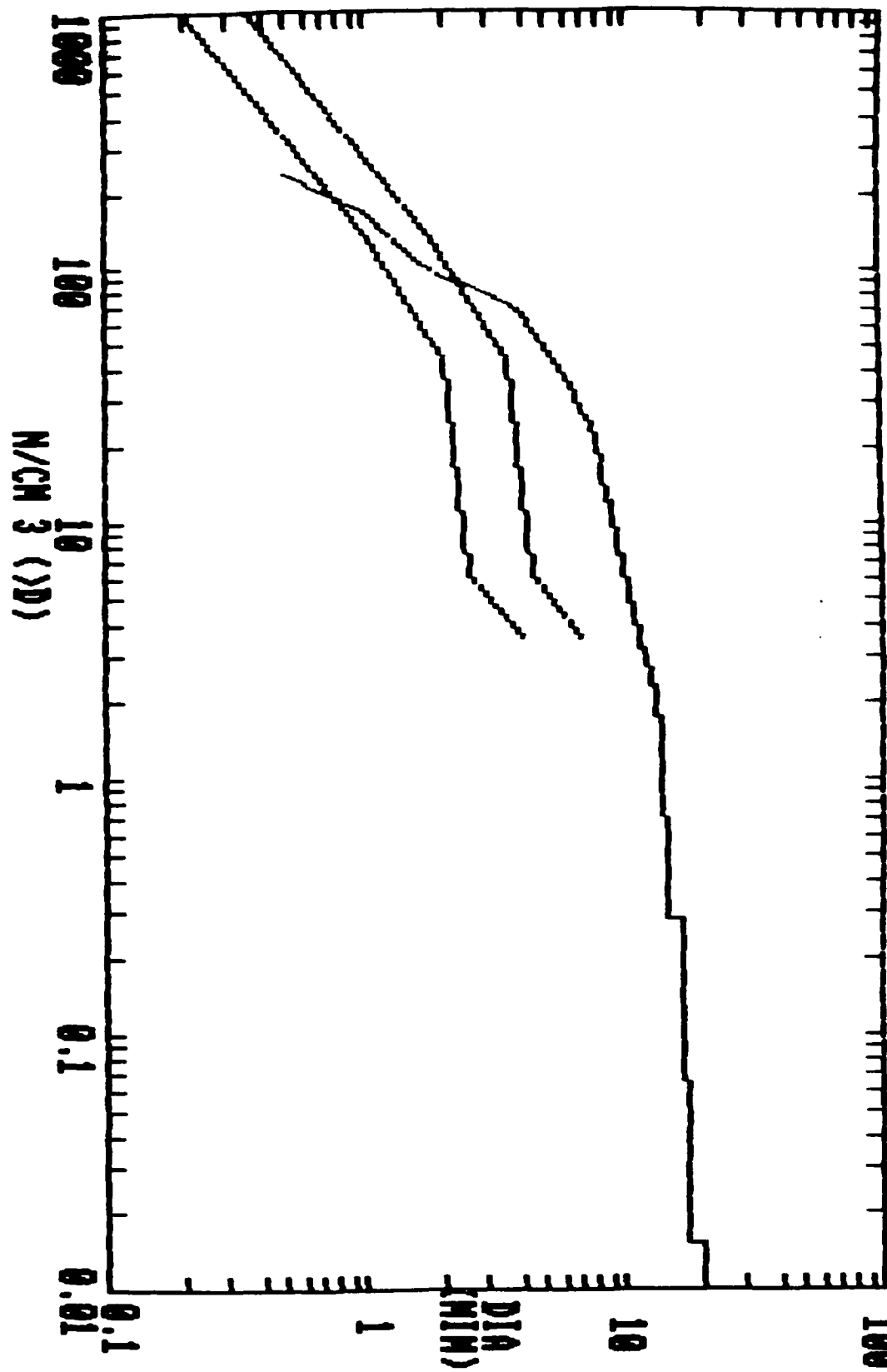
CUM. CCN SPECTRA
03:10-03:20 OCT. 14
N/CM 3 (>D)
1000
100
10
1
0.1
0.01
0.1
1
10
100
DIA (MICRONS)

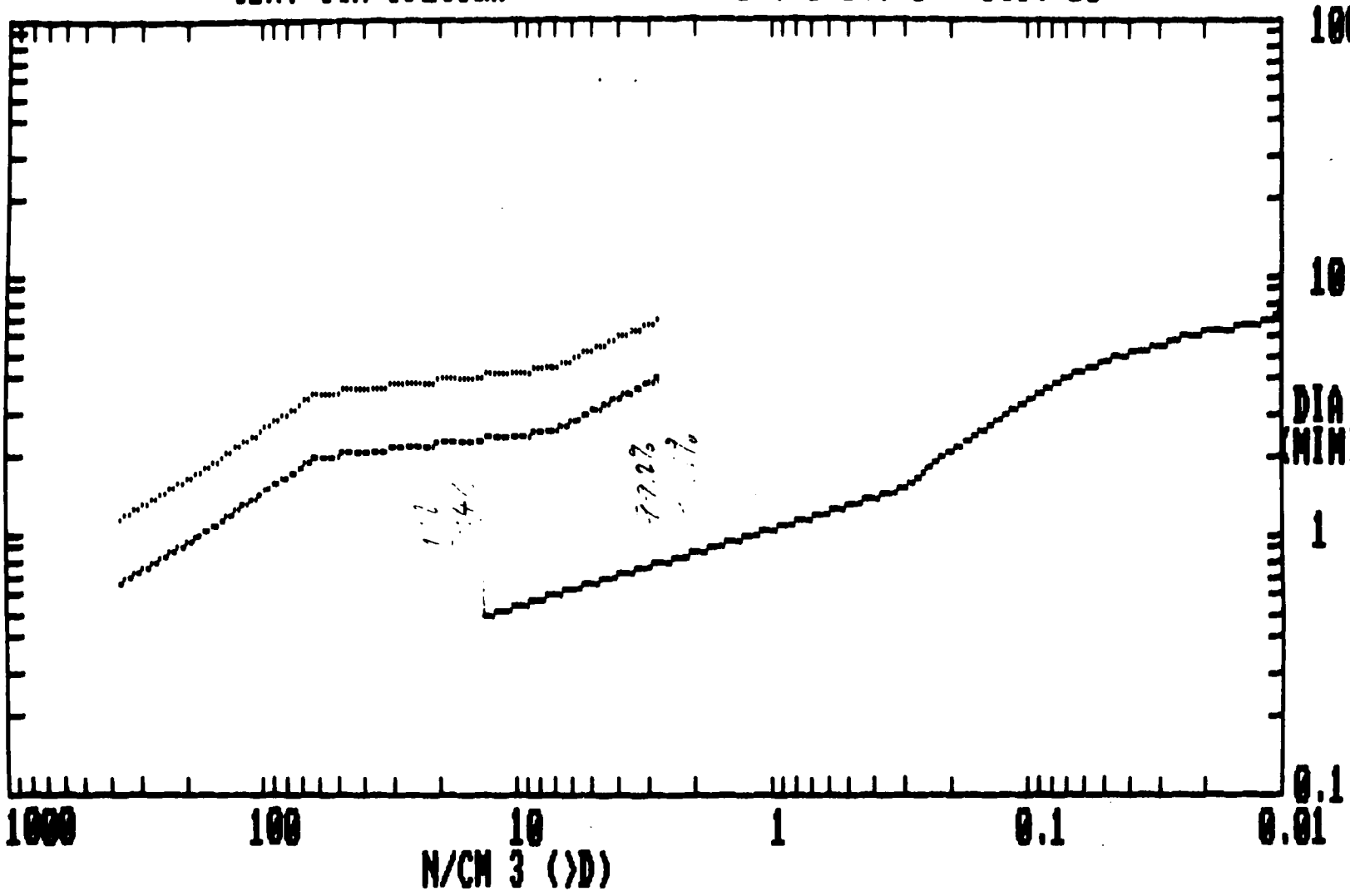
CUM. CCN SPECTRA
01:00-01:10 OCT. 25
100
10
1
0.1
DIA (MIN)
1000
100
10
1
0.1
0.01
N/CM 3 (>D)

A-87

CUM. CCN SPECTRA
01:10-01:20 OCT. 25
DIA (MIN)
100
10
1
0.1
0.01
0.1
1
10
100
1000
N/CM 3 (>D)

CUM. CCN SPECTRA
04:00-05:00 OCT. 27
DIA (MIN)
100
10
1
0.1
0.01
1000
100
10
1
0.1
N/CM 3 (>D)

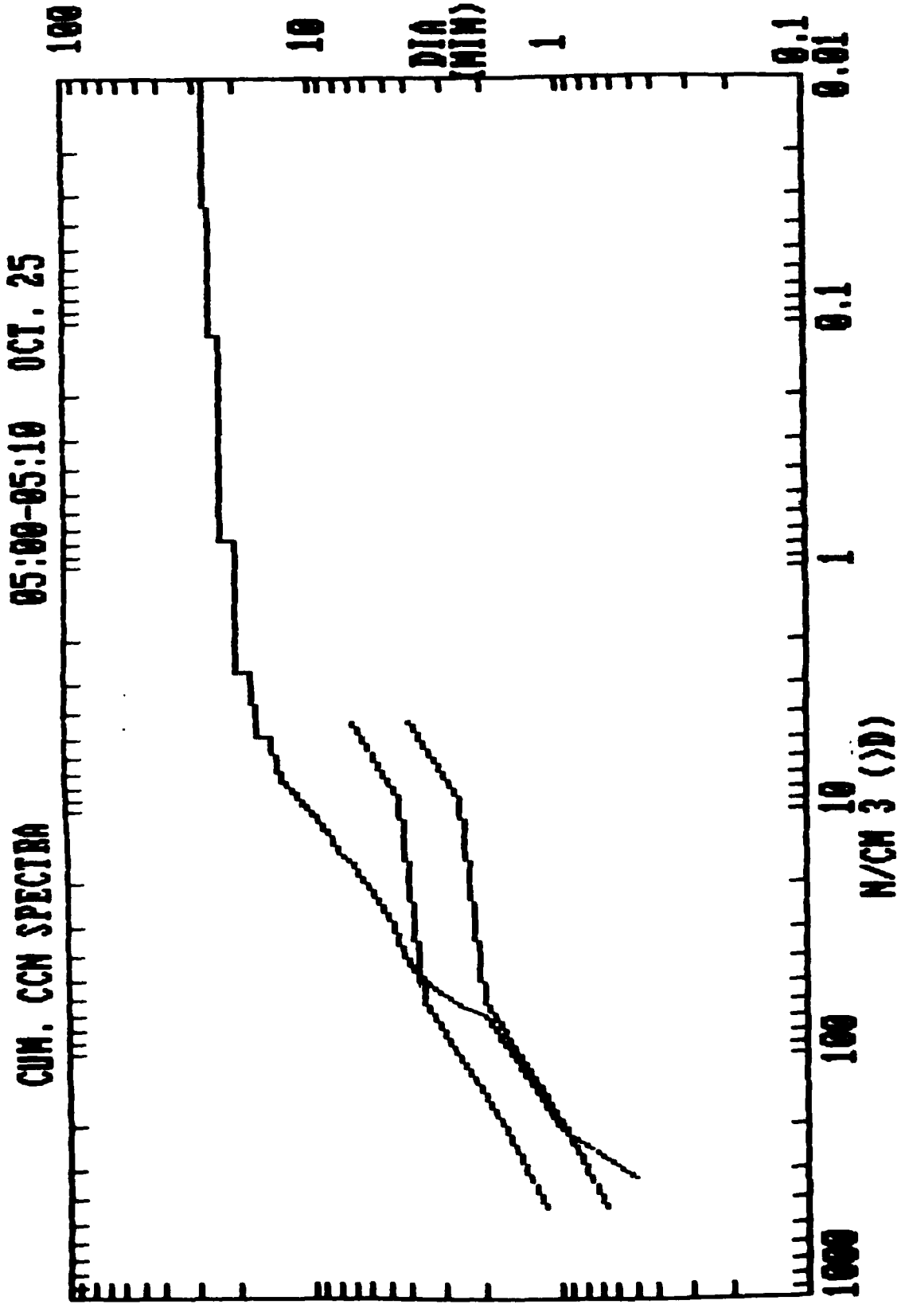
CUM. CCN SPECTRA
05:00-05:10 OCT. 25
100
10
DIA (MIN)
1
0.1
0.01
0.1
1
10
100
1000
N/CM 3 ( )D)

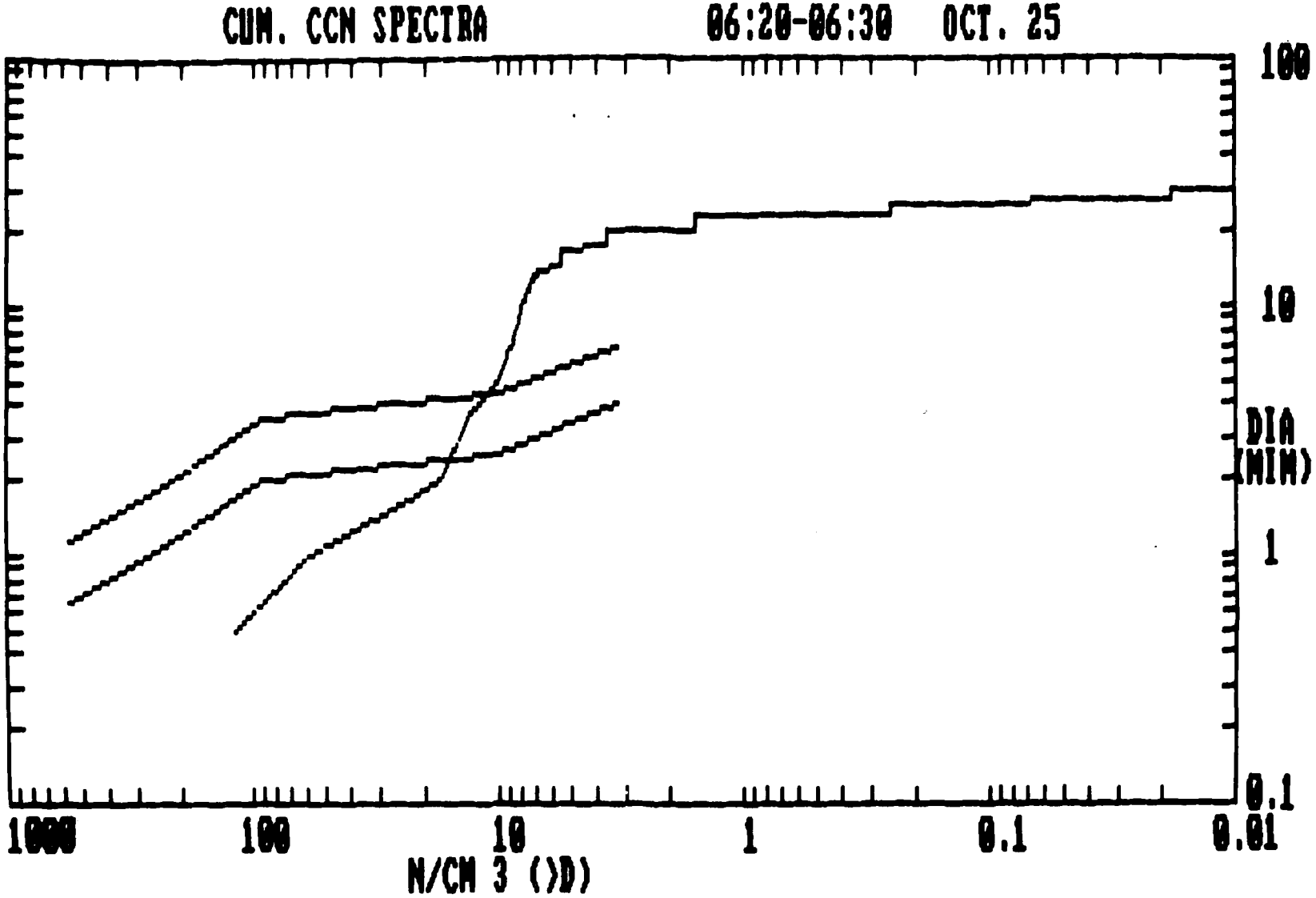
CUM. CCN SPECTRA
06:20-06:30 OCT. 25
100
10
DIA (MIM)
1
0.1
1000
100
10
1
0.1
0.01
N/CM 3 ()D)

CUM. CCN SPECTRA
07:30-07:40 OCT. 25
DIA (MIM)
100
10
1
0.1
0.01
0.1
1
10
100
1000
N/CM 3 (>D)

CUM. CCN SPECTRA
07:40-07:50 OCT. 25
100
10
DIA (MIN)
1
0.1
0.01
0.1
1
10
100
1000
N/CM 3 (>D)

CUM. CCN SPECTRA
06:40-06:50 OCT. 27
100
10
DIA (MIN)
1
0.1
0.01
0.1
1
10
100
1000
N/CM 3 (>D)

CUM. CCN SPECTRA
06:50-07:00 OCT. 27
DIA (MIN)
100
10
1
0.1
0.01
0.1
1
10
100
1000
N/CM 3 (>D)

CUM. CCN SPECTRA
07:10-07:20 OCT. 27
100
10
DIA (MIN)
1
0.1
0.01
0.1
1
10
100
1000
N/CM 3 (>D)

CUM. CCN SPECTRA
07:20-07:30 OCT. 27
100
10
DIA (MIN)
1
0.1
0.01
0.1
1
10
100
1000
N/CM 3 (>D)

AD-A179 776 EFFECTS OF CCN-FCN (CLOUD CONDENSATION NUCLEI-FOG CONDENSATION NUCLEI) SP..(U) NEVADA UNIV RENO DESERT RESEARCH INST J G HUDSON 05 MAR 87 ARO-22342.1-GS 3/3

UNCLASSIFIED DAAG29-85-K-0037 F/G 4/1 NL

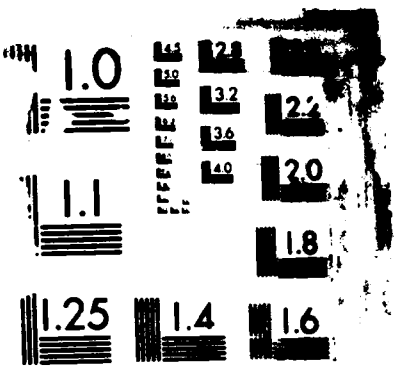
1.0
1.1
1.25
1.4
1.6
2.0
1.8

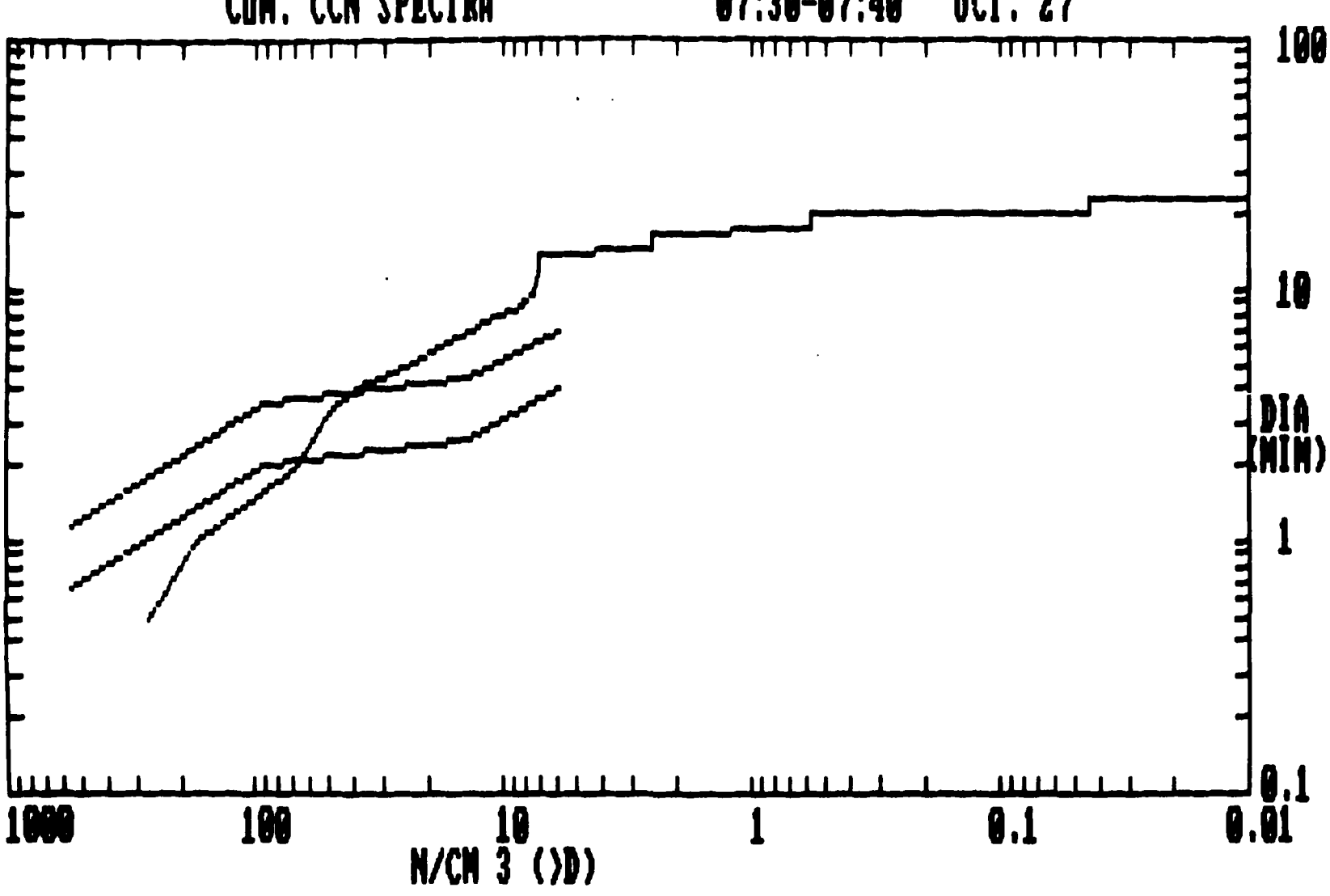
CUM. CCN SPECTRA
07:30-07:40 OCT. 27
100
10
DIA (MIM)
1
0.1
1000
100
10
1
0.1
0.01
N/CM 3 (>D)

A-98

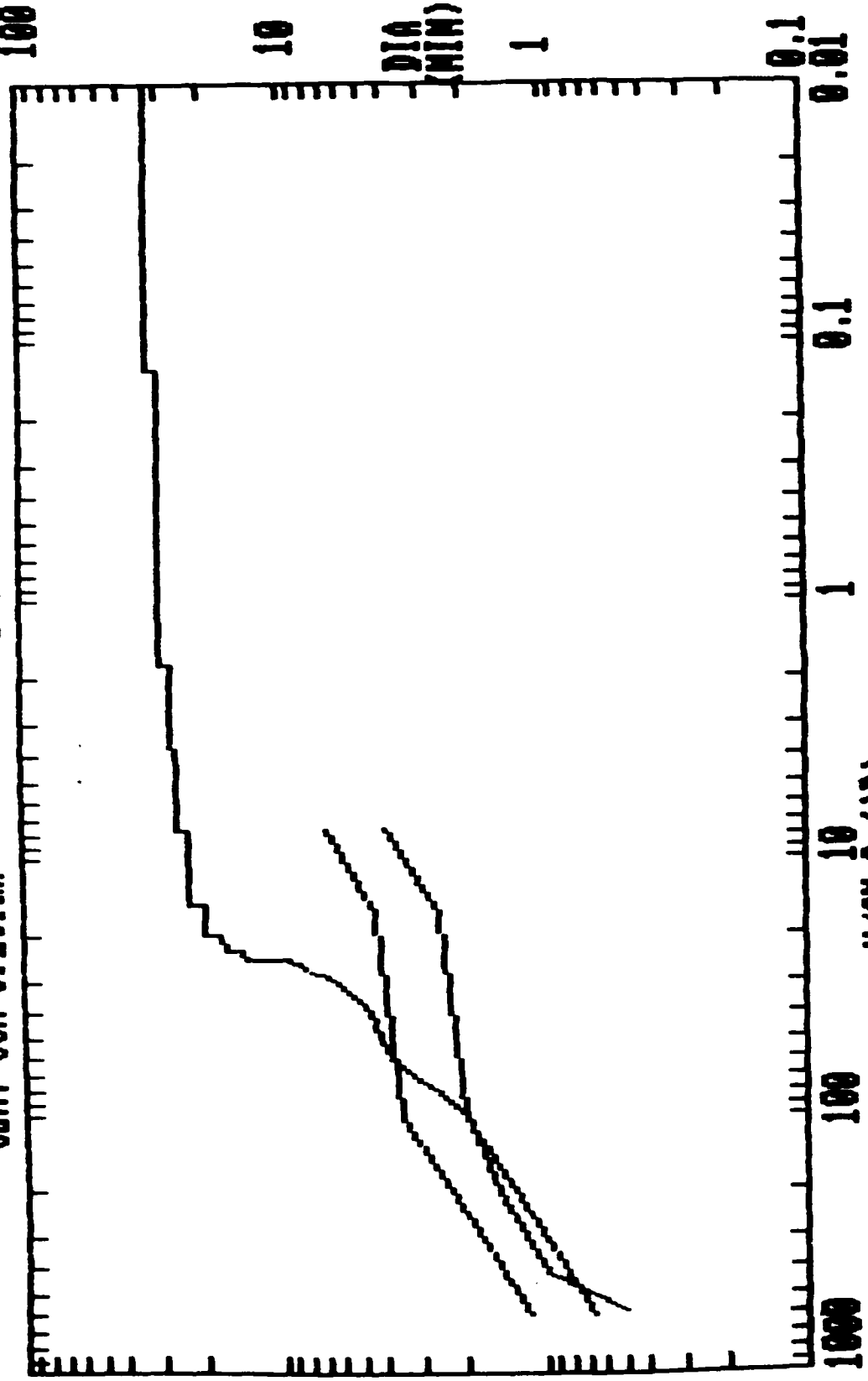
CUM. CCN SPECTRA
07:50-08:00 OCT. 27
DIA (MIN)
100
10
1
0.1
0.01
0.1
1
10
100
1000
N/CM 3 (>D)

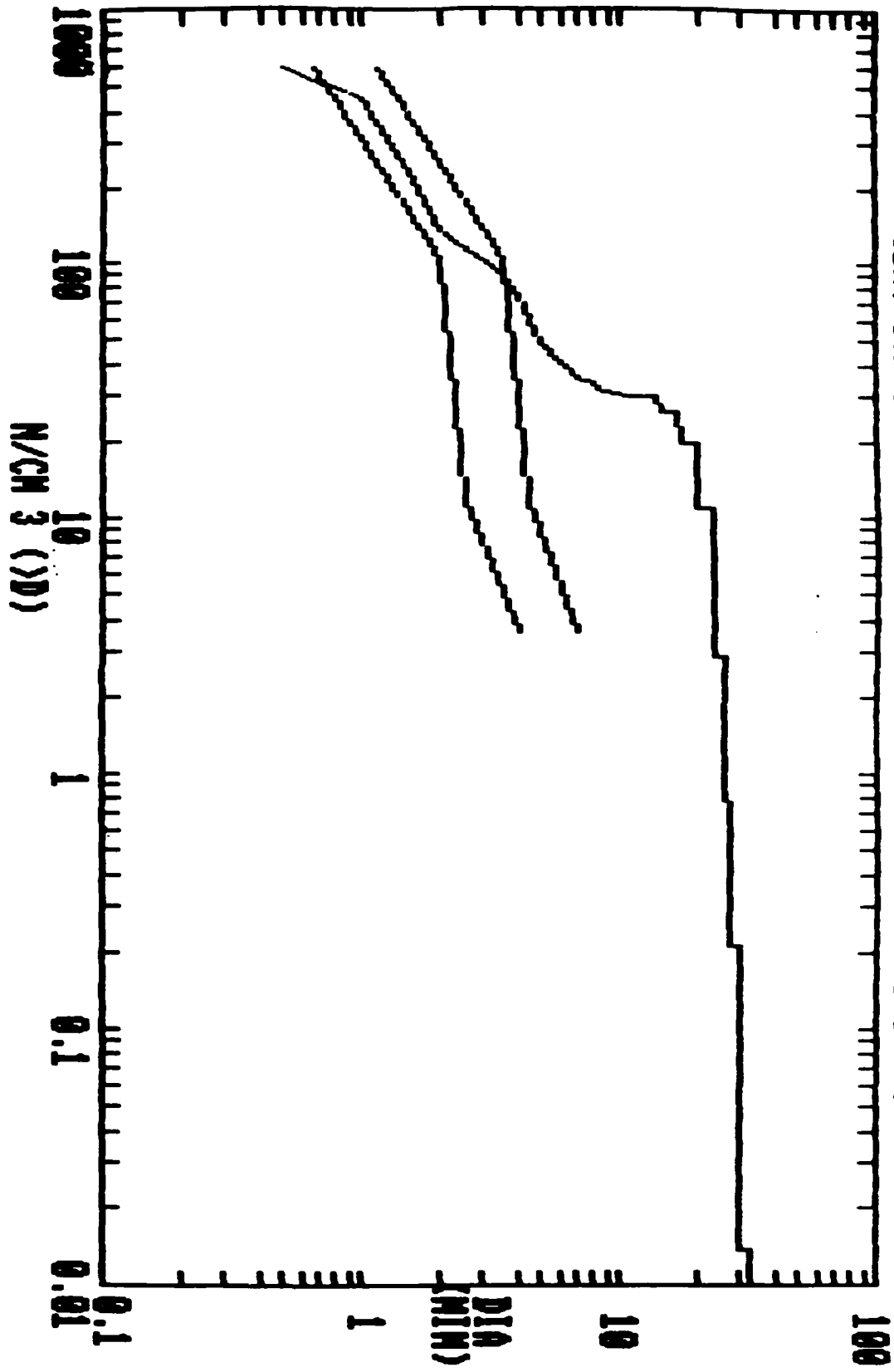
CUM. CCN SPECTRA
08:10-08:20 OCT. 27
N/CM 3 (D)
DIA (MIN)
0.01
0.1
1
10
100
1000

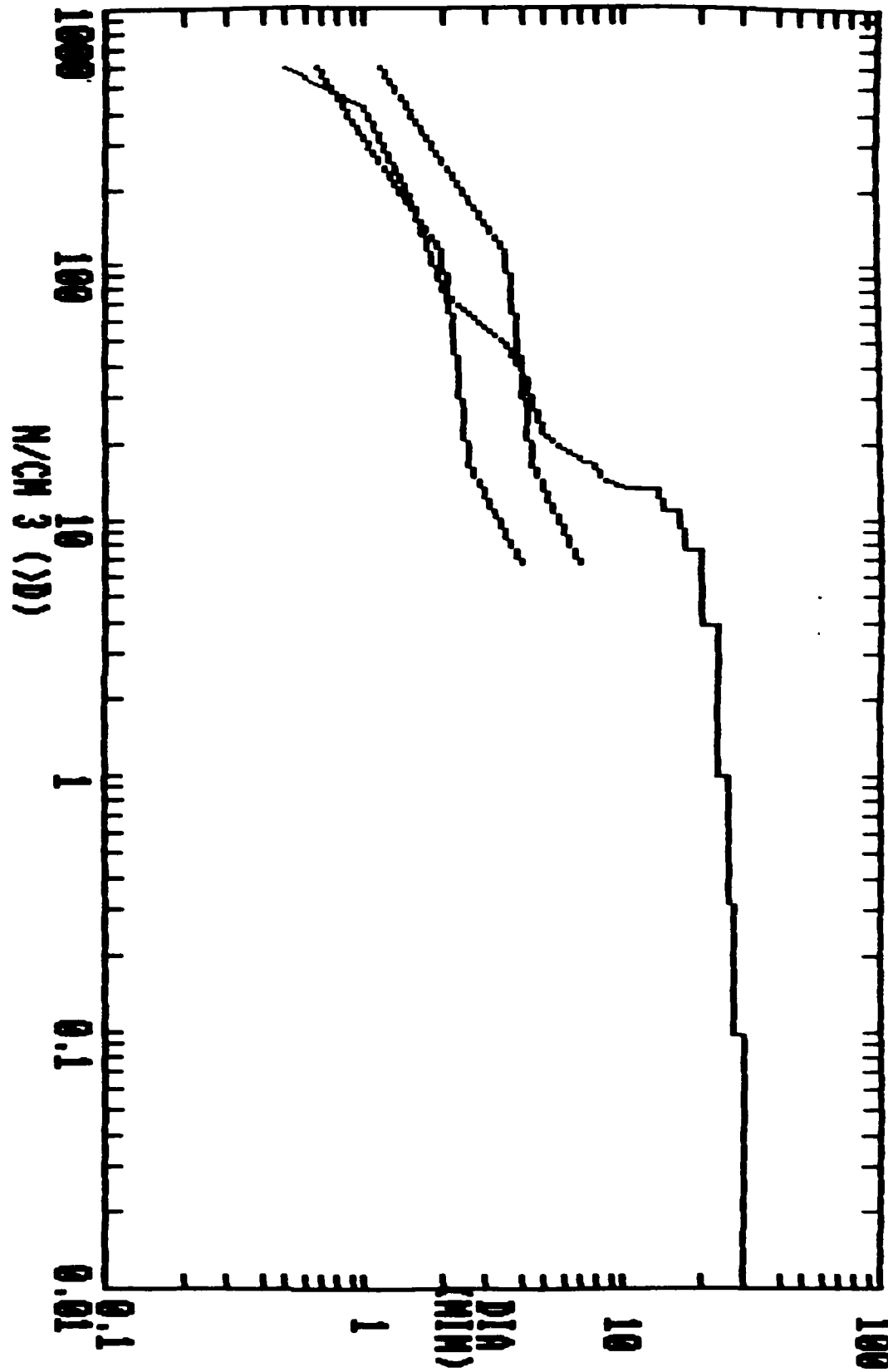
CUM. CCN SPECTRA
08:20-08:30 OCT. 27
N/CM 3 (D)
DIA (MIM)
0.01
0.1
1
10
100
1000

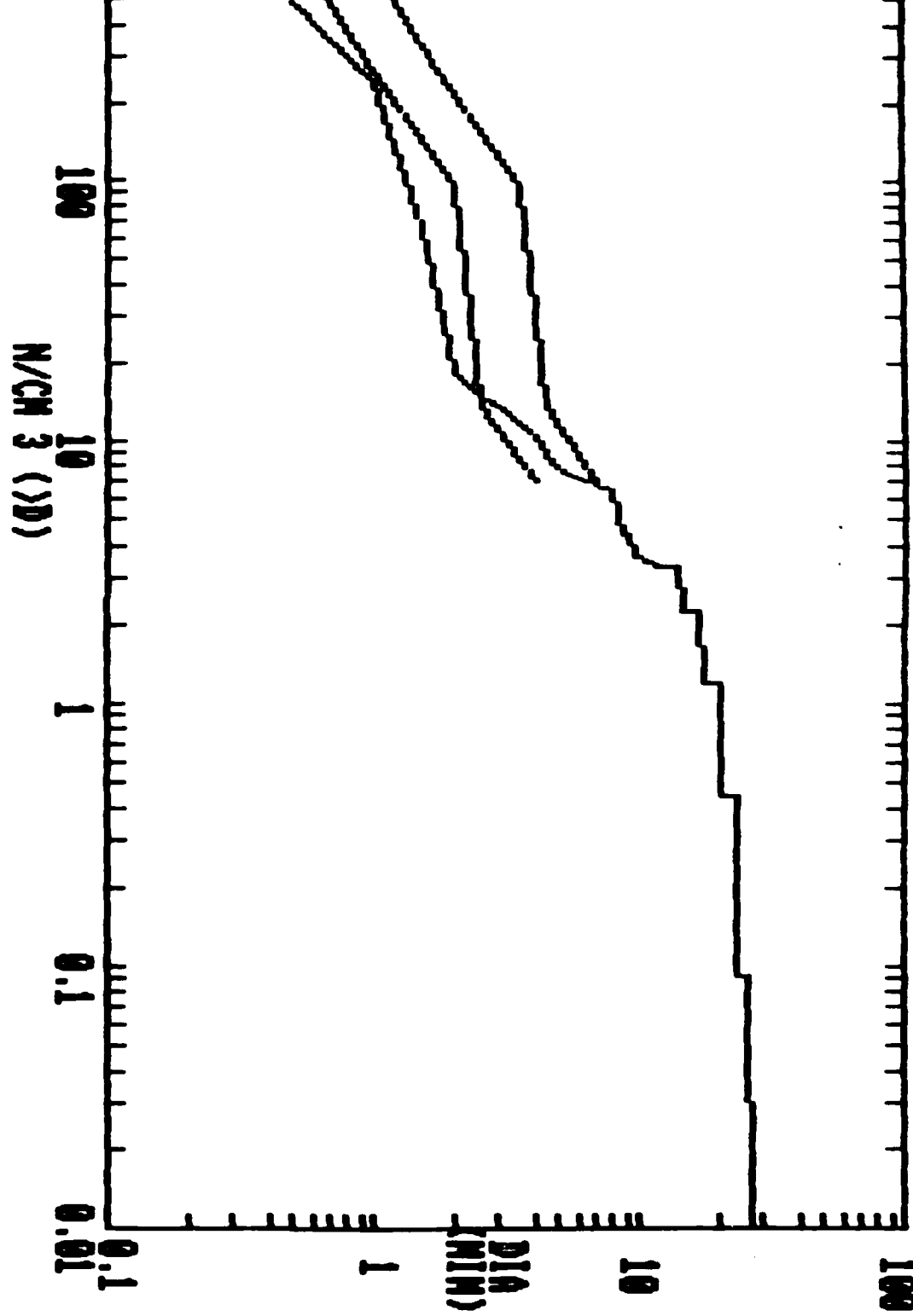
CUM. CCN SPECTRA
08:30-08:40 OCT. 27
N/CM 3 (>D)
D(MIN) (UM)
0.01
0.1
1
10
100
1000

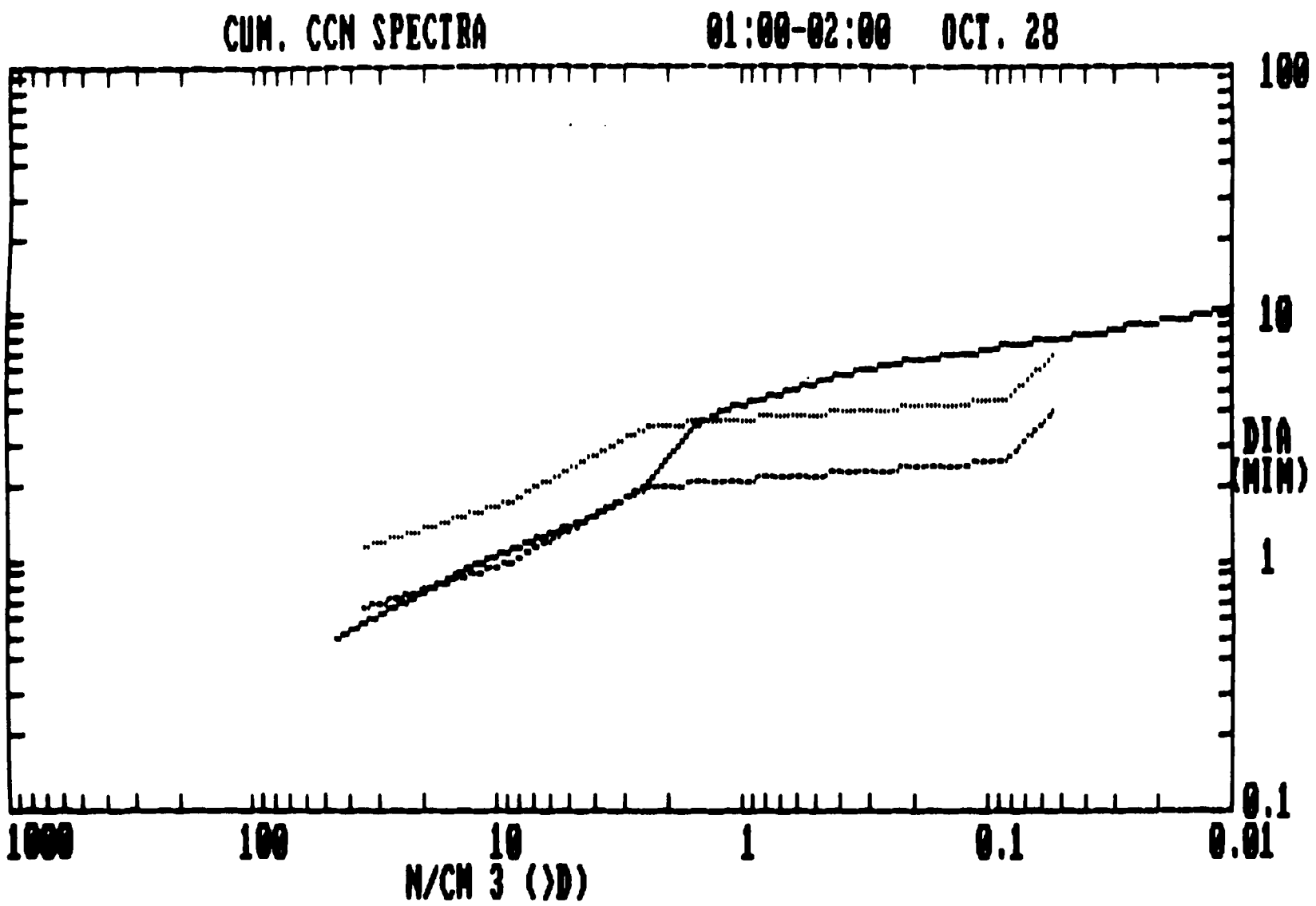
CUM. CCN SPECTRA
01:00-02:00 OCT. 28
100
10
DIA
(MIM)
1
0.1
1000
100
10
1
0.1
0.01
N/CM 3 ()D)

CUM. CCN SPECTRA
02:00-03:00 OCT. 28
100
10
DIA (MICRONS)
1
0.1
0.01
0.1
1
10
100
1000
N/CM 3 (>D)

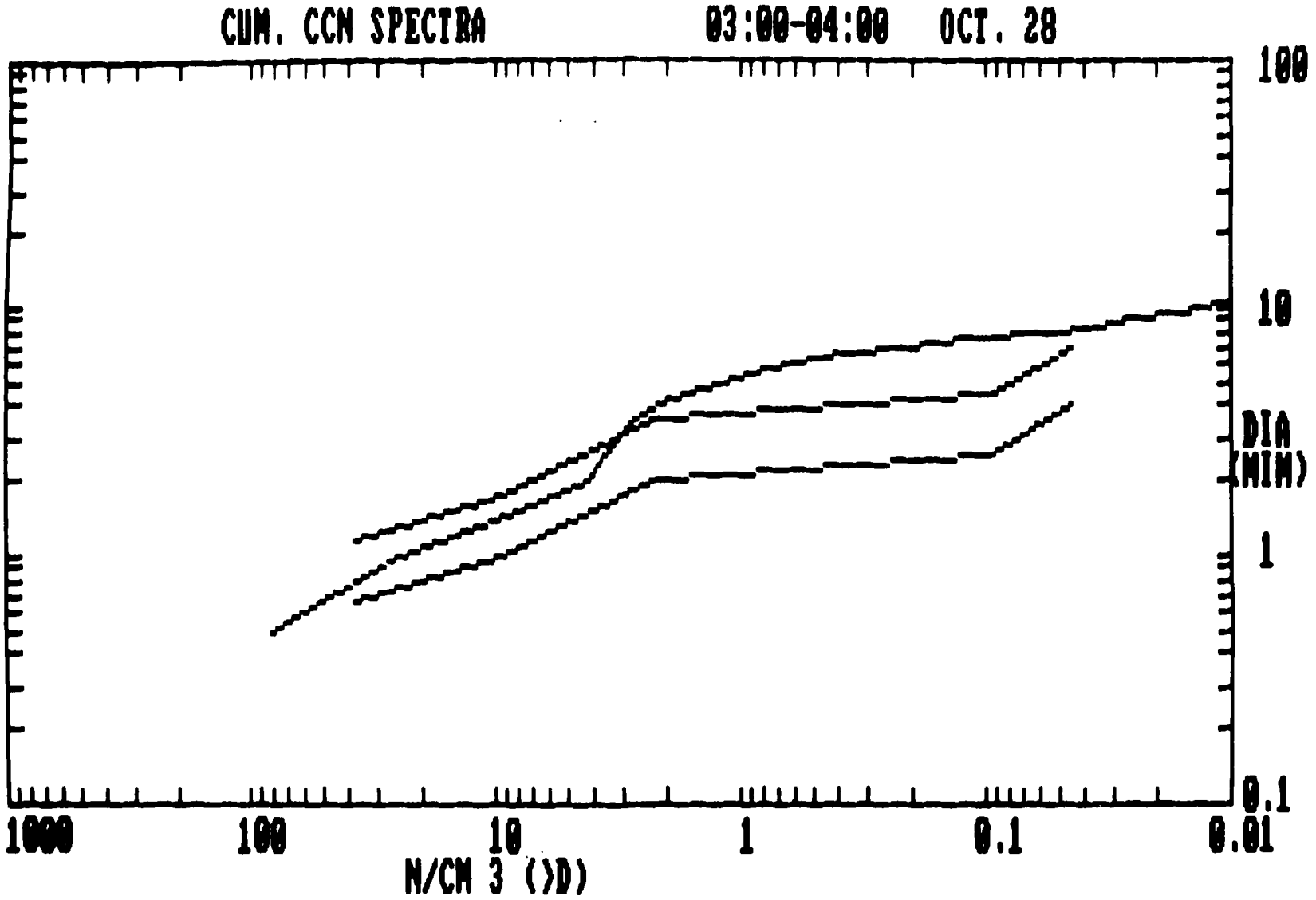
CUM. CCN SPECTRA
03:00-04:00 OCT. 28
100
10
DIA
(MIM)
1
0.1
1000
100
10
1
0.1
0.01
N/CM 3 ()D)

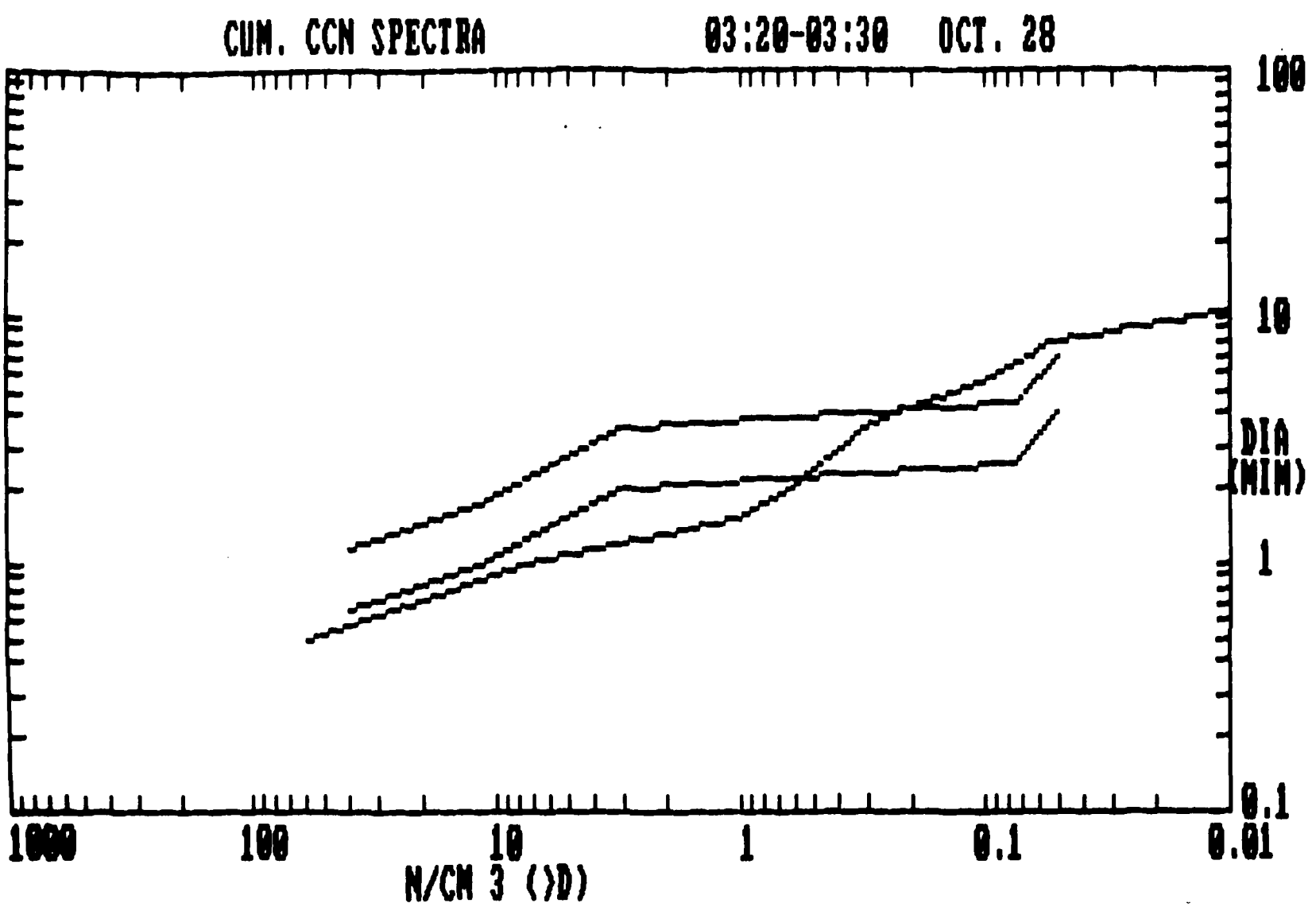
CUM. CCN SPECTRA
03:20-03:30 OCT. 28
100
10
DIA
(MIN)
1
0.1
1000
100
10
1
0.1
0.01
N/CM 3 ()D)

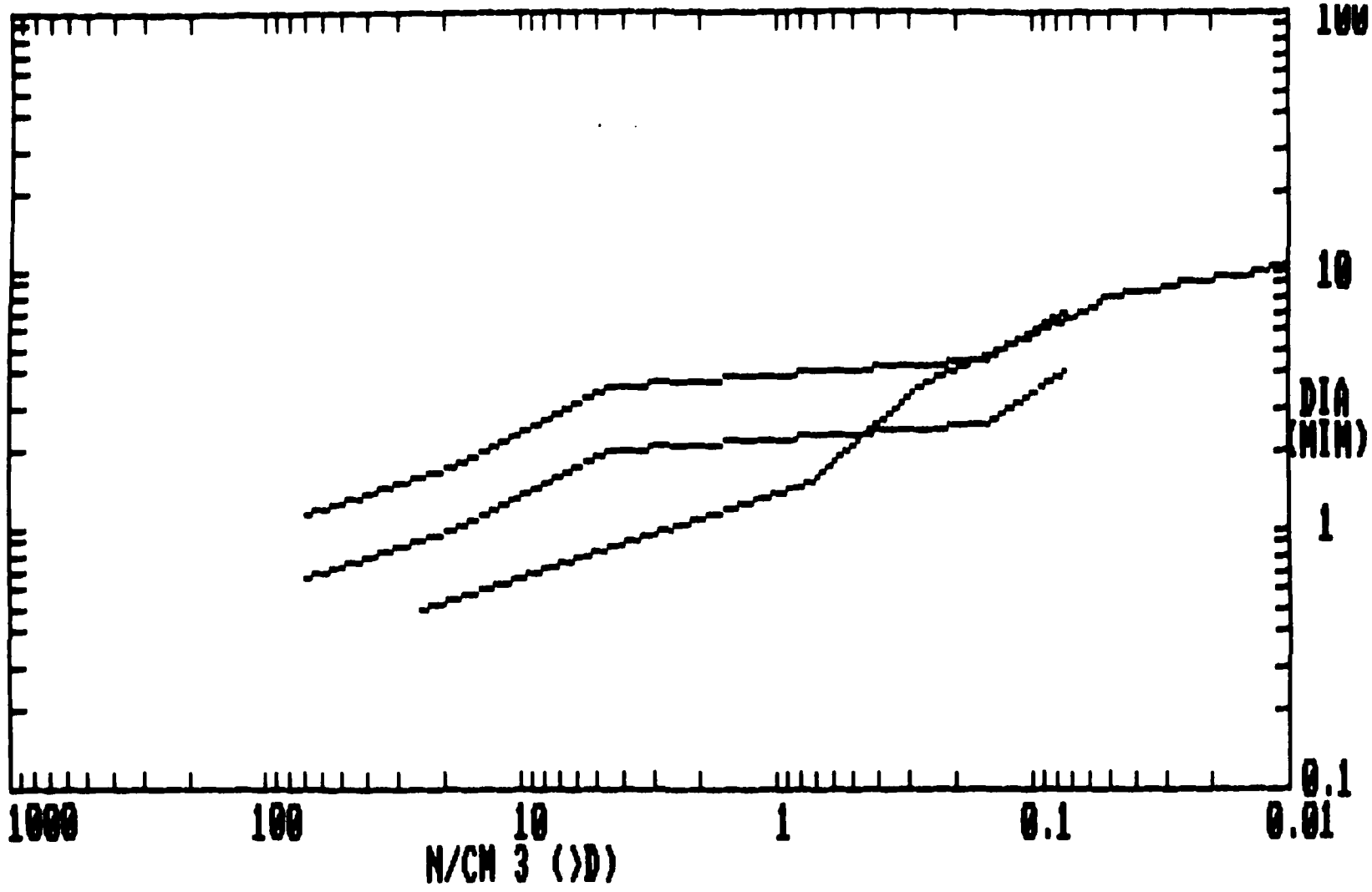

A-107

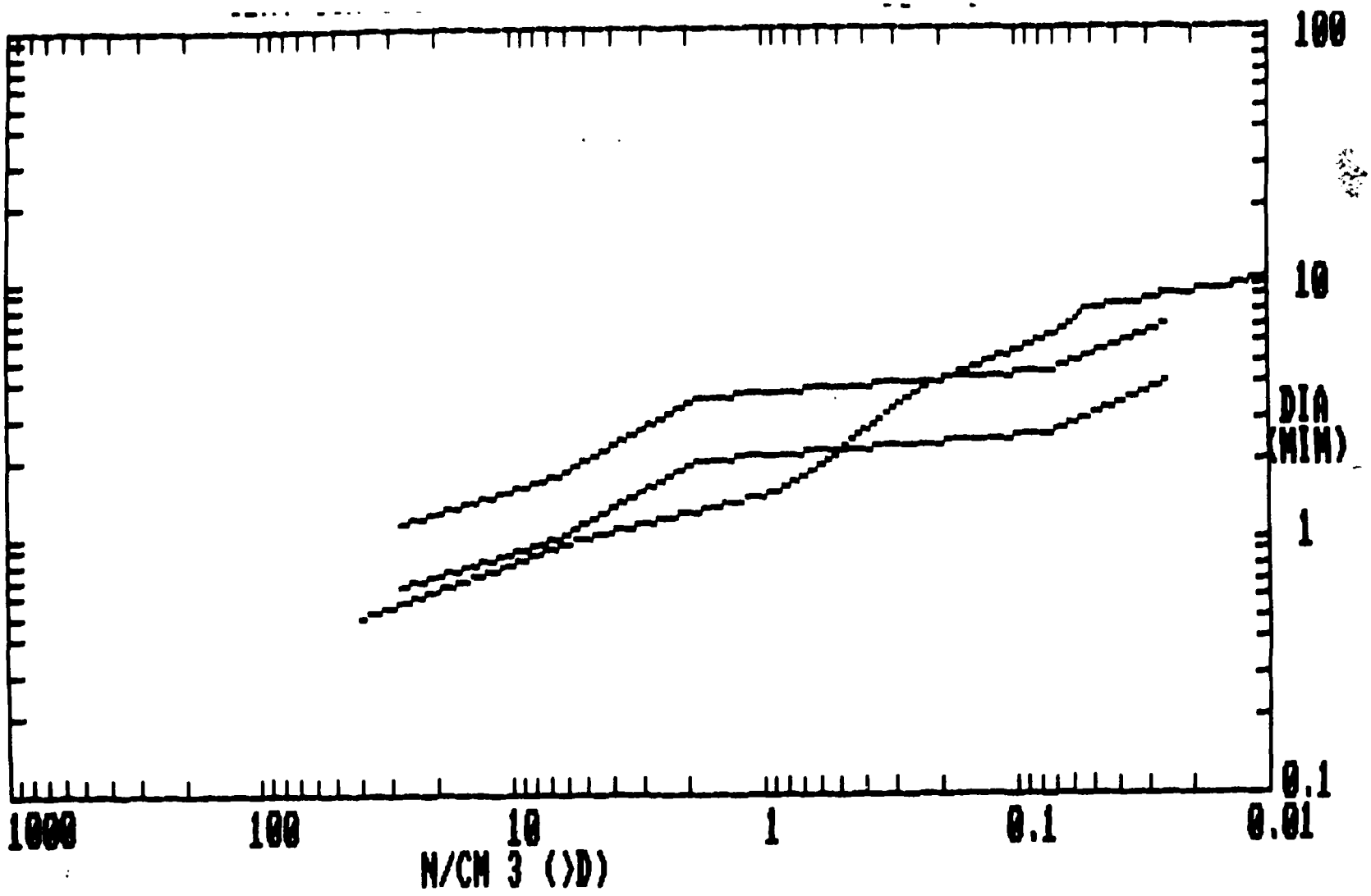
100
10
DIA
(MIN)
1
0.1
1000
100
10
1
0.1
0.01
N/CM 3 (>D)

END

5-87

DTIC